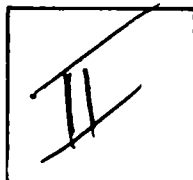


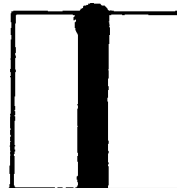
PHOTOGRAPH THIS SHEET

AD A119360

DTIC ACCESSION NUMBER



LEVEL



INVENTORY

Rept. No. NP30/78, Final Rept., Aug 77-Oct 78

DOCUMENT IDENTIFICATION

Sept. '78

Contract F33615-77-C-2059

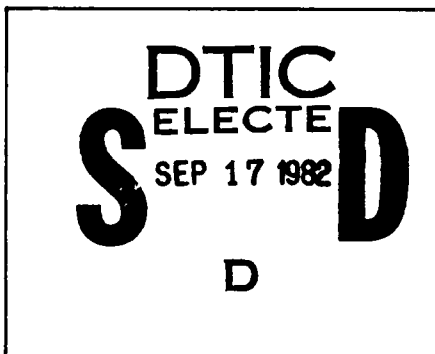
**DISTRIBUTION STATEMENT A**

Approved for public release;  
Distribution Unlimited

**DISTRIBUTION STATEMENT**

ACCESSION FOR	
NTIS	GRA&I
DTIC	TAB
UNANNOUNCED	
JUSTIFICATION	
BY	
DISTRIBUTION /	
AVAILABILITY CODES	
DIST	AVAIL AND/OR SPECIAL
A	

DISTRIBUTION STAMP



DATE ACCESSIONED



82 09 17 042

DATE RECEIVED IN DTIC

PHOTOGRAPH THIS SHEET AND RETURN TO DTIC-DDA-2

**NP30/78**  
**SEPTEMBER 1978**

# **A CRITICAL ANALYSIS AND ASSESSMENT OF HIGH POWER SWITCHES**



DR. TOM R. BURKES, PRINCIPAL INVESTIGATOR  
ELECTRICAL ENGINEERING DEPARTMENT  
TEXAS TECH UNIVERSITY  
LUBBOCK, TEXAS 79409

SUBMITTED TO:  
**NAVAL SURFACE WEAPONS CENTER**  
**DAHLGREN, VIRGINIA 22448**

**DISTRIBUTION STATEMENT A**

Approved for public release  
Distribution Unlimited

This report represents the first of a series of reports on high power switching which seeks to establish the state-of-the-art and provide direction for funding decisions. It is expected that an upgrade of this report will occur every 2 to 5 years. Comments concerning this report and suggestions for future reports should be directed to:

NAVAL SURFACE WEAPONS CENTER

SPECIAL APPLICATIONS BRANCH

ATTENTION: H. B. ODOM, CODE F12

DAHLGREN, VIRGINIA 22448

A CRITICAL ANALYSIS AND ASSESSMENT  
OF HIGH POWER SWITCHES

Final Report

Submitted as Partial Fulfillment  
Subcontract  
SCEEE-SIP/77-20

Electrical Engineering Department  
Texas Tech University  
August 1, 1978

T. R. Burkes, Principal Investigator  
M. O. Hagler  
M. Kristiansen  
J. P. Craig  
W. M. Portnoy  
E. E. Kunhardt



## Abstract

This work represents an evaluation and summary of the current state-of-the-art in pulsed power switching. Specifically, tube type switches (thyratrons, ignitrons, etc.), thyristors, transistors, spark gaps, mechanical switches and various other switches are described. The emphasis is on single element devices and switch performance achieved by series-parallel combinations of small devices is not included. A comparison of the capabilities of commercially available switches is made. Switch characterization and evaluation of those parameters responsible for switching performance, including standoff voltage, peak current,  $di/dt$ , pulse width, and pulse repetition rate, are presented.

# TABLE OF CONTENTS

	Page
ABSTRACT. . . . .	ii
ACKNOWLEDGEMENT . . . . .	x
LIST OF FIGURES . . . . .	v
CHAPTER I. GENERAL CONSIDERATIONS. . . . .	1
A. Introduction . . . . .	2
B. General Switching Constraints. . . . .	4
C. High Power Switch Capabilities . . . . .	12
D. Switch Parameter Description and Definition. . . . .	23
E. References . . . . .	26
CHAPTER II. TUBE TYPE SWITCHES . . . . .	27
A. Hydrogen Thyratrons. . . . .	28
B. Ignitrons. . . . .	49
C. A Thyatron-Ignitron Hybrid Switch . . . . .	68
D. Liquid Metal Plasma Valve. . . . .	70
E. Crossed Field Tubes. . . . .	80
F. Vacuum Tubes . . . . .	90
G. Cold Cathode Vacuum Tube . . . . .	103
CHAPTER III. SOLID STATE SWITCHES. . . . .	105
A. Thyristors . . . . .	106
B. Transistors. . . . .	160
CHAPTER IV. SPARK GAPS . . . . .	176
A. Introduction . . . . .	177
B. Gas Gaps . . . . .	186
C. Triggered Vacuum Gaps. . . . .	266
D. Liquid Spark Gaps. . . . .	278

Table of Contents (cont.)	Page
CHAPTER V. MECHANICAL SWITCHES. . . . .	286
A. Introduction. . . . .	287
B. Mechanical Switch Characterization. . . . .	288
C. Power Circuit Breakers. . . . .	295
D. Other Mechanical Switch Examples. . . . .	307
E. Parameters. . . . .	313
F. Summary . . . . .	321
G. References. . . . .	324
CHAPTER VI. MISCELLANEOUS SWITCHES. . . . .	326
A. Introduction. . . . .	327
B. Vacuum Arc Opening Switches . . . . .	329
C. Electron Beam Triggered and Sustained Switches	335
D. Solid Dielectric Switches . . . . .	341
E. Dielectric Surface Discharge Switches . . . . .	354
F. Fuse Opening Switches . . . . .	358
G. Explosive Opening Switches. . . . .	372
H. Thermally Driven Opening Switches . . . . .	379
I. Superconducting Switches. . . . .	383
APPENDIX I. BASIC THEORY OF GAS BREAKDOWN . . . . .	399
APPENDIX II. HIGH POWER SWITCH DATA AND RATIONALE . .	413
APPENDIX III. POWER CIRCUIT BREAKER DUTIES AND RATINGS	428



# LIST OF FIGURES

FIGURE		PAGE
I-1.	Switch voltage, current and power dissipation for square pulse operation. . . . .	5
I-2.	Approximate Anode Fall Time of Various Switches as a function of Pressure . . . . .	10
I-3.	Peak Rated Standoff Voltage Versus Peak Rated Forward Current. . . . .	13
I-4.	Total Coulomb Transfer Capability Versus Life Expressed as the Total Number of Pulses	15
I-5.	Charge Transfer per Pulse Versus Pulse Repetition Rate. . . . .	17
I-6.	Peak Repetitive Current Versus Pulse Repetition Rate. . . . .	19
I-7.	Rate of Current Rise Versus Peak Forward Current. . . . .	20
I-8.	Rate of Current Rise Versus Peak Standoff Voltage. . . . .	21
II-1.	Basic Thyatron Configurations and Materials Summary. . . . .	29
II-2.	Peak Standoff Voltage Versus Pulse Current for Large Commercial Thyatrons. . . . .	32
II-3.	Average Current Versus Peak Current for Commercially Available Thyatrons. . . . .	33
II-4.	Cathode Limitations as a Function of Power Density and Pulse Width, Current Density and Specific Resistance. . . . .	36
II-6.	Experimental Results . . . . .	41
II-7.	Basic Ignitron Configurations and Materials Summary. . . . .	50
II-8.	Rated Switching Voltage and Current for Commercially Available Ignitrons . . . . .	51
II-9.	Average Current Versus Peak Pulse Current for Crowbar Ignitrons. . . . .	53

List of Figures (cont.)

FIGURE	PAGE
II-10. Structural Features of the Liquid Metal Plasma Valve. . . . .	71
II-11. Crossed Field Switch Configuration. . . . .	81
II-12. Vacuum Tube Schematic . . . . .	91
II-13. Rated Standoff Voltage Versus Rated Pulse Current . . . . .	93
III-1. Thermal Connections to a Thyristor. . . . .	107
III-2. Basic Thyristor and Thyristor Equivalent Circuit . . . . .	110
III-3. SCR Current-Voltage Characteristics . . . . .	111
III-4. Typical SCR Construction. . . . .	113
III-5. Repetitive Peak Blocking Voltage vs. Turn-off Time. . . . .	115
III-6. Double Bevel Control of Surface Breakdown . .	117
III-7. Forward Voltage Drop at $200 \text{ A/cm}^2$ as a Function of Hole Lifetime in the n-Base and of Effective Base Width. . . . .	121
III-8. Overlapping Shorted Emitter (a); Multiply Shorted Emitter (b) . . . . .	123
III-9. Time Dependence of Trapezoidal Forward Current Pulse (a); of Forward Voltage (b) . . . . .	126
III-10. Effect of Emitter Shorting and Lifetime on Plasma Spreading Velocity (a); Relationship between Plasma Spreading Velocity and Blocking Voltage (b) . . . . .	129
III-11. Representative Interdigitated Contacts. . . .	131
III-12. Firing Sequence for Shorted Emitter Auxiliary Gate Thyristor (a); Auxiliary Gate Thyristor Equivalent Circuit (b). . . . .	132
III-13. Regenerative Gate Structure . . . . .	134

8

# List of Figures (cont.)

FIGURE	PAGE
III-14. Effects of Minority Carrier Lifetime on Forward and Reverse Blocking characteristics. . . . .	137
III-15. Light Triggered Thyristors. . . . .	141
III-16. Laser Activated Semiconductor Switch (LASS) .	142
III-17. Reverse Conducting Thyristor, Antiparallel Structure (a); p-i-n Structure (b). . . . .	144
III-18. Field Controlled Thyristor. . . . .	146
III-19. Basic Transistor Structure (a); Transistor Terminal Connections (b). . . . .	161
III-20. Impurity Profiles for an $n^+p-n^+$ Transistor (a); for an $n^+p-v-n^+$ Transistor (b). . . . .	166
III-21. Output Characteristics for an $n^+p-n^+$ Transistor (a); for an $n^+p-v-n^+$ (b). . . . .	171
III-22. Turn-On Behavior of $n^+p-n^+$ and of $n^+p-v-n^+$ Transistors . . . . .	173
IV-1. Effect of Metastable Atoms. . . . .	187
IV-2. The Trigatron Arrangement . . . . .	204
IV-3. Field Distortion Spark Gaps . . . . .	206
IV-4. Field Distortion Switch . . . . .	207
IV-5. Basic Laser Triggering Methods. . . . .	214
IV-6. Delay vs Laser Power. . . . .	215
IV-7. Jitter vs Laser Power . . . . .	216
IV-8. Arc Recovery Strength in $N_2$ at 1 atmosphere (6.4 mm Gap, 19 mm) Cylindrical Electrodes (Cu), 400-Ampere Arc) . . . . .	222
IV-9. Rep Rate Spark Gap Switch Assembly. . . . .	225

List of Figures (cont.)

FIGURE	PAGE
IV-10. Turbulent Flow Switch. . . . .	227
IV-11. Spark Gap Cross Section. . . . .	231
IV-12. Electrode Surface Temperature vs Rate of Current Rise for Copper, Tungsten, Lead and Aluminum . . . . .	236
IV-13. Anode Jet Velocity vs Rate of Current Rise for Copper, Tungsten and Aluminum. . . . .	237
IV-14. Erosion of MK V Gap Main Electrodes. . . . .	243
IV-15. Effect of gas pressure an erosion rate in a 2 mm gap, electrodes 30 mm diam., $Q = 7 \text{ Cb}$ Const. . . . .	244
IV-16. Erosion Rate for Different Electrode Metals (13 mm, 1 atm) . . . . .	247
IV-17. Erosion Rate for Different Electrode Metals (1.5 mm, 6.5 atm). . . . .	248
IV-18. The Erosion at a Constant Coulomb Rating But Varying Current. . . . .	249
IV-19. The Erosion of Copper. . . . .	250
V-1. Elementary Mechanical Switch Components. . .	292
VI-1. Vacuum Arc Interrupter . . . . .	330
VI-2. Electron Beam Triggered and Sustained Switches	336
VI-3. Dielectric Switch Schematic. . . . .	343
VI-4. Typical Switch Package Construction. . . . .	345
VI-5. Solid Dielectric Switch Breakdown Process. .	347
VI-6. Multichannel Solid Dielectric Switch . . . .	348
VI-7. Metal-Metal Switch . . . . .	351
VI-8. Dielectric Surface Discharge Switch. . . . .	355

List of Figures (cont.)

FIGURE	PAGE
VI-9. Time to Explosion $\Delta t$ of Copper Wires Versus Current Density $j$ . . . . .	359
VI-10. Peak Voltage per Length $V^*$ of Copper Wires Versus Time to Explosion. Parameter: Surrounding Medium. . . . .	361
VI-11. Peak Voltage per Length $V^*$ and Current Shapes of Slowly Exploding Wires in Different Surrounding Media . . . . .	363
VI-12. Explosive Switches . . . . .	374
VI-13. Possible B-Field Orientations for S.C. Switch Quenching . . . . .	385
VI-14. Superconducting Opening Switch . . . . .	392
AI-1. Evolution of Voltage and Current in Gap. Voltage is applied at $t = 0$ . . . . .	401
AI-2. Typical Paschen Curve. . . . .	408
A3-1. Short Circuit Current with Decaying D-C Offset . . . . .	432
A3-2. A Symmetry Factor for Symmetrical Rating Standard . . . . .	432



### Acknowledgement

This work was funded by the Naval Surface Weapons Center/Dahlgren Laboratory, Special Applications Branch, through the Air Force Aero-Propulsion Laboratory, Senior Investigator Program, Wright-Patterson AFB, Contract F33615-77-C-2059 (Southeastern Center for Electrical Engineering Education). Numerous individuals and organizations, both domestic and foreign, generously contributed much of the necessary information to compile this report. Rather than risk offending individuals or organizations due to an inadvertent oversight, the authors wish to thank collectively those who assisted Texas Tech University in the preparation of this report.

CHAPTER I  
GENERAL CONSIDERATIONS

T. R. Burkes

et. al.

### A. Introduction

New developments in high-technology areas, such as lasers and fusion, often require electrical switching capabilities beyond what are currently available. New requirements may result in new switch studies and development programs devoted to the specific needs of a particular application and, consequently, to a narrow range of switching parameters. Few studies, however, have considered broad areas of high power switching and the general comparison of various switching technologies as well as the identification of those factors which appear to limit a particular switching concept. This report describes a study conducted at Texas Tech University to analyze and assess high power switches. This effort includes the evaluation of the more popular switches and describes some of the most promising concepts. A few novel switches are also described. This report represents a one man year effort.

The meaning of the term "high power switches" is subject to varying definition depending on the user. For this report, the meaning of "high power switches" is constrained to those switches or switching concepts which are capable (or appear capable) of "standing off" kilovolts and conducting currents in the "ON" state of the order of kiloamperes. Small switches can be connected in parallel and/or series to achieve

a high power capability. Although this is a legitimate approach to increased switching capacity, this study is confined to single element switches.

Both opening and closing as well as single shot and rep-rated switches are included within the scope of this report. Obviously the scope is so broad that it is difficult (if not impossible) to cover every possible switch. Thus, the more interesting and important concepts form the principal topics. The major types of switches described are spark gaps, vacuum tubes, gaseous tubes such as thyratrons and ignitrons as well as solid state devices and mechanical switches.

In general, all switches have certain aspects in common. Many switches are governed by general concepts such as Paschen breakdown and the glow-to-arc transition. It is worthwhile then to review briefly the fundamental aspects of switch operation and those concepts which are applicable to switches in general. This section is followed by a short review of the state-of-the-art of the major commercially available switches. A few of the more important switches which are not readily available commercially are also included. For uniformity a consistent set of switch parameters is required. The parameters used in this report are described at the end of this chapter.

### B. General Switching Constraints

Fundamentally, most switches in the "open" state may be viewed as a set of capacitor plates separated by a dielectric. The properties of the dielectric are such that it can be made conductive in some manner such as ionization of a gas (thyratrons), injection of charge carriers into the conduction band (solid state), etc. or by injection of a conducting medium into the separating region (vacuum spark gaps). Even the closure of mechanical contacts is usually preceded by an arc. In most cases a charge transport phenomenon through the previously insulating medium is required to achieve switch closure. To recover to the "open" state, a deionization process is usually required.

The voltage standoff capabilities (see Fig. I-1) of a switch are determined by the breakdown characteristics of the dielectric and/or the field emission characteristics of the separating electrodes. For example, in low pressure devices such as thyratrons or vacuum devices the electrodes are usually separated by less than one mean free path of the insulating (or residual) gas and field emission dominates. For others, such as solid dielectric spark gaps, the breakdown of the dielectric is usually exceeded before field emission from the separating electrodes becomes a problem.

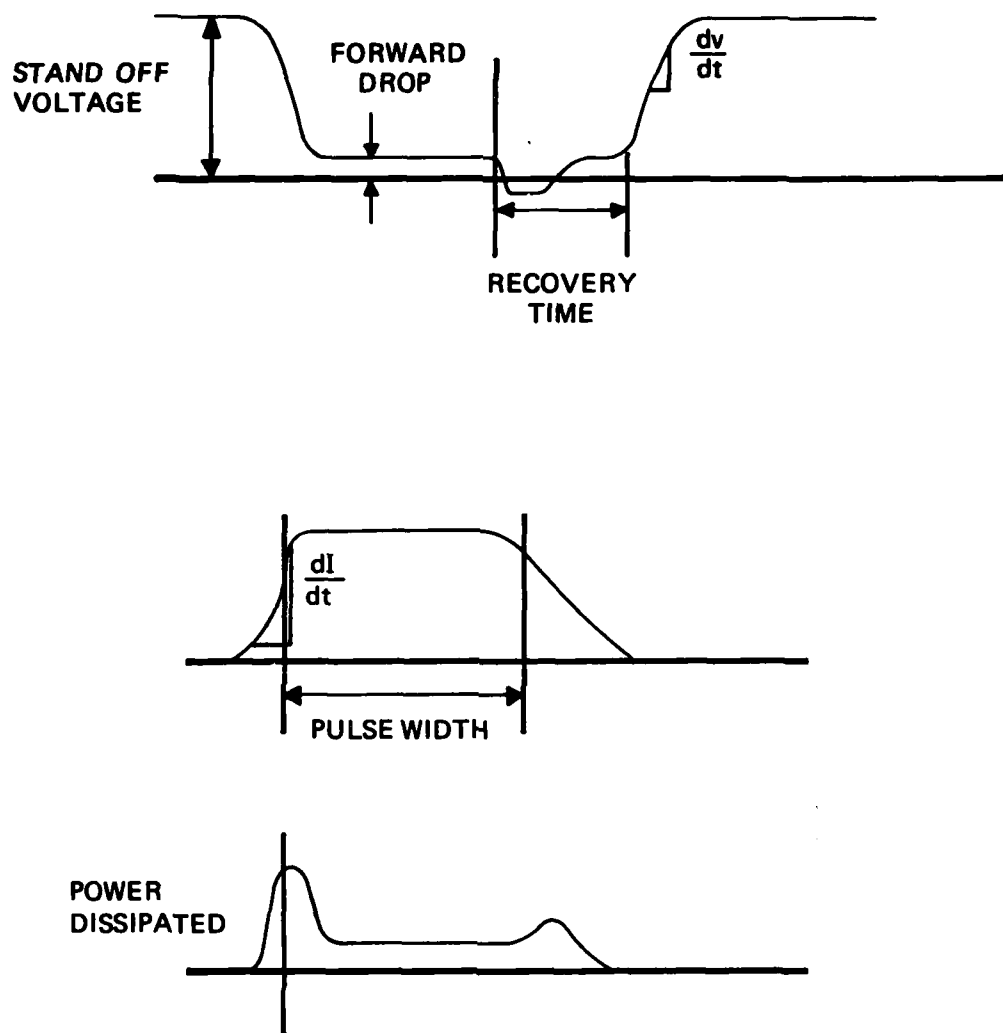


Figure I-1. Switch voltage, current and power dissipation for square pulse operation.

Problems associated with breakdown of insulators or envelopes, etc. are not considered, for purposes of this report, to be limiting factors as they can usually be solved by proper voltage grading, oil submersion, etc. Size constraints imposed by the application may be such that envelope constraints dominate switch performance. However, this type of problem doesn't in itself, constitute a switch constraint except as imposed by the specific application.

Because charge transport is required for switch closure, sufficient energy must be available to accelerate the carriers within the gap. For triggered switches a source of charges is usually provided in some manner (ignitors in ignitrons, trigger electrodes in spark gaps, etc.). Because these charges will have some initial velocity distribution, some of the carriers will cross the gap sooner than others. This results in a finite closure rate determined by the initial conditions in the charge source, the accelerating voltage, and the insulating medium. Considerable energy may be dissipated during the closure phase (referred to as the "resistive" phase in spark gap terminology). X-rays will be emitted for high voltage switches and electrode damage due to heat generation is possible. Thus, some switches have  $di/dt$  constraints imposed by their heat capacity and conductivity or a  $di/dt$  limitation imposed by carrier formation rates.

The switch voltage in the "on" state (forward drop in Fig. I-1) is important in determining overall switch efficiency. For most switches the forward voltage is determined

by complex processes and in general is not constant with time. This is especially true for short, fast rising pulses. Thus, a spark gap may have a forward drop of 100-150 volts shortly after the initial "turn on" phase, but only 20-30 volts for the same current in "steady state."

The recovery time of a switch generally refers to the time for the recovery of the dielectric properties of the switch so that voltage can be withstood. Most switch concepts require the recombination of charge carriers in the recovery process. This recombination is a function of the plasma characteristics of the conducting medium; i.e., charge density, mobility, temperature, collision and attachment cross sections, mean free paths, external fields, etc. After a certain time, recombination or recovery has progressed to a point that some voltage can be withstood and the recovery process continue at some rate,  $dv/dt$ . This leads to a  $dv/dt$  constraint for many switches. If a certain rate of reapplication of voltage is exceeded, then there is a high probability that the conducting state will be reestablished. In some switches, the application of a high  $dv/dt$  will result in switch closure, even from the open state. Many solid state devices suffer from this characteristic. In any event, the recovery characteristics of a switch clearly



limit the rate at which the switch may be operated. In general, an increased dissipation is associated with the recovery phase of a switch (Fig. I-1). This dissipation is a straight forward process in "opening" switches (at least in principle) but may be imposed by external circuitry in "closing" switches. If a negative voltage is applied to the anode immediately after the main pulse, significant ion bombardment of the anode may occur, increasing dissipation.

A switch in its "open" state is required to withstand a voltage determined in part by the properties of its dielectric. Clearly there is a capacitance associated with a switch in its open state, and most of the energy thus stored will be dissipated internally to the switch. Thus, in the extreme, a limitation on switching action may be determined by the switch's ability to dissipate its internally stored energy, especially for high pulse repetition rates.

Switches that do not clearly define initial conditions suffer from jitter. Charge buildup is usually a random phenomenon and the delay in the start of closure is also random. The initial conditions can be well defined as demonstrated by the use of lasers in pressurized spark gaps and solid state devices or "keep alive" electrodes in thyratrons. The result is a greatly reduced jitter.

A great number of important switches are fundamentally limited by an equivalent Paschen's Law. This law relates

the breakdown voltage to electrode separation and gas pressure (See Appendix I). Figure I-2 shows some important characteristics of several switches and their relationship as a function of gas pressure. It is interesting to note that the lower the pressure, the longer the fall time in anode voltage, the exception being the vacuum tube which does not depend on a breakdown process. It is also interesting to note that delay and jitter decrease with increasing pressure but recovery time can be expected to increase with pressure. At very high pressures however, the recovery processes are such that recovery time may decrease with increasing pressure.

Another important process in the breakdown phenomenon is the glow-to-arc transition (GAT). A review of this process was performed by M. A. Lutz [1] who proposes the following model:

"A clear model for the GAT is evident. An insulating particle on the cathode surface charges up by positive ion bombardment to a potential high enough that the field strength causes breakdown, producing a burst of vapor. This can only happen for a range of particle sizes, this range in turn depending on the glow current density and discharge voltage. Once the vapor is produced, any volatile contamination in the vicinity increases the amount and duration of the vapor burst, thereby increasing the probability of subsequent arc formation. If the circuit current exceeds

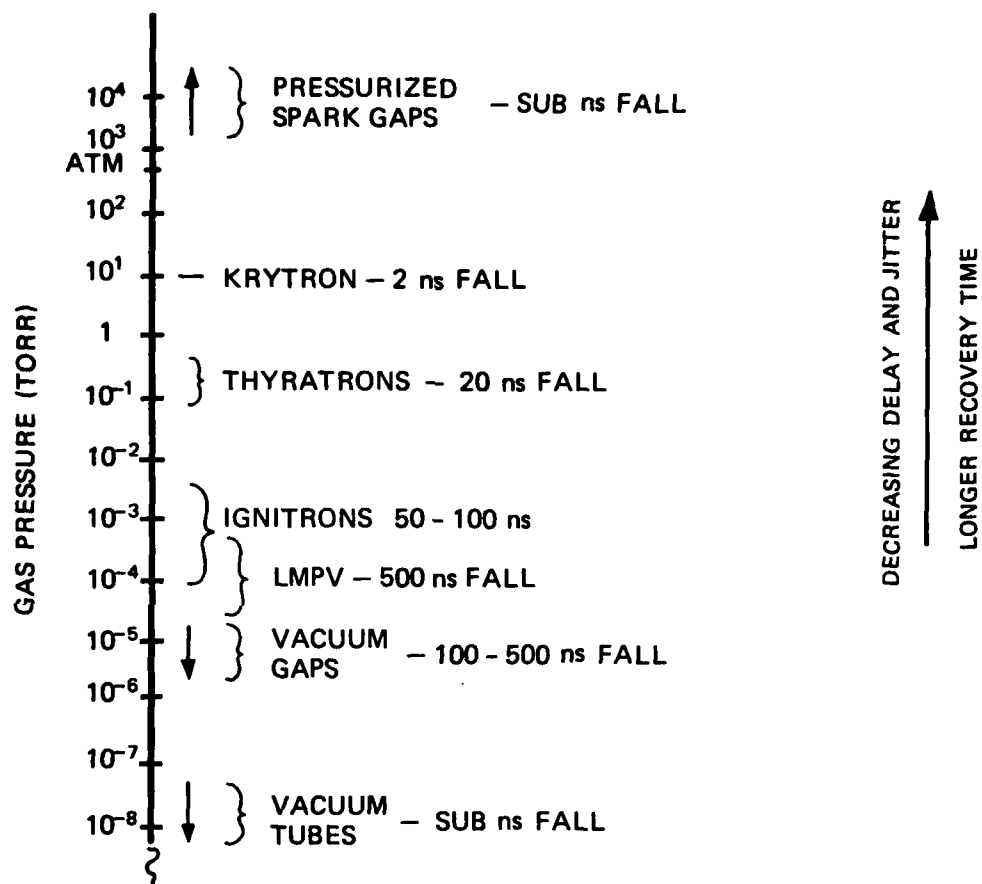


Figure I-2. Approximate Anode Fall Time of Various Switches as a function of Pressure.

the vapor arc chopping current, an arc forms immediately. If not, arc formation can occur only if the circuit current can rise above the chopping current in a time short relative to the duration of the vapor. It is in this regard that the amount of stored energy which can be delivered on the nano-second time scale (to sustain the embryonic arc) and the external circuit play a role."

Clearly, the GAT is very important in switches operating in the arc mode and equally important to switches where an arc is to be prevented. The reader is referred to this article [1] for more detailed information.

### C. High Power Switch Capabilities

Reviews of the state-of-the-art of the high power switches has been previously reported [2,3,4]. A portion of this work [2,3] is represented here to establish an overall perspective for the present status of the more popular, high power switches. The switch selection for this presentation is based primarily on off-the-shelf availability (the exception being some spark gaps). This evaluation then omits many important switches such as fuses, mechanical "opening" switches, etc. A description of the capabilities of these concepts is deferred to subsequent chapters.

Even with the deletion of many competing technologies, a meaningful and fair comparison is difficult. Most switches can be operated in a manner to enhance some switch parameter over the others. Thus, taken out of context so to speak, the operation of a switch can be manipulated to show advantage in one regard or the other. In this presentation, simultaneous operation at maximum rated standoff voltage, and peak pulse current are taken as the primary operating constraints. The data and the rationals used are presented in Appendix II.

Figure I-3 shows the rated standoff voltage plotted for the rated pulse current for the various switches. No

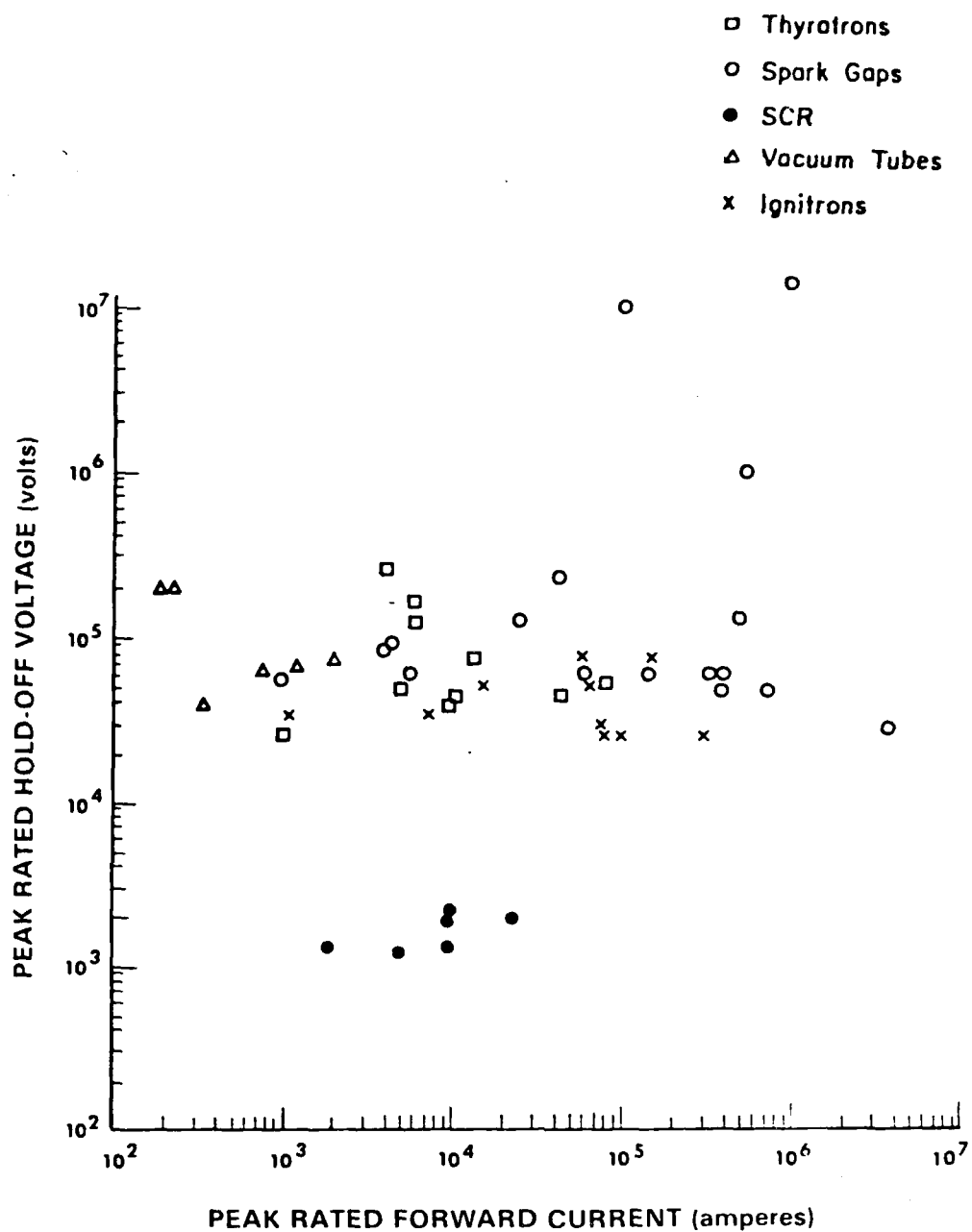


Figure I-3. Peak Rated Standoff Voltage Versus Peak Rated Forward Current

obvious trends exist in the data, which suggest that the state-of-the-art in these devices is determined more by application requirements than fundamental limitations. Clearly, spark gaps have achieved a higher level of performance as far as voltage and current are concerned. In terms of peak switched power the ranking is spark gaps, ignitrons, thyratrons, vacuum tubes and lastly, SCR's. Of course, voltage and current are only part of the overall picture. Figure I-4 shows the total Coulomb transfer of the switch versus life time expressed as the total number of shots obtainable. The best device in this regard is the SCR but little data are available and the expected life is so great in comparison to the other devices as to be off scale in Fig. I-4. It is likely that ignitrons operated in square pulse operation would also demonstrate enormous total Coulomb transfer. However, little data are available on this type of operation for ignitrons. The data shown for ignitrons came from tests which were terminated, for various reasons, before actual device failure. The best total Coulomb transfer for ignitrons used in ringing type discharges is  $3 \times 10^5$  C.

Thyratrons can be expected to transfer between  $10^8$  and  $10^9$  Coulombs with greater than  $10^{10}$  shots. This fact, coupled with the peak power capabilities shows the enormous advantage that hydrogen thyratrons have over most other type switches which have similar peak power capabilities but lower

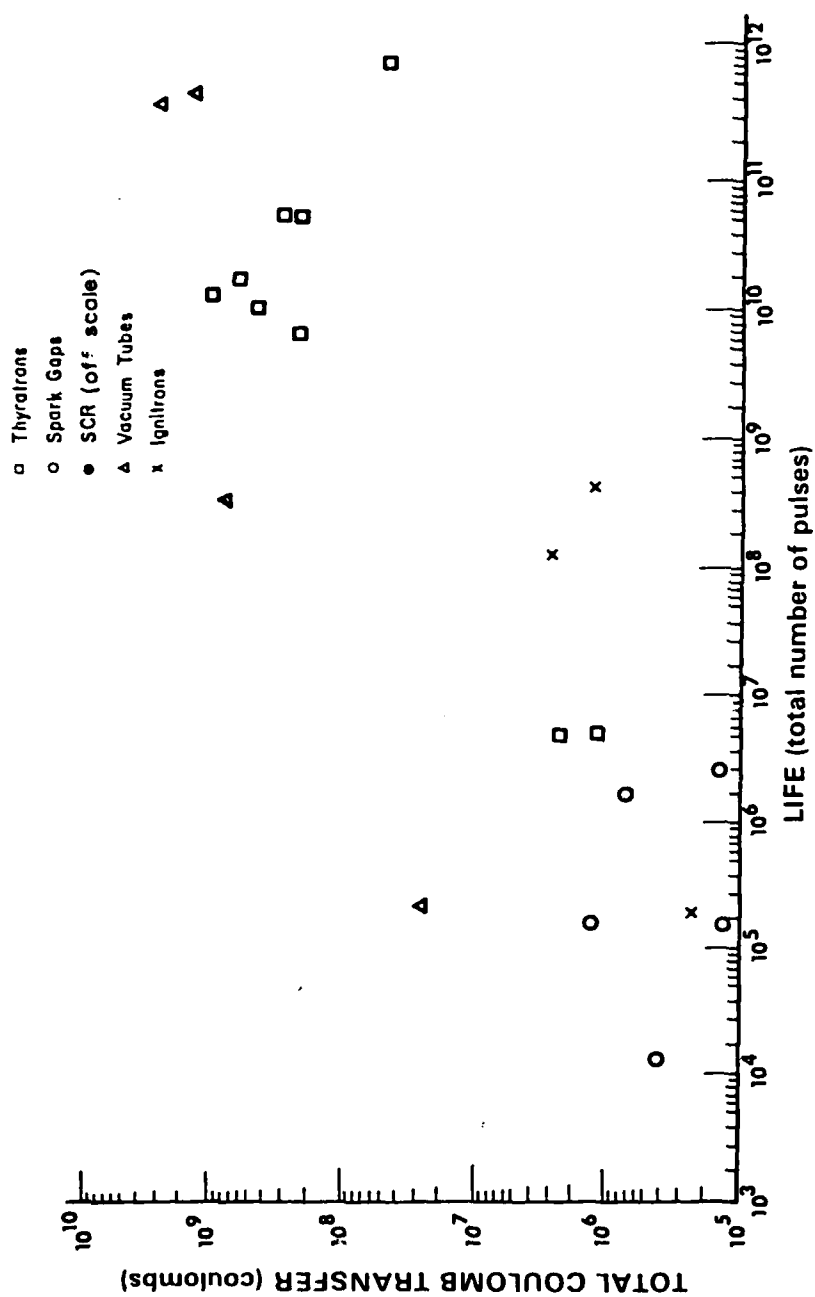


Figure I-4. Total Coulomb Transfer Capability Versus Life Expressed as the Total Number of Pulses.



life expectancies. Vacuum tubes are capable of similar Coulomb transfer but at much reduced peak power. Spark gaps operating at high peak powers have not demonstrated a great ability for total Coulomb transfer capability (see Appendix II). Some spark gaps have demonstrated a respectable total Coulomb transfer, however, but extensive life test data are not available. It is obvious that the true capabilities of spark gaps are not well defined in this regard.

The total Coulomb transfer capability shown in Fig. I-4 gives, of course, no indication of the rate of charge transfer. Thus, the charge transfer per pulse versus pulse repetition rate is shown in Fig. I-5 and the peak repetitive current versus repetition rate is shown in Fig. I-6. The general fall-off in charge transfer per pulse at high rep-rates results from device heating limitations and from the reduced pulse width resulting from high rep-rates. Figure I-6 would be identical to Fig. I-5 if the pulse lengths were the same for all devices. Notice that vacuum tubes are capable of considerable Coulomb transfer per pulse but at low repetition rates (Fig. I-4). By reducing the pulse width or Coulombs/shot, much higher repetition rates can be achieved. Operation at higher than rated current usually reduces the life expectancy of all switch types. Figure I-5 shows only a modest Coulomb/shot capability for thyratrons

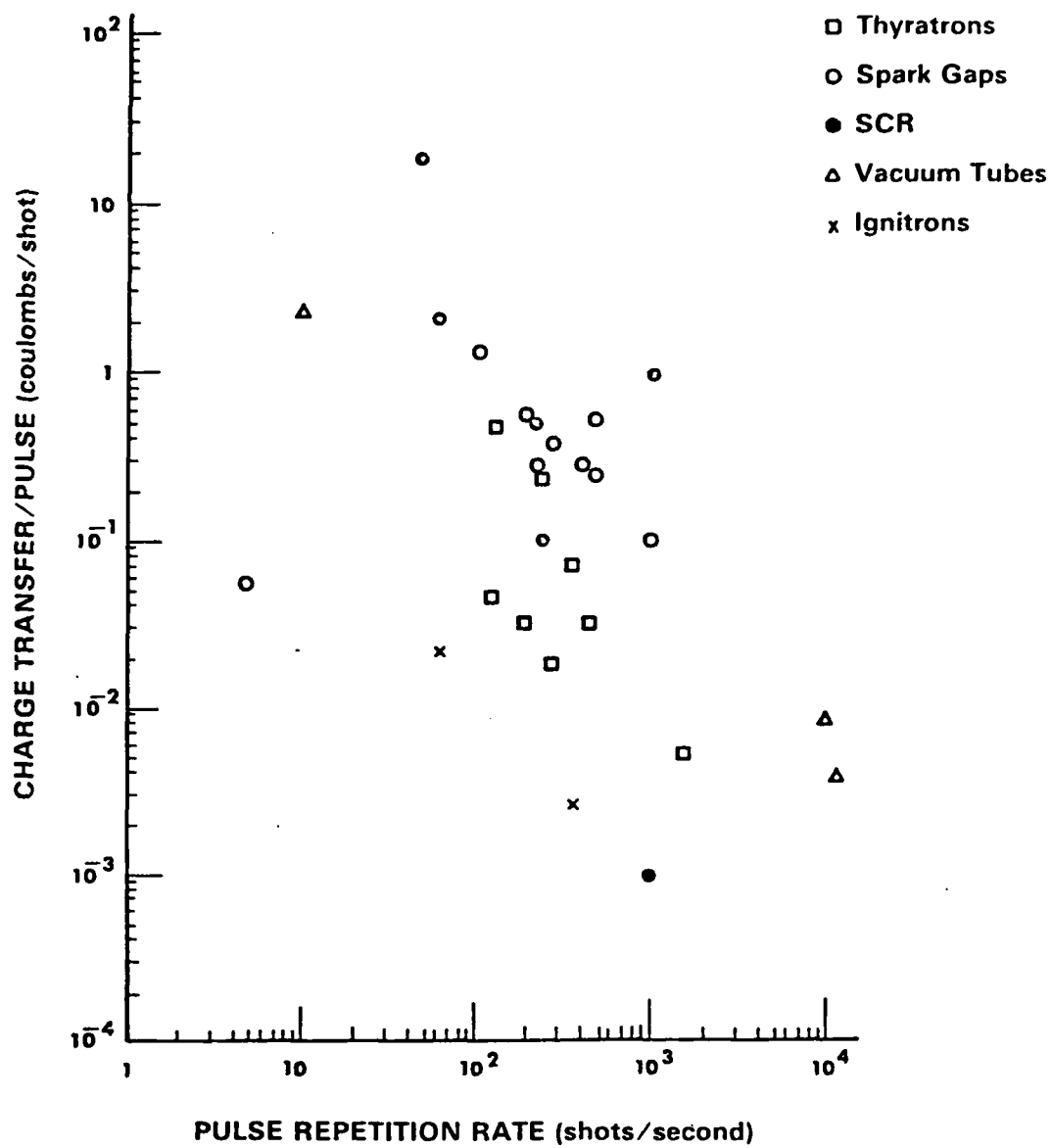


Figure I-5. Charge Transfer per Pulse Versus Pulse Repetition Rate.

because operation at maximum current (Fig. I-6) is assumed. Reduction of the peak current will allow a considerable increase in pulse width allowing for a much greater Coulomb per shot capability.

Spark gaps have been tested in short-circuit discharges and shown to have extremely high  $di/dt$  capability. Generally, spark gaps can be designed with multichannel discharges to provide such a low inductance that the current risetime is limited by the load rather than the switch itself. Many spark gaps with liquid or solid dielectric media also have spectacular performance characteristics in single shot service but it is difficult to envision how one can extrapolate these parameters to rep-rated service. The data presented here are, therefore, mostly for gas filled gaps except for one vacuum gap listed in Table IV, Appendix II.

The  $di/dt$  versus the peak current and maximum hold-off voltage for the various switches are shown in Figs. I-7 and I-8. The characteristic turn-on time,  $\tau = I_p/(di/dt)$ , for the devices described in Fig. I-7 generally seems to decrease as the peak current capabilities increase. Although vacuum tubes seem capable of reaching their peak rated current somewhat faster than the other devices, spark gaps show the greatest capability for combined speed and peak current. Little data were found on  $di/dt$  capabilities or limitations of ignitrons. Also, the  $di/dt$  capabilities

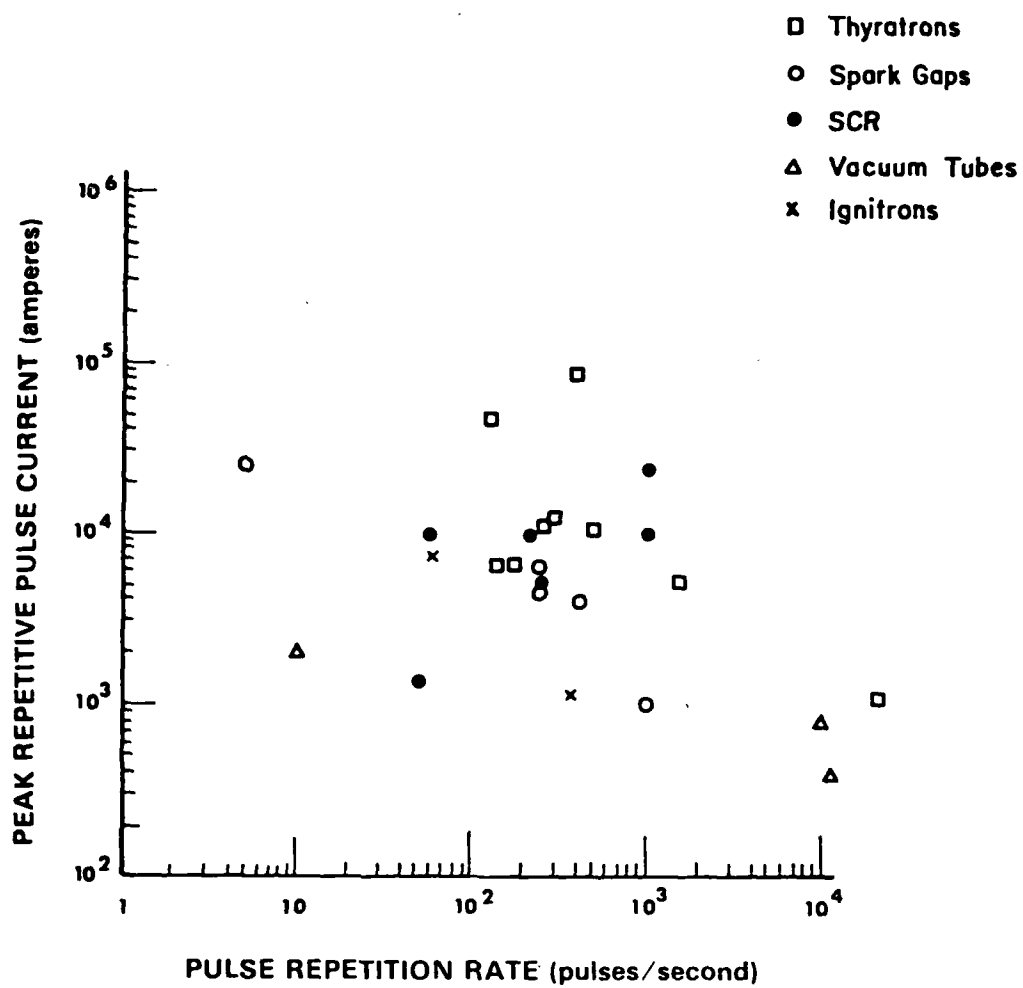


Figure I-6. Peak Repetitive Current Versus Pulse Repetition Rate.

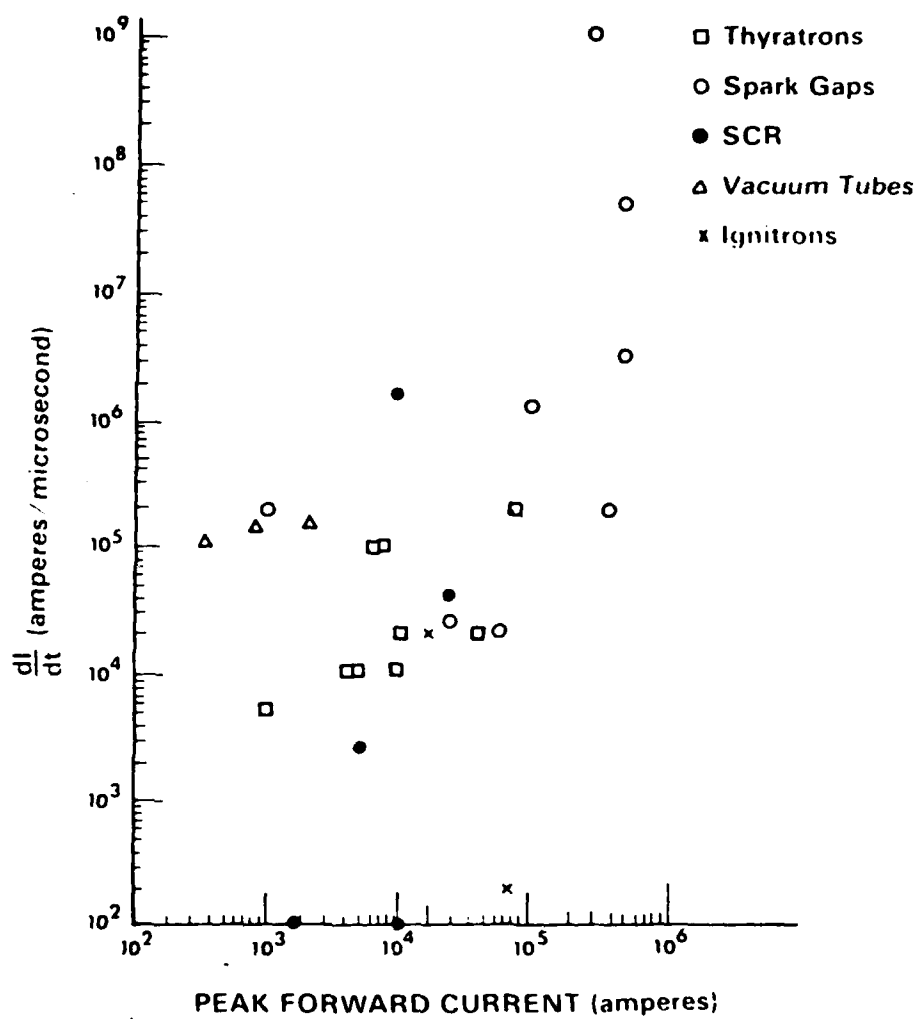


Figure I-7. Rate of Current Rise Versus Peak Forward Current.

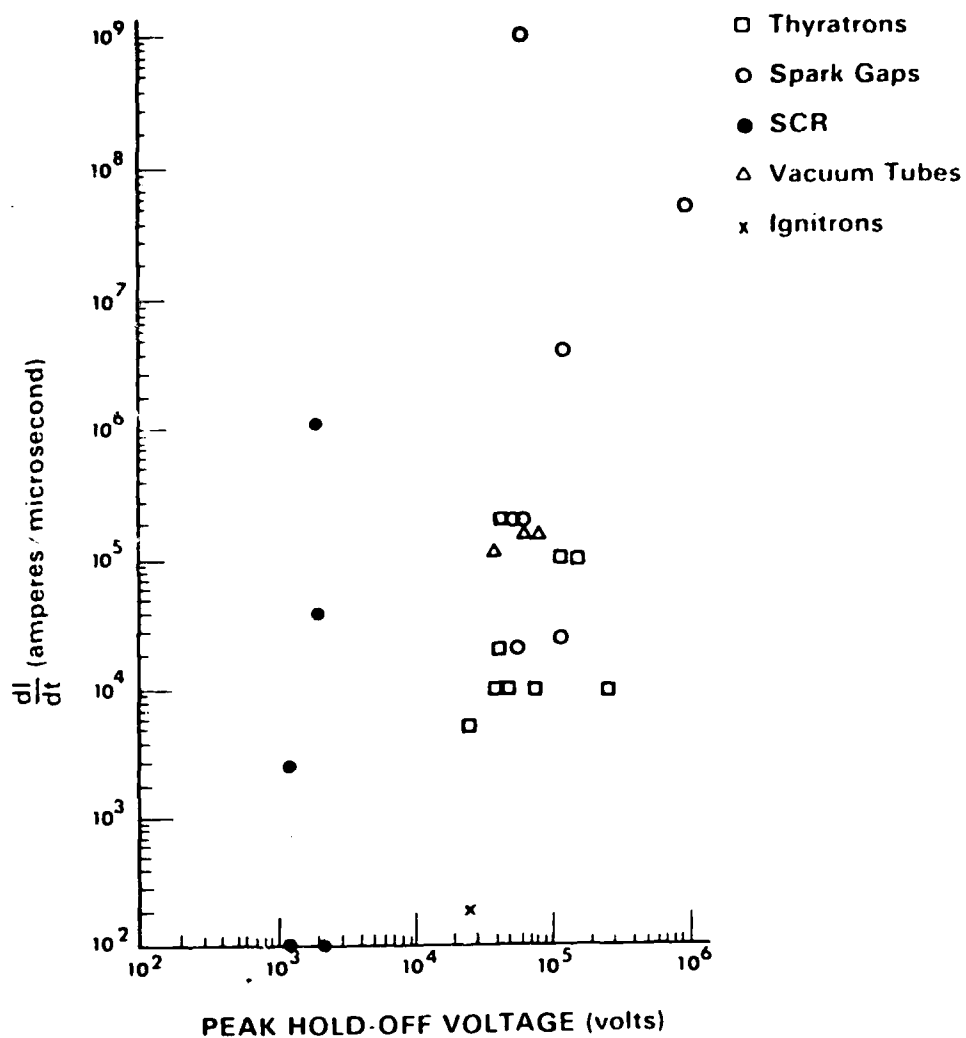


Figure I-8. Rate of Current Rise Versus Peak Standoff Voltage.

of vacuum tubes is a function of the drive capabilities as mentioned in Appendix II and little actual data were found.

The  $di/dt$  limitation of thyratrons is, to a degree, determined by the application. At high repetition rates and high  $di/dt$  operation, considerable tube heating may occur and the life of the tube is thus reduced. However, sufficient data were found to say that reliable operation from  $10^4$  to  $10^5$  amperes/microsecond can be expected for most commercially available devices.

#### D. Switch Parameter Description and Definition

In any reasonably well defined switching concept (such as thyratrons) there are many terms and parameters used to describe the operation or character of a particular device. Because different concepts may use different terminology for the same parameter and because some parameters are not universally applicable to the various switching concepts, it is not feasible to define a universal set of switch parameters.

If a switch, regardless of whether it is a spark gap, solid state device, etc., is viewed as a black box with power terminals and control terminals, then a set of parameters describing the black box can be defined. Of course, this approach ignores the internal workings and character of the particular switch.

There are many parameters which are functions of a particular application. Examples are the effect of environment on voltage, circuit layout on inductance or  $di/dt$  capabilities. For purposes of this report, this type of application induced parameters are largely ignored and the major effort is directed toward the determination of factors which form ultimate limitations.

A description and definition of the switch parameters used in this report is as follows:



Voltage Standoff-Manufacturers rating for commercially available devices. The limitation is defined as that voltage for which breakdown of the device will occur based on the internal characteristics rather than those limitations imposed by device packaging, etc.

Peak Current-Manufacturers rating for commercially available devices. The limitation is defined as the current at which the "health" of the device is in jeopardy. More often than not, the current is also a function of the pulse width.

Pulse Width-Time for the beginning of conduction to termination of conduction.

di/dt-That rate at which current can be applied without device damage or, in some cases, that value of current rise limited by the switch itself.

Delay Time-That value of time between the application of a trigger command and the initiation of conduction. To the extent possible, the effects of the character of the trigger pulse are ignored.

Jitter-Variations in the exact time of the initiation of conduction.

Pulse Repetition Rate (rep-rate)-The rate at which the switch can be "opened" and "closed" without degradation of characteristics.

Recovery Time-That time between the end of a current pulse and the point at which the switch recovers the ability to withstand voltage.

dv/dt-That rate of change of applied voltage which can be safely applied to a device after conduction and/or the rate at which voltage can be applied to a device without causing a switching operation.

Forward Drop-The voltage drop across the switch after the initial "turn on" phase.

Life-The life expectancy of switches is measured in different ways. In some cases, the number of "shots" or operations is sufficient. In others, the amount of time (usually stated in hours) of repetitive operation is more appropriate.

### E. References

- [1] Michael A. Lutz, "The Glow to Arc Transition-A Critical Review," IEEE Transactions on Plasma Science, March 74.
- [2] T. R. Burkes, M. Kristiansen, W. Portnoy and M. Hagler, "High-Power Switching Capabilities," Thirteenth Pulse Power Modulator Symposium, June 1978.
- [3] "Proc. Workshop on Switching Requirements and R&D for Fusion Reactors," EPRI ER-376-SR, July, 1977, (M. Kristiansen, Editor), Electric Power Research, Institute.
- [4] P. Felsenthal and J. M. Proud, "Nanosecond Switch Development," AFWL-TR-65-119, Nov. 1965.

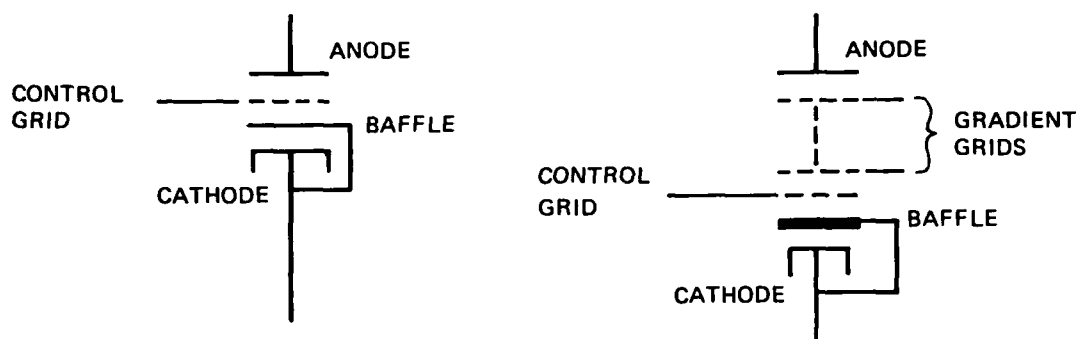
CHAPTER II  
TUBE TYPE SWITCHES  
T. R. Burkes

## A. Hydrogen Thyratrons

### 1. Introduction

The thyatron is primarily a unidirectional "closing" switch. Switch closure is achieved by grid control. The tube is filled with low pressure hydrogen although deturium is occasionally used [1] and operation is on the left hand portion of the Paschen curve (see Appendix I). An electrical pulse applied to the grid will cause switch closure by the ionizing the fill gas. A hot cathode is used to emit electrons into the neutral plasma formed by the gas. Once the thyatron is "triggered," the control grid is quickly surrounded by an ion sheath and thus loses control over the discharge. Thus, recovery depends on a current zero, maintained for sufficient time to allow deionization of the conducting plasma.

The usual configurations and a list of electrode materials of hydrogen thyratrons are shown in Fig. II-1. In the single gap version, the control grid is placed in close proximity to the anode. The anode-control grid spacing is less than one mean free path at the tube operating pressure. This spacing prevents spurious "firing" of the switch but also limits the voltage standoff due to field emission. The cathode is located many mean free paths from the control grid, usually at a Paschen type minimum to reduce grid drive requirements. A baffle (at cathode potential) is placed between the control grid and the cathode. In addition, or instead, a baffle at grid potential may be



a. BASIC THYRATRON

b. ITERATIVE GRID THYRATRON

ANODE -	MOLYBDENUM, COPPER
GRID -	COPPER, MOLYBDENUM
CATHODE -	BaO, SrO, CaO COATING ON TUNGSTEN BARIUM ALUMINATE IMPREGNATED TUNGSTEN
GAS -	HYDROGEN OR DEUTERIUM AT APPROX. .5 Torr
RESERVOIR -	HYDRIDE MATERIAL, TITANIUM, TANTALUM, ETC.

Figure II-1. Basic Thyratron Configurations and Materials Summary.

placed over the grid apertures. These baffle geometries prevent a line-of-sight path between the anode and cathode. Baffles help prevent spurious triggering and the control grid may be maintained at zero volts without tube breakdown.

The multigap or iterative grid version of the hydrogen thyratron (Fig. II-1b) is employed to achieve high stand-off voltages. Additional grids (gradient grids) are employed to grade the voltage drop between the anode and cathode. The control grid-cathode geometry is essentially the same as in the single gap version.

Other versions of the thyratron are possible. An important version is the "double ended thyratron" [2,3,4]. Essentially, this thyratron is symmetrical in that it has a cathode at each end. Thus, this tube can operate as a bidirectional switch. This ability is important in applications where large voltage reversals are likely. Versions of the "double ended" thyratron are available with voltage capabilities above 100 kV (gradient grids are employed) and pulse currents in the 10 kA range.

The usual envelope material is either glass or a ceramic. The use of ceramics allows for compact designs as well as very high average power. A distinction is made between the operational characteristics of "glass" thyratrons and "ceramic" thyratrons. Under heavy pulse conditions, ion pumping occurs so that a pressure differential exists within the tube. In ceramic tubes, the gas density in the grid-anode region may

become too low for operation and the tube refuses to trigger [5]. Glass tubes are not prone to suffer from this problem because of their geometry. Glass thyratrons employ a bulb structure and the anode is completely surrounded by the grid structure. Holes in the grid structure allow gas to penetrate quickly into the grid-anode region thus equalizing pressure differences. Ceramic thyratrons are more compact and employ an in-line geometry so that the only access for gas to the grid anode region is through the grid aperture utilized for the discharge. Thus, the essential difference between the two tubes is one of geometry rather than materials.

Thyratrons operating in pulse modulators are typified by kiloampere pulses with delays of 20 to 30 ns, jitter of 1 to 5 ns and forward voltage drops of approximately one hundred volts. Among the commercially available tubes, one offers a standoff voltage of 260 kV and another has a peak repetitive current rating of 80 kA (see Fig. II-2). Typical rates of current rise are from  $10^4$  to  $10^5$  A/ $\mu$ s although  $5 \times 10^5$  A/ $\mu$ s has recently been achieved [6]. Some new tubes offer average currents to 50 A (Fig. II-3) and smaller versions are capable of pulse repetition rates to 100 kHz although a few hundred Hertz is more typical among the large, high power tubes. The technological factors defining thyatron limitations are reasonably well established. The major factors are discussed below.

## 2. Voltage Standoff

In single gap tubes (no iterative grids), the control grid-anode spacing is less than one mean free path. The obvious



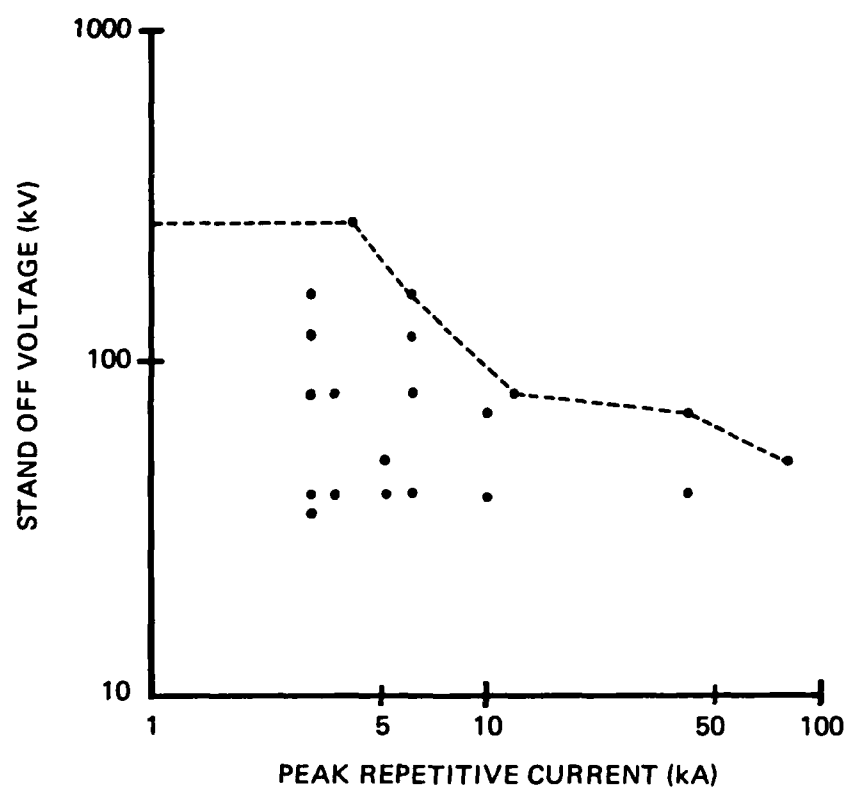


Figure II-2. Peak Standoff Voltage Versus Pulse Current for Large Commercial Thyratrons.

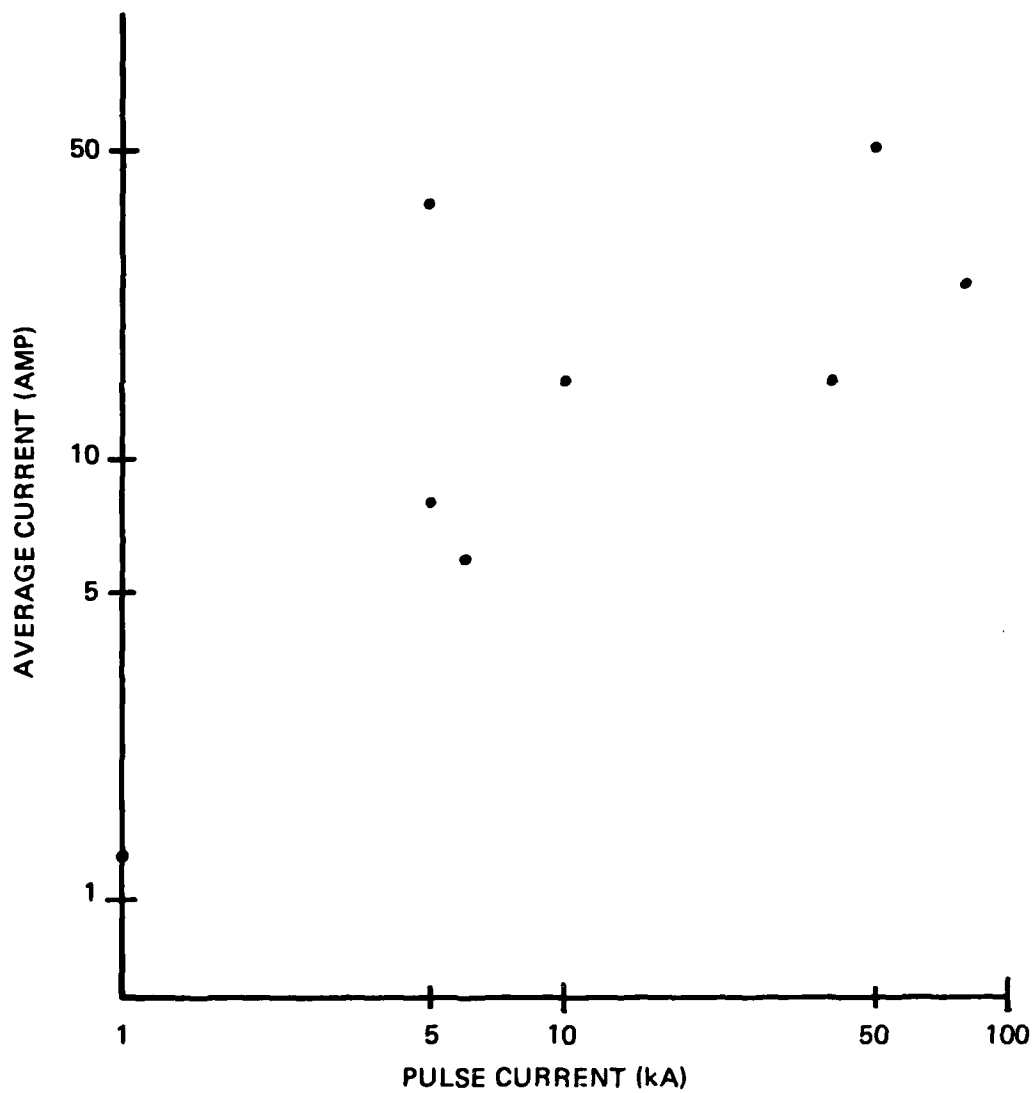


Figure II-3. Average Current Versus Peak Current for Commercially Available Thyratrons

limitation on standoff voltage is then due to field emission or vacuum breakdown between the grid and anode structures. Manufacturers typically precondition or "cure" thyratrons to 70 kV or more but typically rate single gap tubes at only 40 to 50 kV. Under repetitive pulse operation, other breakdown mechanisms may occur, thus limiting the standoff voltage. The primary mechanism for breakdown under high repetition rate conditions is thought to be due to charge accumulation on the tube walls (ceramic tubes). By careful design, the operating voltage may be considerably increased. An experimental, single gap thyatron has demonstrated good reliability operating at 100 kV [7]. Although this tube had a glass envelope, it serves to demonstrate that the ultimate voltage limitation of thyratrons is considerably above the ratings of present devices. Present packaging constraints, mass production techniques and user operational requirements combine to form the "practical" limitation of 40 to 50 kV per gap. These numbers are somewhat vague and operation beyond manufacturers ratings has been achieved on many occasions. (See for instance ref. 8). Suffice it to say that of the present commercially available thyratrons, reliable operation with long life can be expected, in general, if the standoff voltage is limited to 40 to 50 kV per gap. When iterative grid structures are used to obtain higher stand-off, the per-gap-voltage is reduced further. Typical gap voltages may be 30 to 40 kV in this case.

### 3. Pulse Current

The cathode is the primary limiting factor on the peak current capability of thyratrons. As indicated in Fig. II-1, thyratrons use an oxide coated or impregnated cathode. At operating temperature, the oxide coating is slowly evaporated. The rate of oxide evaporation is a strong function of temperature and under pulsing conditions, the oxide layer is further heated by the pulse current. Thus, the combined peak repetitive current, pulse width and repetition rate capability is a tradeoff with the life expectancy of the tube [9,10]. Figure II-4 gives an indication of the current-pulse width capabilities versus the specific resistance of the cathode coating. The RMS current rating of thyratrons is a guide in this regard. By appropriate manipulation of heater power under a specific set of operating conditions, cathode life can be considerably extended (see section on life expectancy).

If life expectancy is not a major concern but rather the peak current capability on a single shot or low repetition rate basis, the peak temperature of the cathode coating must be limited to prevent arc formation. Because of the resistivity of the oxide layer, the temperature of this layer rises rapidly during the pulse. At the hottest spot on the cathode considerable material is evaporated and a metal vapor arc may develop between the cathode and anode. Thus, on a single shot basis, the combination of peak current and pulse width limits thyatron capabilities [11]. The important current-pulse quantity is  $I^2 t$  but factors such as the specific heat of the oxide layer, emissivity,

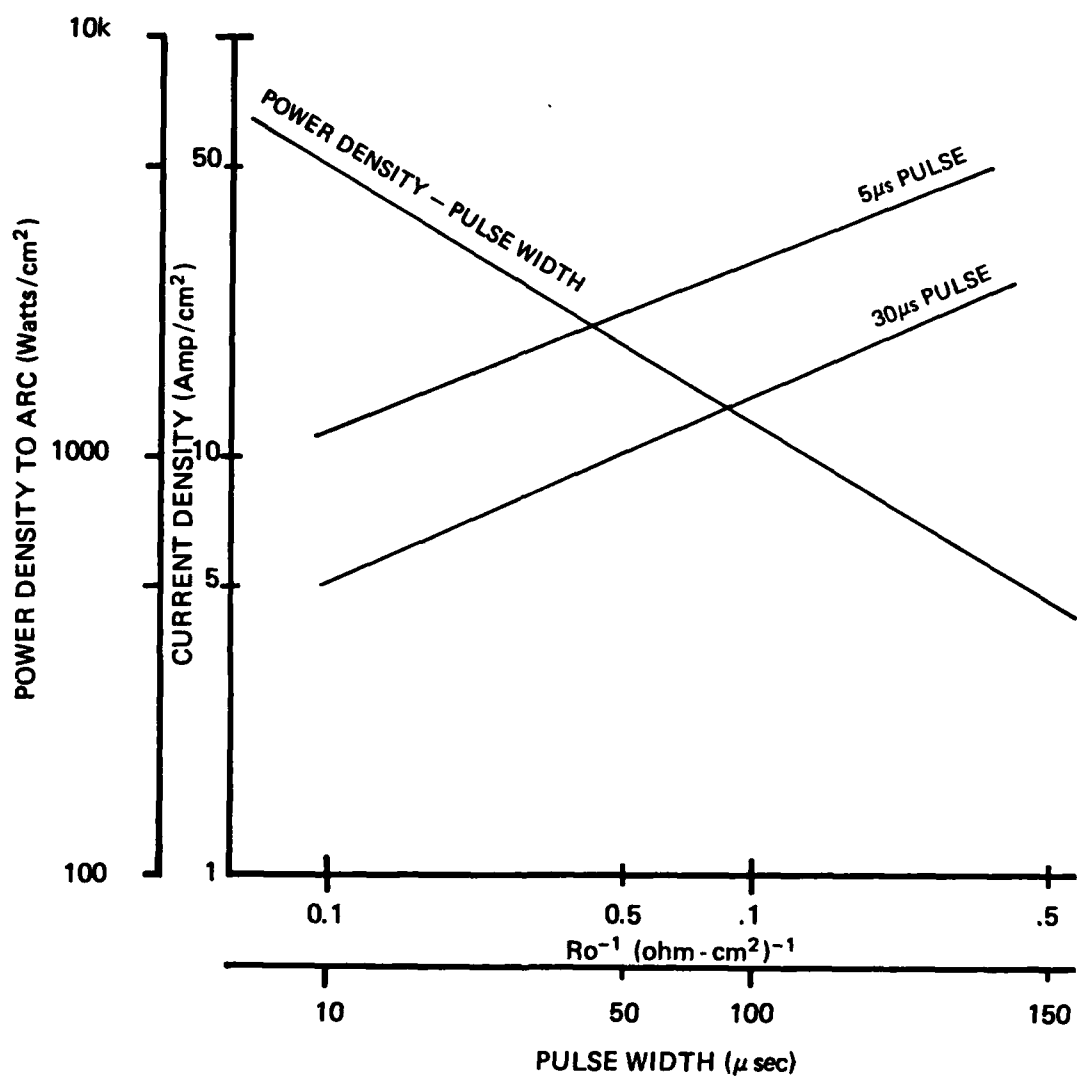


Figure II-4. Cathode Limitations as a Function of Power Density and Pulse Width, Current Density and Specific Resistance.

thermal conductivity and initial temperature are, of course, also important. Obviously an exact formulation would be extremely difficult and of doubtful use because of the difficulty in obtaining uniform emission from the cathode. For a particular tube, the power density versus pulse width which resulted in a metal vapor arc is shown in Fig. I-4 [11].

Typical cathode structures employ a vertical vane or similar structure to obtain a large surface for emission. It is difficult to expose these geometries to a uniform electric field and the emission from the cathode is, therefore, not uniform [9, 10]. This situation is further aggravated by temperature gradients within the cathode itself. One of the major problems in thyatron design is thus cathode utilization. That portion of the cathode that is hottest and nearest the anode will emit the most electrons and will in turn become hotter. Manufacturers have managed to work with this problem, and average current densities from a few amperes/cm<sup>2</sup> to 60-70 amperes/cm<sup>2</sup> and higher are obtained. An advance in the switching capabilities of thyatrons is possible if means can be found to obtain better cathode utilization.

Another factor affecting the peak current capabilities of thyatrons is the grid aperture area. Apparently, if this area is too small, the tube has a tendency to form plasma instabilities and an MHD type pinch may occur under high current, long pulse conditions. It has been found that this problem

does not occur if the aperture current density is limited to approximately  $10 \text{ kA/in}^2$ .

#### 4. Pulse Width

The essential factors affecting pulse width capabilities are covered in the pulse current section. Essentially, the magnitude of the pulse current, cathode temperature and the desired life expectancy combine to determine pulse width capabilities. High current for too long a pulse duration will result in a metal vapor arc [11] or, if an arc does not form, a reduced life will result [9]. In addition, very long pulse operation may require a greater grid aperture area than the general rule of thumb number,  $10 \text{ kA/in}^2$ . This number is used to design thyratrons intended for use in applications requiring pulse widths of a few tens of microseconds or less.

#### 5. Repetition Rate

There are two principal factors affecting the rep-rate capabilities of thyratrons, life expectancy and recovery time. The effect of peak current, pulse width, and pulse repetition rate on cathode life are discussed in the section on pulse current. Tube heating and cathode evaporation do not directly effect rep-rate capabilities except in terms of the long term capabilities of the tube.

Recovery time, however, is a fundamental limitation of pulse repetition rate capabilities of thyratrons. "The time between the end of the current pulse and that at which positive voltage may be reapplied to the anode without causing

breakdown is called the recovery time. It is strongly affected by negative bias on the grid. It is less affected by the peak discharge current, which determines plasmas densities at the onset of the deionization interval. ... The presence of inverse voltage has no effect on recovery time" [10]. These conclusions were derived by thyatron researchers in the mid fifties. It should be pointed out that the research was conducted on small tubes by today's standards.

These facts are borne out today by available manufacturer data for small tubes. However, large tubes present greater problems and little published data are available on recovery characteristics of large thyatrons.

The exact mechanism for deionization of the plasma is not well understood. Ambipolar diffusion theory seems to best account for the observed responses [10]. Uncertainties in the plasma conditions such as number density, temperature, etc. lead to ambiguities in the theory and, consequently, difficulties in engineering new tubes. From a qualitative point of view, the diffusion distances must be kept small and the confining walls should be cool. Clearly, the recovery aspects of thyatrons represents an area for research which may lead to higher performance tubes.

#### 6. Current Rate of Rise ( $di/dt$ )

Aside from the obvious circuit limitations, the  $di/dt$  capabilities of thyatrons are determined, in a large measure by the rate of plasma formation. The rate of plasma formation



depends on many complicated factors not well established at this time. Breakdown phenomena have been studied for many years and a clear model of the many processes has yet to be established. However, several factors are established, which assist in obtaining high  $di/dt$  operation. A large initial ion density is desirable in high  $di/dt$  operation. This can be achieved by employing a tetrode configuration and using low impedance grid drives. Also, higher  $di/dt$  can be obtained using a higher gas pressure [10]. Clearly, this latter condition is a tradeoff with voltage standoff capabilities.

Cathode utilization may also be a factor in the  $di/dt$  capability of thyratrons. Data derived in the mid-50's [10] may provide a clue to better understanding of the phenomenon. The essentials of this experiment are shown in Figs. II-5 and II-6. A voltage pulse was applied to the anode as shown and the current response measured in each of the three cathodes. The leading edge of the voltage pulse and the current response of the cathodes is shown in Fig. II-6. (For a more detailed description of the experiment, the reader is referred to the literature [10].) As expected, the cathode nearest the anode begins to emit first, followed by the others. Each current pulse is delayed by a time required for the anode field to penetrate through the forming plasma. Although there is a definite saturation characteristic to the current emitted by each cathode, this fact is more the nature of the experimental arrangement than the cathode emission limitations. However,

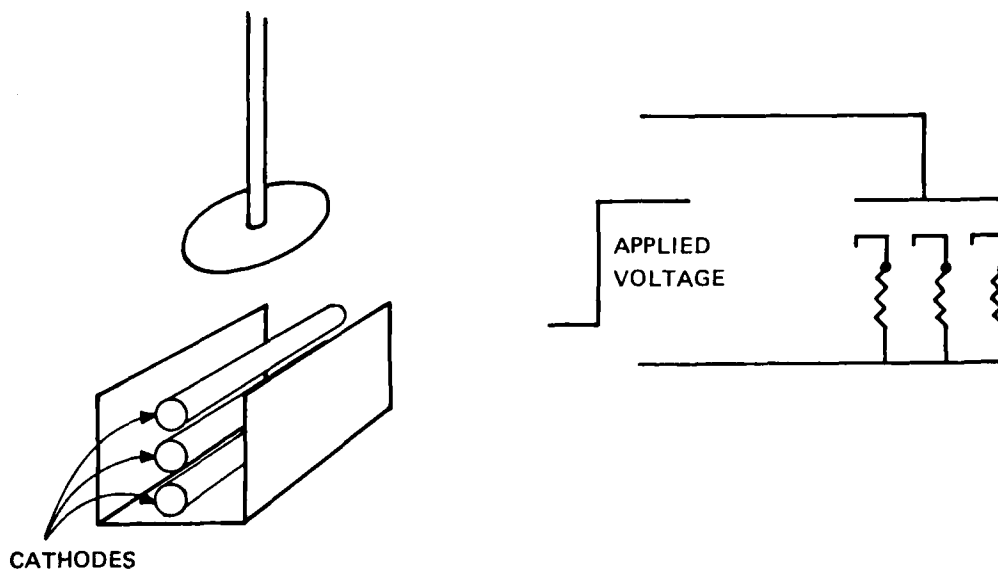


Figure II-5. Experimental Setup to Determine Cathode Utilization Effects [10].

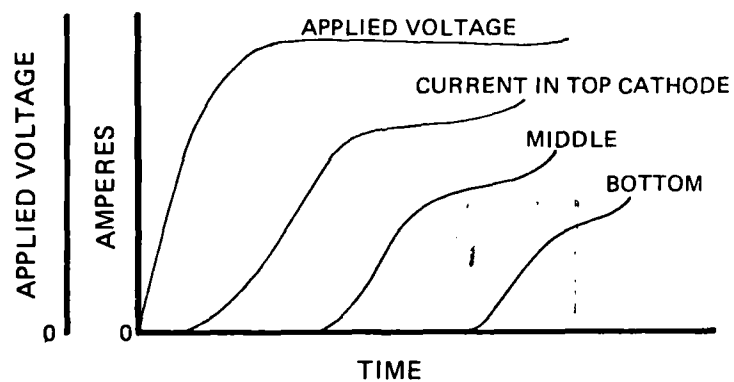


Figure II-6. Experimental Results [10].

it may be inferred that under a given set of circumstances, the peak current density emitted from the cathode is limited and that increased current comes from the discharge spreading to the other cathodes.

Cathodes are usually composed of vanes oriented normal to the plane of the grid-anode structure. When the tube is triggered, the discharge begins at the top of the vanes and penetrates between vanes until an equilibrium exists between the plasma and the emission characteristics of the cathode [10]. The rate at which the discharge spreads over the cathode surface together with the emission characteristics of the cathode clearly limit the rate of current rise.

The  $di/dt$  capabilities of most commercially available thyratrons is approximately  $10^5$  A/ $\mu$ s although  $5 \times 10^5$  A/ $\mu$ s has been reported recently [6]. It seems clear that if higher  $di/dt$  is to be obtained, a change in tube geometry is required. Possibly a cylindrical geometry might allow a greater cathode surface to be utilized in the initial breakdown process.

## 7. Delay

Because a plasma must form to constitute switch closure, a delay time is inherent in thyratrons. This delay is a strong function of the initial ion density, gas pressure, and the grid-cathode spacing. Also, to a degree, delay is dependent on the magnitude of the trigger voltage and the internal impedance of the grid drive circuit. Tetrode configurations can be used to increase the initial ion density

and closer grid-cathode spacing would allow for a shorter delay. However, grid-cathode spacings closer than that for a Paschen minimum would increase the grid drive power requirements. Delay times of 20 to 30 ns are typical among modern thyratrons.

#### 8. Jitter

The time variation between the trigger pulse and anode current rise is a function of the plasma formation time. At the time of the application of the trigger pulse, free charges (especially electrons) will be accelerated and collision processes will account for the initial portion of the overall breakdown process. Clearly, the greater the number of initial free charges, the greater the probability of switch closure at a specified time (delay). Thus, jitter can be considerably reduced by using the tetrode configuration. The extra electrode (sometimes referred to as the "keep alive electrode") will provide a large number of initial charges. For these devices, jitter can be limited to a few nanoseconds.

Jitter may be reduced further by using D.C. for the filament power. This fact bears out the importance of initial conditions on the breakdown process.

#### 9. Life

The predominant factor limiting thyatron life is the cathode. As indicated in Fig. II-1, various materials are used to coat or impregnate the cathode structure so that

high emission is obtained. At operating temperatures from 700°C to 900°C this material is slowly evaporated. Eventually, the cathode will have very low emission capabilities and the useful life of the tube is ended. The usual design life of thyratrons is 10,000 hours of continuous operation. However, under a given set of operating conditions, this number can be considerably changed.

Since the cathode coating has some characteristic resistance, the current pulse will cause a rise in cathode temperature. Because the rate of evaporation of the cathode coating is a strong function of temperature, appropriate reduction of filament power under operating conditions can dramatically increase the life expectancy of the cathode [9].

Other factors affecting thyatron life are usually associated with operation outside manufacturer specifications. Heavy pulse operation usually leads to excessive heating and thus high temperature in some portion of the tube. Failure may then occur because of electrode sputtering, etc.

#### 10. Other Factors

An increasingly important consideration in thyatron design is heat management considerations. Excessive dissipation in the various tube elements can lead to premature failure or malfunction. In order to switch high average powers, some tubes have been operated in the so called "Adiabatic Mode" [12]. In this mode of operation, the temperature of the tube elements is allowed to rise without the application of additional

cooling. The filament and reservoir power may, however, be modified to obtain satisfactory operation throughout the run. By operating thyratrons in this mode, much higher average powers can be switched for short periods of time

As tubes become larger, the details of dissipation become more important. The grids of high average power and high repetition rate thyratrons have become more massive and some designs use "metal-ceramic" envelopes. In these devices, the grid is attached to massive external cooling fins.

The forward voltage drop in thyratrons is approximately 100 volts and exhibits a rising characteristic during the pulse [11]. A portion of the loss is obviously in the cathode (see discussion on pulse current and life). The majority of the remainder of the loss must be conducted through the anode and grid structures. Some heat is lost through the walls but this loss is minor. Heating of the anode and grid occurs in very short times (microseconds) so that surface temperatures may become very high and sputtering may occur. This area of thyatron design bears further investigation because of the obvious effects on switching high average power at high repetition rates.

Another consideration important to thyatron design is the support structure to the cathode itself. This structure must conduct the current pulse as well as thermally isolate the cathode so as to reduce filament power. Good thermal isolation can lead to designs of high resistance and inductance resulting in reduced tube capabilities.

### 11. Summary

Hydrogen thyratrons have many advantages when all things are considered. No other switch is yet capable of switching the same average power (1 MW) at the same efficiency (>90%) on a continuous basis. High  $di/dt$  and pulse repetition rate capabilities along with reasonably long life make the thyatron invaluable in many applications since no other switch has its demonstrated capabilities. Even so, improvements in hydrogen thyratrons are continually being made.

A significant improvement could be made if a scheme can be found to utilize the capabilities of the cathode better. Such an improvement could lead to higher  $di/dt$  as well as peak current capabilities. An improvement in the emissivity of the cathode material would also help. It has been many years since a significant improvement has been made in cathode capabilities [13].

The capabilities of some switches has been greatly increased by the use of optical triggering techniques (laser triggered spark gaps and SCR's). A similar technique might be applied to a thyatron. This technique might eliminate the effects incurred by the necessity of propagating a plasma (delay and jitter) and greatly increase the  $di/dt$  capability and cathode utilization of thyratrons.

Higher voltage in single gap tubes has been achieved [7]. Present packaging techniques do not make use of this technology. Present designs emphasize small size and high average power more than voltage capabilities.

## 12. References

- [1] H. N. Price, "Deuterium Versus Hydrogen In Thyatron Modulator Switch Tubes," Proceedings of the Eighth Symposium on Hydrogen Thyratrons and Modulators, May 1964.
- [2] H. Menown and B. P. Newton, "A Multigap, Double-Ended, Hydrogen Thyatron," Conf. Record of 11th Modulator Symposium, Sept., 1973.
- [3] R. B. Molyneux-Berry, "Symmetrical Double-Ended Thyratrons in Pulse Modulators," Conf. Record of 12th Modulator Symposium, Feb., 1976.
- [4] H. Menown, R. J. Wheldon and N. S. Nicholls, "Double-Ended Hydrogen Thyratrons for Crowbar Protection of High Power TWT Systems," Thirteenth Pulse Power Modulator Symposium, June, 1978.
- [5] S. Schneider, J. Creedon and N. Yeamans, "Hydrogen Cleanup," Prod. of 8th Symp. on Hydrogen Thyratrons and Modulators, May, 1964.
- [6] S. Friedman, S. Goldberg, J. Hamilton, S. Merz, R. Plante, and D. Turnquist, "Multigigawatt Hydrogen Thyratrons with Nanosecond Rise Times," Paper presented at 13th Pulse Power Modulator Symposium, June, 1978.
- [7] L. Mancebo, "A High Power Hydrogen Thyatron Without Gradient Grids," Proc. 10th Modulator Symposium, May, 1968.
- [8] B. R. Gray, "Evaluation of State-of-the-Art Hydrogen Thyratrons at Extended Ratings," Conf. Record of 11th Modulator Symposium, Sept. 1973.
- [9] S. Goldbert, "Cathode Phenomena and Life in Hydrogen Thyratrons," Proc. 7th Symp. on Hydrogen Thyratrons and Modulators, May, 1962.
- [10] S. Goldberg, "Research Study on Hydrogen Thyratrons," Volume II, Research Report to Evans Signal Laboratory, Ft. Monmouth, N.J., 1956.
- [11] J. Creedon, S. Schneider and F. Cannata, "Cathode-Grid Phenomena in Hydrogen Thyratrons," Proc. 7th Symp. on Hydrogen Thyratrons and Modulators, May, 1962.
- [12] J. Creedon, J. McGrowan and A. Buffa, "Adiabatic Mode Operation of Thyratrons for Megawatt Average Power Applications," Conf. Recd. of 12th Modulator Symposium, Feb., 1976.



- [13] R. L. Remski, "1978 Tri-Service Cathode Workshop,"  
Microwave Journal, Vol. 21, No. 7, July, 1978.

## B. Ignitrons

### 1. Introduction

The ignitron employs a mercury pool as the cathode and is essentially an unidirectional closing switch. Often however, the ignitron is utilized in "ringing" discharges where it is required to conduct in the reverse direction. This kind of operation results in an "arc back" and is destructive to the internal components of the ignitron thereby severely limiting its useful life.

The usual configurations of ignitrons and the component materials used are indicated in Fig. II-7. The distinguishing feature of the ignitron is of course its use of mercury as a cathode which allows this device, in principle, to be capable of massive Coulomb transfer. The mercury vaporized during the discharge is condensed on the walls and returned again to the cathode pool. In pulse service, the single shot rating of this switch exceeds that of any other commercially available switch. It is characterized by reasonably high standoff voltages (20 kV to 50 kV) and by a very, low forward drop at kiloampere currents (typically from 20 to 30 volts). In addition, this device is "triggerable" for anode voltages down to approximately 100 volts. A plot of the standoff voltage and peak rated current of large, commercially available ignitrons is shown in Fig. II-8. It should be noted that these data are derived from manufacturer's specifications

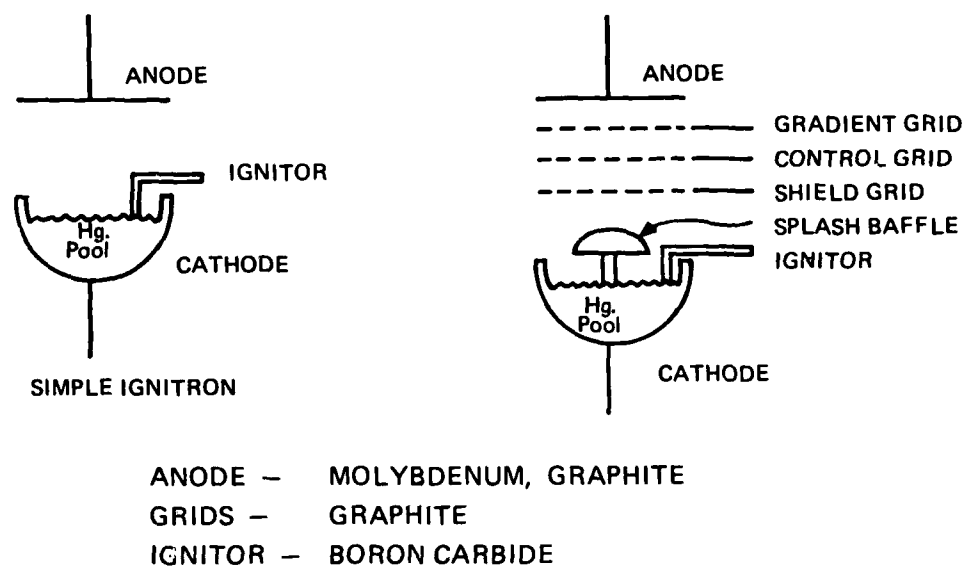


Figure II-7. Basic Ignitron Configurations and Materials Summary.

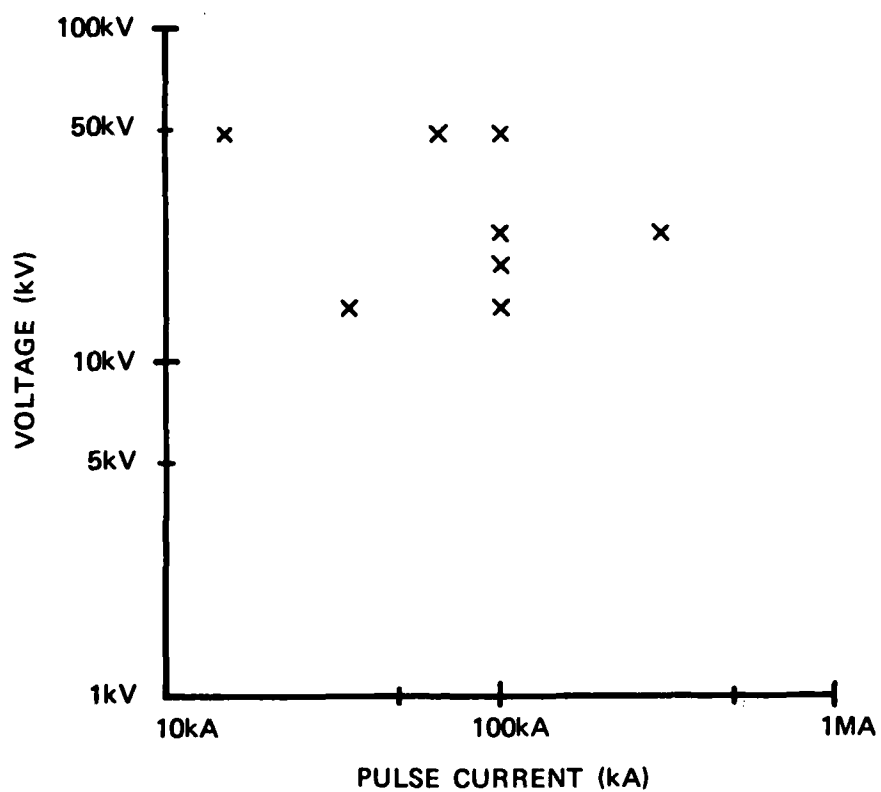


Figure II-8. Rated Switching Voltage and Current for Commercially Available Ignitrons.

for crowbar or ringing discharge service [1,2,3]. Only limited data are available for ignitrons operating in "square" pulse operation.

Figure II-9 is a plot of the rated average current versus the peak pulse current. Most devices are rated below 10 A average current. The usual pulse repetition rate is specified at two pulses per minute. Thus, most commercial, pulse type ignitrons are relatively low power and are not designed for rapid, continuous pulse operation.

The available literature for this study indicates that little or no development work has been done on ignitrons since the early 1960's. Essentially sixteen years have passed without any significant improvements in mercury pool devices. Work has been done on the liquid metal plasma valve (LMPV) which is a close relative to the ignitron. The LMPV is sufficiently different that it warrants a separate section and is covered elsewhere in this report. This investigation indicates that the present state-of-the-art of classical ignitrons does not indicate the true potential of this device (see Summary). It is clear to this investigator that much remains to be done on switches utilizing the mercury pool cathode.

Switch closure is achieved by electrically pulsing an "ignitor" electrode (see Fig. II-7). The ignitor electrode material is such that it is not "wetted" by the mercury and is mounted so that it penetrates into the mercury pool. Thus, the electrical resistance between the ignitor and the mercury

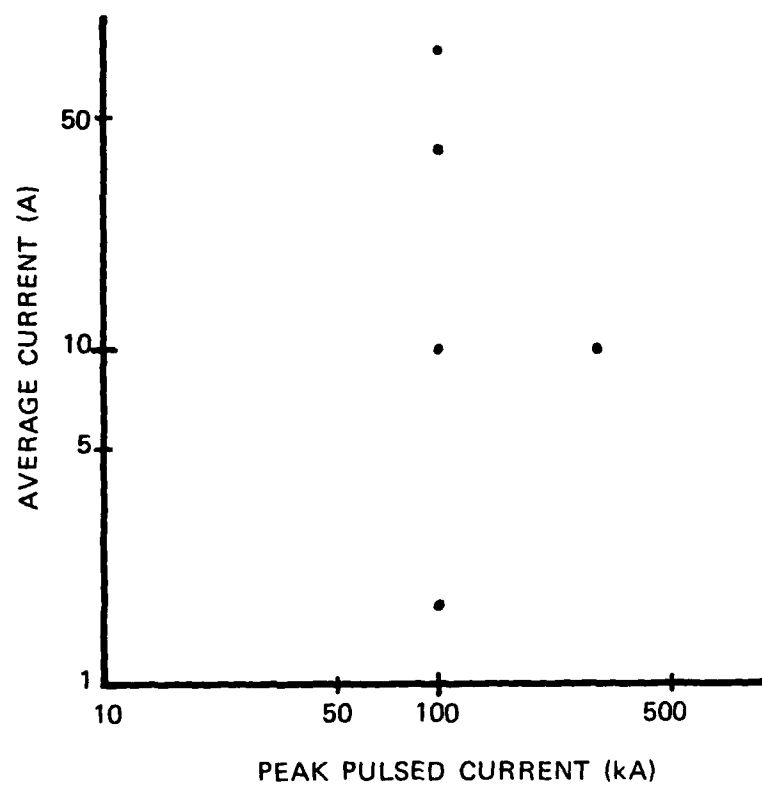


Figure II-9. Average Current Versus Peak Pulse Current for Crowbar Ignitrons.

is significant, typically from 20 to 100 ohms at room temperature. The vapor pressure of mercury is low (.0012 Torr at room temperature) so that prior to the trigger pulse, the tube pressure is very low. The trigger pulse is of sufficient power so that mercury is vaporized and a "cathode spot" develops at the junction of the ignitor and the mercury pool and, subsequently, an arc forms between the cathode spot and the top of the ignitor post [4,5]. A plasma then diffuses into the tube volume and a glow-to-arc transition takes place between the anode and the mercury pool cathode.

In order to achieve precision in closure time, a control grid may be added (see Fig. II-7). This electrode is placed less than one mean free path from the anode (or gradient grid) and held at zero (or negative) potential relative to the cathode. Thus, pulsing the ignitor electrode does not "fire" the tube, and closure is delayed until the control grid is pulsed positive. Closure then proceeds rapidly in a thyatron-like manner and the grid loses control over the discharge.

## 2. Standoff Voltage

Ideally, the voltage capabilities of ignitrons are determined only by the electrode separation (and geometry) and mercury vapor pressure (Paschen-like breakdown). For very low pressures, field emission or vacuum breakdown dominates. Because the vapor pressure of mercury approximately doubles for each 10 °K increase in temperature, it is necessary to control the temperature of the ignitron carefully to obtain

reliable voltage standoff. This is especially true for repetitive pulse operation where the average temperature is likely to rise because of internal losses.

There are several practical factors that limit the voltage capabilities of ignitrons. Mercury droplets that condense on the anode lead to low voltage breakdown by causing a glow to arc transition [6]. In addition, mercury may condense on the insulators leading to breakdown along the tube walls. To prevent these modes of premature breakdown, heat may be applied to the anode and anode seal regions to prevent mercury condensation [7, 17].

The splash baffle (Fig. II-7) is employed to help prevent mercury ejected from the cathode spot(s) (see pulse current section) from being sprayed directly onto the anode and insulation elements. Although the baffle may reduce one mode of voltage breakdown, it and the ignitor structure may cause another, namely, field emission induced breakdown due to electric field concentration at these structures.

Although gradient grids have been employed in pulse tubes, they do not appear to be particularly successful in increasing voltage standoff capabilities, but the recovery time may be reduced [8].

Reliable standoff voltages of 75 - 80 kV have been obtained and 100 kV for short periods of time in developmental designs [9]. This was achieved by careful design and by heating the anode to prevent mercury condensation. This



result clearly indicates that ignitrons are capable of considerably greater standoff voltage than those currently available.

### 3. Pulse Current

For low repetition rates in applications where the ignitron is not expected to standoff voltage soon after the pulse, there appears to be no obvious limitation to the peak current capability of the mercury cathode. However, under heavy current operation, considerable mercury may be dispersed throughout the tube volume so that recovery and voltage standoff are reduced. The ultimate current limitations are probably determined by plasma instabilities. Certain irregularities (plasma instabilities) may be explained by gas starvation in the arc [4, 10]. Also, some irregularities are eliminated by using an axial magnetic field [11]. In any event, the ultimate capabilities of the mercury cathode do not appear to have been reached.

For pulse repetition rates of a few per second and higher, the peak current must be reduced. Because the mercury vapor pressure will roughly double for each 10 °K temperature rise, a compromise must be established between pulse current, pulse width, standoff voltage, pulse repetition rate and the ambient environment. The ignitron is very sensitive to temperature and, for reliable repetitive operation, the case temperature should be closely controlled [12]. If this is done, reliable operation can be obtained.

#### 4. Pulse Width

The pulse width under high current conditions is limited by the tendency of the cathode spot(s) to migrate to the confining wall of the mercury pool. The velocity of the spread of the cathode spots has been measured at up to  $2 \times 10^6$  cm/sec [4]. Thus, for most tubes, the arc may reach the confining wall within a few tens of microseconds. In the case of metal envelope tubes, this action results in erosion of the envelope material, outgassing, etc. so that tube performance suffers and failure will eventually occur. The application of only a modest axial magnetic field results in stabilization of the cathode arc and prevents its movements to the wall(s). Thus, the pulse width capabilities are considerably increased.

Other methods of eliminating the limitation imposed by arc migration have been used or attempted. Insulated mercury pools, envelopes of ceramic [13] and composite materials have been utilized. Also, refractory metals have been employed to minimize the effects of the cathode spot running at the container-mercury interface. The only commercially available variation utilizes the composite envelope. Otherwise, coaxial mounting is recommended.

The ultimate limitation on pulse width is, of course, formed by the combination of pulse current and tube drop, i.e., the tube loss. The mercury pressure will continue to increase during the pulse until recovery is impaired and the pulse repetition rate must be reduced.

### 5. Current Rise ( $di/dt$ )

The  $di/dt$  capabilities of ignitrons are not well defined. Clearly, the  $di/dt$  capability is determined by the plasma formation time and its density. Ambient mercury vapor pressure is then a determining factor. "The rate of ionization, indicated by the rate of collapse of the anode-cathode voltage, increases as the anode-cathode spacing is reduced" [11]. Thus, it appears that the  $di/dt$  capabilities and standoff voltage form a trade-off in ignitrons. In addition, the cathode spot formation time may be a limiting factor. The effects of  $di/dt$  and magnetic fields on cathode spot formation time have been studied [11]. This study shows that as  $di/dt$  is increased, the spot velocity increases. Under the action of a transverse electric field and high current operation, the cathode spot takes the form of a line [4]. Also, the spot movement is opposite to the direction predicted by Ampere's Law.

There seems to be a limitation in the current density that any particular cathode spot may emit and the discharge remain stable (approximately  $5 \times 10^6$  A/cm<sup>2</sup>). Thus, "when the current was increased rapidly, the spots expanded as a circular line of almost continuous emitting sites with a velocity up to  $10^4$  cm/sec. At values of  $di/dt$  greater than  $10^7$  amp/sec, new spots formed ahead of the old. At  $10^9$  amp/sec, this "leap-frogging" was pronounced. The front velocity approached  $10^5$  cm/sec although the spot velocity remained approximately  $10^4$

cm/sec" [4]\*. The mechanism for this phenomenon is not well understood. It seems clear, however, that the formation of the discharge on the cathode does require some finite time and thus forms an ultimate limitation on the  $di/dt$  capabilities of the mercury cathode. A  $di/dt$  of  $3 \times 10^6$  A/s was achieved in this study although the peak current for this condition was not mentioned.

#### 6. Pulse Repetition Rate

Deionization time (recovery time) and tube dissipation are the principal factors affecting the pulse repetition capabilities of ignitrons. The recovery time is a function of the peak current conducted, tube temperature, the physical dimensions, etc. as well as how the tube is operated. By experiment it has been determined that "...the deionization time (1) increases with increasing grid resistance, (2) decreases with increasing bias voltage, (3) increases with increasing pulse repetition frequency, (4) increases with increasing cooling water temperature and (5) increases with increasing pulse current"[12]. In addition, a small reverse voltage is helpful in obtaining the fast recovery. It should be noted that these results were obtained on gridded ignitrons operating up to 800 pps. A diffusion process of some kind (probably ambipolar) best describes the deionization mechanism.

\*This quote is a summary of work done by Froome. His paper's were not available at the time of this writing.

For crowbar operation, the limitation on repetition rate is primarily thermal. Manufacturers typically warrant tubes to only a few pulses per minute. Thus, recovery time is not so important and little work has been done on recovery of ignitrons after conducting crowbar type currents (100's kA in a ringing discharge). The recovery process is undoubtedly complicated by the presence of metal vapor generated during reverse conduction and the likelihood of other gases being released by the hot tube elements.

#### 7. Delay

The time delay between trigger and switch closure is of course determined by the plasma formation time. For simple ignitrons, delays as low as 50 nsec have been measured [7]. This study showed that the delay was not a strong function of anode voltage and that some tubes made by different manufacturers, but otherwise similar, have significantly different responses. These tubes were intended for use in 10 kV, 30 kA capacitors discharge service.

Control grids have been employed to control the delay and jitter in ignitrons better [12, 13].

#### 8. Jitter

Variations in closure time or delay are primarily caused by the ionization level in the tube prior to the trigger pulse. At very low mercury pressure, the jitter can be expected to be considerably larger than at high pressure.

For the simple tube geometry, average jitter as low as 12 ns has been measured although a value of 50 ns would appear to be more typical [7]. The use of a control grid helps maintain the jitter at approximately 10 ns [13].

## 9. Life

The useful life of ignitrons is a very strong function of its application. In ringing or crowbar discharges, the life is usually limited to a few thousand operations. In the few cases where data were obtained for square pulses, short duty cycle operation, many hundreds of hours of operation were obtained without failure (see Appendix II). However, the peak current for these tests was much reduced over that typically incurred in crowbar service (10's to 100's kA in a damped sinusoid). Also, it should be noted that in phase controlled applications, ignitrons have functioned for many years without failure.

The predominate failure mode is the loss of the ability to trigger the tube due to wetting of the ignitor by the mercury. This phenomenon is associated with metallic sputtering by the arc running on the tube wall-mercury pool interface or in an arc-back condition associated with a ringing discharge. The sputtered metals may contaminate the mercury, and the ignitor becomes "wetted." The electrical resistance between the ignitor and the mercury pool may drop below one ohm (normally 20 to 100 ohms) and the tube thus fails to fire.

Another means of ignitor failure results from the trigger circuit characteristics. Specifically, if the trigger current reverses (normally the ignitor is driven positive with respect to the mercury cathode) the ignitor surface is affected in some manner (primarily by erosion) so that it eventually becomes "wetted" by the mercury as described before.

The life of an ignitron is strongly affected by the operating stress in capacitor discharge applications. One manufacturer states, "a rule-of-thumb guide is that these tubes will provide in the order of 1000 shots when maximum ratings are applied simultaneously. Reduction of one key parameter, current, energy transfer, or voltage by 50% will increase life by a factor of ten" [14].

The life capabilities of ignitrons under repetitive, square pulse operation is not well established. Information on testing performed under this condition is limited. However, the data available indicate that ignitrons should have a very long life expectancy under low duty cycle, square pulse operation if care is taken to prevent excessive voltage reversals, etc. For instance, an ignitron has performed satisfactorily for 600 hours at 35 kV, 8 kA, 3  $\mu$ s in a line modulator operating at 60 pps [12] and another ran for 350 hours at 35 kV, 1.1 kA, 2.45  $\mu$ s operating at 360 pps [19].

#### 10. Other Factors

The performance of ignitrons is subject to several other factors. Obviously, the tube is sensitive to orientation

because of the mercury pool. In addition, acoustic waves on the surface of the mercury are likely to affect the delay and jitter of the switch. The surface waves may be induced by mechanical vibrations of the tube mounting or possibly by the discharge itself so that anomalous behavior may occur as the pulse repetition rate is varied.

Under pulse repetition rates above a few per second, the case temperature control becomes critical. The advantage of low standby power is apparently lost. Short bursts at high power can still be obtained. For instance, pulse operation at 20 kV, 2 kA, 20  $\mu$ s at 250 pps has been obtained for bursts of several seconds [15]. However, for continuous operation, the case temperature must be controlled to fairly close tolerances [8, 12]. This control is necessary to maintain the proper mercury vapor pressure as determined by the particular set of operating conditions required.

#### 11. Summary

The potential of the mercury pool cathode has not been fully realized [18]. The apparent capability of conducting massive amounts of Coulombs without damage has resulted in many attempts to develop "super-switches." For example, the objective of one development program was a switch capable of conducting 30 MA with a rise time of 2 1/2  $\mu$ s [7]. A 19-inch diameter, low profile ignitron was constructed and partially tested. This tube subsequently conducted a current



of 22 kA. Delay and jitter were measured at .25  $\mu$ s and 4 ns respectively. A switch inductance of 17 nh was also measured. Unfortunately, some practical difficulties were encountered and apparently no further work was done. Another switch, combining some of the characteristics of a thyratron and a mercury pool cathode, is described elsewhere in this report.

The ignitron seems to be best suited for pulse applications at low repetition rates. Although relative high rep-rates are possible (~1 kpps) the operational sensitivities of the ignitron exceed those of thyratrons. The cost savings possible may warrant further investigation of high rep-rate ignitrons but a truly high power, high rep-rate ignitron is not likely because of the characteristics of the mercury vapor and the practical difficulties associated with the control of the tube pressure.

As a matter of conjecture, it should be possible to build an ignitron capable of switching voltages on the order of 100 kV, 100's of kA at several pulses per second. Reasonable delay and low jitter have been demonstrated as well as peak current. The way to high voltage and high power may have been demonstrated by the use of a ceramic envelope [16]. A gradient grid version of this tube switched 60 kA at 50 kV several times but eventually failed due to wall tracking. The investigator suggests that a metal shield would prevent this problem but no further work was done.

The ceramic tube had another interesting feature. The usual ignitor was eliminated and the tube was dielectrically triggered by a trigger electrode surrounding the mercury pool. This scheme worked but no further information on trigger characteristics is available. A scheme of this sort eliminates the prominent ignitor structure (important for high voltage) and eliminates the failure mode most characteristic of present ignitrons, wetting of the ignitor.

12. References

- [1] National Electronics data sheets, "Ignitrons, Application Notes," G.E. Co., Nov. 74.
- [2] "Professional Electron Tubes," Abridged Data, G.E.C. Electronic Tube Company Limited, 1976/77.
- [3] "Ignitrons, Capacitor Discharge and Crowbar Service," G-E Tube Products Department, PT 57A.
- [4] D. Cummings, "Ignitron Discharge Growth During High Current Pulses," IEEE Transactions on Communication and Electronics, 68, 514, 1963.
- [5] Y. Gosho, "Ignitron Phenomena of Discharge Tube with Ignitor," Scientific Papers of the Institute of Physical and Chemical Research, Vol. 58, No. 2, June, 64.
- [6] Michael A. Lutz, "The Glow to Arc Transition - A Critical Review," IEEE Transactions on Plasma Science, March 1974.
- [7] D. Cummings, "Development of Switching Tubes for Controlled Fusion Research," Electrical Engineering, 79, 1960.
- [8] J. Romanelli, "Pulse Characteristics of a GL-5630 Ignitron," Proceedings of the Eighth Symposium on Hydrogen Thyratrons and Modulators, May 64.
- [9] A. Booth, J. Holliday, "High-Voltage Mercury-Arc Switch for Heavy Current Pulse Duty," Proceedings of IEE, Vol. 110, Nov. 63.
- [10] H. C. Steiner and R. W. Strecker, "Voltage Transients Due to Arc Extinction," AIEE Transactions, pt. I (Communications and Electronics), Vol. 79, May 1960.
- [11] H. Knight, L. Herbert and R. Maddison, "The Ignitron as a Switch In High-Voltage Heavy-Current Pulsing Circuits," IEE, April 59.
- [12] T. F. Turner and H. S. Butler, "Performance of Ignitrons in Pulse Service," Proceedings of Seventh Symposium on Hydrogen Thyratrons and Modulators.
- [13] "Ignitron Excitation Circuits and Their Requirements," G-E Power Tube Department Publication PT-50, Dec. 60.
- [14] "Ignitrons, Application Notes on Capacitor Discharge and Crowbar Service," G. E. Tube Products Department, Publication M-1256, November 1974.

- [15] Personal communication, J. O'Loughlin, AFWL, Albuquerque, N.M.
- [16] G. Reiling, "Development of a Metal Anode Ignitron Switch Tube," AIEE Transactions on Applications and Industry, Part 3, Vol. 80, Jan. 1962.
- [17] G. Boicourt and E. Kemp, "Development of Reliable 20 kV, Size A Ignitrons for Thermonuclear Research," Los Alamos Scientific Laboratory Report - LAMS-2416: Dec. 59.
- [18] E. A. Baum and H. E. Zuvers, "Utilization of the Mercury Pool Cathode for Industrial and Military Tubes," Proceedings of Fifth Symposium on Hydrogen Thyratrons and Modulators, May 58.
- [19] Fred Vorwerk, "Evaluation of the Z-5233 Ignitron," Technical Report ECOM-2512.

### C. A Thyatron-Ignitron Hybrid Switch

#### 1. Description

An interesting switch concept is formed by the combination of the thyatron and the mercury pool ignitron. A device has been constructed and tested to illustrate this concept [1].

Basically the device is similar in design to thyatrons and is filled with a low pressure gas, but this device has a mercury pool for a cathode rather than the standard hot cathode typical of thyatrons. Thus, the switch is a "closing" switch and triggering is achieved with a control grid.

Several gases were tried in this device. However, hydrogen (or deuterium) is the primary one because the gas pressure could be controlled with a standard reservoir. A baffle helped prevent mercury vapor jets from contaminating the grid structure. Also, anode heating similar to that used in ignitron operation was employed to help prevent breakdown around the anode seal and to help prevent Hg condensation on the anode structure. Cathode cooling was also employed. In fact, satisfactory operation was obtained with a frozen cathode.

The major difficulty described is the tendency of the tube under high current, long pulse operation to form a cathode-to-grid arc and a grid-to-anode arc resulting in grid erosion. It is likely that the grid aperture was insufficient to prevent this type of failure (see section on hydrogen thyatrons).

The voltage standoff capabilities of this device are not clearly stated although 40 kV is mentioned with 5 mm grid-anode spacing and .4 torr deuterium or .3 torr hydrogen pressure. As in standard thyratrons, the grid-anode spacing and gas pressure determine the hold-off capability.

In operation in a half sine wave discharge, this tube has conducted a peak current of 50 kA with a pulse duration of about 1 msec. It is mentioned that this device has a higher  $di/dt$  capability than other mercury pool devices but no numbers are stated. The delay time is a function of the trigger voltage and a mean value of 80 ns is stated for a  $H_2$  pressure of .26 torr. No information is stated in regard to jitter. The repetition rate capability of the device was apparently not tested. Thus, the recovery time was not investigated.

The true potential of this device has not been established. Its apparent advantages would be high peak current capabilities typical of mercury devices and a high  $di/dt$  capability, low jitter and delay typical of hydrogen thyratrons, especially if a "keep alive" electrode were employed. No ignitor is employed so some reduction of failure modes is possible compared to ignitrons. It is not likely that this device will perform well at high repetition rates because of the long recovery time associated with the mercury vapor.

## 2. References

- [1] B. O. Baker and K. G. Cook, "A High Power Gas Discharge Switch," Proceedings of the Seventh Symposium on Hydrogen Thyratrons and Modulators, May 1962.

#### D. Liquid Metal Plasma Valve

##### 1. Introduction

The Liquid Metal Plasma Valve (LMPV) is very much like the ignitron. It is essentially a unidirectional closing switch and uses a mercury cathode with an ignitor to establish switch closure. The primary feature of the LMPV that distinguishes it from the classical ignitron is the structure and operation of its mercury cathode [1]. The usual temperature of operation is room temperature or lower so that the mercury vapor pressure is low ( $\leq 3 \times 10^{-3}$  Torr) and the LMPV thus qualifies as a vacuum switch.

The structural features of the LMPV are shown in Fig. II-10. Instead of a mercury pool, the LMPV uses a cathode structure of annular cross section. Mercury is fed into the channel shown in Fig. II-10. The mercury wets the cathode structure material, molybdenum, and the combination of the cathode shape and the mercury wetted surface leads to the unique operation of the LMPV.

During conduction, considerable mercury is evaporated from a pool cathode, much more than is required to sustain the arc. In the LMPV, much less mercury is evaporated and the vapor pressure in the tube is much lower after conduction than would be the case in a conventional ignitron [1,2]. Thus, the recovery time is reduced over what might normally be expected in a mercury pool device. (Apparently, the LMPV was

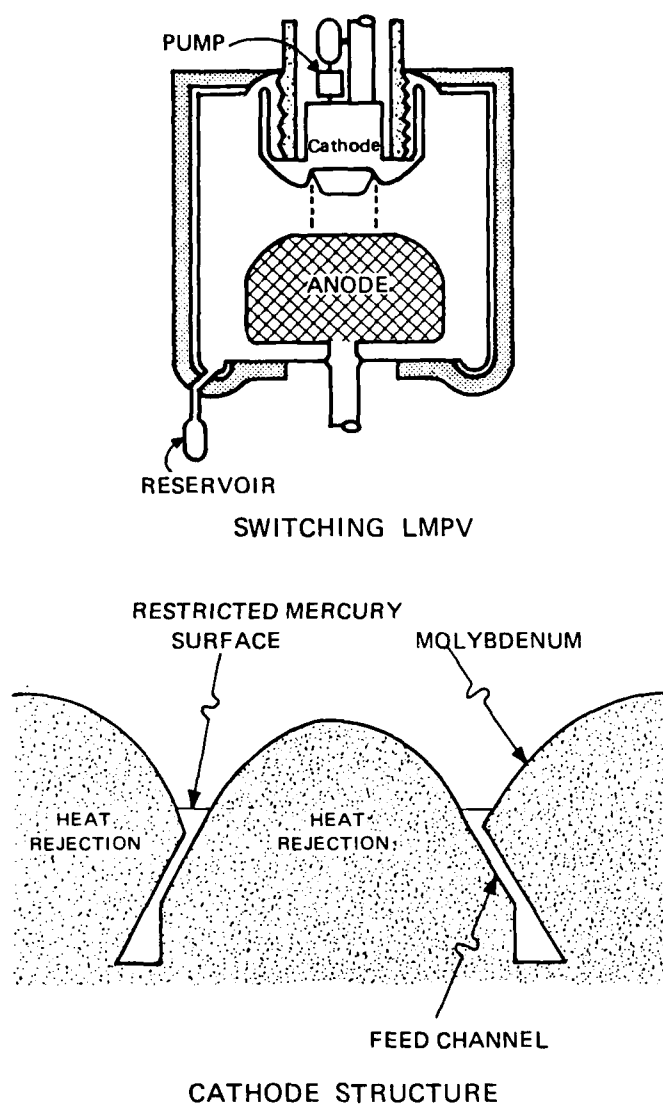


Figure II-10. Structural Features of the Liquid Metal Plasma Valve



originally intended for applications requiring fast recovery at low repetition rates.)

The small free surface of the mercury and its intimate contact with the molybdenum structure results in rapid heat transferal from the arc spots. Thus, the mercury temperature in the vicinity of an arc spot is lower than for a pool cathode. Clearly, the combination of a small mercury surface and rapid heat removal by the cathode structure results in reduced mercury evaporation. In addition, the shape of the cathode more or less directs the vapor jets from the arc spot toward the anode. Thus, the design of the LMPV cathode results in a high electron to atom ejection ratio during the discharge.

A major feature of the LMPV cathode is its greatly increased ability to anchor the cathode spots so that the probability of spot migration to the tube walls is much reduced. Also, because of the surface tension of the mercury and the small dimensions of the feed channel, the cathode is insensitive to orientation. The mercury sump is, of course, sensitive to orientation, but the flexibility of design is greatly increased over conventional ignitrons.

The LMPV has operated successfully as an "opening" switch. In this mode, the arc is "forced commutated" by external circuits so that a current zero is established within the tube. LMPVs have interrupted 40 kA to 30 kV on a single shot basis and 21 kA to 20 kV at .003Hz [2]. These tubes were employed in inductive energy storage systems.

As a closing switch in a PFN application, a LMPV has achieved the performance parameters indicated in Table I [5]. The particular tube failed during the test so that no real life data were obtained. The failure was due to a crack in the anode, apparently due to excessive heat dissipation.

The LMPV is a relatively new device and does not have an extensive history of operation. The factors that affect its performance as a switch are discussed below.

## 2. Voltage Standoff

Because of the low operating pressure, the LMPV is essentially a vacuum device and the voltage limitation is determined by field emission or vacuum breakdown. Thus, the electrode materials and surface conditions determine the voltage capabilities of the LMPV [1]. One LMPV has been impulse tested to 450 kV and operated dynamically to over 270 kV [2]. Clearly the LMPV can be made to operate at very high voltages.

## 3. Pulse Current

The peak current capability of the LMPV would seem to be similar to that of the ignitron. However, "For the proper functioning of the LMPV at all current levels, it is necessary that the (cathode) spots remain anchored" [1]. Thus, the current limitations are based on the character of the cathode spots and the ability of the cathode design to maintain the stability of the discharge. The intimate contact of the mercury

Table I (Reference 5)

		<u>Navy I</u>	<u>Navy II</u>	<u>Air Force</u>
Peak Voltage	kV	100	150 <sup>1</sup>	53
Peak Current	kA	8.0	2.9 <sup>2</sup>	3.8 <sup>4</sup>
Average Current	A	4.5 <sup>1</sup>	4.5 <sup>1</sup>	7.5 <sup>5</sup>
Pulse Length	$\mu$ s	50	50	20
Repetition Rate	pps	13 <sup>1</sup>	36 <sup>1</sup>	100 <sup>6</sup>
Average Power	MW	.26 <sup>1</sup>	.38 <sup>1</sup>	.2 <sup>7</sup>
Run Time	Min	1	.25 <sup>3</sup>	1
Recharge Time <sup>8</sup>	ms	11	44	4

## Notes:

1. Power supply limitation
2. PFN breakdown limitation
3. Charging resistor overheating
4. Using 7 ohm PFN; LMPV failed before getting to 3.5 ohm test
5. LMPV misfiring at higher repetition rate
6. Ran at 250 pps, but at 15 kV
7. LMPV limitation
8. To 90% of anode voltage

with the molybdenum structure and the small free surface combine to help anchor the cathode spots. Considerably higher current densities have been obtained from anchored cathode spots in the LMPV (700 to 750 A/cm<sup>2</sup>) than in mercury pool devices (40 to 50 A/cm<sup>2</sup>) [1]. However, the largest peak current quoted is 40 kA [1] and the available literature does not discuss the design factors and tradeoffs required to maintain stability of the cathode spots at high peak currents.

#### 4. Pulse Width

The factors affecting the duration of conduction in the LMPV are not clear, except of course, for the obvious temperature limitations due to conduction losses. The relationship between the ability of the LMPV cathode to anchor the cathode spots and the pulse time are not discussed in the available literature. However, the pulse width capabilities at low pulse repetition rates is considerable. One LMPV, operating as an "opening" switch in an inductive energy storage application, has conducted a peak current of 21 kA with a conduction time of 1 sec. [3].

#### 5. Repetition Rate

The rep-rate capability of the LMPV is determined essentially by recovery time and heat generated due to losses (see di/dt section). The recovery time is a function of the plasma density, temperature and tube geometry. Because the LMPV is

essentially a vacuum device, recovery is relatively rapid. In "opening" switch operation, a LMPV has withstood a re-application of voltage at the rate of 3 kV/ $\mu$ s after a current zero [4]. Another LMPV has operated up to 250 pps [5].

#### 6. Current Rate of Rise ( $di/dt$ )

The  $di/dt$  capability of the LMPV is limited by the plasma formation time. The vapor required for plasma formation must come from the cathode. The initial vapor is generated by the ignitor pulse. The ionization of this vapor, the formation of cathode spots and the subsequent increase in vapor pressure combine to form the  $di/dt$  limitations of the LMPV. Tests on the LMPV indicate that the initial turn-on is a time consuming process. In these tests [5] the fall in anode voltage (roughly corresponding to the rise in anode current) was variously measured at 3 to 5  $\mu$ s although an anode fall of .5  $\mu$ sec. is quoted elsewhere [6]. This long anode fall time leads to considerable anode heating. (The test LMPV failed due to a crack in the anode.) Increasing the ignitor power decreased the fall time somewhat but the fall time was still long compared to that of usual "closing" switches.

#### 7. Delay

The time lapse between the beginning of the ignitor pulse and the rise in anode current in the LMPV is characteristic of vacuum devices. Since the vapor necessary to establish an arc must propagate from the cathode to the anode and a plasma must then form, a long delay can be expected.

#### 8. Jitter

The statistical nature of the turn-on mechanism of the LMPV is evident from the previous discussion. The establishment of the initial vapor density and ionization (ignitor pulse) and the establishment of the arc itself lead to a considerable randomness in the beginning of conduction in the LMPV. Tests have measured jitter at approximately 4  $\mu$ s [3].

#### 9. Life

The failure mechanisms of the LMPV are not well established and no extensive life data exist. It should be kept in mind that the LMPV is a relatively new device and failures can be expected in developmental models.

Available life data indicate that the LMPV operating as an "opening" switch has performed 4,000 operations interrupting about 15 kA against about 10 kV [4]. As a converter operating at power frequency, the LMPV apparently has obtained more than  $10^8$  closures without failure. Operation as a "closing" switch in short pulse operation has been disappointing.

#### 10. Other

The temperature of the LMPV is closely controlled in order to establish the proper ambient pressure in the tube. Thus, a cooling system is required as auxiliary equipment. In addition, a pump is required to maintain the mercury level in the cathode aperture.

## 11. Summary

The LMPV has demonstrated a high voltage capability. This ability is achieved by using very low tube pressure so that the character of the LMPV is similar to vacuum devices. Relatively long delay and jitter can be expected but the recovery time will be correspondingly short.

Many of the objectional features of the LMPV, long delay, jitter and anode fall time can be improved by increasing the tube pressure. Of course, this results in lower standoff voltage and longer recovery time. However, increased pressure might allow expanded use of the LMPV in short pulse service.

The unique design of the cathode in the LMPV allows conduction of long pulses without migration of the cathode spots. This design possibly points the direction toward fuller exploitation of the mercury cathode.

## 12. References

- [1] W. Eckhardt and G. Hofmann, "A 10-kA, 30-kV Liquid-Metal Plasma Valve Switch for Inductive Energy Storage," Proc. 6th Symp. on Engineering Problems of Fusion Research, IEEE Pub. No. 75 CH 1097-5-NPS, 656, 1975.
- [2] W. Eckhardt and G. Hofmann, "Ohmic Heating DC Circuit Breakers with Liquid-Metal Plasma Valves," Proc. 9th Symp. on Fusion Technology; Pergamon Press, 1976.
- [3] Personal Communication with A. F. Dickerson, Hughes Research Laboratories, Malibu, Calif.
- [4] W. Eckhardt, G. Hofmann, E. Bernhardt, R. Kunze and D. Dorst, "LMPV Circuit Breakers: Operation of a 15-kA Unit with Wendelstein VII A, and Laboratory Tests of the Next Breaker Generation," Proc. 7th Symp. on Engineering Problems of Fusion Research, Oct. 1977.
- [5] W. Wright, J. Creedon and J. Bayless, ERAD COM Test Report, ERAD COM, Jan. 1978.
- [6] J. R. Bayless and J. P. Heckl, "The Liquid Metal Plasma Valve Closing Switch," Proc. 1st IEEE Int. Pulsed Power Conf. Lubbock, Texas, Nov. 1976.



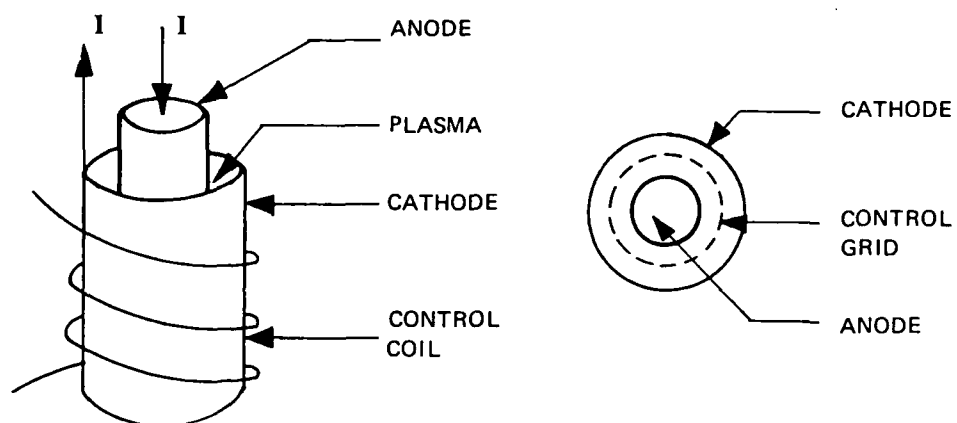
## E. Crossed Field Tubes

### 1. Introduction

Magnetic fields can be employed to expand the capabilities of low pressure, gas discharge devices. Crossed field tubes operate to the left of the Paschen minimum breakdown region and at sufficiently low pressure ( $\sim .03$  Torr) that field emission or vacuum breakdown phenomena limit the stand-off voltage. At operating pressure, the electrode spacing is less than one mean free path and a glow discharge cannot be sustained unassisted. The application of a magnetic field, normal to the electric field, will result in a spiral path for charges within the fields and the opportunity for collisions and thus the possibility for cumulative ionization to occur is greatly enhanced. Thus, a glow discharge can be established and maintained so that switch closure is achieved. Removal of the magnetic field will result in deionization of the conducting plasma. Thus, the crossed field tube can be made to open as well as close.

In some versions of crossed field tubes, an arc is allowed to form so that spark gap operation is achieved. The advantage of this device over ordinary vacuum spark gaps is its simpler trigger requirements and the opportunity to control delay and jitter more adequately.

The usual configurations of crossed field tubes and a materials summary are shown in Fig. II-11. The cylindrical geometry allows easy application of the magnetic field. The current path shown prevents the magnetic fields gener-



CATHODE - STAINLESS STEEL, TANTALUM  
ANODE - STAINLESS STEEL, TANTALUM  
GAS - HELIUM

Figure II-11. Crossed Field Switch Configuration.

ated by the switch current from interfering with the discharge. A grid may be added to "trigger" the tube more precisely while conduction interruption can still be accomplished by removal of the magnetic field.

The usual gas in modern crossed field tubes is helium. Other gases have been tried [1,2] but He gives the best overall performance.

Crossed field tubes are relatively new devices and do not have a long operation history. Most of the devices tested to date are experimental or prototype tubes. Standoff voltages on the order of 100 kV have been achieved and currents up to 10 kA have been interrupted [1]. For glow mode operation, the forward voltage drop is approximately 500 volts. As a closing switch (arc mode), repetitive operation at 40 kA, 40 kV has been achieved [3]. The Artatron [2], apparently in the arc mode, has conducted 200 kA for a total charge transfer of 60 Coulombs. The standoff voltage for this device was 70 kV.

The conditions necessary to establish a glow discharge in a crossed field tube lead to design constraints that determine the switching capabilities. The combination of applied voltage, magnetic field and tube pressure combine to limit the capabilities of crossed field tubes, especially for tubes intended for "opening" applications. A crossed field discharge cannot be maintained at low voltage for pressures below approximately .01 Torr [4]. This, coupled with

the electrode spacing, combine to limit the design choices (recall that operation is to the left of the minimum in the Paschen curve). Thus, vacuum breakdown considerations and pressure limitations combine to limit the tube dimensions. For a given design and tube pressure, the magnetic field must be above a certain minimum to maintain the discharge. Clearly, too weak a field will not allow sufficient collisions to maintain the discharge. For an excellent review of the conditions affecting the design parameters of a crossed field tube, the reader is referred to Reference 4.

The peculiar combination of a discharge voltage and magnetic field required to sustain (not cause) a discharge, allow the use of a grid to control the initiation of the conduction [5]. The best configuration for a grid device is the grounded grid configuration. The main pulse is then conducted between the anode and grid. The sequence of events to achieve switch closure is easily summarized. First, a magnetic field insufficient to cause breakdown between grid and anode is applied. However, the field strength is sufficient to maintain a discharge in the grid-anode region if one were somehow established. The grid-cathode region allows this possibility. Conditions in the grid-cathode region are such that a discharge can be established there by the application of a modest voltage pulse (approximately 1 kV). The carriers generated in this discharge diffuse

the grid into the grid-anode region in sufficient number to result in the establishment of a stable glow and thus switch closure. The switch can now be "opened" by the removal of the magnetic field.

Those factors affecting crossed field tubes as switches are summarized below.

## 2. Voltage Standoff

The maximum voltage capabilities of crossed field tubes are limited by the peculiar requirements for the discharge. Gas pressure restrictions, Paschen and vacuum breakdown combine to limit the voltage capabilities (see introduction). The maximum useful holdoff voltage is approximately 150 kV for a single gap tube using helium [4]. For tubes intended to operate in the arc mode, the voltage standoff capabilities may be somewhat less than those tubes intended for glow operation. Since the goal is to establish an arc, the surface of the electrodes need not be highly conditioned as required for the glow mode.

## 3. Pulse Current

In the glow mode, the maximum current density is limited in part by the glow-to-arc transition phenomena. At high current densities, the probability of establishing an arc is great and the surface condition of the electrodes is extremely important if arcs are to be prevented. A value of  $10 \text{ A/cm}^2$  seems to be a reasonable upper bound at this time.

The peak power dissipation is also a limiting factor on the allowable current density, especially when the tube is interrupting or turning "off" [1]. High peak power may cause an arc or the evolution of gases which eventually lead to Paschen breakdown. Also, the electrodes may be damaged so that the tube can no longer stand off rated voltage. For arc operation, the peak current is limited by life considerations and electrode damage tolerances.

#### 4. Pulse Width

Several factors affect the pulse width capabilities of crossed field tubes. Aside from thermal considerations, transient gas cleanup problems may become important. Under high current operation, the gas density falls and pressure differences may develop to a point that a glow-to-arc transistion occurs or the tube interrupts due to too low a gas pressure [4]. This limitation can be relieved to some extent by having a perforated anode so that its interior acts as a gas reservoir. For pulses exceeding one millisecond, a current density of approximately  $.3 \text{ A/cm}^2$  or higher is required to utilize the gas in the anode reservoir effectively [4].

#### 5. Repetition Rate

The primary limitation on pulse repetition rate for crossed field tubes is thermal considerations. The glow mode switches must simultaneously handle high voltage and current so that considerable dissipation is incurred in turning "ON"

and "OFF." To turn "OFF," the conducting plasma must deionize. The rate of deionization is such that a 2 kV/ $\mu$ s rise in the tube voltage is typical.

For arc mode operation, the recovery time is similar to that of a vacuum spark gap. A tube of this type has been operated satisfactorily at 526 pps at 22 kV, 5.5 kA [3].

#### 6. Current Rate of Rise ( $di/dt$ )

The allowable  $di/dt$  in crossed field tubes (glow mode) is determined by the likelihood of arc formation. The peak power dissipated during turn-on may lead to an arc so that the maximum rate of rise is a function of the allowable current density and thus, tube size. Also, once the tube is "ON," the current must not rise too rapidly or the discharge may extinguish [4]. This occurs because of plasma formation time (more plasma is needed) and the character of the crossed field discharge. If the current rises faster than the rate at which plasma can form, the tube voltage will rise and the cathode electrons may strike the anode without having had enough collisions to maintain the discharge. Thus, the tube interrupts. A stronger magnetic field will help alleviate this limitation.

The  $di/dt$  of arc mode switches is limited by the plasma formation time, similar to vacuum gaps.

#### 7. Delay

The delay between the time at which the minimum critical magnetic field is established and the rise in anode current is

a function of the plasma formation time [4]. If a source of initial charges is present, sufficient time must lapse for collisions to occur in sufficient number so that an avalanche occurs. Typically a low power DC discharge is maintained in the tube as a "keep alive" source of free charges. Because of the low pressure, the mean free paths are long and the delay may be as long as approximately 1  $\mu$ s [3].

#### 8. Jitter

Jitter is a strong function of the initial charges available [4] as well as the peak magnetic field, anode voltage and gas pressure [3]. Jitter as low as 10 ns can be achieved for closing (arc) switches [3].

#### 9. Life

Extensive life data are not available on crossed field tubes. Gas clean-up is likely to be the long term limitation [4]. Although helium is essentially inert, it is, none-the-less, slowly trapped by various mechanisms. The primary cause of gas clean-up is cathode sputtering due to ion bombardment. This results in the loss of gas and eventually the tube will not trigger. In addition, the sputtered material may eventually cause a lowering in the ability of the tube to hold off rated voltage. The conditions are far more severe in the arc mode switches where electrode damage due to erosion is an additional factor limiting tube life.



The use of hydrogen as a fill gas would allow the use of a hydride reservoir to control gas pressure over the long term. The Artatron utilized such a scheme. The article describing this device [2] is somewhat vague about the mode of operation of the device (arc or glow?) but 6000 hours of life as a low current (3 A) rectifier is quoted. No other life data are available.

#### 10. Other

Crossed field discharges can be maintained up to approximately  $10 \text{ A/cm}^2$  with a reasonable probability of stability (no arc formation) [4]. For kiloampere discharges, glow mode tubes are obviously large.

It is interesting to note that crossed field tubes are not sensitive to voltage polarity. In principal, this device would conduct in either direction and, in the glow mode, would have an interrupt capability regardless of the polarity. This ability would allow the application of crossed field tubes in ringing application with a controllability not commonly encountered in high power switch devices.

#### 11. Summary and Conclusions

Crossed field switches offer many advantages where a hard tube pulser application is required. Its ability to establish and maintain a glow discharge with a low magnetic field makes control simple and the forward drop is only a few hundred volts as opposed to a few kilovolts for vacuum

tubes. Although forward conduction losses are comparatively low, losses at the leading and trailing edge of the pulse are comparatively high. However, crossed field tubes offer a viable alternative to vacuum tube switches and have the advantage of low auxiliary power requirements, simple drive arrangements and a higher current capability (10 kA as opposed to 2 kA). Also, the tube can conduct in either direction making it a candidate for use in ringing applications.

As a closing switch (arc mode) the tube has demonstrated considerable capabilities. The advantage over normal vacuum spark gaps is lower jitter and simpler trigger requirements. However, the maximum voltage is limited to approximately 150 kV so that the range of application is somewhat limited.

## 12. References

- [1] R. J. Harvey and M. A. Lutz, "High Power ON-OFF Switching with Crossed Field Tubes," IEEE Trans. on Plasma Science, Vol. PS-4, No. 4, Dec., 1976.
- [2] G. Boucher and O. Doehler, "The Artatron, A High Power Switching Device," Proc. of 8th Symposium on Hydrogen Thyratrons and Modulators, May, 1964.
- [3] R. J. Harvey, R. W. Holly, J. Creedon and H. Gauch, "The Crossed-Field Closing Switch - A Status Report," 13th Pulse Power Modulator Symposium, June, 1978.
- [4] M. A. Lutz and G. A. Hofmann, "The Gamitron - A High Power Crossed-Field Switch Tube for HVDC Interruption," IEEE Trans. on Plasma Science PS-2, 1, March, 1974.
- [5] M. A. Lutz, "Gridded Cross Field Tube," IEEE Trans. on Plasma Science, Vol. PS-5, No. 4, Dec., 1977.

## F. Vacuum Tubes

### 1. Introduction

The classical vacuum tube uses a thermonic cathode as an electron source and a control grid to establish control over the electron flow from cathode to anode. The control mechanism is essentially the same whether the tube is conducting or not. Thus, in pulse applications, the classical vacuum tube qualifies as a true "opening" switch. It will interrupt or "open" with approximately the same speed that it closes. (Circuit configuration is usually the determining factor.) The vacuum tube has led to a class of pulse generators known as hard tube modulators. Few other switching concepts allow as much flexibility of pulser design. The primary limitation is one of size and auxiliary power requirements and peak current capabilities.

A vacuum tube is represented schematically as shown in Fig. II-12. Typical materials used in the construction are as indicated. The vacuum tube has had a long development history and its governing principles and limitations are well understood. In fact, the understanding of vacuum tube design probably exceeds that of any other switch.

Of the commercially available types, standoff voltages are limited to 100-200 kV and pulse currents to a few kiloamperes. Much higher voltages have been demonstrated in individual cases. A graph of standoff voltage versus peak current as determined from the available manufacturers data

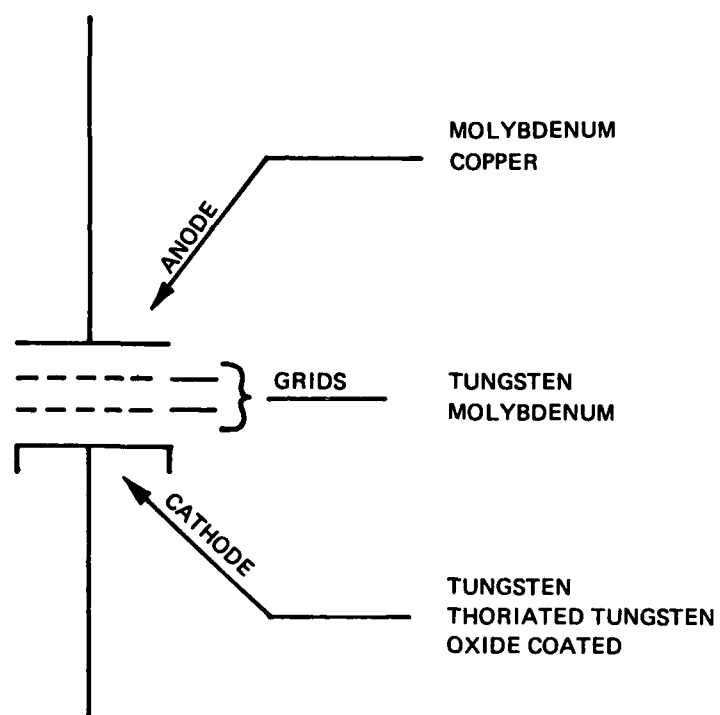


Figure II-12. Vacuum Tube Schematic.

sheets is shown in Fig. II-13. Also indicated in Fig. II-13 are a few of the more interesting tubes reported in the literature. The commercial ratings are determined by the manufacturers and are based on manufacturing tolerances, expected user tolerances, etc. so as to achieve a specified life expectancy. According to Dr. H. D. Doolittle, in connection with oxide cathode tubes, "...whereas any individual tube may operate satisfactorily under conditions considerably beyond the published limits, one cannot be sure that any tube bearing the same type number will do likewise" [1]. The present state-of-the-art in vacuum tube design seems to be more a function of commercial requirements (markets) rather than technological limitations.

For instance, the cathode is probably the single most important feature which limits the capabilities of vacuum tubes as switches. Thoriated tungsten with a carbide coating is by far the most popular cathode material. This material can emit up to 60 mA per cathode watt of heater power and peak current densities of  $3 \text{ A/cm}^2$  can be achieved with a life expectancy of approximately  $10^4$  hours. Higher emission will result in reduced life [1]. Thus, tubes capable of high peak currents are large in part because of cathode limitations. Of course, high voltage considerations place additional requirements on tube size (see standoff voltage section).

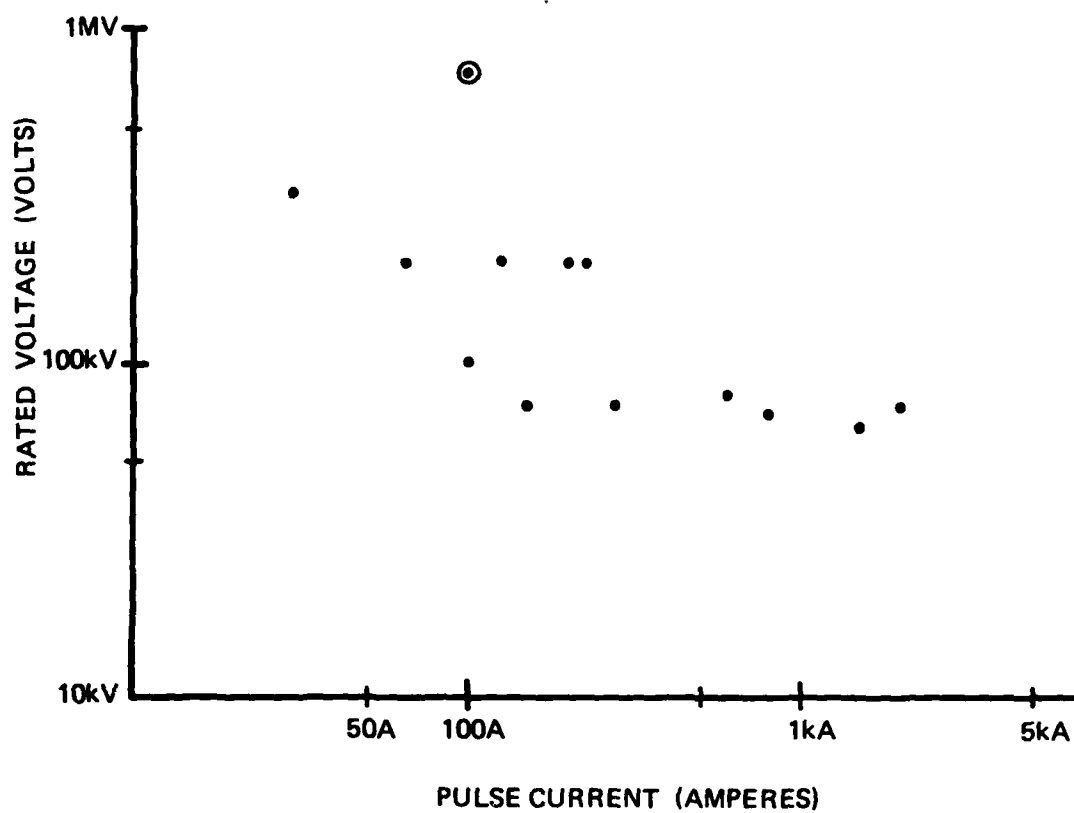


Figure II-13. Rated Standoff Voltage Versus Rated Pulse Current.  
⊗ -Unconfirmed

Increased emission is possible by using rare earth oxides as cathode coatings (200 mA per cathode watt filament power). However, this material has a considerably reduced life compared to thoriated tungsten. Evaporation of the oxide coating and its extreme sensitivity to ion bombardment are the major factors. Also, because of heating of the oxide layer under pulsed conditions, the pulse width strongly affects the cathode temperature and thus the tube life. Because of life limitations, oxide coated cathodes have not found the application one might expect and are presently limited to applications requiring peak currents of only a few hundred amperes.

The theoretical considerations for vacuum tube design have been well established. For general tube theory, the reader is referred to reference 2 and for vacuum tubes operated as switches, references 1 and 3 are excellent.

In addition to the cathode, the grids and anode affect the vacuum tube's performance as a switch. Their effects are included in the description of the switch parameters.

## 2. Standoff Voltage

The essential feature limiting standoff voltage is vacuum breakdown induced by field emission and/or ion bombardment [1, 4, 5]. The ions are, of course, due to residual gases in the tube. The electrodes most concerned with voltage standoff are the anode and the grid nearest the anode (control grid in triodes and screen grid in tetrodes).

For the usual "birdcage" geometry, breakdown is more likely to originate on the grid rather than the anode because of higher field stress and the structure of the grid (fine wires). Thus, anode-to-grid spacing and surface conditions are the primary factors determining standoff voltage.

It should be noted that the anode-grid spacing is not an arbitrary design factor [1]. Other factors such as tube efficiency and amplification factor form tradeoffs with high voltage capability.

Some field emission is usually present in high voltage tubes. Thus, these tubes are impossible to "cut off" completely and x-rays may be present. The control grid cannot affect this condition.

The voltages between the other grids or the control grid and cathode are usually not critical. These voltages are determined by parameters such as required emission, cut-off, etc. and are usually too low to cause breakdown.

Problems with envelopes, seals, etc. are not major limitations in that they can usually be avoided by good engineering practices.

### 3. Pulse Current

The peak cathode current is obviously a function of the cathode material, temperature, cathode area, etc. In most pulsed applications the anode current is the current of interest rather than the cathode current. The current emitted by the cathode is not, in general, equal to the anode



current. To achieve maximum emission from the cathode, the control grid is usually required to be driven positive. Thus, a portion of the emitted current will be intercepted by the control grid. The screen grid (tetrodes) will also intercept a portion of the cathode current. The grids in high gain tubes will, in general, intercept a greater portion of the cathode current than low gain tubes. Thus, the efficiency will be lower for high amplification factors. Also, under the "on" condition or low plate voltages, the relative potential of the grids and plate will be greatly reduced and thus excessive grid current is not only possible but likely. In fact, it is possible to calculate from geometry, etc. the maximum plate current possible under any given set of circumstances [2]. Thus, for practical reasons, the "on" voltage is limited to a value of approximately 1.5 times the control grid voltage for triodes or 1.5 times the screen voltage for tetrodes.

#### 4. Pulse Width

Grid heating is usually the limiting factor on pulse width for vacuum tubes having tungsten or thoriated tungsten cathodes [1]. Because the grid(s) intercepts a portion of the cathode current, heating occurs and a sufficiently high temperature may be reached to achieve thermionic emission from the grids. This condition is undesirable as control of the tube becomes difficult and an arc may occur when the

tube is switched "off." Thermal capacity and conductivity of the grid material, grid current and emissivity combine to determine the critical grid temperature and thus, the "safe" pulse width. Of course the pulse width can be increased by actively cooling the grid, which is being done for some new tube designs.

Oxide cathodes may impose an additional limitation on the pulse width. The oxide coating sublimates at operating temperatures (see life section on hydrogen thyratrons) and the grids may become coated with the oxide material. This would sharply reduce the pulse width capabilities as grid emission would begin at a much lower temperature. In addition, the oxide coating is heated by the emitted current so that the coating temperature increases during the pulse. Increased evaporation of the oxide layer occurs and for high current, long pulse operation the tube life suffers and a point may be reached where an arc may be formed.

By using grid water-cooling and beam forming techniques, some new tubes have extended their pulse width capabilities to several seconds or more [6, 7, 8].

##### 5. Pulse Repetition Rate

The pulse repetition rate is a strong function of the grid power a designer is willing to expend. The inter-electrode capacitance must be charged and discharged to turn the tube "on" and "off." Also, for high pulse currents,

the control grid is driven positive (see section on pulse current) and additional power is expended. It is conceivable to arrive at a condition where the power required to drive a tube "on" and "off" exceeds the power being switched. Thus, the limitation on pulse repetition rate is imposed by practical considerations rather than theoretical considerations.

A finite time is required for the electrons to move from the space charge region to the anode (transit time). Thus, it is possible, at least in principle, to drive the grid on and off so fast that no switching action occurs at the anode.

#### 6. Current Rate of Rise ( $di/dt$ )

The  $di/dt$  capabilities of a vacuum tube are a function of grid drive characteristics and power and the inductance and capacitance associated with the tube elements (for an explanation of these effects, see chapter 16, reference 2). In addition the cathode must not become saturated in order to supply the peak current required to charge the stray capacitances [3]. If the cathode becomes emission limited in this process, the rate of anode current rise will suffer. If one postulates that no circuit or cathode limitations exist, then the  $di/dt$  capability would be determined by the initial velocity distribution of the electrons in the grid-cathode region. Thus, practical considerations limit the  $di/dt$  capabilities of vacuum tubes.

## 7. Delay

The delay in anode switching action is a function of the capacitance and inductance of the overall circuit (essentially transmission line effects) and the electron transit time.

## 8. Jitter

Jitter is usually very small in vacuum tubes. The use of A.C. power for filament heating may result in some jitter due to temperature modulation effects.

## 9. Life

The usual failure mechanism of vacuum tubes is the loss of emission from the cathode. The life expectancy of tubes using thoriated tungsten cathodes is approximately  $10^4$  hours and for oxide cathodes approximately  $3 \times 10^3$  hours [1]. The loss mechanism is essentially the same in both cases, namely, the evaporation of the carbide or oxide coating. The rate of evaporation is a function of cathode temperature and, in the case of oxide cathodes, the peak current and pulse width.

## 10. Other

The thermal and mechanical properties of materials utilized in vacuum tubes are extremely important. At high temperatures, expansion of various structures may cause severe distortion of the electrode spacings so that it becomes difficult to maintain uniformity. Failure or reduced life is a likely result.

As tubes are made larger, the probability of parasitic oscillations increases [8]. These oscillations may occur internally to the tube envelope as a result of favorable geometries (inductance of grid supports, spacings etc.). The net effect of parasitic oscillations is they tend to use up the available emission from the cathode and little is left for switching action at the anode.

#### 11. Summary

The size of vacuum tubes using thoriated tungsten cathodes is approaching a practical limit. Thermal distortion of tube elements and parasitic oscillations combine to make large tubes difficult to design. New materials (such as the pyrolytic graphite grids developed in Europe) as well as modular cathodes [7, 8] may help reduce the thermal problems. Careful lay-out could help control parasitic oscillations but this promises to be a difficult process because of the likelihood of small changes in geometry as the tube ages. All things considered, a new cathode development would appear to offer the shortest path to higher performance in vacuum tubes.

The oxide cathode is known to offer several advantages in this regard [1,3]. Little work appears to have been conducted on oxide cathodes since the mid 60's. Advances in supporting technologies (materials, breakdown suppression, high vacuum techniques, etc.) make the use of oxide cathodes a logical next step in the advancement of vacuum tube switches.

The use of a field emission cathode has been successfully tried (see next section) and also remains a strong possibility for further tube development.

12. References

- [1] Dr. H. D. Doolittle, "Vacuum Power Tubes for Pulse Modulation," Cathode Press, Vol. 21, No. 1, 1964.
- [2] K. R. Spangenberg, Vacuum Tubes, McGraw-Hill Book Co., Inc., 1948.
- [3] Dr. H. D. Doolittle, "Interactions Between Pulse Modulator Tubes," Cathode Press, Vol. 21, No. 2, 1964.
- [4] M. A. Lutz, "The Glow to Arc Transition," IEEE Transactions on Plasma Science, March 1974.
- [5] M. M. Chrepta & G. W. Taylor, "High-Voltage Vacuum Breakdown Considerations for Tube Design," Proceedings 10th Modulator Symposium, May 1968.
- [6] A. Deitz, H. Murray and R. Winje, "HV Switch Tube Development Program-TFTR," Eighth Symposium on Engineering Problems of Fusion Research, 1978.
- [7] D. H. Preist, "High Voltage Switch Tubes for Neutral Beam Injectors-A New Design Approach," Conference Record of the 12th Modulator Symposium.
- [8] J. T. Mark and J. A. Eshleman, "Recent Developments in High Power Switch Tubes for High Power Radar and Fusion Research," Proceedings of 1st IEEE International Pulsed Power Conference, Lubbock, Tx., 1976.

### G. Cold Cathode Vacuum Tube

High power vacuum tubes that utilize field emission cathodes have been investigated [1]. The intended application was as a switching radar pulser.

Very high current densities can be obtained from field emission cathodes ( $>100\text{A}/\text{cm}^2$ ). In these experiments, cathodes consisting of several hundred tungsten needles were utilized. Because of the small cathode size, tubes can be designed which have very small drive requirements. The interelectrode capacitance is also very small compared to classical designs. The geometry of the models resulted in a "beam forming" device so that very little current was intercepted by the grid.

The practical limitations of this device are not clearly defined although it may be surmised that the "art of construction" rather than theoretical considerations will be the most important factor. Apparently, extreme vacuums ( $<10^{10}$  torr) are required and it is likely, in the larger sizes, that the sensitivity to geometric tolerances will become great.

The voltage standoff of this device is, obviously, field emission limited (vacuum breakdown) and 75 kV was obtained in one of the test devices. The total leakage current in the "off" condition for this tube was 3  $\mu\text{a}$ .

The peak current obtained was 15 A for the 75 kV tube although one test device obtained a peak current of 26 A.



For the 75 kV, 15 A case, a 10 kV tube drop was sustained. No other information is described pertaining to switch parameters.

The primary advantages of a field emission tube would be no heater power requirements, no warm-up time, and low power drive requirements. It should be mentioned that part of the rationale for the investigation [1] was that commercial flash x-ray machines produce 1000 A pulses with current densities above  $1000 \text{ A/cm}^2$ .

The future possibilities of this concept are not clear. No scaling information has been found so that a meaningful technical assessment can be made.

## 2. References

- [1] E. E. Martin and F. M. Charbonnier, "Field Emission Switch Tube Study," Proceedings of the Seventh Symposium on Hydrogen Thyratrons and Modulators, May 1962.

CHAPTER III  
SOLID STATE SWITCHES

W. M. Portnoy

## A. Thyristors

### 1. Thyristor Properties

A thyristor, generally speaking, is a semiconductor closing switch whose switching action depends on regenerative feedback. It is a four-layer, three-terminal device, with connections to a cathode, an anode, and a control gate (Fig. III-1). A number of different types of thyristors have been reported: gate-triggered, light-triggered, laser triggered, non-reverse blocking, gate-assisted turn-off, gate turn-off, reverse-blocking diode, and field-controlled. (Field controlled thyristors are not, strictly speaking, thyristors; they have no regenerative gain and do not latch on.)

The gate-triggered thyristor is the conventional SCR which is triggered on by an electrical pulse. Both forward and reverse blocking are obtained with this structure, switching times being relatively long for large blocking voltages because of the amount of charge which must be injected into or extracted from the base regions during switching.

Light-triggered SCRs are similar to gate-triggered devices, but use a weak light pulse for triggering; light-triggering is useful for electrical isolation, but has no other obvious advantage over electrical triggering. Laser triggering involves higher light energies; turn-on is probably obtained through a narrow region of very high carrier density, generated by the light pulse, and dissipating very low

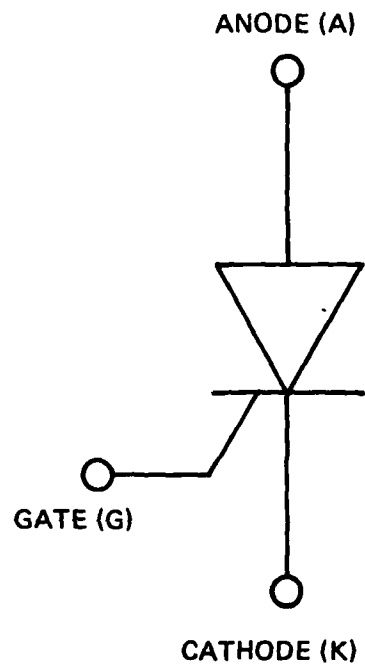


Figure III-1. Terminal Connections to a Thyristor.

power, permitting high  $di/dt$  and high peak currents. The non-reverse blocking thyristor (or reverse-conducting thyristor (RCT or ASCR)) has an asymmetrical structure. One blocking junction has been eliminated, and voltage blocking takes place only in the forward direction. The charge-modulated volume is smaller than in the conventional SCR, so that faster switching is obtained.

A negative gate pulse is applied to assist turn-off in the gate-assisted turn-off thyristor (GATO) to help reduce switching times; however, anode current must be commutated. The turn-off mechanism has not been completely identified; one explanation is the rapid withdrawal of carriers from the base by the negative pulse; and another is the prevention of a forward voltage on the cathode.

The gate turn-off thyristor (GTO) does not require commutation; a reverse gate bias squeezes the conduction plasma into a high current filament which is pinched off. The reverse blocking diode thyristor (RBDT) is essentially self-gated, using  $dv/dt$  switching. Finally, the field controlled thyristor (FCT) is a modified vertical channel field-effect transistor containing a reverse blocking junction. In the on-state, the structure behaves like a p-i-n diode; when the gate is reverse-biased, the internal field distribution is such that the device is off.

## 2. Operation of a Thyristor

The operation of the SCR can be understood by considering it as a p-n-p transistor in tandem with an n-p-n transistor, such that the two transistors share a collector junction (Fig. III-2). Each transistor base is driven by the collector current of the other transistor. The gate is connected to the base of the n-p-n transistor. When the anode, A, is positive relative to the cathode, K, the center p-n junction is reverse-biased, and the SCR is in the forward blocking state. The SCR remains in the blocking condition as long as the applied voltage does not exceed the breakdown voltage of the center p-n junction, or the sum of the breakdown voltages of the diode and cathode junctions, and as long as no forward gate-cathode bias is applied.

When a forward bias is applied to the gate in the forward blocking state, the n-p-n transistor turns on, and collector current flows, turning on the p-n-p transistor. The collector current in the p-n-p transistor drives the base of the n-p-n transistor, and regenerative feedback takes place; when the total loop forward current gain exceeds unity, both transistors turn on, all three junctions become forward biased, and the thyristor latches on. (Current gain is current dependent and generally not uniform over the conducting area of the device.) Because the switching point depends on the gate current, a family of current-voltage characteristic curves are obtained (Fig. III-3). Figure

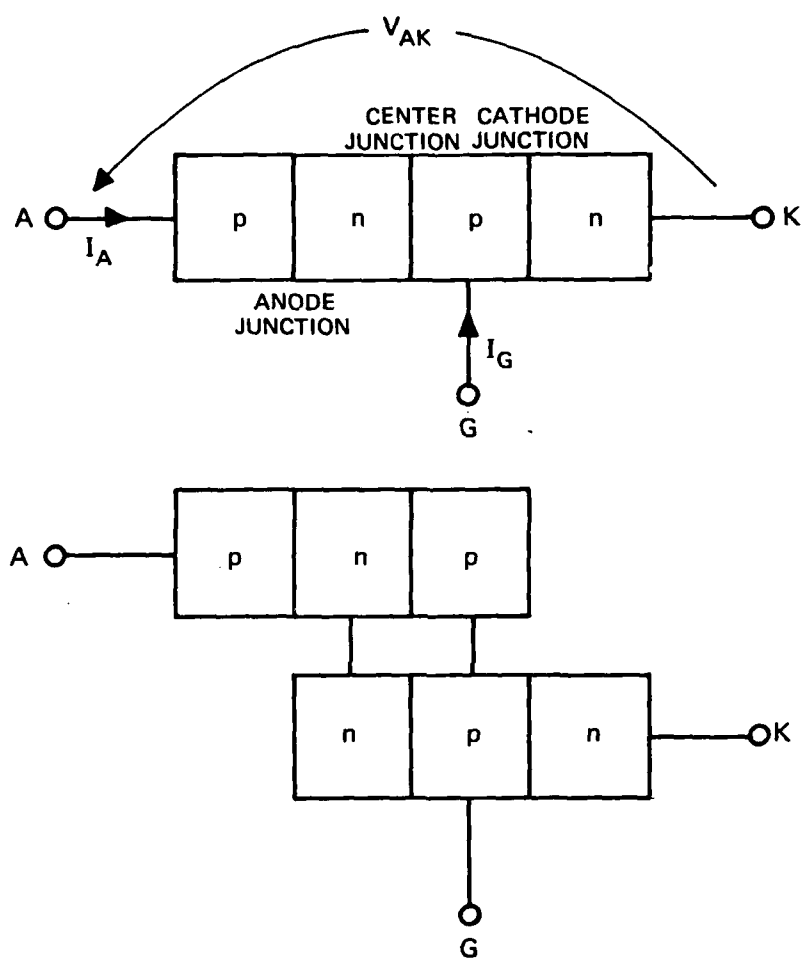


Figure III-2. Basic Thyristor and Thyristor Equivalent Circuit.

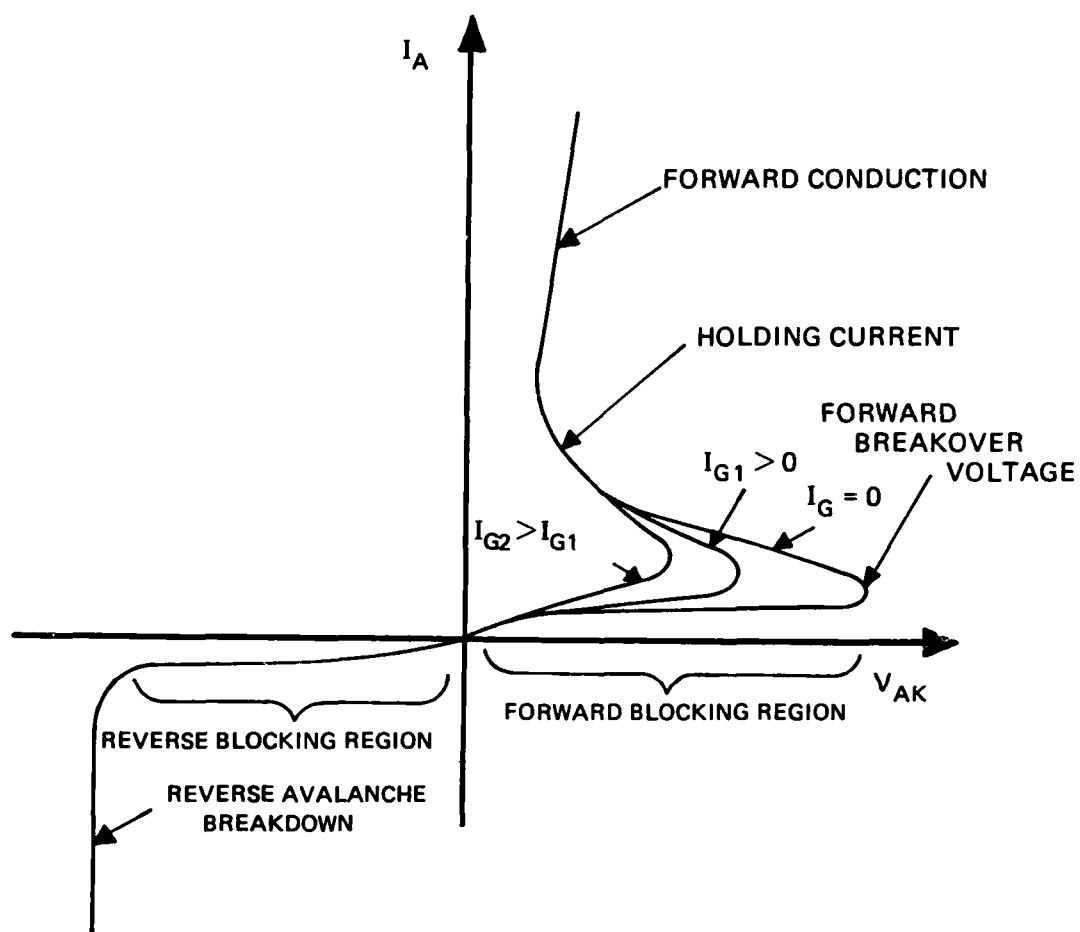


Figure III-3. SCR Current-Voltage Characteristics.



III-4 illustrates the construction of a typical SCR, with a central gate and a shorted emitter.

### 3. Voltage Standoff (Blocking Voltage)

Commercial reverse blocking SCRs are usually symmetrical, that is, both p-regions are identically diffused, and have the same concentration and thickness. In the reverse blocking condition, the anode and cathode junctions are both reversed-biased; however, the breakdown voltage of the cathode junction is usually very low compared with that of the anode junction, so that the reverse bias is supported essentially by the latter junction. In the forward blocking state, the center junction supports the reverse bias. In either blocking state, the depletion region extends primarily into the n-region, because of its light doping relative to the p-regions. The breakdown, and hence the blocking voltage, is controlled by the properties of the n-base, that is, by its doping and width, or by the character of the n-type surface near the center or the anode junctions. The blocking voltage itself is less than the breakdown voltage, being reduced through the effects of the forward current gains of the two transistors, particularly the p-n-p transistor, making up the thyristor.

Most thyristors are designed around the bulk breakdown voltage of the n-region. The depletion width must always be less than the n-base width in order to prevent punch-through

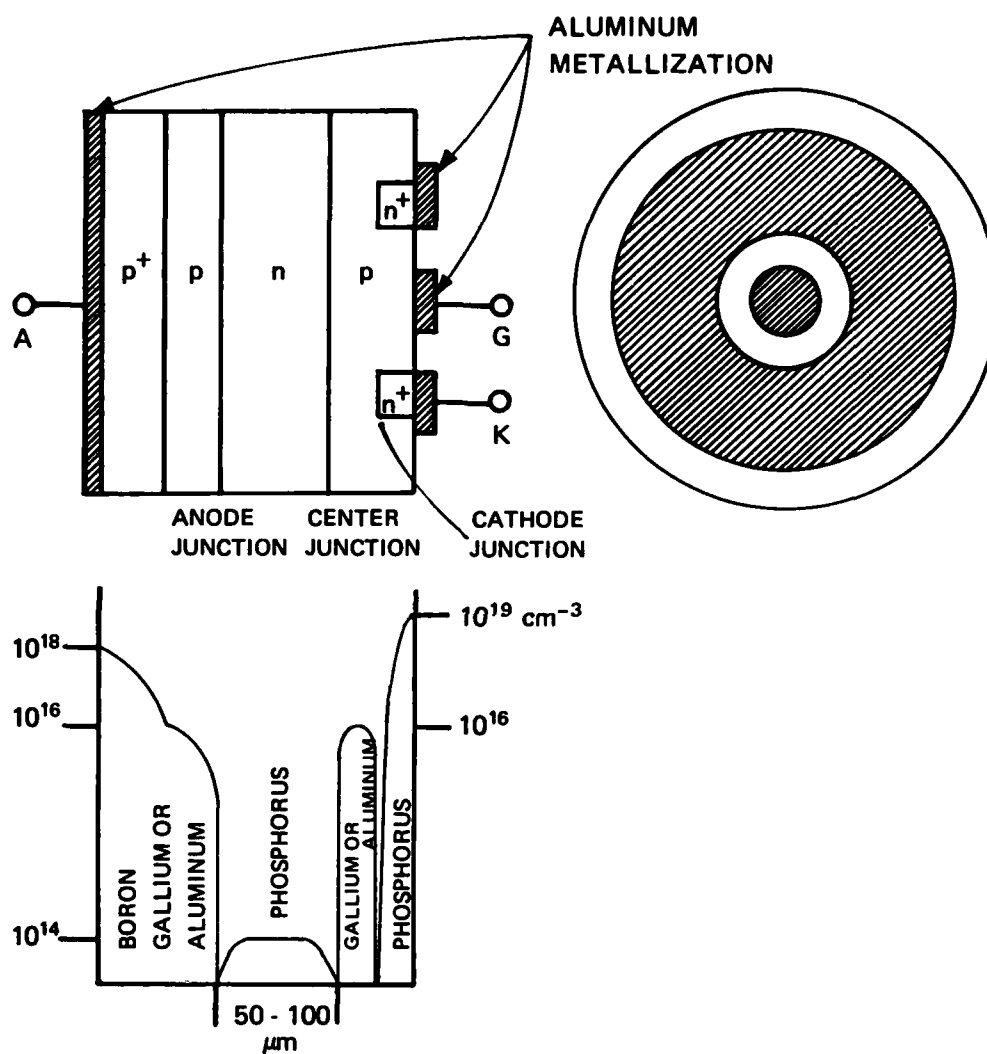


Figure III-4. Typical SCR Construction.

at a given doping level. Because both the breakdown voltage and the depletion width increase with decreasing impurity carrier concentration, the base width must be increased as the blocking voltage is increased. However, the dynamic properties of the thyristor [such as turnoff time (Fig. III-5)] degrade with increasing base width, so that a compromise between blocking voltage and other thyristor characteristics is required.

The impurity concentration of the n-base is established by the resistivity of the thyristor starting material. Doping is usually performed during initial growth of the silicon ingot. Because control of the process is limited, resistivity variations occur from wafer to wafer, and radially across individual wafers themselves. For large area, high current devices, such variations must be compensated by making the n-base wide enough to contain the depletion width for the lowest anticipated resistivity. Such a worst-case design results in a large variation in breakdown voltage for a given base width, affecting yield, and degrades the dynamic performance of the thyristor at a given breakdown voltage. However, this problem has recently been circumvented by the introduction of the technique of neutron doping, in which silicon is transmuted into phosphorus by neutron bombardment; this procedure introduces a uniform and precise impurity concentration. The primary application of neutron doping has been for high voltage (above 2 kV) phase control

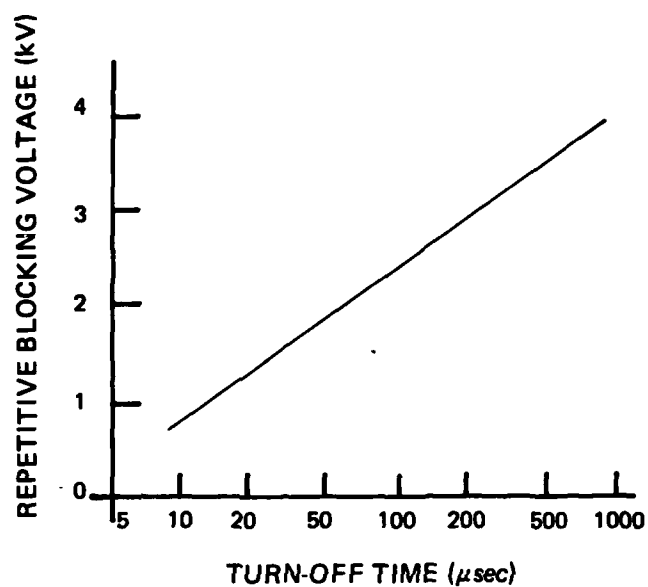


Figure III-5. Repetitive Peak Blocking Voltage vs. Turn-off Time.

devices, but it will undoubtedly be used wherever base width control is critical, such as in fast inverters.

In order to take advantage of the bulk breakdown in the n-base, the junction breakdown voltage where the junction intersects the surface must be maximized. Surface breakdown is controlled by bevelling the junction; bevelling spreads the space charge region at the surface, reducing the electric field strength and increasing the breakdown voltage. The standard edge contour is the double bevel, a low angle negative bevel for the forward blocking junction, and a positive bevel for the reverse blocking junction (Fig. III-6). Additional control is obtained by passivating the junction, normally by coating with an RTV type compound, which protects against contamination and also prevents arcing.

#### 4. High Pulsed Current Effects

High power switches operate at peak current densities between several hundred and several thousand amperes per  $\text{cm}^2$ ; at these levels, injected minority carrier densities approach or exceed equilibrium values of majority carrier concentrations. Device properties under these conditions are considerably different than at low currents, and can no longer be described in terms of small-signal parameter values.

Normally, carrier mobilities (and diffusivities) are limited by lattice scattering, and at high impurity concentrations, by impurity scattering. At high injection levels,

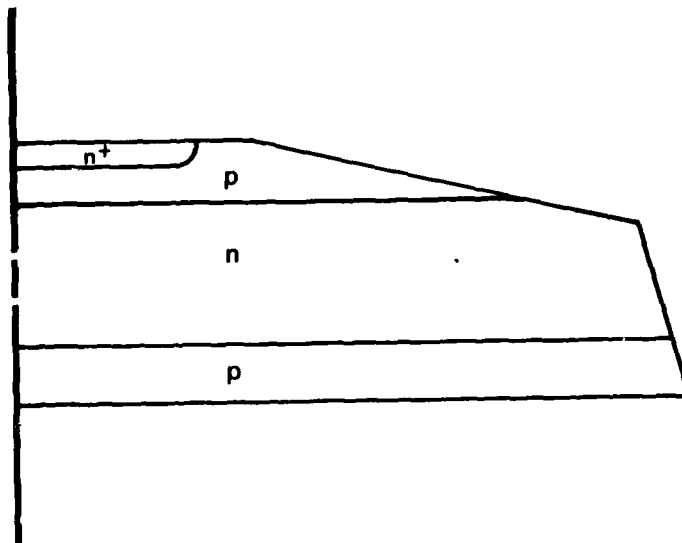


Figure III-6. Double Bevel Control of Surface Breakdown.

carrier-carrier scattering becomes significant; electron and hole transport can no longer be treated separately. New mobilities and diffusivities, (the ambipolar values), must be defined; these are expressed in terms of small-signal values. Ambipolar mobilities and diffusion constants decrease rapidly with increasing carrier concentration, so that forward voltage drops are strongly affected at high current levels. Also, current gain falls off significantly at high current densities because of conductivity modulation in the base, although this effect is more important for transistors than for thyristors.

At high injection levels, recombination is inadequately described by Reed-Shockley statistics, and minority carrier lifetime is affected by processes which are not important at low levels. Direct band-to-band recombination of two carriers without intermediate trapping occurs, and Auger recombination, which is a three-carrier process, takes place.

##### 5. Forward Voltage Drop

All the junctions in a thyristor are forward biased in the on-state. The forward voltage drop consists of the drop across the contact regions, across the regions between the p-n junctions, and across the junctions themselves. At low injection levels, the current density is small, and the voltage drops across the metal contacts, the high-low  $p^+-p$  junction, and the region between the junctions, are negli-

gible; the significant voltage drop is across the forward biased junctions. (At low injection levels, the injected carrier density into the n-base remains less than the equilibrium carrier density, typically  $10^{14} \text{ cm}^{-3}$  for power switches; values of the forward current density under these conditions are below around  $100 \text{ mA/cm}^2$ .) The drop across the center junction is opposite to those across the cathode and anode junctions, so that the total voltage drop is around 0.8 volt.

When the injected carrier density becomes greater than the n-base doping level, but is still less than the impurity concentrations in the p-regions, then injection levels have become moderate; these levels occur between around 10 and 50  $\text{A/cm}^2$ . Under these conditions, the voltage drops across the anode and center junctions become equal and opposite. The voltage drops across the contacts, the  $p^+$ -p junctions, and the p-regions are still negligible, but a significant drop now occurs across the n-base, which is conductivity modulated. The drop is independent of current, and varies directly as the square of the width of the n-base, and inversely as the hole lifetime. The total voltage drop, around .9 volt, is obtained by adding the n-base drop to the drop across the forward biased cathode junction.

At high current densities, between 50 and 5000 amperes per  $\text{cm}^2$ , all regions of the thyristor, except the heavily-doped  $p^+$ - and  $n^+$ -regions, are conductivity modulated; opera-



tions of power switches take place at these levels. At these injection levels, ambipolar effects are such that the electron and hole currents are equal. The device resembles a p-i-n diode, the effective i-width being the sum of the widths of the two p-regions and the n-base. Again, all voltage drops except the drop across the cathode junction and the n-base are negligible (the drops across the anode and center junctions are equal and opposite). The voltage drop across the n-base, which varies inversely as the square root of the hole lifetime in the n-base and directly as the effective base width, is the important term in the forward voltage drop at high forward currents; the dependence is illustrated in Fig. III-7 [2].

#### 6. Voltage Triggering and $dv/dt$

There are two modes of voltage triggering of a thyristor, by avalanche multiplication and by a rapidly rising anode voltage, that is, by a high  $dv/dt$ . If a forward voltage exceeding the forward standoff voltage is applied to the anode, bulk avalanche breakdown begins, and considerable carrier multiplication takes place in the center junction depletion region. The increased reverse current flow stimulates carrier injection at the anode and cathode junctions, regeneration begins, and the thyristor turns on. This mode of voltage triggering can be avoided by limiting the applied forward anode voltages.

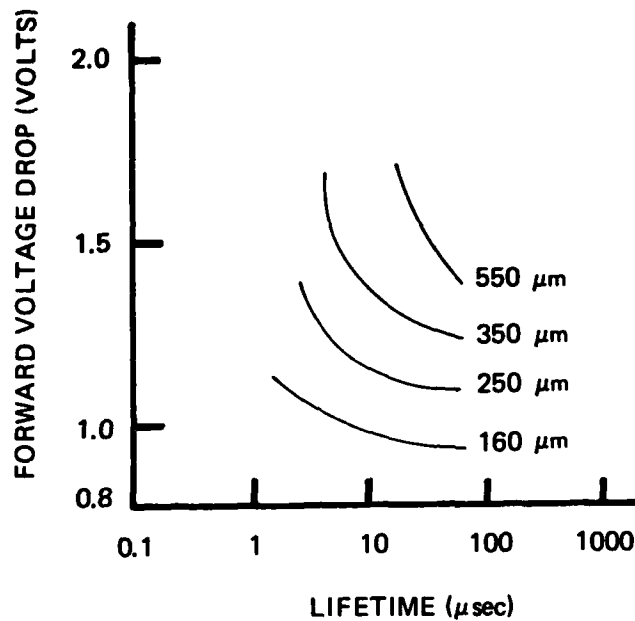


Figure III-7. Forward Voltage Drop at  $200 \text{ A/cm}^2$  as a Function of Hole Lifetime in the n-Base and of Effective Base Width [2].

The second mode is the result of displacement current flow through the reversed biased center junction capacitance. Forward displacement current flow through the thyristor increases the effective current gain so that regeneration occurs and the device turns on. (The value of  $dv/dt$  is usually specified for non-repetitive voltage ramps. It is also possible to describe it in terms of the rate of application of forward voltage while the thyristor is returning to its forward blocking condition following a previous turn-off from the on-state). The value of  $dv/dt$  for which the device will self-trigger can be increased by reducing the center junction capacitance, either by reducing the junction area or by increasing the n-base doping. The former method requires a reduction in the current handling capability of the device, and the latter causes a reduction in blocking voltages. Neither of these are conventionally used; the common procedure for increasing  $dv/dt$  is by shorting the emitter.

A shorted emitter (Fig. III-8) has low injection efficiency, hence low current gain, at high voltages and low currents; when the voltage is low and the current is high, injection efficiency and current gain are also high. These are the conditions required for high  $dv/dt$  self-triggering. The emitter short collects the displacement current preventing the lateral voltage drop under the  $n^+$ -emitter, that is, the cathode, from reaching its turn-on value, around 0.5 volt. The

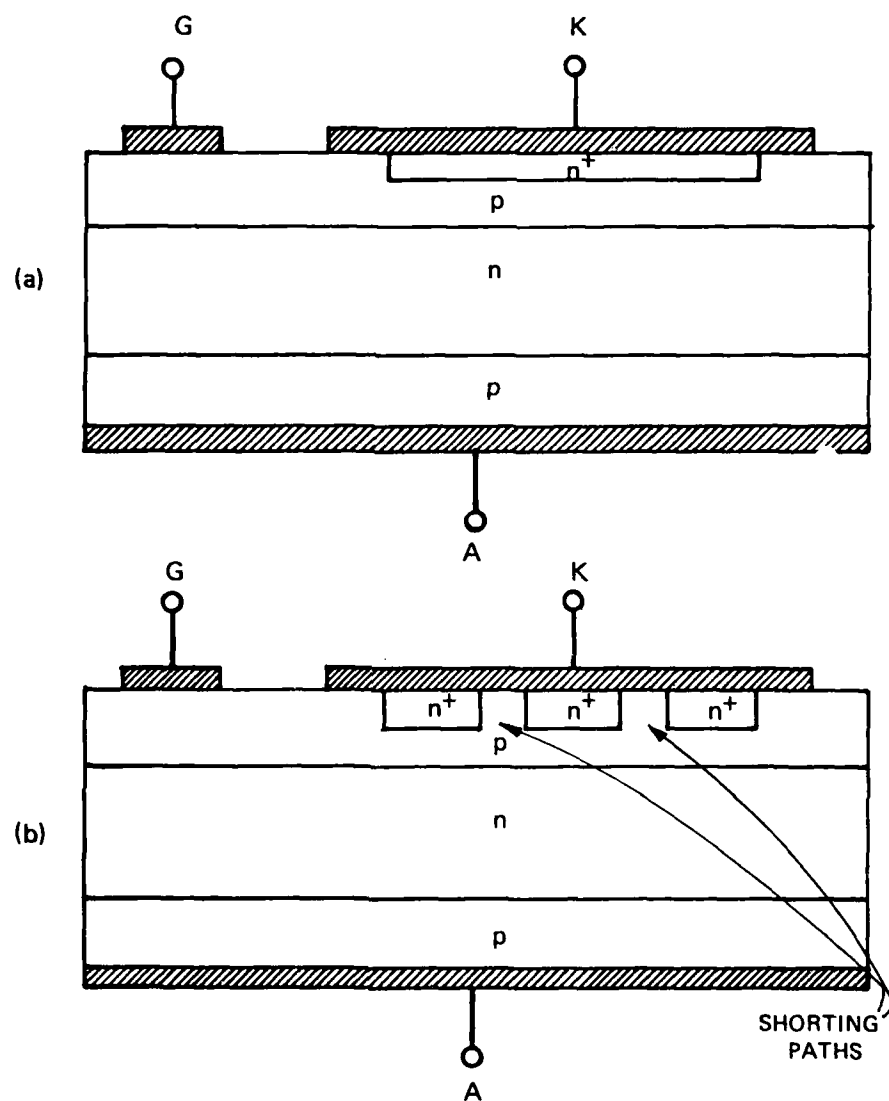


Figure III-8. Overlapping Shorted Emitter (a);  
Multiply Shorted Emitter (b).

simplest method for obtaining an emitter short is to overlap the cathode metallization onto the gate (Fig. III-8a); a more effective method for increasing the emitter shorting area without losing cathode area is to use multiple shorting paths, in which portions of the base region are shorted to the emitter contact, (Fig. III-8b). A high density of small paths will provide high  $dv/dt$  capability, but it is not practical to reduce the diameter of the shorting below 100  $\mu m$  because of surface roughness.

Forward voltage drop is not greatly affected by shorting the emitter; forward blocking voltage is increased. The greatest effect of an emitter short is on the plasma spreading velocity, which is reduced, which, in turn, reduces the  $di/dt$  capabilities of the thyristor.

#### 7. Turn-on and $di/dt$

The rate at which a device turns on depends on the amount of current which can safely flow through the small region where switching is initiated. In center gated thyristors, only a small part of the device immediately adjacent to the gate electrode turns on; the high reverse bias is shorted out by the conducting region, and the electric field collapses, so that regenerative effects essentially vanish, and the remainder of the device must turn on by lateral propagation of the on-region plasma. A considerable time may elapse before the entire cathode area turns on, and during this time, the entire anode current

flows through only a small part of the total conducting area; at high values of  $di/dt$ , high power dissipation and localized heating can cause considerable damage to the device.

It is possible to obtain a rough estimate of leading edge limitations by assuming that power is dissipated only during the turn-on transient, and that device heating is adiabatic. Figure III-9 illustrates the turn-on events. The trapezoidal pulse has a peak current,  $I_p$ , and a leading edge slope,  $di/dt$ ; the rise time,  $t_r$ , is the time required for the current to reach its peak value, that is,  $t_r = \frac{I_p}{di/dt}$ . The voltage is assumed to fall exponentially from its forward blocking value,  $V_{DRM}$  with a fall time,  $t_f$ . Both the time dependence of the voltage and the value of  $t_f$ , are assumed to be independent of the turned on area in the thyristor, through which the instantaneous current must flow. Then

$$i(t) = I_p \frac{t}{t_r}$$

and

$$v(t) = V_{DRM} e^{-t/t_f}.$$

The instantaneous power during turn-on is

$$P(t) = v(t)i(t) = I_p V_{DRM} \frac{t}{t_r} e^{-t/t_f}.$$

For fast rise times, the power is assumed to be dissipated adiabatically, so that

$$P(t) = m(t) c_p \frac{dT}{dt},$$

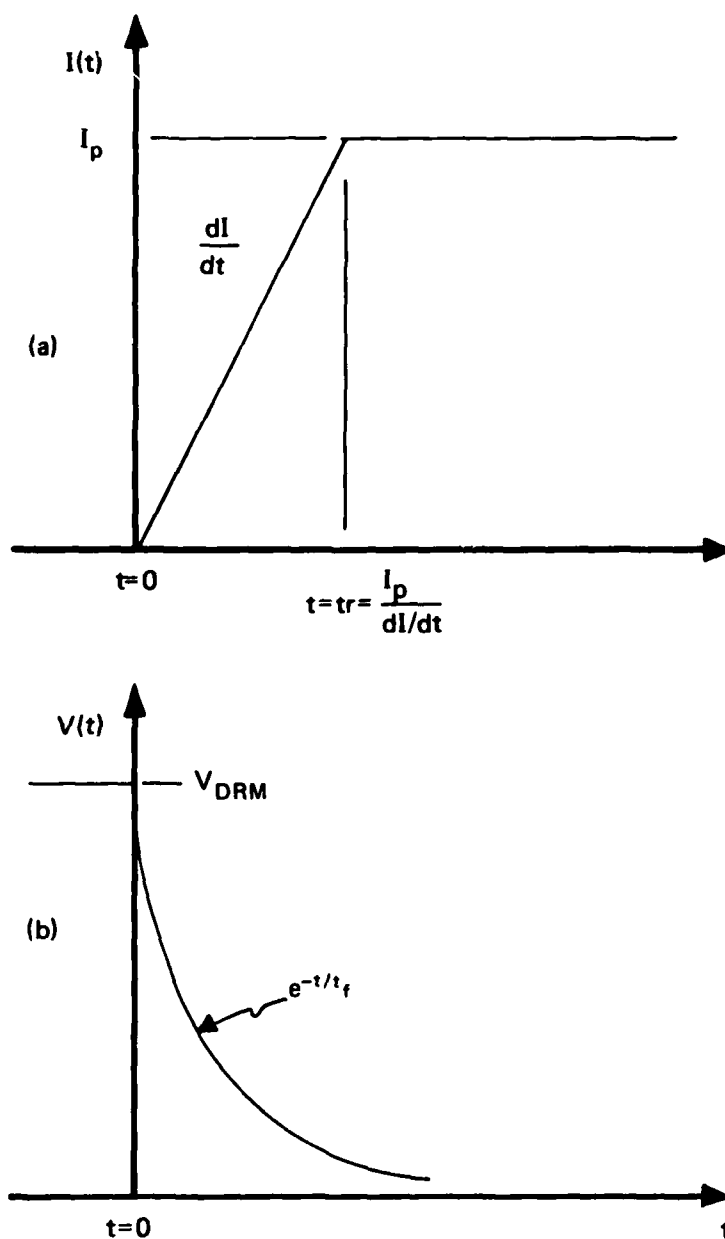


Figure III-9. Time Dependence of Trapezoidal Forward Current Pulse (a); of Forward Voltage (b).

where  $T$  is the instantaneous temperature,  $c_p$  is the specific heat capacity, and  $m(t)$  is the mass of silicon in which the power is dissipated. The conduction area through which current flows will depend on time through the plasma spreading velocity,  $v_p$ . The instantaneous conduction area is just the product of the plasma spreading velocity, the time, and the total gate length,  $\ell$ , that is,

$$A(t) = v_p \ell t,$$

so that the mass,  $m(t)$ , is

$$m(t) = \rho w A(t) = \rho w v_p \ell t,$$

where  $\rho$  is the density of silicon and  $w$  is the thyristor wafer thickness. Combining all the expressions,

$$I_p V_{\text{DRM}} \frac{t}{t_r} e^{-t/t_f} = \rho w v_p \ell t c_p \frac{dT}{dt},$$

or,

$$\frac{I_p V_{\text{DRM}}}{t_r} \int_0^{t_r} e^{-t/t_f} dt = \rho w v_p \ell c_p \int_{T_a}^{T_m} dT.$$

$T_a$  is the ambient temperature at turn-on,  $T_m$  is the maximum safe temperature, that is, the maximum temperature which can be sustained without physical damage to the device. The minimum current rise time is just the voltage fall time; for this condition,

$$I_{p\text{max}} = 1.58 \rho w v_p \ell c_p \frac{T_m - T_a}{V_{\text{DRM}}}.$$

Using room temperature (300°K) values for  $\rho$  (2.33 gm per cm<sup>3</sup>)



and for  $c_p$  (0.7 joule per gram per  $^{\circ}\text{K}$ ), and typical values for  $v_p$  ( $10^4$  cm/sec [1]), for  $w$  ( $3.81 \times 10^{-2}$  cm) and for  $\ell$  (20 cm), the expression for  $I_{p\max}$  becomes

$$I_{p\max} = 1.96 \times 10^4 \frac{T_m - T_a}{V_{\text{DRM}}}.$$

If  $T_m$  is the silicon-aluminum eutectic temperature,  $577^{\circ}\text{C}$  ( $850^{\circ}\text{K}$ ) then, for  $V_{\text{DRM}} = 1000$  V,

$$I_{p\max} = 10800 \text{ A},$$

and, for a rise time (fall time) of 100 nsec,

$$\left(\frac{dI}{dt}\right)_{\max} = 1.08 \times 10^5 \text{ A}/\mu\text{s}$$

Lower temperature failure mechanisms, such as thermal fatigue [3, 4], that is, damage which occurs because of expansion and contraction of the silicon material with heating and cooling, will reduce these values.

The velocity of the lateral plasma spreading has been found to increase with increasing current density and increasing minority carrier lifetime, but decreases as the effective base width and the amount of emitter shorting increase. Figures III-10a[1] and III-10b[5] illustrate the effects of emitter shorting and lifetime on plasma spreading velocity, and the relationship between plasma spreading velocity and blocking voltage, respectively. According to Fig. III-10a, the spreading velocity saturates at around  $10^4$  cm/sec for high current densities, and decreases significantly with emitter shorting and low minority carrier lifetime (gold-doped material). Increasing blocking voltage in

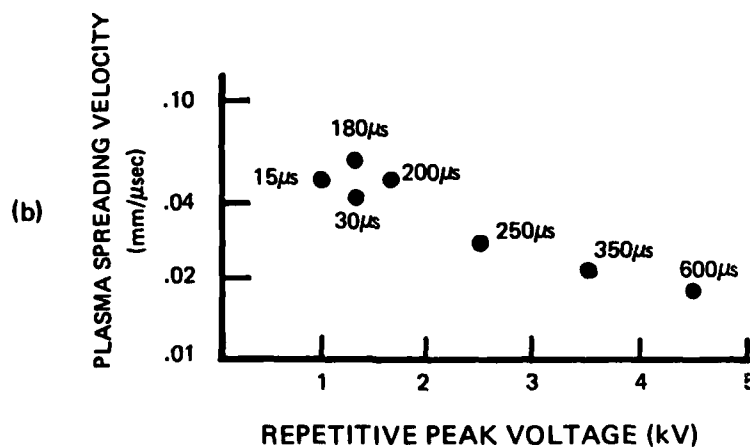
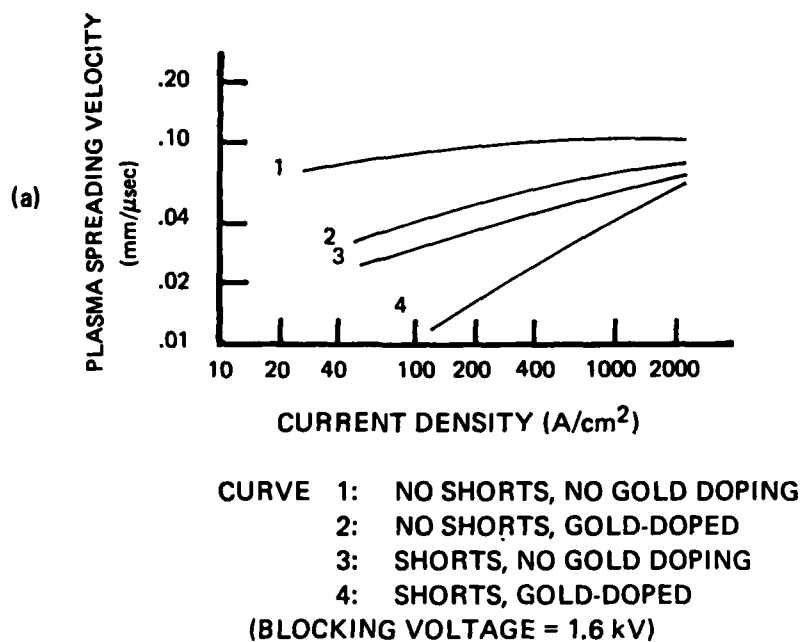


Figure III-10. Effect of Emitter Shorting and Lifetime on Plasma Spreading Velocity [1] (a); Relationship between Plasma Spreading Velocity and Blocking Voltage [5] (b).

Fig. III-10b is directly related to increasing n-base width, a relationship demonstrated also by the increasing turn-off times.

It is not possible to increase plasma spreading velocity in the device without affecting other thyristor parameters, but independent improvements in turn-on time may be obtained by appropriate contact geometries. The effective turn-on area is increased by a large gate periphery (and by driving the gate at several times the critical gate current for turn-on), and the distance over which the plasma must spread is reduced by making the gate-cathode electrode separation small. Figure III-11 illustrates a representative interdigitated contact structure. Interdigititation provides an increased initial turn-on area, hence higher  $di/dt$ , and also reduces the instantaneous forward voltage drop, but because triggering current is proportional to total emitter periphery, interdigitated devices require higher gate drives than conventional geometries. In order to maintain high gate sensitivities at the same time as providing large gate drives, a small driving thyristor, triggered by low currents, is often used with interdigitated contacts. The auxiliary thyristor is integrated on the same wafer as the main device; the arrangement is called an amplifying gate.

A central amplifying gate structure is illustrated in Fig. III-12. The auxiliary thyristor, being small, is turned on rapidly by a small gate current. The cathode current for the auxiliary device, which is much higher than

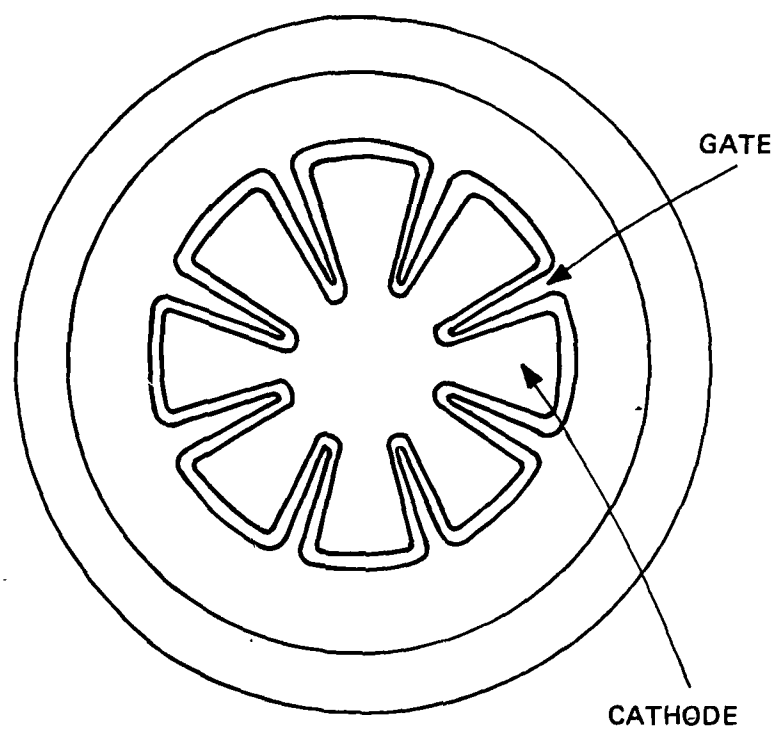


Figure III-11. Representative Interdigitated Contacts.

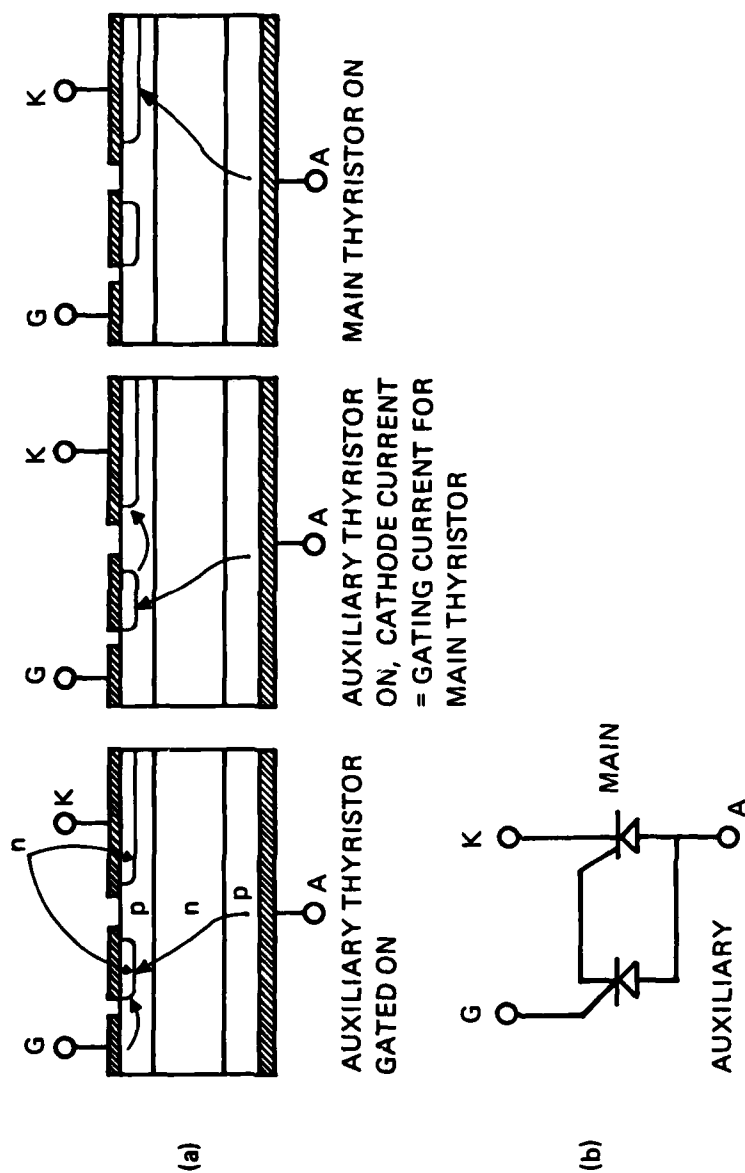


Figure III-12. Firing Sequence for Shorted Emitter Auxiliary Gate Thyristor (a); Auxiliary Gate Thyristor Equivalent Circuit (b).

the original gate current, is now the gate current for the main thyristor, and turns on a large initial area. The main thyristor turns on not only more uniformly, but rapidly; the auxiliary thyristor carries the major part of the load current for less than one microsecond. Large auxiliary gate currents in an amplifying gate are not desirable; they cause the main thyristor to turn-on at the same time as the auxiliary thyristor and the advantage of the amplifying gate is lost.

There are other multiple stage thyristor structures, such as the emitter gate, the field initiated gate, and the regenerative gate. The regenerative gate (Fig. III-13), is frequently found in inverter devices. The emitter area is not completely metallized, and the lateral current flow in the high resistance narrow unmetallized n-region causes a positive voltage drop relative to the metallized portion of the cathode; this is picked off and fed to one or more gate contacts to the p-gate region. The initiating gate signal triggers current flow at the end of the emitter near the standard gate, and the regenerative gate simultaneously initiates anode flow at the far end. A distribution of regenerative gates around the cathode enhances uniform and rapid turn-on.

#### 8. Recovery Time (Turn-off)

A conventional SCR latches on, that is, remains on after the gate trigger signal has been removed, and can be turned

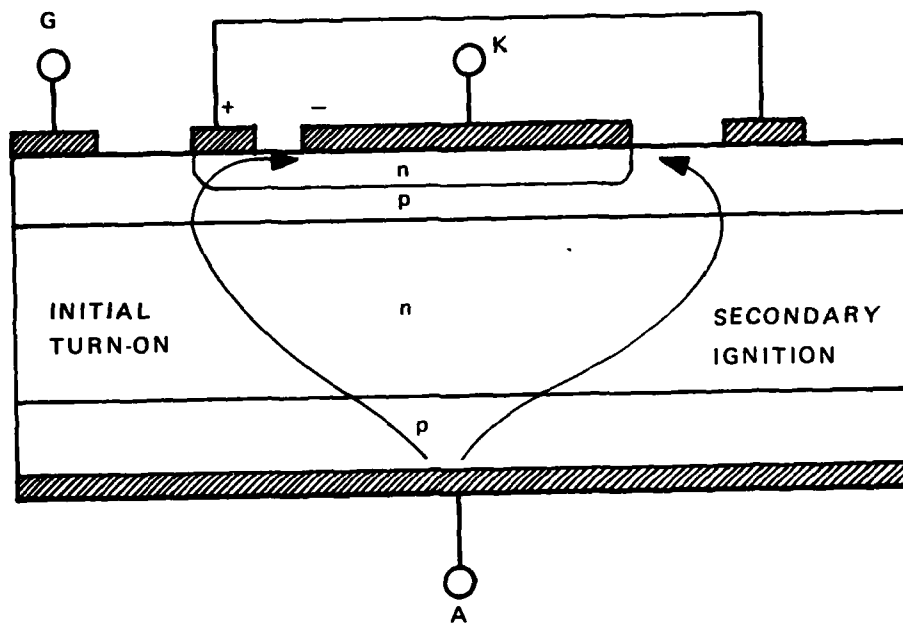


Figure III-13. Regenerative Gate Structure.

off only by interrupting the anode current (commutation). The turn-off time, that is, the time which must elapse before forward blocking capability is reestablished is usually long; the charge stored in the p-and n-base regions which is injected by the on current cannot be removed rapidly during reverse blocking. Charge in the base regions is removed via ambipolar diffusion to the depletion regions, where it is extracted, or by recombination; both processes are slow. The reapplication of a forward voltage while substantial charge still remains in the base regions will turn the device on again, so that  $dv/dt$  following commutation of the anode current may be considerably less than  $dv/dt$  relative to a single ramp. If sufficient charge has already disappeared, emitter shorting will help recovery by extracting any remaining stored charge, but considerable emitter shorting cannot be introduced without affecting the plasma spreading velocity (and hence,  $di/dt$ ).

Turn-off time is usually adjusted by introducing suitable impurities, such as gold, to reduce carrier lifetime; with gold-doping, turn-off times can be reduced to 10  $\mu\text{sec}$  without seriously affecting other device parameters. However, if minority carrier lifetime is reduced excessively, forward voltage drops are increased, and leakage currents become large enough to affect leakage power dissipation.

#### 9. Adjustment of Minority

Minority carrier lifetime is adjusted in order to reduce turn-off time; the turn-off time is around ten times as



great as the minority carrier lifetime in the base regions. However, turn-off time cannot be independently reduced without affecting other parameters; the forward voltage drop in the on-state increases sharply at low lifetimes (Fig. III-7), plasma spreading velocity is reduced (Fig. III,10), and the reverse leakage currents at the blocking voltages become high enough to exceed permissible leakage power levels. However, a lower lifetime in the n-base reduces the current gain of the p-n-p transistor section of the thyristor, and a higher blocking voltage is obtained (Fig. III-14).

The most widely used method for reducing lifetime is gold diffusion; however, gold doping causes high leakage currents, may affect background impurity levels, and is gettered by other impurities, such as phosphorus, and by dislocations, so that good lateral distributions are hard to obtain. On the other hand, vertical concentrations can be sufficiently controlled to permit some individual adjustments of otherwise interdependent turn-off time and forward voltage drop.

Platinum is occasionally used to adjust lifetime, rather than gold, but it introduces excessive forward voltage drops. Electron irradiation is beginning to compete with gold for lifetime adjustment. Damage is introduced into the lattice by a flux of electrons at 1 to 2 MeV, and annealed out above 250°C (523°K) to desired levels. Good lateral uniformity of recombination centers is obtained. The greatest advantage of electron irradiation is that

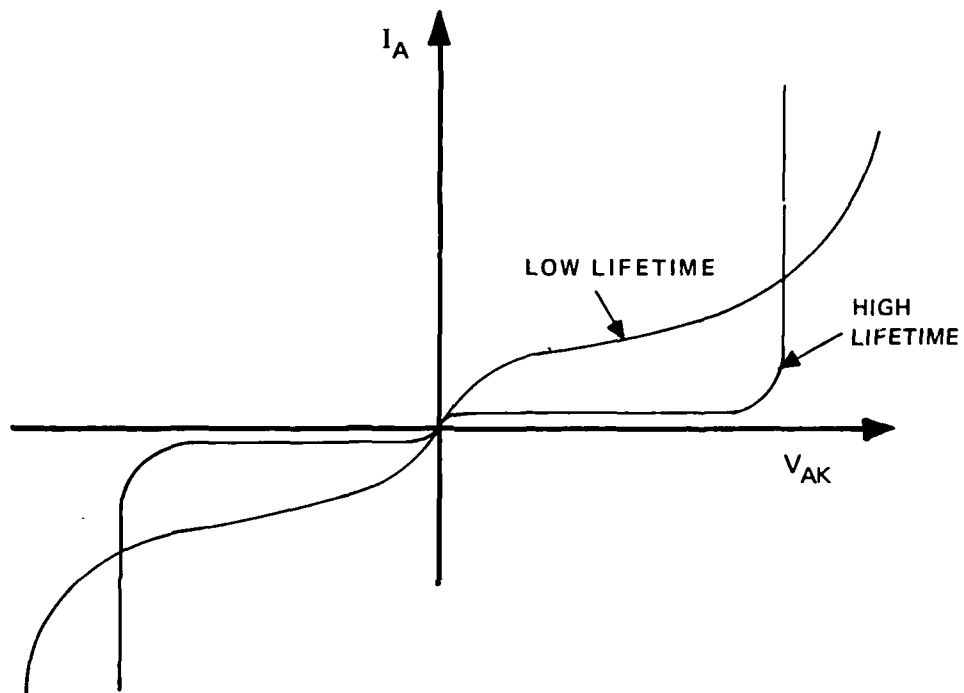


Figure III-14. Effects of Minority Carrier Lifetime on Forward and Reverse Blocking Characteristics.

lifetime adjustment can be performed on packaged devices. A few electron irradiated thyristors are commercially available, but there is some industry reservation to this process because of possible additional annealing at high operating temperatures, and subsequent uncontrolled changes in lifetime.

#### 10. Types of Thyristors

Various modifications to the conventionally structured SCR can be made in order to improve certain performance characteristics; however, these are frequently compromises, inasmuch as other parameters will usually suffer. Seven major types (other than the normal SCR) have been developed. Although these several types have found specific applications, in general, none have been completely characterized nor, excepting the RBDT, are they commercially available. However, for completeness, and to demonstrate current thyristor design philosophies, the seven structures will be described here. They are the gate-assisted turn-off thyristor (GATO), the gate turn-off thyristor (GTO), the light triggered thyristor, the laser triggered thyristor, the reverse conducting thyristor (RCT) or asymmetrical SCR (ASCR), the reverse blocking diode thyristor (RSR or RBDT), and the field controlled thyristor (FCT), which is, strictly speaking, not a thyristor at all.

##### a. Gate-Assisted Turn-Off Thyristor (GATO)

In the GATO, a reverse bias is applied to the gate after commutation, while the forward anode voltage is reapplied, to help reduce turn-off time and increase the frequency

capability. One model [6] describes reverse gating effects in terms of removal of excess carriers faster than they can be removed by recombination alone; this model excludes the use of shorted emitters. A more recent explanation [7] suggests that the gate assist prevents a forward voltage from developing at the cathode junction, inhibiting refiring. A shorted emitter structure is consistent with the latter model. When there is no cathode shunting, the negative gate bias directs forward recovery current laterally in the p-gate region from the cathode to the gate; the cathode junction becomes less forward biased and fewer electrons are injected from the emitter, reducing the likelihood of refiring. (This model is not inconsistent with the carrier sweep-out model.) If cathode shunting is present, lateral current flows through the p-gate region from the cathode shunts to the gate, in a direction opposite to the forward recovery current, reducing the total lateral voltage drop, inhibiting refiring.

b. Gate Turn-Off Thyristor (GTO) [8]

If the negative gate drive is sufficient, debiasing will be great enough so that the current flowing to the cathode will be pinched into a narrow channel. Under certain conditions, regeneration in the conducting filament will not be sufficient to sustain it, and it will collapse, turning off the device. This effect can be used to turn-off the device without external commutation, while anode current is still flowing, and is called gate turnoff. A GTO thyristor must

be carefully designed; local overheating in the current channel may damage the device. (This effect is similar to current channeling at high collector currents in transistors.) The maximum reverse gate-cathode bias is limited to the breakdown voltage of the cathode junction.

c. Light Triggered Thyristors.

Turn-on in a light triggered thyristor [1] is initiated by carrier generation in the bulk via light conducted into the gate region through a light pipe. It has the advantage of total isolation of the gating circuit from the other circuitry, which is useful when thyristors are series stacked for high voltages and when stray capacitance is a problem. The basic light-gated thyristor is illustrated in Fig. III-15a. Light, usually from a gallium arsenide LED, is conducted through a glass fiber. Another design, which appears in devices used as auxiliary gates in two-stage gate structures, is shown in Fig. III-15b. Weak light triggering is generally used for phase control devices.

d. Laser Triggered Thyristors.

If the energy which is contained in the light pulse is great enough, high carrier concentrations generated throughout the bulk of the thyristor will permit fast, simultaneous turn-on of large areas, for very high  $di/dt$  and peak currents. Figure III-16 represents a laser activated semiconductor switch (LASS) [9, 10]. If high intensity  $1.06 \mu\text{m}$  radiation (YAG laser) is used to irradiate the thyristor junctions

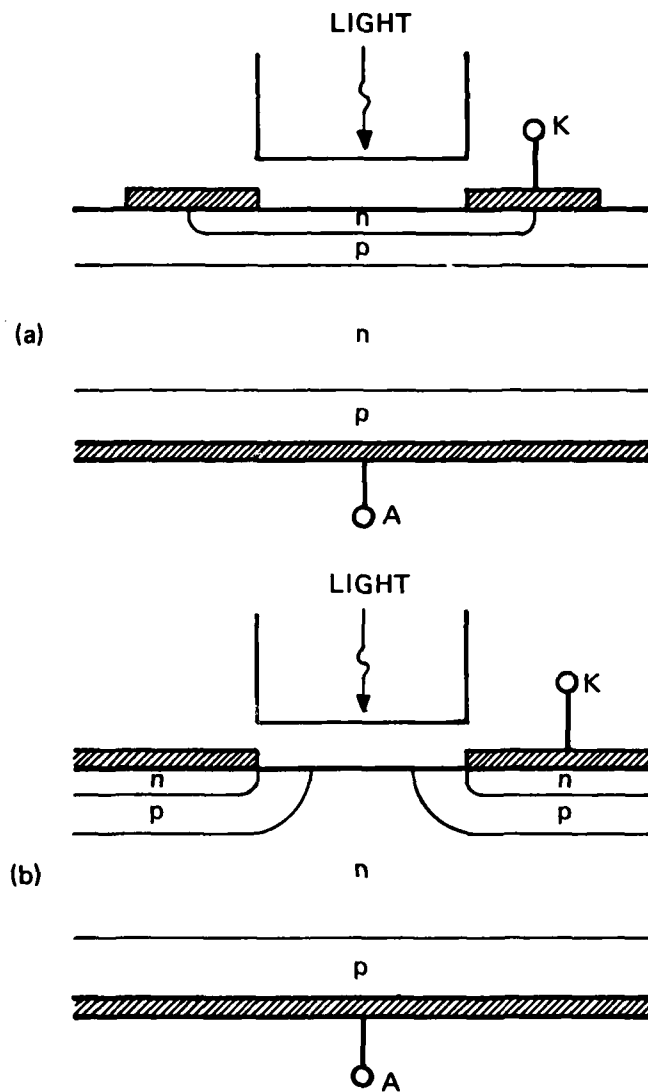


Figure III-15. Light Triggered Thyristors.

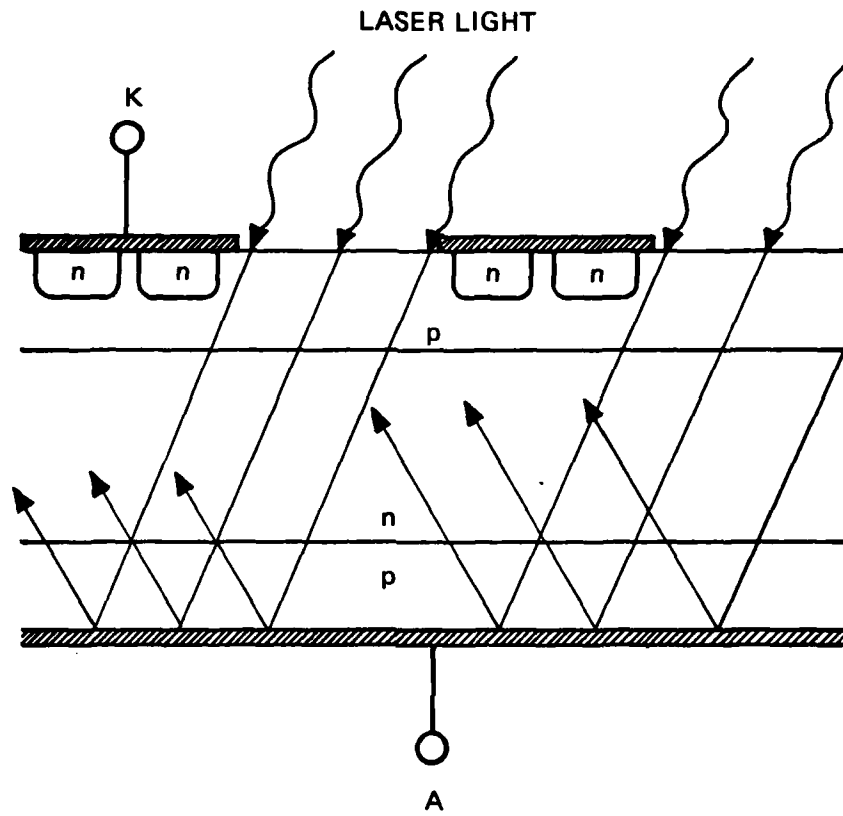


Figure III-16. Laser Activated Semiconductor Switch (LASS).

through openings in the contact metallization, the light, which traverses the silicon by way of internal reflections, will generate hole-electron densities which are great enough to swamp the background concentrations in the base regions, and the device will turn on very rapidly. In principle, switching speeds of 1 psec can be obtained, which is the time required for the light to traverse the wafer. (It is not clear if the light does, in fact, traverse the wafer completely to turn on the entire area, or if a relatively small region is carrier modulated to such an extent as to create an effective short circuit, in which the instantaneous power density is very small.) Mode-locked YAG lasers will generate pulses as short as 20 psec; to obtain carrier densities of  $10^{18} \text{ cm}^{-3}$  in this time requires around  $9 \text{ GW/cm}^2$  peak power.

e. Reverse Conducting Thyristor.

It is possible, by sacrificing reverse blocking capability, to reduce the n-base width while maintaining forward blocking; forward voltage drop and turn-off time are thereby reduced. The basic RCT consists of a thyristor and an integrated antiparallel diode [11], illustrated in Fig. III-17a; the cathode junction has low breakdown voltage, and the anode junction is shorted out by the antiparallel forward biased diode when the thyristor is biased in the reverse direction. It is possible to employ an epitaxial n-p-i-n-p structure [12] to obtain very high forward blocking voltages.



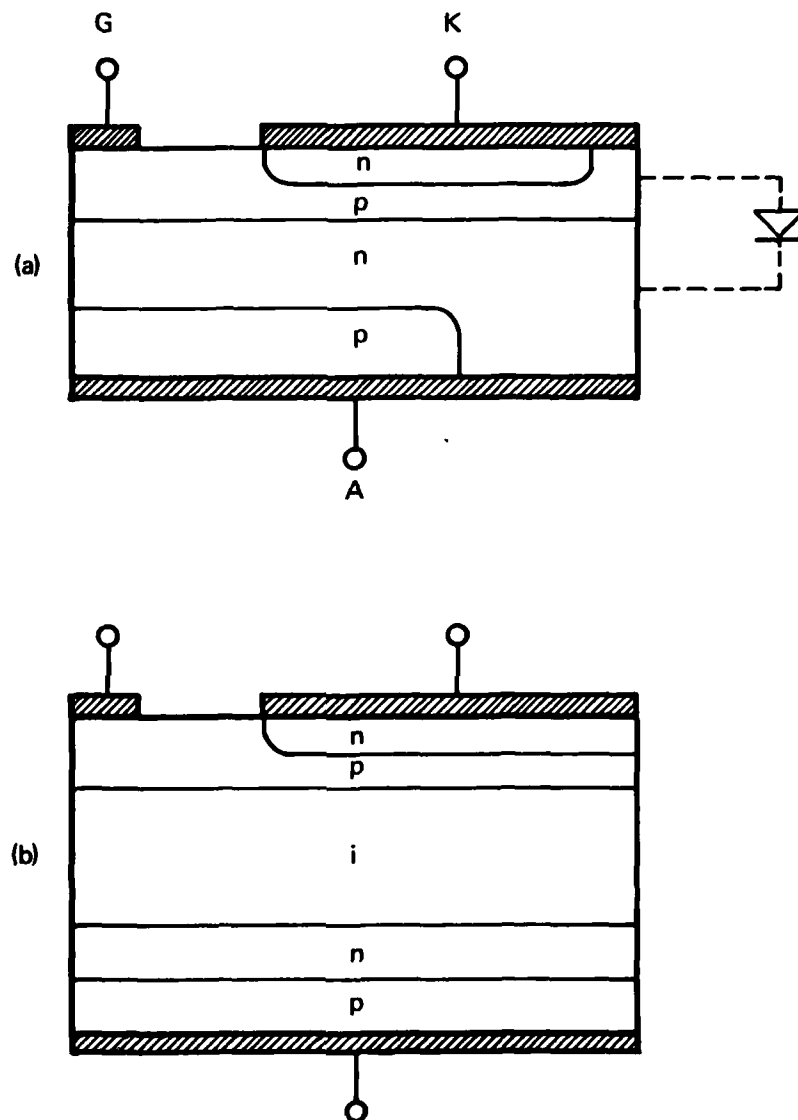


Figure III-17. Reverse Conducting Thyristor. Antiparallel Structure (a); p-i-n Structure (b).

The cathode and anode p-n junctions have low breakdown voltages for the reverse biased thyristor, but forward blocking voltage is dropped across the central reverse biased p-i-n junction (Fig. III-17b).

f. Reverse Blocking Diode Thyristor.

The RBDT, or RSR [13], has essentially the same structure as a conventional SCR, but has no external gate lead. It is self-gated by applying a ramped cathode-to-anode voltage with a time rate of change great enough to exceed its  $dv/dt$  rating.

g. Field Controlled Thyristor.

Strictly speaking, the FCT [14] is not a thyristor, inasmuch as it is not gated on by the conventional thyristor latching mechanism, and, in fact, has turn-off capabilities without commutation. It is more properly described as a vertical channel field effect transistor in series with a reverse blocking diode (Fig. III-18). Reverse blocking is obtained when the p-n anode blocking diode is reverse biased. If a reverse bias is placed on the grid relative to the cathode, the depletion region formed in the lightly doped n-region around the reverse biased cathode p-n junction pinches off the vertical channel, and forward blocking is obtained. The FCT is turned on simply by removing the negative gate bias; in the on-state, the device behaves like a forward biased p-i-n diode. The FCT is turned off simply by reapplying the negative grid voltage.

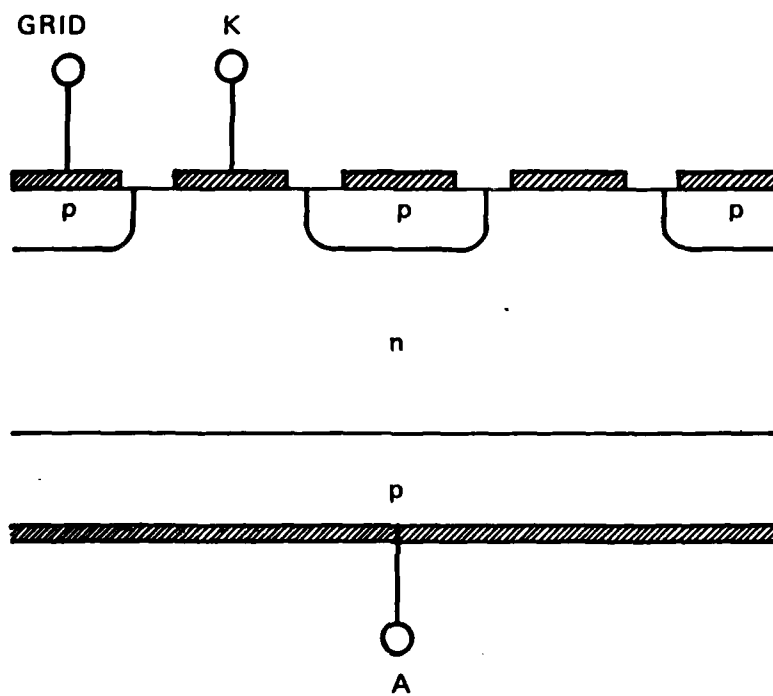


Figure III-18. Field Controlled Thyristor.

## 11. Packaging

High power switches are normally packaged in a flat pack configuration. In the normal package, the wafer is hard soldered between a pair of thermally matched plates such as tungsten or molybdenum. One plate (the anode) is hard soldered to a threaded copper stud, which is the anode connection and heat sink; the other plate is hard soldered to the cathode terminal. The entire assembly is hermetically sealed by a ceramic cap. This method is not practical for the large wafers (greater than 25 mm in diameter) used for high power devices, because of thermally induced stress on the larger wafers. The flat pack, which employs floating contacts, is required. Several configurations are possible [15, 16]; in one, the upper anode plate floats on a pressure contact and a pressure contact separates the cathode from the cathode plate [15]. Another design [16] eliminates all solder joints and has pressure contacts throughout. Both arrangements are contained in a relatively flat cylindrical ceramic package. External pressure on the package is required to assure good electrical and thermal contact. The floating contacts make the package and internal structure less subject to thermal fatigue; for one such configuration, 37 mm devices were cycled three and one-half million times at junction temperatures between 125°C (398°K) and 45°C (318°K) at 1600 amps rms forward current, with no failures [16].

A new package technology has been developed, the transcalent package [17]. The package consists essentially

of two hollow evacuated copper cylinders, each sealed at one end (the device end) with a brazed molybdenum disc, the interior surfaces of which are coated with a thin sintered copper layer which forms a surface of high capillarity, that is, a wick. Anode and cathode currents are conducted through the walls of the tubes, into and out of the device. A separate wire conducts the gate current. A section of one conducting tube wall is made thin with respect to the rest of the tubing. If thermal overloading occurs, perhaps because of repeated excess surging, this segment will melt and open circuit before the silicon device short circuits, and prevent the formation of damaging high short circuit currents. Anode and cathode sections are electrically separated by a segment of high strength alumina.

The active regions of the silicon device wafer are vacuum soldered between the molybdenum discs. The device contacts are chemically vapor deposited tungsten, overplated with nickel for solderability; the discs are lapped for optimum thermal contact and nickel plated also. The thyristors are fabricated on 38 millimeter diameter wafers; the active device region is 21 millimeters in diameter. The additional silicon material is included for greater reliability. All exposed junctions are bevelled and passivated to increase stand-off voltage. Anode and cathode contacts are solid circles; the gate wire is connected to a non-amplifying gate.

A small amount of working fluid is introduced under vacuum into the wicks; water is used because of its thermal

properties in the operating temperature range and its compatibility with the package materials. Thin layers of the fluid are held in the wicks against the molybdenum end-plates. When heat is evolved in the device, the water evaporates and recondenses on the cooler tube walls, which are at uniform case temperature. Heat is exchanged through the copper tube walls and dissipated through cooling fins. The water is pumped back to the molybdenum interface by way of capillary action. Such heat pipe action permits the mounting of the device in any attitude, without clamping.

## 12. Life

The factors which affect the life expectancy of thyristors are not well-defined. The lifetimes of phase control devices are measured in tens of years, as long as they are adequately heat-sinked, and failure modes, excepting those associated with thermal cycling, have not been identified. Package failure, that is, thermal stresses developing at the contact-wafer interface, is probably more important than device failure, that is, electrical failure in the wafer itself.

Thermal failure is important for short pulse, high power switching also, but the failure mechanism is considerably different than for phase control devices. Because the thyristor does not turn on uniformly, high values of  $di/dt$  can cause local burnout; however, even when the  $di/dt$  is kept low enough to prevent catastrophic failure, repeated thermal shocks caused by localized high power dissipation in a small turned on region

can cause eventual mechanical wafer fracture and mechanical destruction of the device [3, 4]. Heating is probably substantially adiabatic in this case, and heat sinking is not effective. Thermal mismatching between the package contact and the silicon wafer also is probably exaggerated, and fracture may occur because of thermally induced contact stress.

More stress test and failure rate data are required under real operating conditions before the important failure mechanisms for switches can be characterized. The measurements are complicated, because localized heating is adiabatic and essentially a non-equilibrium phenomenon, whereas the temperature of the junction is obtained from the temperature dependence of certain device parameters under equilibrium conditions, after the heat has been more-or-less distributed.

### 13. Fast Thyristors

#### a. Commercial

Development of large phase control thyristors has been emphasized in Europe and Japan, where electric railways have been an important market, whereas fast inverters have been a US specialty, although quality European inverters are also available. Commercial power inverters have the conventional thyristor structure, and, in general, their features are similar, depending more on market applications than on the manufacturer. Table 1 lists the important characteristics of ten high power, high frequency switches, available from both US

Table 1. Characteristics of fast, high power, thyristors.

Device Number	Standoff Voltage (volts)	Peak Current (amps)	Forward Voltage Drop (volts)	di/dt A/ $\mu$ s	dv/dt V/ $\mu$ s	Delay Time ( $\mu$ s)	Recovery Time ( $\mu$ s)	Pulse Width	Measurement Rep Rate (pps)	Duty Cycle	Coulombs Per Shot
1	2100	11500	1.4	800	500	1.5	50	200 $\mu$ s	60	1.2%	1.6
2	1200	1700	2.9	800	500	2.5	25	4.2 ms	60	25%	7.1
3	1300	20000	1.8	800	400	0.7	40	200 $\mu$ s	60	1.2%	2.0
4	1200	1500	1.6	800	700	.4	45	1 ms	400	40%	1.5
5	1200	4000 (4000)	1.7	1500	1000		25	100 $\mu$ s (50 $\mu$ s)	600 (60)	6% (.3%)	.32 (.16)
6	1300	1800	1.4	200 (repetitive)	500	1.5	25	10 ms	50	50%	18.0
7	1200	1200	2.0	800	500	.4	25	500 $\mu$ s	690	34%	0.6
8	1200	1700	1.5	400	1000	1.5	30	2.5 ms	200	50%	4.2
9	2200		2.5	1000	400	1.5	40				
10	1200 (forward)	5000	10.0	4500	5000 (trigger voltage)	.1	200	20 $\mu$ s	250	0.5%	0.05



and foreign suppliers. Devices numbers 1 through 9 are conventionally triggered thyristors, with interdigitated gate-cathode structures; all have amplifying gates, devices number 3 and 5 being regenerative. Device number 10 is an RBDT. Performance data were obtained from manufacturer's data sheets for their highest power inverters, except for device number 10; those data were obtained from reference 13.

Voltage standoff is defined as the peak repetitive forward or reverse blocking voltage, except for device number 10, for which it is the forward breakover voltage. Peak current is the highest value which could be obtained from the data sheets for trapezoidal pulsed operation, independent of duty cycle. It should be emphasized that the  $di/dt$  for the leading edge of the pulse for all tabulated peak currents was only 100 A/ $\mu$ s, which is an industry standard, and which does not correspond to the maximum  $di/dt$  which can be sustained at those peak currents, without damage to the device. (Device number 5 is an exception; it has been tested at  $di/dt = 1000$  A/ $\mu$ s, and corresponding results are shown parenthetically in Table 1.) The peak currents themselves are generally not leading edge limited, but are based on thermal impedance and duty cycle. The values for forward voltage drop are not completely consistent, inasmuch as they correspond generally to different

values of peak forward current, but they provide a reasonable comparison between the devices. The tabulated values of  $di/dt$  correspond to non-repetitive conditions, except for device number 6, which has a repetitive value. The values of  $dv/dt$  in Table 1 are self-triggering values, and do not include recovery time limits imposed by rapid reapplication of forward blocking voltage after turnoff. The delay time is the time interval between the beginning of a gate pulse and the time when the forward voltage has dropped to some fraction of its blocking value. (The fraction depends on the standard, which may or may not include the fall time, typically 100 to 125 ns) Recovery time is the circuit commutated turn-off time, that is the interval between the time when the forward anode current goes to zero and the time when the forward blocking voltage can be reapplied at its full  $dv/dt$  value.

Typical jitter is less than 2 nsec [15] if the gate is overdriven at two to three times its minimum trigger value; factors affecting jitter have not been clearly identified. Lifetime information was generally not available, except for a commercial version of device number 10, which is being life-tested as part of a larger life-test program of a radar modulator. This device has been operated continuously, except for minor interruptions, for 2000 hours, switching a 3  $\mu$ sec, 2200 A current pulse at 365 pulses per second. Reliability calculations have been made [3, 18, 19] on

selected devices, but are not included as part of the data issued by manufacturers. Thermal impedance data are usually provided so that safe operating conditions may be determined; these are related to the safe peak current values for pulsed operation at various pulse repetition rates and duty cycles. For normal applications, employing relatively wide pulses, safe operation is related to power dissipated during the on-state, as long as the leading edge  $di/dt$  is low enough to prevent localized burn-out. However, when fast, high power pulses are involved, the rise times become so short that the limiting constraint is  $di/dt$ , and data respecting safe operation are not available.

b. In Development

Although non-conventional thyristor structures, such as the ASCR, are being developed for higher frequencies and voltages, these still depend on carrier diffusion to spread the conduction plasma through the device and are limited, according to the previous estimate, to peak currents of around 10 kA and to  $di/dt$  values of around  $1 \times 10^5$  A/ $\mu$ s. It is possible to reduce the voltage fall time sufficiently so that the value of  $di/dt$  can be substantially increased, and to reduce the power dissipated during turn-on so that safe peak currents can be increased also; these improvements can be made by direct laser triggering.

The light activated semiconductor switch (LASS) has a conventional thyristor structure, but is designed for optical,

rather than electrical triggering. The light pulse, typically produced by a Q-switched laser, provides the energy to generate carrier concentrations throughout the illuminated portion of the base regions at least as great as those occurring when the thyristor is on. Turn-on is free of the usual transit time delays, and very high values of  $di/dt$  can be sustained. Table 2 contains the results of several experiments [9, 20] which indicate the capability of the LASS. A Q-switched neodymium-doped YAG laser ( $1.06 \mu\text{m}$ ) was used to illuminate the switch wafer; the laser output was around 3 to 5 mJ per pulse, and the duration of the light pulse was around 10 nsec. The optically generated carrier density in the base regions was approximately  $10^{18} \text{ cm}^{-3}$ . If the previous calculation for limiting  $di/dt$  is reasonable, and it is assumed the current rise times are comparable to the voltage fall times, then the voltage fall times associated with laser triggering are in the order of 10 nsec, a factor of ten faster than the fall times associated with electrical triggering. It is likely that jitter is minor with laser triggering.

#### c. Summary

Switching thyristors which can be obtained commercially today have several common features: they have conventional thyristor structures, amplifying gates, and are, with one exception, gate-triggered with an electrical pulse. They can sustain high peak currents (some as high as 20 kA) for low duty cycles and low  $di/dt$  (although device number 5

Table 2. Characteristics of the LASS.

Test Number	Line Voltage (volts)	Peak Current (amps)	di/dt (A/ $\mu$ s)	Pulse Risettime (ns)	Pulse Width	Measurement Rep Rate (pps)	Duty Cycle	Coulombs Per Shot
1	1000	5000	$1.6 \times 10^4$	316	40 $\mu$ sec			.02
2	1100	7100	$6.5 \times 10^5$	11	50 nsec	1000	.005	$73.6 \times 10^{-4}$
3	1000	9800	$7.5 \times 10^5$	13	50 nsec	1000	.005	$5 \times 10^{-4}$

tolerate high values of peak current up to 1000 A/ $\mu$ s for low duty cycles). It is not possible to establish the limits of operation with respect to pulsed power for existing thyristor switches from manufacturer's data alone. If device number 5 is representative, the data may be too conservative, and additional measurements are required adequately to define thyristor capabilities in short pulse, low duty cycle operation.

14. References

- [1] A. Herlett and P. Voss, "State-of-the-art in power semiconductor devices," IEEE International Semiconductor Power Converter Conference, Orlando, Florida, March, 1977.
- [2] J. Burtscher, F. Dannhäuser and J. Krausse, "Die Rekombination in Thyristoren and Gleichrichtern aus Silizium: ihr Einfluss auf die Durchlasskennlinie and das Freiwertzeitverhalten," Solid-St. Electronics 18, 35 (1975).
- [3] I. L. Somos, "Current conditions for meaningful di/dt test," World Electrotechnical Congress, Moscow, USSR, June, 1977.
- [4] G. Karady and R. Casse, "Design philosophy of the 600 MW pulsed energy converters for the toroidal field coil of TFTR at Princeton," Proceedings of the Seventh Symposium on Engineering Problems of Fusion Research, IEEE Publication Number 77CH1267-4-NPS, 874 (1977).
- [5] R. Rosch, "Über die laterale Zundausbreitung in Leistungsthyristoren," Ph.D. Dissertation, Aachen, 1973.
- [6] P. S. Raderecht, "The development of a gate assisted turn-off thyristor for use in high frequency applications," Int. J. Electronics 36, 399 (1974).
- [7] E. S. Schlegel, "Gate-assisted turn-off devices," IEEE Trans. El. Dev. ED-23, 888 (1976).
- [8] A. Blicher, Thyristor Physics, Springer-Verlag, New York, 1976.
- [9] O. S. Zucker, J. R. Long, V. L. Smith, D. J. Page and J. S. Roberts, "Nanosecond switching of high power laser activated silicon switches," International Topical Conference on Electron Beam Research and Technology, Albuquerque, New Mexico, November, 1975.
- [10] L. R. Lowry and D. J. Page, "Light activated semiconductor switches," Westinghouse Research and Development Laboratories Scientific Paper 77-1F5-SW1TS-P1, May, 1977.
- [11] R. A. Kokosa and B. R. Tuft, "A high-voltage, high-temperature reverse conducting thyristor," IEEE Trans. El. Dev. ED-17, 667 (1970).
- [12] P. Smith, I. Martin and K. Gooen, "High power, high frequency epitaxial ASCR," Technical Digest, Page 298, International Electron Devices Meeting, Washington, D.C., December, 1977.

- [13] R. A. Gardenghi, "A super power RSR," International Electron Devices Meeting, Washington, D.C., December, 1975.
- [14] D. E. Houston, S. Krishna, D. E. Piccone, R. J. Finke and Y. S. Sun, "A field terminated diode," IEEE Trans. El. Dev. ED-23, 905 (1976).
- [15] General Electric SCR Manual, Fifth Edition, 1972.
- [16] S. D. Prough and J. Knobloch, "Solderless construction of large diameter silicon power devices," Record of the IEEE IAS Twelfth Annual Meeting, Los Angeles, October 1977.
- [17] S. W. Kessler, R. E. Reed, H. Shoemaker and K. Strater, "Transcendent solid-state power devices," RCA Report PE-679, 1976.
- [18] W. H. Tobin and S. J. Wu, "Safe junction temperature criteria for thyristors in high frequency pulse applications," Proceedings of the IEEE Industry Applications Society Conference, 477.
- [19] I. L. Somos and D. E. Piccone, "Temperature excursion in thyristors due to short current pulses during forward conduction and reverse recovery time," Proceedings of the IEEE Industry Applications Society Conference, 495.
- [20] J. R. Davis and J. S. Roberts, "Ultra-fast, high-power laser-activated switches," IEEE PESC Record, 262 (1976).



## B. Transistors

### 1. Transistor Properties

A transistor is a semiconductor opening and closing switch, whose switching action is controlled by the presence or absence of current flow through a p-n junction (the emitter-base junction). When the p-n junction is forward biased, and forward diode current flows, the switch is closed and it conducts collector current. When the emitter-base junction is short-circuited or reverse biased, the switch is open. The transistor is a three-layer (Fig. III-19a) three-terminal (Fig. III-19b) device, with connections to an emitter, a collector and a control base. Specifications of a transistor as a switch are similar to those for a thyristor, except that transistors do not self-trigger, that is, there is no  $dv/dt$  specification for transistors.

### 2. High Power Transistors

Three commercial transistors are of particular interest; their characteristics are listed in Table 3. All three transistors are triple diffused n-p-n devices, with the  $n^+ - p - v - n^+$  (where  $v$  represents a very lightly doped, high resistivity near intrinsic n-type region) structure obtained by a double diffusion, but having a third, separate, collector diffusion instead of simultaneous emitter and collector diffusions.

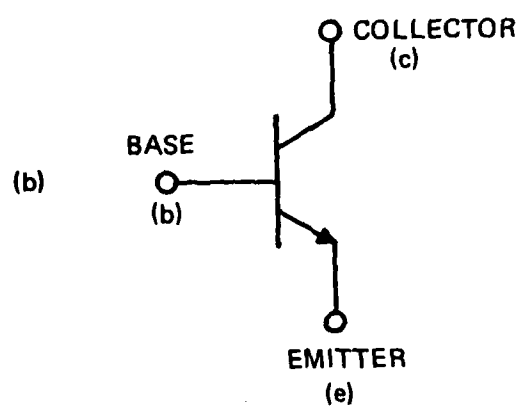
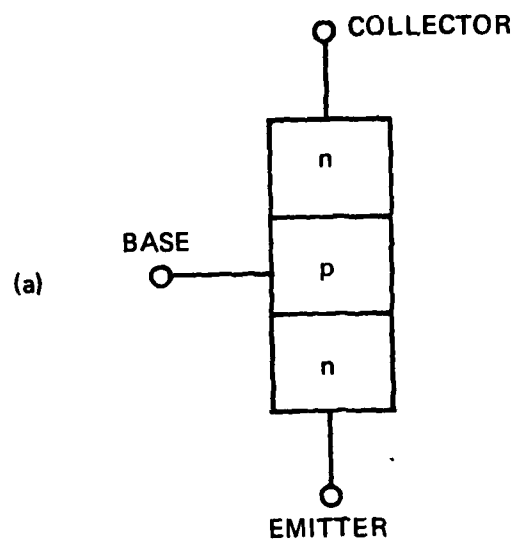


Figure III-19. Basic Transistor Structure (a);  
Transistor Terminal Connections (b).

Table 3. Characteristics of high power transistors.

Device Number	Standoff Voltage (volts)	Peak Current (amps)	Forward Voltage Drop (volts)	$h_{fe}$	$di/dt$ (A/ $\mu$ s)	Delay Time ( $\mu$ s)	Recovery Time (ns)	Pulse Width ( $\mu$ s)	Measurement (pps)	Duty Cycle	Coulombs Per Shot
1	500	60	.8	10	62	.8	5.3	20	5000	10%	.0012
2	500	50	.8	15	100	.6	3.0	100	200	2%	.005
3	300	400	2.0	1500	800	.5	16.5	300	100	3%	.12
	(60)	(60)	(1.0)	(620)		(.5)	(17.7)				
	(50)	(50)	(.9)	(500)		(.5)	(17.5)				

The values for standoff voltage are the  $V_{cesat}$  values for the transistors; peak current is the value of the collector current switched. Devices number 1 and 2 were tested under similar conditions; the collector current switched in device number 3 was considerably higher. Values of several parameters obtained from the manufacturer's curves for device number 3 are shown parenthetically for comparison with those for devices number 1 and 2. The values of  $di/dt$  were estimated by dividing the peak current by the pulse rise time. The delay is the sum of the elapsed time from the initiation of the base current pulse to the beginning of the collector current pulse and the rise time of the collector current pulse. The recovery time is the sum of the storage time measured from the end of the base drive pulse to the beginning of collector current turn-off and the fall time of the collector current pulse.

Device number 2 appears to have characteristics quite similar to those of device number 1. It is difficult to compare the performance of device number 3, inasmuch as it is a monolithic Darlington arrangement; that is, a drive transistor is formed on the same wafer as the main transistor at the time that the latter is fabricated, and integrated with it in a Darlington configuration. The gain limitations of the main transistor are obscured, and the performance of the combination may not be superior to a Darlington amplifier

formed by devices number 1 and 2 with a second discrete transistor. Turn-on times for device number 3 might be expected to be comparable to or better than those for devices number 1 and 2, if the drive transistor is small and its base is overdriven, and its gain is high enough to overdrive the base of the main transistor. Turn-off times, under these conditions, would be longer than for devices number 1 and 2, consistent with the data shown in Table 4.

Devices number 2 and 3 are contained in the flat pack; device number 1 has a transcalent package [1, 2]. However, the emitter in the transcalent package is not soldered to the emitter disc, but has an emitter ballast resistance wafer clamped between the emitter disc and seventy-two emitter fingers. The emitter ballast wafer is mesa-etched to align with the emitter fingers, then gold-plated to obtain conformable pressure contacts; its purpose is to force a uniform emitter current distribution, and inhibit the occurrence of thermal instabilities. A molybdenum ring is soldered to the base contact for uniform base current distribution; the base wire is connected to the ring. Collector and emitter thermal impedances are somewhat different, emitter thermal impedance being somewhat higher because of the presence of the emitter ballast wafer.

#### a. Standoff Voltage

The principal design consideration for high power transistors is the standoff voltage, that is, the collector-base junc-

tion breakdown voltage. Starting resistivity, diffusion depths and base widths are all chosen with respect to the voltage requirements, and switching performance is affected by those choices. Fabrication processes are affected as well; device configurations must be consistent with high voltage operation. These processes and structures are discussed below.

Several types of processing are involved in the fabrication of power transistors: a single two-sided diffusion into a lightly doped substrate (Fig. III-20a); a double diffusion (Fig. III-20b); a double-diffused epitaxial process; and a double epitaxial process. The single-diffused device ( $n^+ - p - n^+$ ) requires wide bases to prevent punch-through before avalanche breakdown occurs at the collector-base junction, reducing the current gain. The current gain is additionally reduced by the reduced injection efficiency which is a consequence of the deep emitter diffusion required in a simultaneous collector and emitter single diffusion.

The high voltage performance of power transistors can be improved by starting with low resistivity n-type material and performing a second diffusion. In the double-diffused structure of Fig. III-20b ( $n^+ - p - v - n^+$ ), the high reverse voltage of a  $p - v - n^+$  diode of comparable width can be supported by the  $v$ -region, which also inhibits punchthrough. The  $n^+ - p - v - n^+$  structure is the most common high power transistor structure.

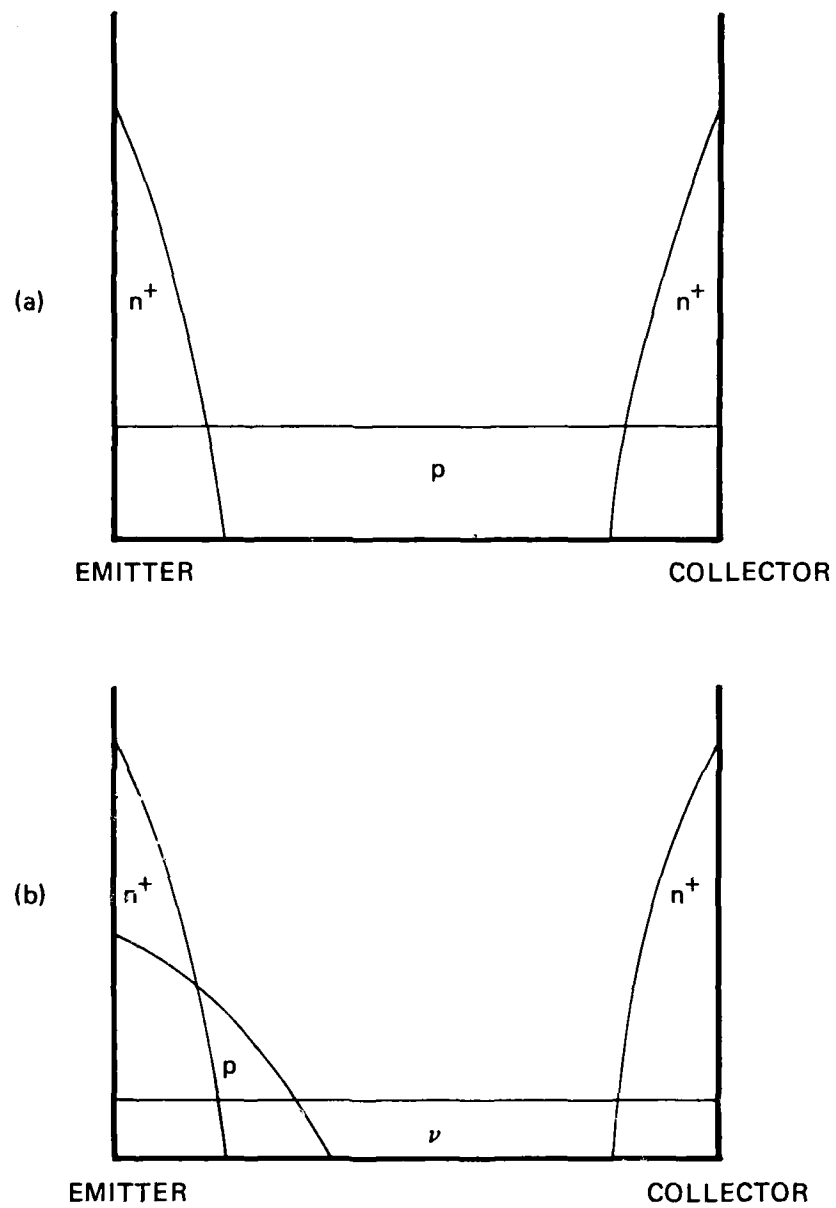


Figure III-20. Impurity Profiles for an  $n^+p-n^+$  Transistor (a); for an  $n^+p-v-n^+$  Transistor (b).

### b. Pulse Current and Gain

The current gain (the ratio of collector current to base current) of a transistor falls off considerably at high forward current densities. As emitter current increases, the minority carrier density injected into the base becomes large enough to cause the conductivity of the base region to increase, (conductivity modulation) and the emitter injection efficiency falls off. Emitter debiasing, the result of voltage drops in the base at high base currents, causes emitter current crowding which exaggerates base conductivity modulation. The increase in base conductivity at high forward currents in an  $n^+p-n^+$  transistor also reduces the collector-base depletion width, which increases the effective base width. Additional stored charge in the base reduces the injection efficiency even further, and the increased base width also reduces the base transport factor.

In an  $n^+p-v-n^+$  device, the effect of high currents is to conductivity modulate the  $v$ -region, reducing its resistivity relative to the  $p$ -base, so that the depletion width in the  $p$ -region will expand, reducing the effective base width. However, the voltage drop across the undepleted portion of the  $v$ -region increases with increasing forward currents; less voltage is available to maintain wide depletion at the  $p-v$  junction and the depletion layer shrinks, increasing the base width. The net effect is a wider base width and gain fall-off at high currents. In general, forward current gain will be low for all types of power transistors at high collector currents.



Destructive effects at high currents are generally the result of high temperatures which follow the formation of current constrictions. The constrictions themselves can be initiated by emitter debiasing or enhanced local avalanche multiplication or microplasma formation; the latter events are more likely to occur under reverse bias conditions, when the transistor is turning off. Narrow current channels are regenerative; increased temperature enhances increased current flow, which increases temperature. High forward current stability can be enhanced by interdigitation of the emitter and base contacts. The emitter area can be maintained by employing a large number of narrow emitter fingers; if the fingers are narrow enough, relatively little debiasing occurs. Current hogging (that is excess emitter current flowing through one finger), which tends to be regenerative, is avoided by ballasting the fingers, that is, by inserting a temperature dependent resistance, with a positive temperature coefficient, in series with each finger. One such ballasting arrangement occurs in the transcalent package previously described.

#### c. Delay and Recovery

Delay and recovery effects in transistors are the result of junction depletion and charge storage capacitances. When a base signal is first applied, the emitter base depletion capacitance must be charged through the

source output resistance and transistor input resistance before base current can flow. The charging time constant is the intrinsic delay time of the transistor, which, when added to the rise time of the collector current pulse, establishes the transistor switching delay time. As the base current increases, and the transistor turns on, charge is stored in the base region as base current flows. This stored charge represents an equivalent storage capacitance which must be charged up as the collector current increases, and which affects the rise time of the collector current pulse. Switching delay time may be reduced by overdriving the base with base currents in excess of those required to sustain a given collector current, but such overdriving reduces the effective current gain and introduces excess charge to be stored in the base, increasing the collector current fall time, hence the recovery time.

Switching recovery time is determined by the storage capacitance, which must be completely discharged before the current pulse is off. The recovery time has two components, the storage time required to remove excess stored charge introduced into the base by base overdrive currents and the pulse fall time, which corresponds to the removal of stored charge introduced by normal base drive.

#### d. Current Rise Time

The maximum value of  $di/dt$  is determined by the rise time of the collector current. (Current constrictions, caused by

emitter debiasing, are not important in this respect, except as they are related to the value of the peak current.) Propagation delays, such as those occurring with respect to the turned on region in a thyristor, do not exist in the base of a transistor; the time required for the base signal to propagate through the base region, less than 0.5 nsec, is essentially the velocity of light in the silicon. The pulse rise time may be increased by base overdrive; however, inasmuch as the maximum pulse repetition rate depends on the recovery time, an increase in  $di/dt$  will be accompanied by a diminished pulse repetition rate.

#### e. Output Characteristics

The introduction of a  $v$ -layer affects the output behavior of a transistor. Figure III-21a illustrates typical output characteristic curves for an  $n^+p-n^+$  transistor; these represent the conventional common emitter behavior of a transistor. The collector-base junction is forward biased in the saturation region (region I); the slope of the limiting curve is the inverse of the collector resistance. Region II is the active region in which the collector-base junction is normally reverse biased. The presence of the  $v$ -layer introduces a third region (region III in Fig. III-21b) into the output curves, the quasi-saturation region. In true saturation (region I), the base-collector ( $p-v$ ) junction is heavily forward biased and the  $v$ -region is conductivity modulated, so that the voltage

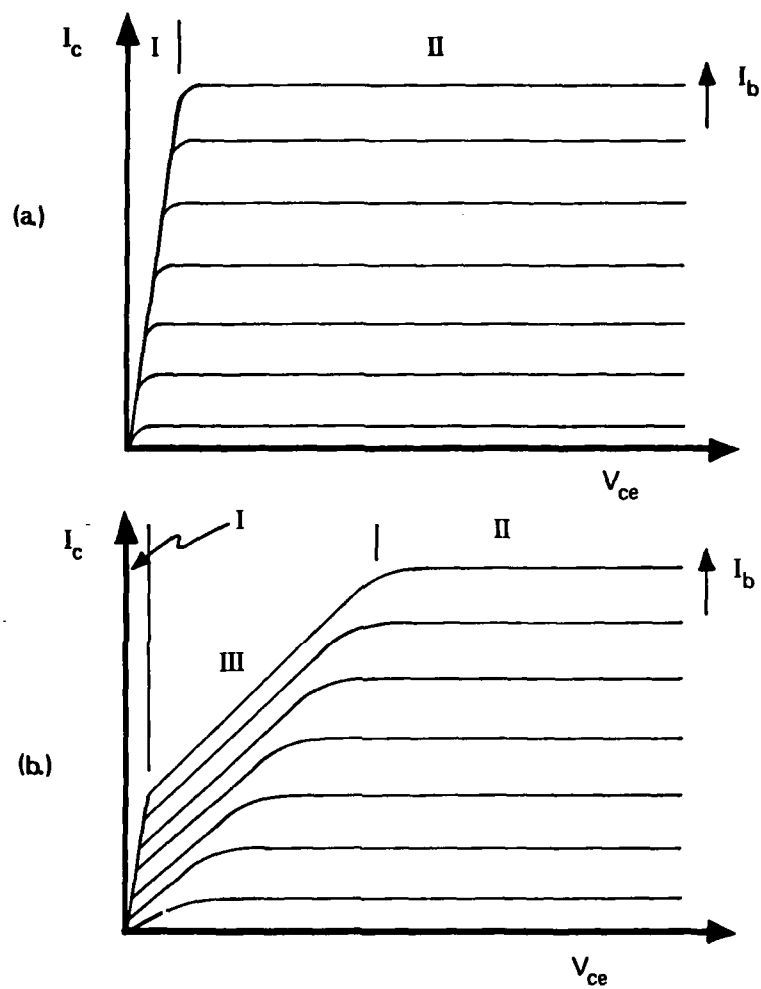


Figure III-21. Output Characteristics for an  $n^+ - p - n^+$  Transistor (a); for an  $n^+ - p - v - n^+$  (b).

drop across it is low. As the transistor begins to come out of true saturation, the base-collector junction becomes less heavily forward biased and the  $v$ -region is conductivity modulated over less of its width so that the collector resistance increases, becoming the resistance of the  $v$ -region for low  $p$ - $v$  forward biases. This resistance is much greater than the resistance of the  $n^+$ -region, and the transistor is in quasi-saturation. In the active mode, the collector-base junction is reverse biased; the  $v$ -region is completely depleted and the output resistance is the resistance of a reverse biased  $p$ - $n$  junction.

f. Forward Voltage

Although breakdown voltage is improved by introducing the  $v$ -region, the forward voltage in the on-state, typically several tenths of a volt, is also increased. Turn-on (delay) time is relatively high in quasi-saturation, so that power dissipation may be increased excessively during turn-on. Figure III-22 compares the turn-on characteristics for  $n^+$ - $p$ - $n^+$  and  $n^+$ - $p$ - $v$ - $n^+$  transistors. It is possible, by increasing the base doping level, to reduce the final on-state voltage drop across the transistor, and to reduce the delay time, but quasi-saturation effects are not eliminated, and turn-on times remain relatively high.

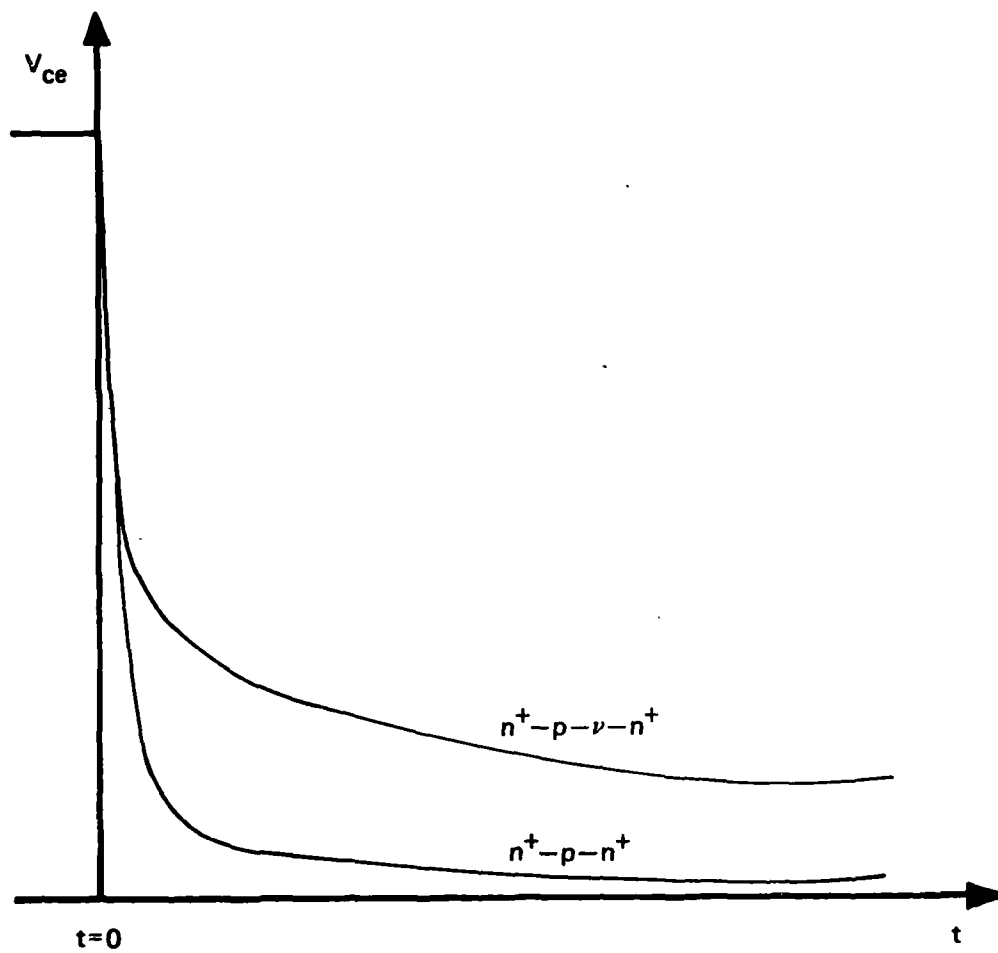


Figure III-22. Turn-On Behavior of  $n^+-p-n^+$  and of  $n^+-p-v-n^+$  Transistors.

### g. Life

The life of transistors is established generally by the same constraints which affect the life of thyristors. If a transistor is well-enough heat sunked, it is reasonable to expect a lifetime in the order of tens of years, providing that transient adiabatic heating is not so great as to cause catastrophic damage. Transistors, moreover, do not experience the pulsed thermal shocks which damage thyristors when high currents are required to flow through small turned-on regions. A transistor with dimensions comparable to those typical for a thyristor inverter will turn on in around 0.5 nsec, the time required for the base signal to propagate across the base. Within the same period of time, approximately 0.001% of the total thyristor area will conduct. However, transistors can be driven into unstable operation relatively easily, particularly when switching inductive loads, and catastrophic failure can quickly result once a transistor has been driven into an unsafe power dissipation region.

### 3. Summary

Transistor switches have an advantage over thyristors insofar as they will turn off, they are not  $dv/dt$  limited, and their  $di/dt$  values are not constrained by small conduction volumes. However, available transistors are not capable of supporting the very high pulsed currents required in pulsed

power switching. Furthermore, the transistor has poor surge capability; that is, for a given base current, it must go out of saturation to accommodate higher collector currents. Simultaneous high voltages and high currents occur, and the possibility of burnout is considerable. Finally, the transistor suffers the same limitations on duty cycle as the thyristor imposed by recovery time and thermal dissipation.

#### 4. References

- [1] R. Eaton, S. W. Kessler, Jr. and R. E. Reed, "Development of a transcendent silicon power switching transistor," Record of the IEEE IAS Twelfth Annual Meeting, Los Angeles October, 1977.
- [2] S. W. Kessler, R. E. Reed and D. R. Trout, "Development of a high voltage and high current transcendent transistor," Final Technical Report, US Army MERADCOM Contract Number DAAK -2-C-0642, RCA, Lancaster, Pennsylvania, November, 1977.



CHAPTER IV

SPARK GAPS

M. Kristiansen and M. O. Hagler

### A. Introduction

Spark gaps are among the most widely employed switches in pulsed power technology. They cover an impressive range of voltages, currents, Coulomb transfer, rep-rate, etc. Whenever a special switch is needed for a special application the first thought is usually to employ a spark gap. Only a limited range of spark gaps are available, off-the-shelf, because of the extremely wide range of applications and requirements.

Because of the widely different applications and the "make-as-needed" manufacturing of spark gaps there has been very little uniform testing and/or specification of spark gap performance parameters. This makes it very difficult to make an organized comparison of the various gaps since most of them have not undergone the same testing procedure. Spark gaps also come with a wide range of shapes (e.g. coaxial or rail geometry), trigger methods (e.g. field distortion or trigatron), and dielectrics (vacuum, gases, liquids, or solids). For the purpose of this report we have subdivided the spark gaps according to the dielectric medium. The solid dielectric spark gap is described, however, in Chapter VI.

The basic factors involved in designing spark gaps are the field geometry, the dielectric material in the gap,

the temporal history of the applied voltage, the load characteristics, and the rep-rate and life requirements. Reference [1] gives an excellent review of the effects of field geometry and the properties of a wide range of dielectrics under various conditions. Suffice it, therefore, to point out here the general concept of "field enhancement" factors [1]. For a general 2-element electrode structure the field enhancement factor  $f_1$  can be defined as the maximum electric field strength divided by the average electric field. The maximum electric field usually occurs at the electrode with the smallest radius of curvature and the "average electric field" is defined as the potential difference between the two electrodes divided by the smallest electrode separation. The factor,  $f_1$ , is thus a measure of how much stronger the field is somewhere in the gap than for the parallel plate geometry. Another field factor  $f_2$  is derived from  $f_1$  by multiplying it by the ratio of the maximum system dimension to the minimum electrode separation ( $R/r = p$ ). The factor  $f_2$  as a function of  $p$  always has a minimum and its importance is in the fact that at  $f_{2min}$  the maximum field stress in the system has its lowest possible value for a given geometry voltage, and system size.

As an example, consider two concentric cylinders of radius  $r$  and  $R$  ( $R > r$ ). The average electric field is  $V_0/(R-r)$ . By definition  $f_1 = E_{max}/E_{avg}$ . It is easy to show

that  $f_1 = \frac{R-r}{r \ln R/r}$  which gives  $f_2 = \left(\frac{R}{R-r}\right) \left(\frac{R-r}{r \ln R/r}\right) = \frac{R/r}{\ln R/r}$ . Setting the derivative of  $f_2$  with respect to  $R/r$  equal to zero, one finds that the minimum stress occurs at  $R/r = e = 2.718 \dots$ . The maximum field values for a given applied voltage,  $U$ , and several typical geometries [2] are given in Table IV-1.

In some cases it may be desirable to have an electrode configuration with the maximum field uniform and in the center of the electrode system. Examples of this kind of electrode arrangement are Rogowski [3] and Bruce [4] profiles. Both are essentially the same but the latter is easier to fabricate. The breakdown strength of a nonsymmetric, non-uniform field gap tends to be polarity dependent. For instance the vacuum insulation of a gap is less when the high field region is negative than when it is positive, due to electron field emission. In gases (depending on pressure) and liquids the opposite tends to be true, probably because space charge effects at the negative electrode modify the electric field [1]. The polarity effect tends to be enhanced for short, fast pulses.

The electric breakdown strength of dielectrics is also area dependent. The larger the cross-sectional area, the lower the dielectric strength. This can be expressed, for a continuous probability distribution, as [1]:

$$\text{cum } P_{bd_n} = 1 - (1 - \text{cump})^n,$$

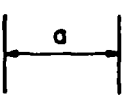
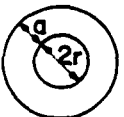
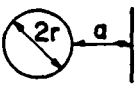
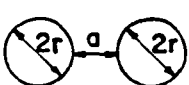
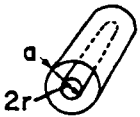


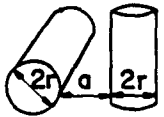
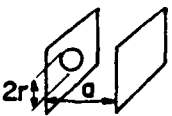
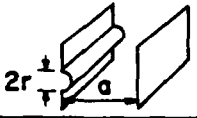
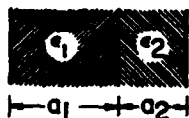
Configuration		Formula for E
Two parallel plane plates		$\frac{U}{a}$
Two concentric spheres		$\frac{U}{a} \frac{r+a}{r}$
Sphere and plane plate		$0.9 \frac{U}{a} \frac{r+a}{r}$
Two spheres at a distance a from each other		$0.9 \frac{U}{a} \frac{r+a/2}{r}$
Two coaxial cylinders		$\frac{U}{2.3 r \lg \frac{r+a}{r}}$
Cylinder parallel to plane plate		$0.9 \frac{U}{2.3 r \lg \frac{r+a}{r}}$
Two parallel cylinders		$0.9 \frac{U/2}{2.3 r \lg \frac{r+a/2}{r}}$
Two perpendicular cylinders		$0.9 \frac{U/2}{2.3 r \lg \frac{r+a/2}{r}}$
Hemisphere on one of two parallel plane plates		$\frac{3U}{a}; (a \gg r)$
Semicylinder on one of two parallel plane plates		$\frac{2U}{a}; (a \gg r)$
Two dielectrics between plane plates ( $a_1 > a_2$ )		$\frac{U \epsilon_1}{a_1 \epsilon_2 + a_2 \epsilon_1}$

Table IV-1 Maximum field strength E with a potential difference U between the electrodes, for different electrode configurations. [2]

where  $\text{cum } P_{bd_n}$  is the cumulative probability of breakdown at a given voltage for  $n$  identical areas in parallel and  $\text{cump}$  is the cumulative probability for breakdown at the same voltage for one area (e.g. If  $\text{cump} = 0.01$  and  $n = 100$  then  $\text{cum } P_{bd_{100}} = 0.634$ ). Impurities or bubbles in the dielectric medium (solid or liquid) tend to lower the breakdown. In liquids this can be particularly severe for long stress-times, polar impurities, or impurities with exceptionally high dielectric constant (such as water). For cavities in solids the dielectric degradation can be a gradual process caused by local discharges inside the cavities.

Electrode materials and surface conditions also affect the electric breakdown strength of a gap. Rough surfaces tend to lower the breakdown strength and at high field values, materials with low work functions tend to (but not always) give a lower breakdown field. Dielectric coatings on the electrode surfaces can often improve the breakdown strength in vacuum [5], gases [6] and liquids [7].

The breakdown field is also time dependent. For a rapidly rep-rated gap the breakdown field depends, of course, on the immediate past history of the gap. Even for a "fresh" gap, however, the breakdown field is time dependent. Pulse charged gaps tend, in general, to exhibit higher breakdown fields than statically charged gaps. If the pulse is shorter than the formative time lag (see Appendix I) of the discharge then the hold off field strength can be dramatically improved (up to factor of 100 for  $t < 100$  ns in large vacuum gaps).

A limiting factor in some spark gap designs is the surface flashover of the insulating spark gap housing. The surface flashover potential is generally less than for the same distance in the gap dielectric medium. Some materials exhibit better tracking properties [1] and less permanent voltage degradation than others. The general topic of surface flashover is a complicated one and still the subject of much research since it is a limiting factor in many high voltage designs. Some general rules such as using voltage grading (e.g. metal plates providing capacitive grading for pulse charged gaps or grooves in the dielectric) and/or materials with dielectric constants which match that of the ambient environment (air, oil, etc.) help to reduce this problem. The issue is not addressed in any detail here since it is not considered to be a basic aspect of the switching operation.

The development of pulsed charged, single shot, spark gaps has reached a high state-of-the-art as shown in Table IV-2 [8]. Some of the experiences with these limited lifetimes ( $< 10,000$  shots) gaps show that  $\text{SF}_6$  and Molybdenum work particularly well and that  $\text{SF}_6$  and brass, which is cheaper, also work quite well.

A brief review of spark gaps, centered around the work at Culham Laboratories is given in ref [10]. This review also has a fairly long list of references to earlier work.

Table IV-2. Pulsed-Charged Sparkgaps [8]

<u>TYPE</u>	<u>OIL</u>	<u>WATER</u>	<u>GAS</u>
Self-Break Single Channel ~ $\mu$ s Charging Time	12 MV ~ ns jitter (Aurora Diode Exp.)	5 MV ~ ns jitter (Gamble II, Pithon)	4 MV ~ 25 ns jitter (Pulserad 738)
Self-Break Single Channel ~ .1 $\mu$ s Charging Time			6 MV ~ 1 ns jitter (Temps)
Self-Break Multichannel ~ .1 $\mu$ s Charging Time	3 MV few ns jitter (Proto I)	4 MV few ns jitter (Pithon)	2 MV ~ 1 ns jitter (Siege II)
Triggered Multichannel	12 MV 5-10 ns jitter (Aurora)	5 MV 5-10 ns jitter (Owl II)	4 MV ~ 1 ns jitter (Gamble II, Pulsar "DQ" Switches)

Maximum  $\frac{di}{dt} \sim 5 \times 10^{14}$  A/s

Maximum  $\frac{dv}{dt} \sim 5 \times 10^{14}$  V/s

Not same system [9]. The  $\frac{dv}{dt}$

in this case does not refer to the recovery voltage but rather the load voltage.



In the following we discuss the basic features of various spark gaps (according to the dielectric medium classification) along with special aspects such as triggering, erosion, and rep-rating.

### References

- [1] A. S. Denholm, et.al., "Review of Dielectrics and Switching," AFWL-TR-72-88.
- [2] A. B. Bowers and P. G. Cath, "The Maximum Electric Field Strength for Several Simple Electrode Configurations," Phillips Tech. Rev. 6, 270 (1941).
- [3] J. D. Cobine, Gaseous Conductors: Theory and Engineering Applications, Dover Publications, N.Y. (1958) (original reference not available).
- [4] F. M. Bruce, "Calibration of Uniform-Field Spark Gaps for High Voltage Measurements at Power Frequencies," J. IEE (London) 94, 138 (1947).
- [5] L. Jedynuk, "Dielectric Coatings in Vacuum Gaps," Proc. Int. Symp. Ins. High Voltages in Vac., 147, Boston, Oct. 1964.
- [6] P. I. McNeall and D. J. Shipper, Proc. Int. Conf. Gas Discharges and the Elect. Supply Industry, CERL, England (1962).
- [7] A. A. Zaky, et.al., "Influence of Electrode Coatings on the Breakdown Strength of Transformer Oil," Nature 202, 687 (1962).
- [8] Ian Smith, ISI, Private Communication.
- [9] J. C. Martin, "Short Pulse High Voltage Systems," Energy Storage, Compression, and Switching, Plenum Press, N.Y. and London, 1976.
- [10] T. E. James, "Fast High Current Switching System for Megajoule Capacitor Banks," CLM-123, Culham Laboratory, 1973.

## B. Gas Gaps

### 1. Introduction

Gas filled gaps are commonly used and have the principal advantages of low losses, self-healing, and moderate shock problems in rep-rated operation. The basic theory of gas breakdown is summarized in Appendix I. The fundamental aspects of gas breakdown theory are reasonably well understood on a static basis. For very high fields and rapid discharges things are less well understood. The admixture of various gases also causes additional complexities. The presence of metastable atoms may, for instance, have profound effects on the recovery rate of a gas. The well-known Penning [1] effect can have drastic effects on the breakdown strength of a gas. This effect occurs if a small gas admixture has an ionization potential which is just below the metastable level of the parent gas such that the probability of energy transfer during a collision is high. This effect is particularly dramatic for argon mixed into neon as shown in Fig. IV-1. In some sealed gaps, radioactive gas mixtures, such as Kr 85 and Tritium, are used to reduce the statistical time lag by providing the seed electrons for the discharge formation.

The breakdown in a gas is strongly dependent upon the Townsend  $\alpha$ -coefficient which is the number of free electrons produced per unit length by one electron through collisions. This then indicates that a high breakdown field strength

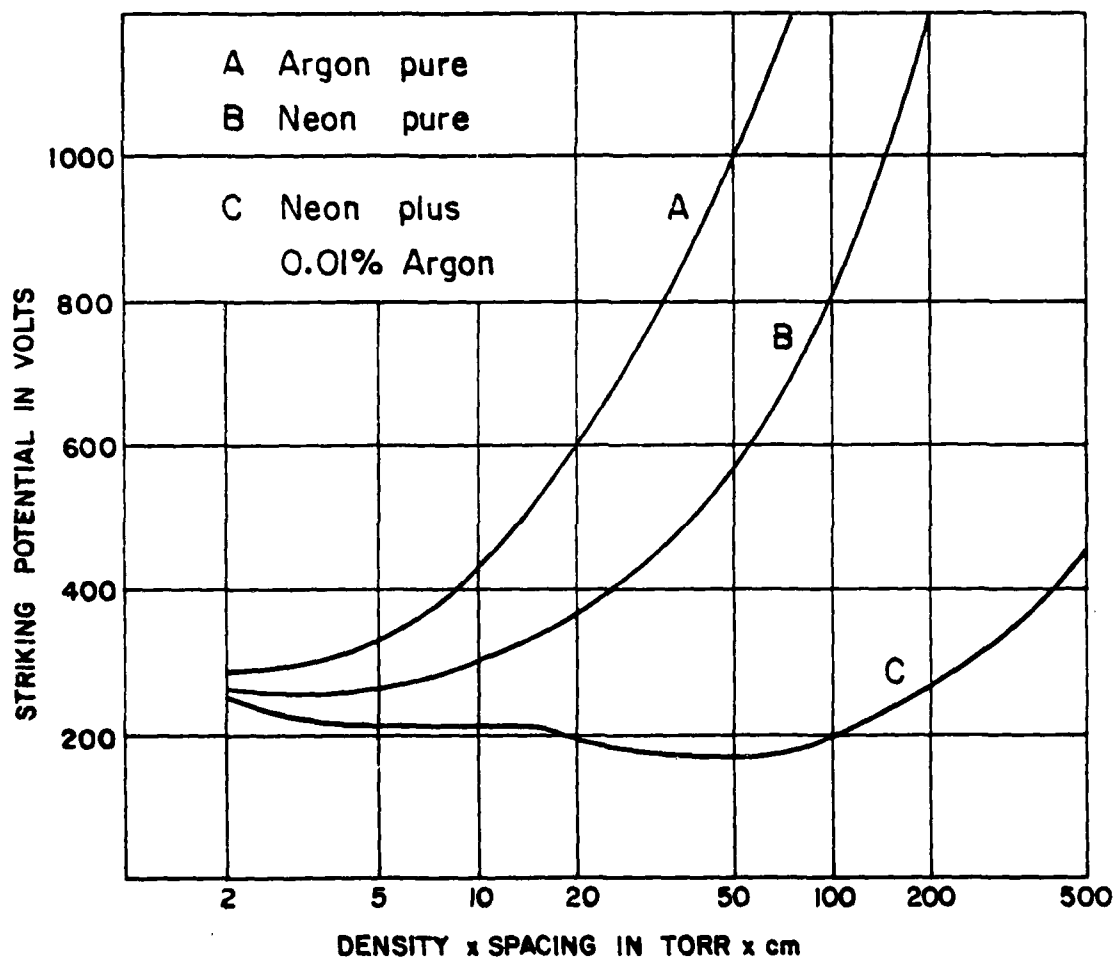


Fig. IV-1. EFFECT OF METASTABLE ATOMS [1]

should be obtained for gases with high ionization potential, large cross-sections (big molecules), and at high pressure (many molecules and high collision frequency). This is in general true, although the pressure effect tends to saturate, but an even bigger effect on the breakdown strength comes from the attachment coefficient of electronegative gases, such as  $\text{SF}_6$  which has an electric strength about 2.5 - 2.8 times that of air. Just a small admixture of  $\text{SF}_6$  into  $\text{N}_2$  or air will increase the electric strength considerably (e.g. 10%  $\text{SF}_6$  in  $\text{N}_2$  about doubles  $E_{\text{BD}}$ ).

The final selection of a particular gas depends upon many factors, such as cost, chemical reactivity, toxicity, etc. Commonly used gases (technical gases) include air,  $\text{N}_2$ ,  $\text{SF}_6$ , Freon, and  $\text{CO}_2$ . One should note, however, that both  $\text{SF}_6$  and Freon decompose into toxic products at high current discharges and that appropriate precautions must be taken. Air is obviously easily available and once dried and purified works quite well in many applications.

Because of field-distorting corona discharges in high voltage gas gaps it is difficult to predict the exact breakdown strength of a nonuniform field gap. Polarity effects can often be both pressure and field enhancement dependent [2] and can be of opposite sign for different pressures and different field enhancement factors.

The breakdown strength is independent on frequency for  $f < 20$  kHz. At higher frequencies the electric breakdown

strength is gradually reduced, especially in gaps with high field enhancement factors.

The breakdown properties for pulse-charged gaps depend upon the pulse shape and length and the statistical and formative time lags of the gas. The formative time lag of various common gases has been studied [3]. An empirical equation [4] relates the breakdown field to the pulse length and gas:

$$k = F t^{1/6} d^{1/6} \quad (\text{IV-1})$$

where  $F$  = Maximum voltage divided by gap length (Average field)

$t$  = time in  $\mu\text{s}$  voltage is above 63%  $V_{\text{max}}$

$d$  = gap distance in cm

$k$  = constant which differs for various gases, pressures, and polarities [4] (Typically  $k \sim 50$ )

A certain "magic" gas mixture of approximately 90% Ar and 10%  $\text{SF}_6$  has gained popularity for use in multichannel switches (e.g. rail gaps). This mixture seems to give better and more reliable multichanneling than other gases. It is speculated that the reason may be the anomalously high resistive phase of  $\text{SF}_6$  at pressures below 10 psig [5]. This may provide an initial resistance which allows the other channels to form. Several past studies review spark gaps in more or less detail [2, 6-10].

## 2. Gap Design and Performance

### a. General Comments

In this section the geometrical configuration, the design and some performance parameters of gas filled spark gaps are

considered. The triggering aspect is discussed separately in the next section.

The main geometrical configurations are coaxial and stripline (rail gaps). The coaxial gaps are the most commonly used ones in fast pulse service. They are relatively easy to construct and typically have an inductance of a few 10's of nh. The rail gaps logically fit certain stripline geometries. They require very fast rise time trigger pulses and typically have an inductance of a few nh. Some highly developed coaxial gaps are described in ref. [11] and an excellent description of rail gaps is given in reference [5]. The field of portion triggered rail or coaxial gaps with off-set trigger electrode can achieve jitters down to about 1 ns rms and can be triggered down to about 35% of self breakdown voltage on the main electrodes. By changing the gas type or pressure in a given gap the range can, of course, be extended considerably. Jitters as low as 0.5 ns have been obtained [12] using UV preillumination of the gap.

A general rule for designing reliable and repeatable spark gaps is to design them so that the operation is dominated by gas physics rather than surface physics. The statistical time lag and hence the jitter can be reduced by strong preillumination\* of the gap gas and the cathode with UV-, and, X-radiation and both the statistical and formative time lags can be reduced with laser irradiation as discussed in the next section.

\*Note added in proof: An extensive discussion of spark gap preillumination is given by T. Noguchi, "Control of the Spark Gap Switch by Irradiation," Translation FTD-1D(RS) T-2354-77.

A discussion of avalanche statistics and the statistical and formative time lags is given in reference [10] (Also see Appendix I). Closure times of 50 ps or less with 25 ps jitter have been observed in highly overvolted, short gaps with UV illumination [13].

An effort to reduce the jitter of overvolted gaps is represented by the "rope switch" [14] which appears to be similar to a switch developed by G. A. Mesyats' group [9] and the "Sequence Spark Gap" [15]. The basic idea is to put several switches (gaps) in series so that if one or two gaps fire early the remaining gaps will keep the overall switch open. The gaps firing late will get the total voltage impressed across them and thus close more rapidly than otherwise. What this achieves is to remove the upper and lower ends of the normal distribution of the individual switch firing. The system has shown to improve the jitter and standard deviation by a factor of 3 over single gap performance. At high electric fields ( $E > 10^5$  V/cm) certain new phenomena take place [9]. The gap is then observed to close faster than explained by the normal avalanche-streamer theory (Appendix I) and microtip explosions occur at the cathode surface.

For the uniform field case Martin [16, 17] has developed a formula for breakdown (essentially the same as Eq. (IV-1)):

$$E_{BD} t_{eff}^{1/6} = K\delta^{-1/6} \quad (IV-1')$$



where  $E_{BD}$  = electric field

$t_{eff}$  = time where field is above 63% of  $E_{BD}$

$K$  = constant for a given pressure and gas

$\delta$  = length of avalanche at instant of conversion to streamer

This equation is useful for determining the length of surface protrusions which will launch streamers.

A study which compared fast pulse breakdown of non-uniform air gaps with that of uniform irradiated gaps [18] showed that the breakdown was essentially inversely proportional to the rate of rise of applied voltage. It was also found by varying the pressure, that, unless  $E > 100$  kV/cm at the cathode surface, the breakdown is delayed due to lack of field emission.

In discharges (RCL series circuit) where the circuit and gap inductance dominate the discharge (high  $Q$  circuit) the maximum  $di/dt \approx \frac{V_o}{L}$ , where  $V_o$  is the initial capacitor voltage and  $L$  is the system series inductance. For very low inductance circuits the channel resistance starts to play a role and for the limiting case where the inductance can be ignored it has been calculated [19] that, for air

$$\left(\frac{di}{dt}\right)_{\max} = \frac{3}{2} \frac{E_o}{R_m t_{mo} \ell} \quad (\text{IV-2})$$

where  $E_o$  = Electric field (V/m)

$R_m$  = Channel Resistance ( $\Omega$ ) at time  $t_{mo}$

$t_{mo}$  = Time (s) at which max  $di/dt$  occurs

$\ell$  = Channel length (m)

It turns out that  $R_m t_{mo}/\ell \sim \text{const} = 10^{-5} \text{ ohm-s/m}$   
 For  $E_0 = 3 \text{ MV/m}$  in air this gives a limiting value of  $di/dt \approx 3 \times 10^{11} \text{ A/s}$  for a single channel gap. This value can be increased by pulse charging or by increasing the gap pressure and hence the electric field [16, 17].

The delay between trigger and main-gap breakdown was studied [20] in an air pressure trigatron gap for various electrode spacings and various main-gap  $V/V_{BD}$  ratios. It is found that  $\tau_{\text{delay}} = f(V)$  is exponential for  $V > .5V_{BD}$  and that  $\tau_{\text{delay}}$  is polarization dependent, especially for high  $V/V_{BD}$  ratios. A parameter study [21] of a given field distortion spark gap may also be useful to other designers in that it provides trend-curves which may have wider application.

The prefire of a gap can often be a problem, especially in large systems where many gaps are supposed to fire in unison. In heavy duty gaps with large erosion this problem can become especially serious. A study [22] of a field distortion gap which passed a peak current of 400 kA and 28 C/shot showed that the prefire probability became less than  $5 \times 10^{-4}$  if the air pressure was 50% above the self breakdown pressure at the 50 kV voltage used. Few studies of this nature have been carried out, probably because of the large number of shots needed to get statistically significant results when the prefire probability is low. Some investigations were

made however, [23] in connection with the Marx generator spark gap development for AURORA.

The Coulomb handling ability of spark gaps is often of interest. In single shot operation, at least 250 C/shot have been successfully handled in a relatively high inductance (100 nh) gap [24]. The Mark IV and V switches at Culham Laboratory, UK also have impressive Coulomb and current handling capabilities. The Mark IV gap, which has 12 nh inductance can handle up to 0.5 MA and pass up to 50 C/shot for a total of some 100 kC. The Mark V gap handles up to 1.5 MA and 100 C/shot (at 200 kA) with a total life in excess of 1 MC. These gaps use brass main electrodes and "heavy metal" trigger electrodes. Tests have been made of similar [25] gaps at currents up to 400 kA at 8 C/shot and 8 ppm for a total of more than 1 MC without significant performance deterioration. Low inductance ( $\sim 10$  nh), multichannel, high voltage ( $\sim 150$  kV), high current ( $\gtrsim 1.5$  MA), high Coulomb (50 C/shot) gaps have also been developed at LASL [26]. Some of these gaps also have exceptionally low minimum main gap switching voltages (wide switching range).

In heavy duty operation various chemical reactions between the gap gas and the electrode material can take place and shorten the lifetime due to build up of the reaction products, unless the gap is carefully flushed. The physical orientation of the gap can therefore sometimes be important due to gravity

settling of these reaction products. The whole topic of "spark gap" chemistry seems to be very poorly understood. Most people refer to the reaction products as "blue crud," "gray crud," etc. Very few chemical analyses of these products seem to have been made.

The best electrode material in spark gaps seems to be some tungsten or maybe molybdenum compositions such as the elkonites which contain various mixtures of tungsten or molybdenum together with copper and/or silver (e.g. elkonite 3W3 has 32% Cu and 68% W). These materials retain some of the refractory properties of tungsten and molybdenum and also the high thermal and electric conductivity of copper or silver. Similiar materials have been used in Europe and the USSR and have generally been found to have superior performance in terms of jitter and lifetime (erosion). Just which composition is best is not clear. Some of the compositions used in the USSR are, for instance, quite different from the ones used in the U.S. The USSR ones often include nickel (e.g. TNC (95% W, 3% Ni, 2% Cu) and TNF (90% W, 7% Ni, 3% Fe)), while others are similar to the elkonites (e.g. AVM (70% W and 30% Cu)). The manufacturing process of these compounds also appears to be important. They apparently can be made either by cintering the tungsten and the high conductivity materials together or by cintering the tungsten first and then letting molten high conductivity material penetrate into this matrix (sponge) structure. Some preliminary experiments

indicate that this difference in manufacturing technique is an important one [27]. A careful investigation into the performance of these different materials is needed.

In many cases, of course, the material selection is also dictated by cost, availability and machinability. A good choice is then often brass which also has good erosion properties (see Section on Electrode Erosion and Heating). A common choice, which by personal experience has proven usually to be poor, is stainless steel which seems to combine "too low melting point" with "too low conductivity" in an unfortunate way. Pure tungsten also seems to have difficulties due to crystalline growth problems [28].

#### b. Summary of Spark Gap Performance

In viewing the following performance parameters one should be aware that the usual case for a spark gap is to measure just the parameters of interest to a given application. Seldom or never are all these parameters carefully checked for a given gap and the values given are thus somewhat unrelated (e.g. the maximum voltage and current are certainly not directly related to the rep-rate values given here).

#### Voltage Standoff

In a gap with proper envelope design the breakdown voltage depends on the field enhancement factors,  $f_1$  and  $f_2$ , discussed in the previous section, as well as the gas type and pressure, the electrode material (for high field

cases), the surface conditions (pits, micro-protrusions, etc.) and the pulse charge time.

For extremely high voltage gaps the standoff is, in practice, more limited by surface flashover, inside or outside the gap envelope, than by the gap design itself. Values as high as at least 12 MV have been obtained for a pulse charged gap.

#### Peak Current

This depends to a large extent on the number of shots one expects the gap to function, within some specified performance limit (usually prefire probability, delay, and jitter). Under the assumption that one would like to have a life of at least 1000 shots it seems as if  $\sim 4$  MA is the limit in practical switches. This depends, however, of ones definition of "a switch." There is, for instance, no fundamental physical reason why one could not build an extremely long, multichannel, rail gap in one housing and call it "a switch." Also, many individual discharge points can be located around a very large circle in co-axial geometry and all be located in one housing. The maximum current number given is thus only a "reasonable number" (which has been achieved at UKAWRE, Aldermasten). The maximum current per arc channel, consistent with a "reasonable lifetime," seems to be about 200 kA and the maximum number of arc-channels about 20-40 per m of electrode length, although this last

number depends strongly upon the rise time and magnitude of the trigger pulse. (For the dielectric surface discharge switch discussed in Chapter VI, channel spacings as short as 0.5 cm were reported.)

### Pulsewidth

Pulse widths as short as 0.4 ns have been produced. The minimum pulse length is a function of the external circuit parameters and the recombination of the gas. Pulse lengths in the  $\mu$ s range are fairly common for spark gap operation and the maximum single shot pulse length at a given current is basically limited by spark gap cooling, especially of the electrodes. (Typical current values for continuous operation are in the kA range.) In rep-rated operation the maximum pulse length depends upon the desired rep-rate and the gas type, pressure, flow, etc. In other words, the recovery time between pulses ( $t_{\text{recov}} \approx .3$  ms) in relation to the rep-rate determines the pulse length.

### di/dt

This is limited primarily by the inductive and resistive time phases of the gap during the formation of the arc.  $di/dt = 5 \times 10^{14}$  A/s has been obtained in multi-channel gaps [29]. For single channel gaps in air at atmospheric pressure a maximum  $di/dt \sim 3 \times 10^{11}$  A/s is calculated (see Section IV.B.2.a). This can be increased by increasing the gas pressure.

### Delay Time

This is primarily limited by the statistical and the for-

mative time lags. At high gap voltages ( $V \sim V_{BD} > 10^5 \text{ V/cm}$ ) and with preillumination or laser triggering the delay can be less than 1 ns.

### Jitter

This depends largely on the statistical time delay (see Appendix I). Jitters in the 100 ps range have been obtained with laser triggering. For regular field distortion or trigatron gaps, it seems like the lowest practical jitter is  $\sim 1$  ns. This can be improved, however, by preilluminating the gap, especially the cathode, to produce electrons and thus reduce the statistical delay  $t_s$  which is the ultimate limitation (i.e. the availability of the first electron(s)). Ultraviolet triggering of overvolted, short gaps has been done with 25 ps jitter.

### Pulse Repetition Rate

This depends upon the plasma deionization, the gas de-excitation, the gas and electrode cooling rates, and the gas flow rate and geometry. It also depends on whether or not one expects 100% voltage standoff recovery between shots. At nearly full voltage recovery in a sealed gap the maximum repetition rate seems to be a few hundred pps, limited primarily by the gas cooling rate. With a flushed gap and full voltage recovery, it seems that approximately 3 kpps is the limit but this may possibly be improved by a factor of a few (not 10) by clever airflow design. The limit is



the flow speed and the fact that the active discharge volume must be moved more than one electrode separation distance away before the gap recovers.

At somewhat reduced voltage recovery, gaps have been operated up to 300 kpps in the "Quenchatron" configuration [30] and up to 100 kpps with 10% recovery in a "regular gap" [31]. The "Quenchatron" operates at about .5 to 5 kA and 6 to 12 kV. A more detailed explanation of the factors affecting rep-rated operation is presented in Section 4.

#### Average Current

This is primarily limited by the gap cooling, especially the electrodes. With only gas flow cooling, average currents of <100 A [32] were obtained for 10 s run times without any apparent excessive electrode damage. The effort in this work, however, was to reach high average power rather than high average current. No information has been found on the average current with water cooled electrodes except for D.C. arcs where kA's are used.

#### Duty Cycle

There is no real limitation since the gap can, in principle, be run continuously. In rep-rated operation, there must, however, be approximately a 0.3 - 10 ms grace period between shots (see "Pulse Repetition Rate"). The exact value depends on the operating conditions as explained earlier.

### Recovery Time

In a sealed gap this is limited by plasma recombination and gas and electrode cooling to about 5-10 ms for recovery to full hold-off voltage. In a gas flow gap it is ultimately limited by sonic flow speed and aerodynamic effects but  $t_{\text{recov}} < 0.3$  ms seems possible. Recovery to and operation at less than 100% hold-off voltage is, of course, possible on shorter time scales.

### dv/dt

The dv/dt is limited by the same basic factors as the pulse repetition rate discussed earlier. No extensive investigations have been found but a  $\frac{dv}{dt} \approx 250$  V/ $\mu$ s was demonstrated [32].\*

### Rise Time

Current rise times ("gap closure") as short as 50 ps have been produced in short, overvolted, UV triggered gaps [13].

### Coulombs/Shot

This depends to a large extent on the expected lifetime without excessive delay, jitter, or prefire degradation. At present, 250 C/shot has been demonstrated [24] but this can probably be extended somewhat. The main limitations are electrode damage and shock damage to the spark gap housing (not a trivial problem).

\*Note added in proof: A dv/dt =  $25 \times 10^6$  v/ $\mu$ s is advertised for a commercially available gap [62].

### Lifetime

2.6 MC total charge transfer has been demonstrated at 53 mC/shot [33]. The ultimate limitation is the allowable electrode erosion before excessive deterioration in performance. In principle, one can use continuous feed electrodes and extend the lifetime considerably. The erosion problem is complicated and poorly understood. The ultimate lifetime is thus a function of many parameters, as discussed in Section 5 and insufficient information is available to give a firm number.

### 3. Triggering of Spark Gaps

#### a. Conventional Triggering

Triggering of gas filled gaps is generally achieved by one of the following methods: Arc initiation (trigatron), field distortion, laser triggering (described separately in section IV.B.3.b. of this report), e-beam triggering (described separately in Chapter VI of this report), and UV irradiation.

The first method involves striking an arc from a trigger electrode to one of the main discharge electrodes, thus initiating the breakdown process, both by providing the initial electrons directly, and by gas volume photoionization and local field distortion. The details of this breakdown process are not completely understood but a fairly comprehensive discussion of it is given in Ref. [8]. The most common arrangement is the trigatron [34] configuration shown in Fig.

IV-2 which can be reliably triggered at gap voltages down to about 50-60% of the self breakdown voltage. The relative polarity of the three electrodes is very important [35] for achieving a wide voltage operating range and a short delay, as indicated in the figure. These results disagree somewhat with those of Shkuropat [36], who agrees that the -, R, + polarity combination is the best but who feels that the +, R, + combination is the worst one. For good performance of a trigatron, the following recommendations are made:

- (1) Use nearly uniform main gap field with a field strength of at least 20 kV/cm.
- (2) Design the trigger electrode location to cause minimum field distortion.
- (3) The trigger voltage should be several times higher than the self-breakdown voltage of the igniter gap and have a fast rise time and low circuit impedance (low voltage drop during pre discharge current phase).
- (4) The igniter gap should be physically large but considerably smaller than the main gap distance.
- (5) The igniter pulse should have about the same voltage as the main gap voltage and last  $\sim 10$  ns.
- (6) Keep a clean gap.

When working at tens of kV and above 80% of self breakdown voltage trigatron gaps can be triggered with a few nanoseconds delay and a few tenths of nanosecond jitter using a trigger

PRIORITY LISTING OF RELATIVE  
ELECTRODE POLARITY FOR  
BEST TRIGGERING ACTION [35]

	A	B	C
1	-	R	+
2	+	R	-
3	+	R	+
4	-	R	-

ELECTRODE B IS THE  
REFERENCE ELECTRODE

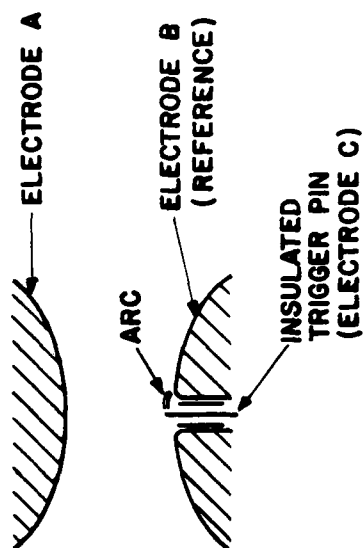


Fig. IV-2. The Trigatron Arrangement

pulse voltage about equal to the main gap self breakdown voltage. A study of the triggering properties of high voltage (MV),  $\text{SF}_6$  filled trigatrons is described in ref. [37].

The field distortion triggering works by driving an inter-gap electrode which was located on an equipotential surface towards or behind the potential of the nearest electrode (see Fig. IV-3). This distortion of the natural field produces a very high field at the edge, initiating the breakdown process.

These gaps can easily be scaled to higher voltages by moving the "distant" electrode away so that the trigger electrode remains at constant potential with respect to the "near" electrode. The trigger electrode is also often located in the midplane between the main electrodes. In general, it appears that the field distortion trigger is better than the trigatron system with regard to reliability and life. A particular trigger mode of three-electrode gaps, known as the Swinging Cascade, [38] helps reduce the breakdown delay and jitter. Preillumination [8] has also been used to improve the performance of these gaps. The various principal trigger configurations for field distortion switches are shown in Fig. IV-4.

A flux of photons which either directly ionize the gas in the gap, or which cause photoemission from the cathode surface can also be used as a trigger. In the latter case,

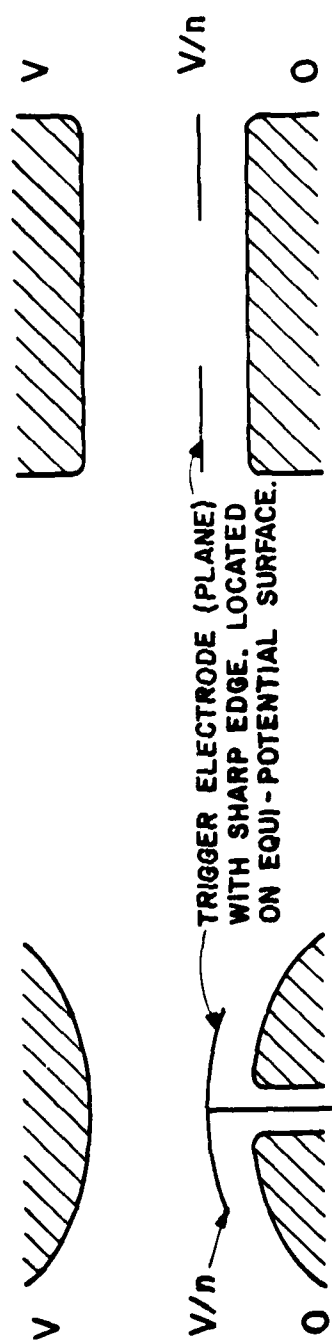


Fig. IV-3. Field Distortion Spark Gaps

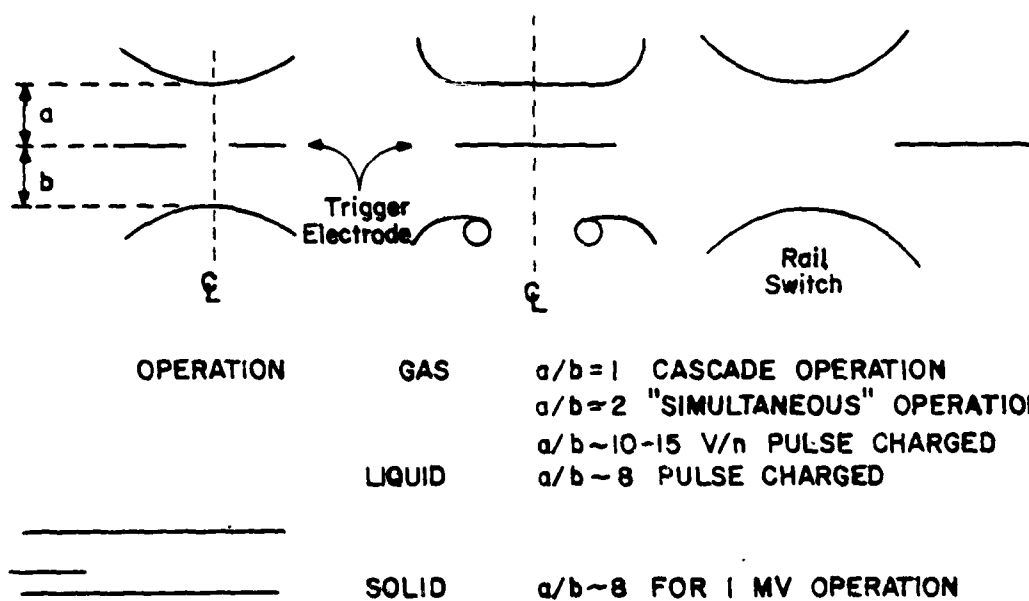


Fig. IV-4. Field Distortion Switch [29]



one wants very short wavelength illumination although this causes problems with absorption in the air if the light source is located too far from the gap. One of the advantages of photon triggering is that the trigger circuit is electrically isolated from the main circuit. This implies, however, operation with relatively low voltage gaps since the light source (usually the arc from another spark gap) otherwise must be moved too far away from the gap. It is obviously possible to improve this somewhat by using an appropriately designed reflector system behind the light source. Also, this trigger method is most useful for gaps which operate very near the self-breakdown voltage, since the photo-emitted electrons only causes about a 10% field enhancement [8] in the gap.

The threshold wavelength for photoemission from most surfaces is 2600-3000 Å, but the emission increases for lower wavelengths. The minimum breakdown delay time when using a statically charged gap is approximately the electron drift time from the cathode to the anode. At this time, a strong field enhancement at the anode causes the gas breakdown. The spread in this delay is less than 2 ns. This spark gap trigger method is often used in Marx generator systems which are arranged so that the light from one gap illuminates the next gap and so on.

Gaps can be thermally triggered [39] using a heating filament which causes a local gas density perturbation. The

breakdown delay in this case is in the 10's of  $\mu\text{sec}$  range and the jitter is relatively large. A spark gap can obviously be triggered mechanically by inserting a mechanical field distortion object into the gap region, e.g. push a rod through a hole in one of the electrodes (used for instance on the Ion Physics Co. FX-15 machine). Spark gaps have also been triggered with exploding wires, [40] plasma jets [41], and x-rays [42].

For multichannel gaps (e.g. railgaps) it is important to have a high  $dv/dt$  in order to obtain the multichanneling. There seems to be little quantitative information about the exact trigger requirements but a  $dv/dt$  of about  $10^{13}$  V/s seems to be needed. From ref. [43] we almost quote:

"The multichannel gap trigger operation is sometimes referred to as simultaneous ignition of a three-electrode gap. The trigger electrode is placed symmetrically between the main electrodes. Multiple channels are obtained by driving the trigger electrode capacitance with a very fast rising voltage. The rapid change in the trigger electrode potential distorts the main gap electric field at the sharp edge of the trigger electrode which produces a cloud of corona electrons at the trigger electrode. This initial corona discharge of electrons and the total voltage applied between the gap

electrodes creates streamers from the trigger electrode to both the main electrodes closing the gap. This behavior is common to all of the switching modes. At this point the characteristics of the trigger circuit and the main discharge circuit enter into the triggering characteristics of the gap. Basically, multichannel triggering operation can be divided into two classes determined by the quantity  $\alpha$ , which is the ratio of the gap self-breakdown voltage to the voltage at which the gap is to be triggered. For  $\alpha \gg 1$ , the trigger system must supply much more voltage and energy to the gap than for  $\alpha > 1$ .

The current risetime of the main discharge circuit,  $\tau_1$ , also affects the trigger system requirements. After the corona streamers have closed the main gap, the trigger system must deliver energy to these arcs to open and sustain the current paths fully until current from the main discharge circuit can sustain the arcs. When  $\tau_1$  is large, the trigger system must deliver much more total energy than when  $\tau_1$  is small, as in a high-voltage, low-inductance circuit. All of the multichannel arcs must be conducting high current on a time scale of 1 to 2 ns. This requires a very low inductance trigger circuit and location of the trigger energy as close to the gap as possible.

For multichannel gaps operating between 10 and 125 kV, a trigger pulse amplitude of 200 kV with a risetime of 20 ns is sufficient to produce multiple channels. The critical parameter is  $dv/dt$ . Generally, a trigger pulse rate of rise of 10 kV/ns is sufficient to produce multiple arc channels in air. However, the faster the rate of rise, the better. A faster rate of rise produces more numerous, uniform arc channels with the trigger energy equally divided. To increase the rate of rise in the trigger electrode potential initiating switching, pulse-sharpening gaps can be used. The pulse-sharpening gap can decrease the trigger pulse risetime to as low as 10 ns.

The polarity of the trigger pulse is important especially in gaps where  $\alpha \gg 1$ . Tests indicate a negative polarity trigger pulse is essential to simultaneous ignition of the gap regardless of the main discharge bank polarity. This is to be expected since the trigger electrode is meant to act as a source of corona electrons. Applying a positive potential to the trigger electrode, especially where  $\alpha \gg 1$ , causes the gap to cascade and delays the current flow randomly from 0.3  $\mu s$  to 100  $\mu s$ . When the cascade delay occurs, the switching action is not the multichannel mode, but a single arc channel. With the negative trigger polarity, however, the delay for

current initiation is less than 1 ns. Similarly, the jitter for a properly triggered multichannel gap is less than 1 ns.

The delivery of trigger energy to a multichannel gap is extremely important. The best results have been obtained when the trigger system has a low impedance (capacitance instead of cable), and is physically located close to the gap. This arrangement provides for low inductance and fast trigger voltage and current risetimes."

It has also been suggested that the voltage risetime of the trigger pulse,  $\Delta T$ , should be [44]

$$\Delta T < 0.1 t_e + 0.8 t_{\text{trans}} \quad (\text{IV-3})$$

where  $t_e$  = total e-folding risetime of main pulse  
 $(t_e = t_r + t_L)$  (See Section IV.B.6 for definitions of symbols)

$t_{\text{trans}}$  = distance between channels divided by local speed of light

Both of these times,  $t_e$  and  $t_{\text{trans}}$ , are functions of the number of channels in a given gap. A study which includes the effect of the external circuit impedance [45] concludes that the most important factors in obtaining multi-channeling are: 1) adequate gap-voltage decay time (say, 15-20ns), 2) small spread in breakdown time between channels, and 3) high ratio of effective arc inductance to total gap inductance. A related study [46] describes the parallel operation of sparkgaps without transit time isolation. An early, but

still very useful analysis of sparkgap triggering is described in ref. [38].

#### b. Laser Triggering

The work on laser triggered spark gaps was pioneered by A. H. Guenther, et.al. at the AFWL and is summarized in two recent, extensive review papers [10, 47]. The basic reason for using laser triggered switching (LTS) is to reduce the jitter and turn-on time and to produce multiple gap and/or multichannel triggering. Triggering of voltages in excess of 3 MV and repetitive switching at rates up to 50 pps with subnanosecond jitter has been achieved. Solid, liquid, gas, and vacuum dielectric media have been used. There is a large body of work in this area and the theory of the LTS is quite well understood. The basic trigger arrangements are shown in Fig. IV-5. The best arrangement for most cases is the coaxial arrangement where the laser strikes the positive electrode. A typical set of measurements (~10 shots/point) of delay and jitter vs laser power are shown in Fig. IV-6 and Fig. IV-7, respectively, and demonstrate that low delay and jitter can be obtained.

The gap is closed by streamer propagation which is 10 to 100 times faster than obtained from Townsend avalanche formation. The details of the streamer formation process also usually results in the fastest discharge when the laser is focused on the positive electrode.

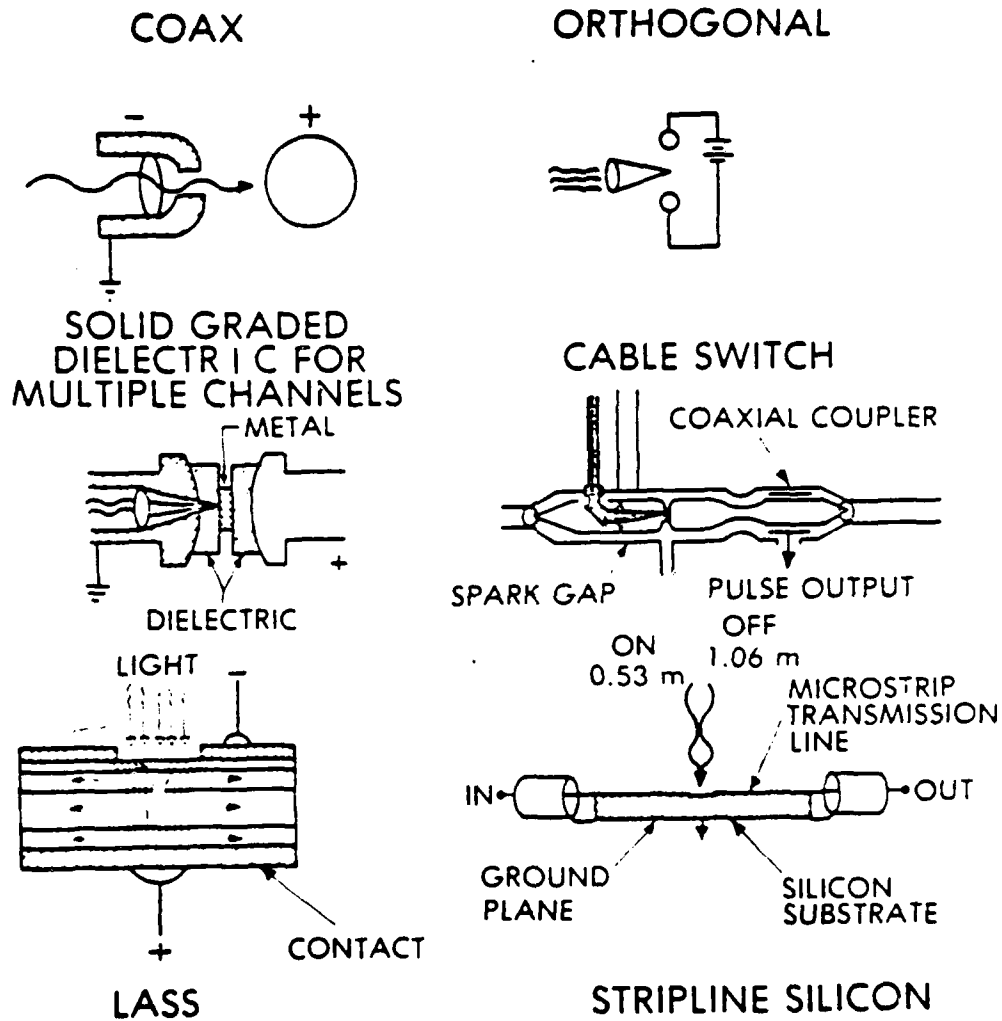


Fig. IV-5. Basic Laser Triggering Methods [47]

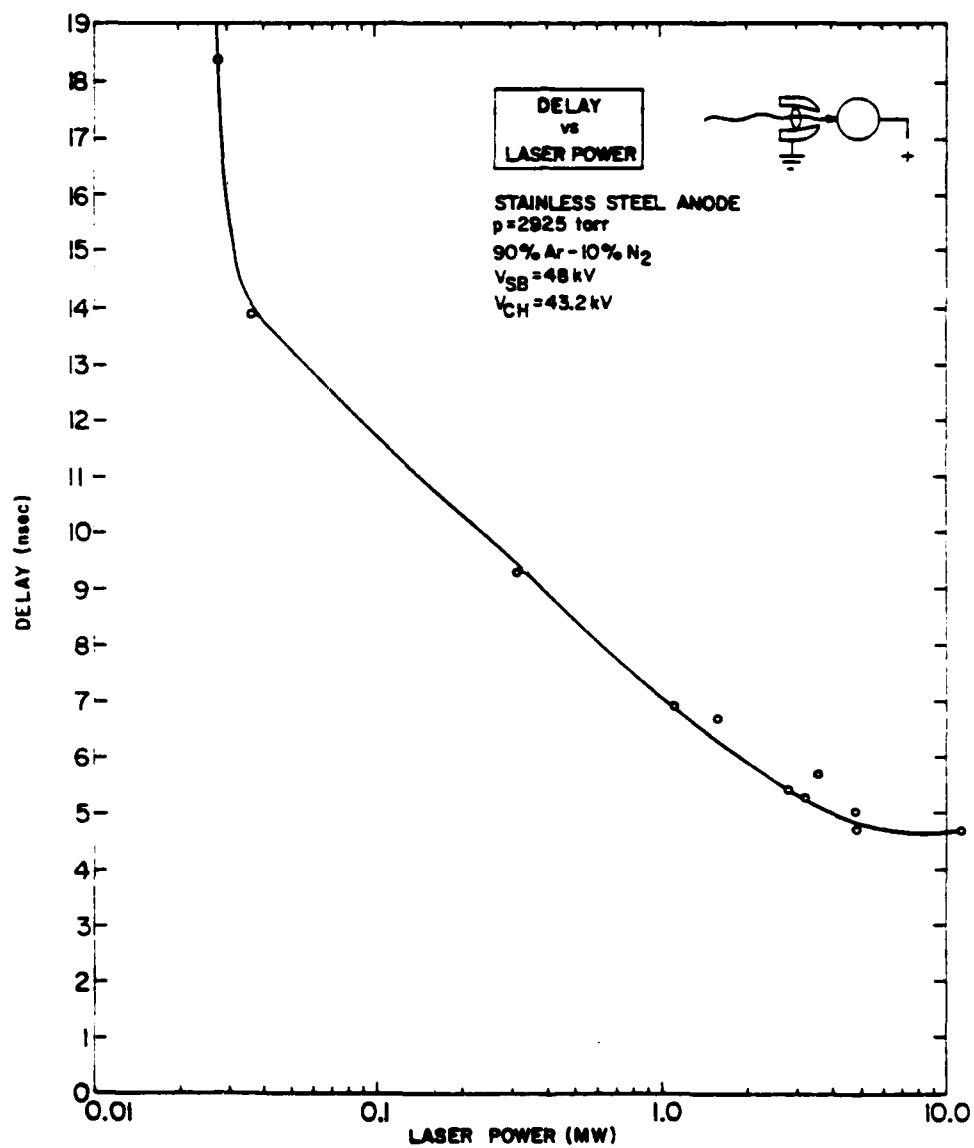


Fig. IV-6. Delay vs Laser Power [47]



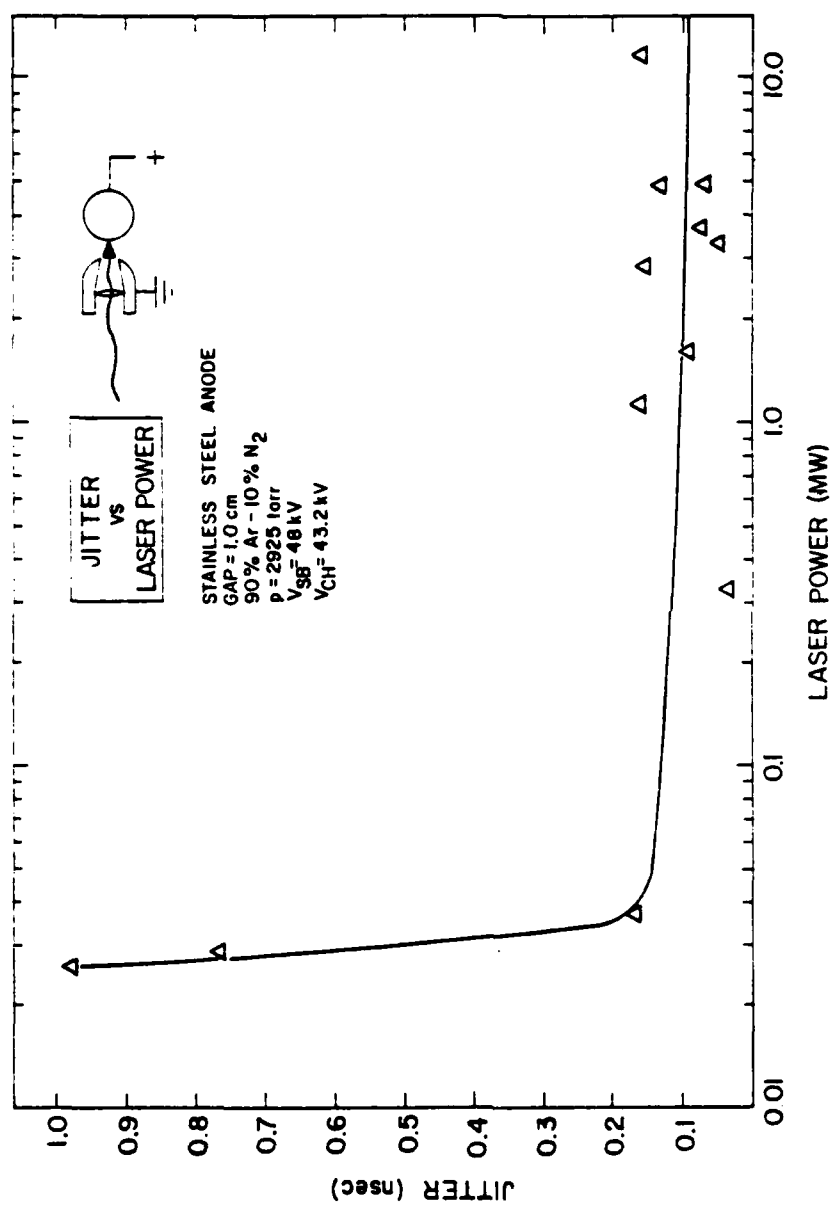


Fig. IV-7. Jitter vs Laser Power [47]

The trigger energy threshold depends upon the experimental conditions, but is typically in the millijoule range (as low as 5  $\mu\text{J}$  has been demonstrated). The effect of the electrode material has been studied and it is generally deemed best (least delay) to use tungsten at the focal spot (followed by SS, Al, and brass).

The main advantage of the LTS is in applications where low delay and jitter ( $\approx 1$  ns) and low prefire probability are required. The criteria for high performance are summarized in Table IV-3 and some demonstrated capabilities in Table IV-4. With the development of reliable, rep-rated lasers it also becomes of interest to consider further the use of laser triggering for rep-rated operations. The combined use of laser triggering and fiber optics for multigap systems may lead to improved system performance with little or no cross-talk between trigger channels. Although much of the LTS work has been carried out with rather long wavelength lasers (up to 10.6  $\mu\text{m}$ ) it should be advantageous to use short wavelength lasers, such as nitrogen with  $\lambda = .3371$   $\mu\text{m}$ .

#### 4. Rep-rated Operation

In order to operate a spark gap in a rep-rated mode one must consider the electrode heating and erosion, the gas cooling rate, the deionization rate of the discharge plasma, and the de-excitation rate of the gas. The recovery rate is

Table IV-3

## High Performance LTS Criteria [47]

1. Use high brightness laser (high power, low beam divergence).
2. Use short focal length lens to increase power density at target electrode.
3. Focus laser beam slightly (few mm) behind target electrode.
4. Use coaxial geometry.
5. Use smallest possible aperture in electrode for laser beam.
6. The target electrode should be charged positive.
7. Use Tungsten insert on target electrode to reduce erosion and maximize ionization.
8. Operate as close to self-breakdown as possible at low prefire probability.
9. Prevent 180° Stimulated Brillouin Scattering.
10. Optical components should be limited in number and be of good quality and have high transmission.
11. In gases use high pressure, high reduced fields (E/P).
12. Add some gas such as Ar which has large photo-ionization and collisional cross-sections.
13. Use short gaps.
14. For solids use graded dielectrics to reduce rise times.
15. For liquids care must be exercised to reduce dynamic loading of optical components which should exhibit good mechanical design and strength.
16. Jitter will be minimized when the delay is less than the laser pulse width.

Table IV-4

## LTS Demonstrated Capabilities [47]

Voltages > 3.5 MV

Repetition rates to 50 pps

Multi-channel (2) rise time reduction of 1/2

Multi-switch synchronization @ 50 pps at < 0.1 nsec jitter

Guidance of long discharges > 40 m @ 5 MV

Low delay << 1 nsec

Low jitter < 0.01 nsec

Discharge voltage control in pulse charged gaps

Dielectrics of solid, gas, liquid, vacuum, semiconductor

a complicated topic for analytical study. A review by Milde [48] lists the following gases in order of increasing recovery times:  $H_2$ ,  $SF_6$ ,  $CO_2$ ,  $O_2$ , He, Air,  $N_2$ , Ar.

Charge carrier removal in a gas can occur through recombination, diffusion, attachment, mass flow (gas flushing), etc. In a non-flowing gas all other processes are all usually slower than the temperature recovery of the gas (recall that the recombination processes release heat in the gas). The limitation on the recovery of a static filled (no gas flow) gap is thus usually the temperature recovery of the gas since the high gas temperature lowers the local gas density and hence the breakdown strength. The temperature recovery is a complicated process which depends upon radiation, conduction, convection, electrode cooling, etc.

Increasing the gas pressure improves the recovery rate as does, obviously, gap gas flushing. The recovery rate is also dependent upon the electrode material and elkonite appears to be one of the best materials [49]. This is probably related to the surface melting and possible electron emission from the electrodes. This then also favors electrode cooling. Früngel [30] has developed a special spark gap ("Quenchatron") with a series of metal discs which effectively constitutes a large number of series connected gaps where the multiple electrode discs help to cool the gas. Because of the larger arc volume and distances involved one expects

the recovery time to increase with the arc length and hence the electrode separation.

The recovery rate is often quite flat (low  $dv/dt$ ) early in the recovery period [50] and care should be taken to tailor the voltage stress pulse accordingly in cases where the maximum rep-rate is needed (see Fig. IV-8). Once the gas has cooled below  $\sim 1800^\circ\text{K}$  the electric strength is largely dependent upon the gas density.

The recovery of air gaps of 2 to 10 mm length with no gas circulation was investigated [51] after the passage of various current pulses in the approximate range of .65 kA, 1500  $\mu\text{s}$  to 20 kA, 10  $\mu\text{s}$ . The electrodes were hemispherical with 3 cm radius and were made of steel and copper. After long, low current pulses the recovery was low for 1-2.5 ms followed by an approximately exponential recovery to 90% over 25-100 ms. For short current pulses the approximately exponential recovery started after  $\sim 200 \mu\text{s}$  and was completed in 5-10 ms. The recovery is shortest for small electrode spacings and about the same for copper and steel electrodes.

The rep-rate that can be used for a certain gap is obviously dependent upon the desired recovery voltage. For a sealed gap with 90% voltage recovery and the parameters indicated above a maximum rep-rate of a few hundred pulses per second is implied.

It seems at first that if a gap can be triggered at a main gap voltage which is small compared to the self breakdown voltage then one can improve the rep-rate by using a

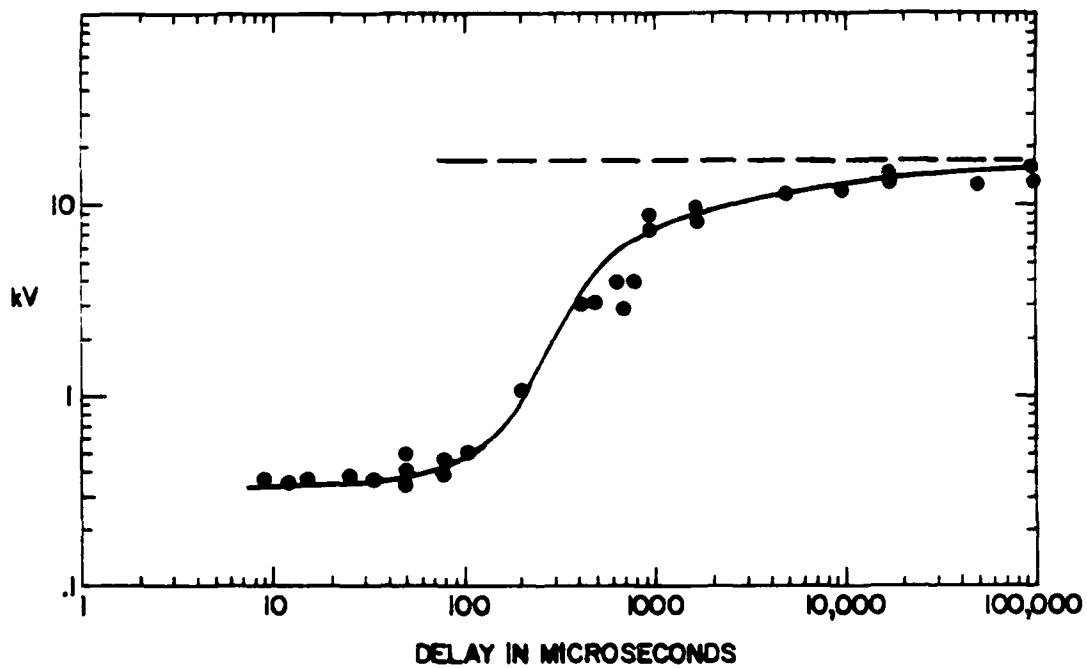


Fig. IV-8. ARC RECOVERY STRENGTH IN  $N_2$  AT 1 ATMOSPHERE  
(6.4mm GAP, 19mm CYLINDRICAL ELECTRODES (Cu),  
400-AMPERE ARC) [50]

large self breakdown to operating voltage ratio. It is, however, not totally clear how the rep-rated operation affects the trigger conditions although it has been suggested [52] that the voltage at which the gap is triggerable decreases with increasing rep-rate.

For heavy duty operation in a rep-rated mode it is necessary to flush the gap in order to achieve a high rep-rate ( $> 100$  pps). Several recent studies address this problem [32, 53-57]. One of the main problems with these investigations is the difficulty in making reliable tests of multimegawatt average power gaps. Most laboratories just do not have the required power supply. One therefore resorts to tricks such as "synthetic testing" [53] where the high current and high voltage supplies are essentially separate. In other words, one supply provides the low voltage, heavy current during the conduction phase and one supply provides the high voltage for the hold-off voltage test. There is always some question in one's mind about the validity of such tests as these or the use of ringing discharges in erosion tests to increase the Coulomb/shot. It is difficult to criticize these approaches, however, until comparisons have been made with a full-power test.

The limiting factor on the rep-rate of flowing gas gaps is the gas flow itself, thus ultimately the sonic flow speed. At very high gas flows one may, however, expect nonrepeatability caused by gas density changes due to compressibility



effects [58]. A rough rule is that the arc volume must be transported at least an electrode separation distance away. The gas flow must also be directed so as to prevent the hot gas from direct contact with the insulator (gap housing). This then generally implies some axially or radially inward directed flow. Some [32, 53, 55] such flow configurations have been investigated with a fair amount of success. An example of one of the flow configurations is shown in Fig. IV-9. This gap [32] was tested to 5.4 MW average power at 250 pps for 10 s runtimes with  $I_p = 4.4$  kA,  $V_p = 90$  kV and  $Q_{max} = 240$  mC/shot. The required gas flow was about 62 SCFM of air at a gap pressure of 35 psig. Elkonite was found to be better than brass as an electrode tip material in order to avoid arc lock-ons. The gap was triggered by an electrode over-voltage pulse and the negative electrode was pre-illuminated with a spark plug discharge. In these investigations [32, 53] gaps operating in the MW average power regime were rep-rated up to 500 pps with a maximum Coulomb transfer as high as 560 mC/shot. It was observed, but not explained, that smaller diameter electrodes (2" vs 4") gave better performance (higher operating voltage and less gas flow). An interesting observation is that increasing the electrode separation at constant gas pressure increases the restrike probability. This is the opposite effect of what is expected for a static gap and is due to the decreased gas flow speed

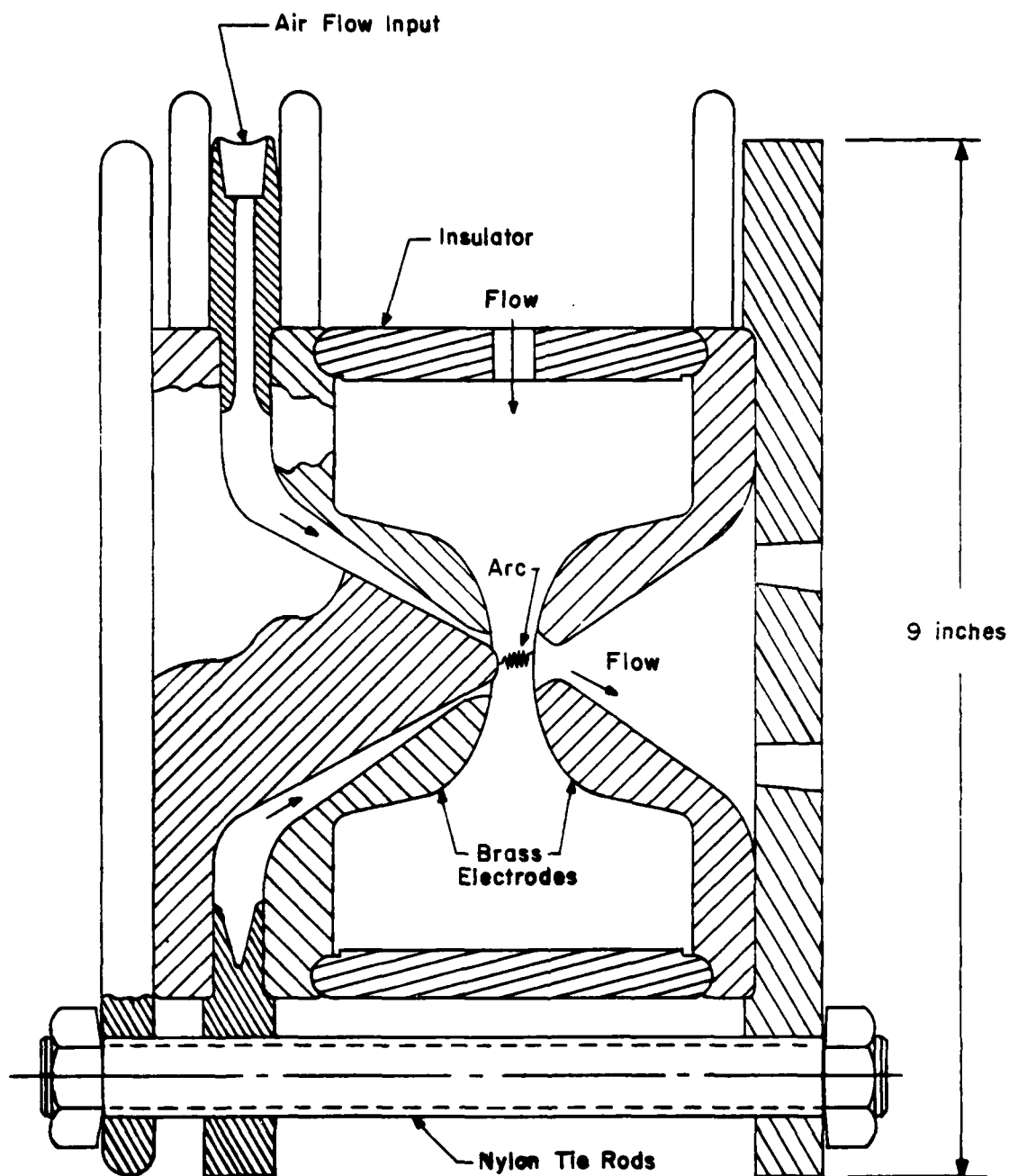


Fig. IV-9. Rep Rate Spark Gap Switch Assembly [32]

in the interelectrode space. The accumulated lifetime, at short runtimes was as high as  $10^6$  shots for one electrode pair with very little noticeable wear.

Although some improvements in the gas flow geometry and hence the gas consumption was made in this [32, 53] work it seems as if this is still an area where much improvement can be made. Charlie Martin [59] has, for instance, proposed a new turbulent flow switch (Fig. IV-10). He predicts that this switch should have a recovery time of  $\sim 0.3$  ms (i.e.  $\sim 3000$  pps rep-rate) at a greatly reduced gas flow (factor 30?). A recent investigation [60] of a similar switch has resulted in a 0.75 ms recovery time. Martin [59] has also proposed some novel ideas involving shock waves and resonant cavities to obtain a very high repetition rate switch.

A theoretical study [54] attempts to develop a numerical model which describes the time history of the gas properties in a gap in order to predict the dielectric recovery rate of the gap. The work was coordinated with some of the experimental work described earlier [32, 53, 55]. Important switch parameters affecting rep-rated spark gap operation were found to be:

Gas Flow Rate	Gap Spacing
Gas Type	Electrode Shape
Gas Pressure	Electrode Material
Current	Grace Period
Voltage	Recharge Time
Charge Transfer	Rep-rate

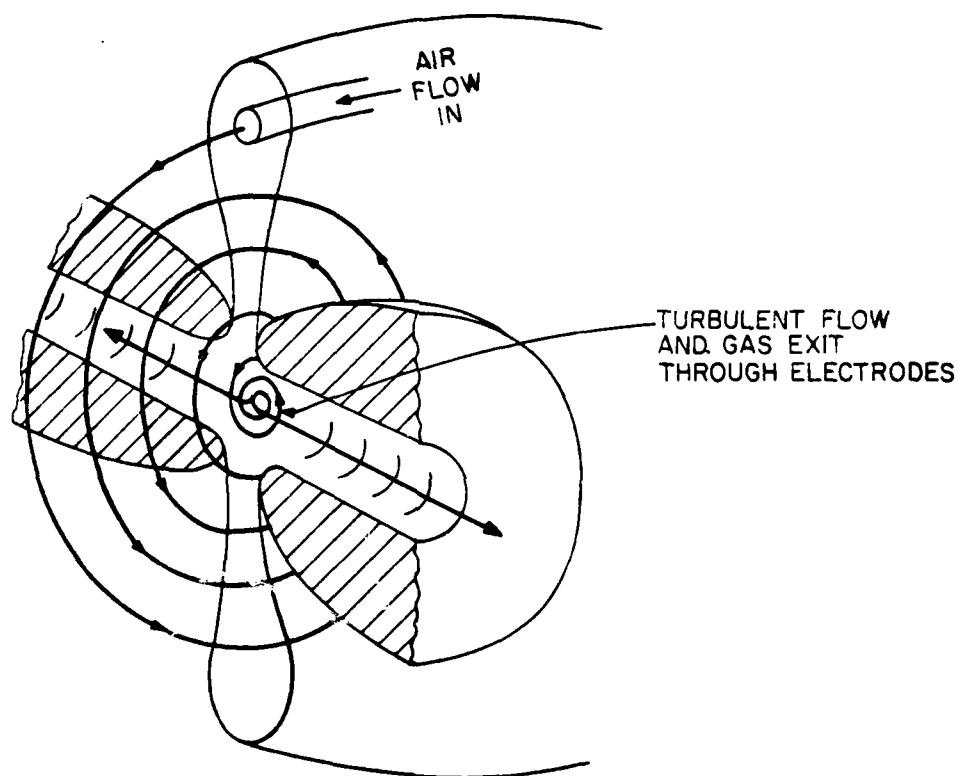


Fig. IV -10. Turbulent Flow Switch. [59]

This number of interrelated parameters indicates the magnitude and difficulty of this study [54] but a successful computer model of the complex physical processes in a rep-rated spark gap is certainly very important. From ref. [54] we borrow a list of some recent rep-rated spark gap studies, as shown in Table IV-5. In this model it is also predicted that flow speeds above Mach 0.5 will actually increase the restrike rate due to low gas densities associated with compressible flow. A useful, empirical equation [54] which gives the breakdown voltage of air as a function of pressure and temperature was determined.

$$V_{BD}(\text{kV}) = \frac{6.958 \times 10^4 \ell(\text{cm})/T(^{\circ}\text{K})}{\ln(668,900 \ell(\text{cm})/T(^{\circ}\text{K}))} \quad (\text{IV-4})$$

In a recent pulser development [56, 60] some interesting switches have been investigated at 40-100 pps operation. The three switches in a pulser unit they investigated were a trigatron gap, a rail gap, and an overvolted gap. The trigatron gap operated only at 30 A and  $24 \times 10^{-3}$  C/shot. The gap is flushed in a vortex manner similar to what is shown in Fig. IV-9. Modest trigger insulator repair is required after about  $10^6$  shots using copper electrodes. The rail gap switch has cooled main and trigger electrodes with a unique flow system to ensure uniform electrode cooling and debris removal. The switch operates at 21 kV, 32 kA, and  $36 \times 10^{-3}$  C/shot. For long runs (in excess of  $10^5$  shots) the rep-rate for the system was 40 pps but shorter runs have been made at 100 pps.

Table IV-5. Recent Repetitive Spark Gap Studies [54]

Author	Reference	Rep Rate pps	Type	P	Gap cm	V <sub>max</sub> kV	I <sub>max</sub> kA	Elec- trodes	Pulse Width μsec	Use	Exceptional Characteristics
Clark, Wayne (Maxwell)	AFAPL TR7541	500	OV2E	1 atm	.5	100	2	W-Ag	20	Lasers	Aircooled parameters tested
Levy, S. (Ft. Monmouth)	ALLRDL TR2454	500	Side AST	1 atm	.4	15	.26	W-Cu	2	Radar	Erosion Tests Aircooled
Anvari (Uppsala Swe)	J Phy 6,73	1,200	SymTrig	1 atm	.4	40	4	Al	.25	Lasers	UV coupling of parallel gaps
Mesyat GA (TomsK USSR)	AD A004599	10,000	SymTrig	1 atm	.01	8	1	Ag	.007	Accel	BaTiO <sub>3</sub> discs in parallel
Gilmour, AS (Calspan)	RADC TR6745	300	LT2E	10 <sup>-13</sup> atm		300	2		100		Laser trig. on electrode
Theophanis (Avco)	AD 608984	Single 1kHz in future	SymTrig	1 atm freon 12	.8	50		Steel		Light Source	Low Jitter
Belkin (USSR)	AD 680860	3,000	QV2E	1 atm			800	Cu			Calculate Erosion
Dashuk (USSR)	IVUZ Phy 1,68 p. 11-16	1.25 MHz or single pulse	OV2E	10 <sup>-8</sup> atm		80	150	SS		Switch	

The trigatron and rail gap received minor service after  $10^6$  shots but it is expected that the use of tungsten alloy electrodes rather than the present copper and brass electrodes will increase the life to at least  $10^7$  shots. Estimates of the lifetime of the overvolted gap which uses elkonite electrodes is  $10^9$  shots. Measurements of the electrode erosions for the various electrodes in these three gaps indicate that the erosion is not just a simple function of Coulomb transfer but also of the current density (see also Section IV.B.5).

Although air is obviously the cheapest gas to use in a rapidly flowing system, such as what is needed in a heavy duty, rep-rated switch, it is important to consider also the use of alternate gases. In particular the use of  $\text{SF}_6$ , Freon, He, or  $\text{H}_2$  either alone or as an admixture to some carrier gas, may prove interesting. For instance,  $\text{SF}_6$  with its high breakdown strength should lead to shorter gap distance and hence reduced flow requirement. In addition one might expect beneficial effects from its recombination and thermal properties [61]. Limited results [56] with  $\text{SF}_6$  indicate that at least the gap spacing argument is valid.

An interesting rep-rated, triggered gap has been developed at Lawrence Livermore Laboratory [57]. The gap uses a coaxial trigger arrangement, as shown in Fig. IV-11. The achieved parameters are: 220 kV, 42 kA, five pulse burst at 1 kHz, 12 ns risetime, 2 ns jitter, 50 ns pulse length. The gap has also been tested at 1.5 kHz. The total lifetest so far is  $10^5$

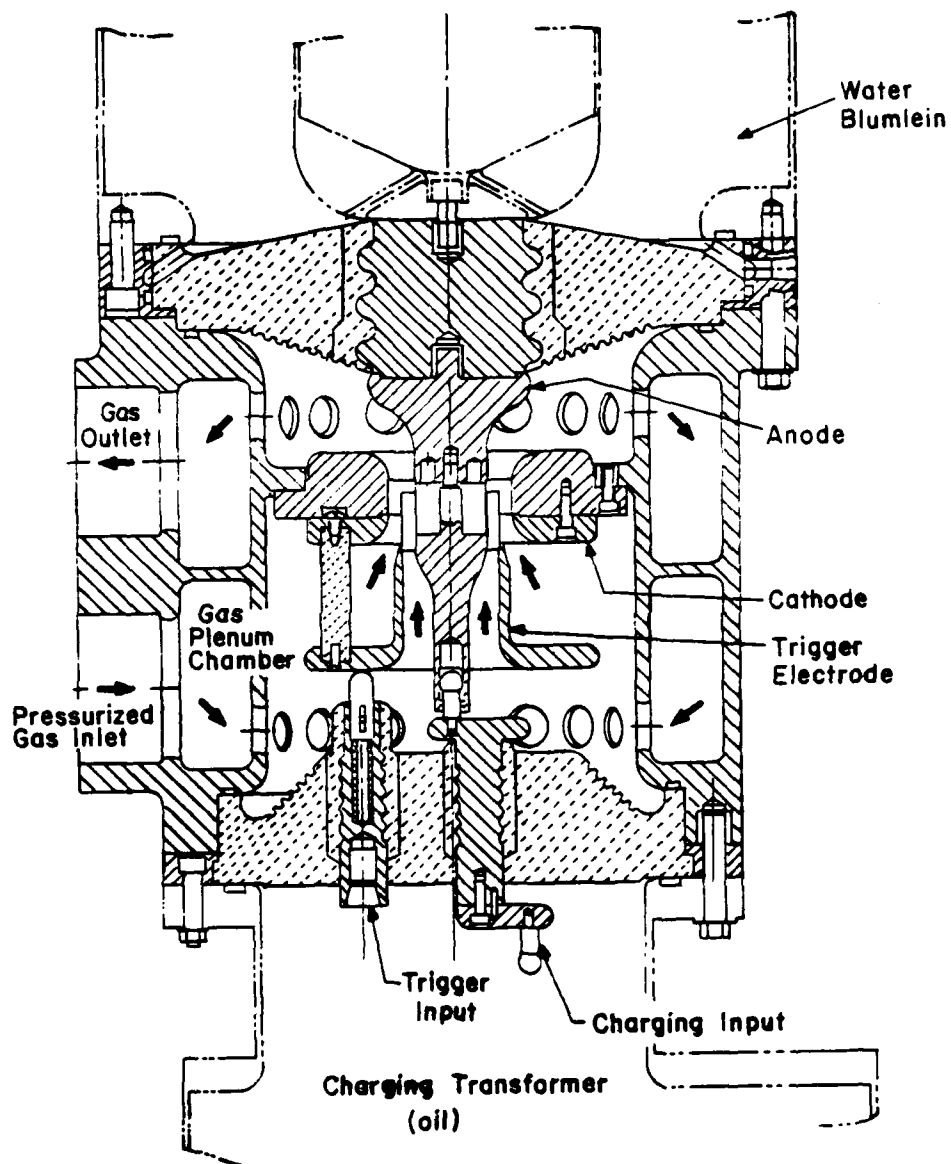


Fig. IV-II. SPARK GAP CROSS SECTION [57]



shots and the projected life is at least  $10^7$  shots. The rep-rate was found to be less when operated near self breakdown of the gap. The operating gas was 80 psig of  $N_2$  with 6-8%  $SF_6$  in an axially flowing system. Tantalum is used for the arc surfaces on the three electrodes.

It is not clear from the reported work [57] how this switch will perform for long bursts or in a continuous rep-rate mode. Switches very similar or identical to the one described above are listed as commercially available [62]. The switches are listed as having a rep-rate from 1-2.5 kHz with no mention of burst mode but it is not clear that they have actually been tested in long continuous runs. The life is indicated as  $10^7$  at currents of 30-40 kA and voltages of 100-250 kV. The jitter is specified as being 1 ns. The recovery rate is  $25 \times 10^{12}$  V/s.

At very low energy or Coulomb per shot, spark gaps have been operated at very high rep-rates in a self trigger mode at reduced recovery voltage. Frequencies in the 100's of kpps have been demonstrated. Special gaps for short (0.6 ns) pulse widths and modest current rating (500-1000 A) have been designed [63] using  $BaTiO_3$  discs in the interelectrode space. These gaps have been rep-rated at  $3 \times 10^4$  pps at 500 A and  $10^4$  pps at 1 kA with a 200 hr lifetime. A rep-rate of 7 kpps at 500-600 A and 3 kpps at 1 kA with a pulse length up to 7.5 ns were also achieved. The voltages were in the 2-8 kV range.

### 5. Electrode Erosion and Heating

The question of electrode erosion and heating is obviously an important one to the design of rep-rated, long life, spark gaps. There has, to our knowledge, been no comprehensive, careful study of this phenomenon. One of the problems is the very large number of possible parameters that may affect the erosion rate. Among these parameters are:  $\frac{di}{dt}$ ,  $I_p$ ,  $\int i dt$ ,  $\int i^2 dt$ , electrode material, gas type, geometry, polarity, trigger method, electrode cooling, gas flow, rep-rate, etc. It is obviously very difficult to arrange, at a reasonable cost, an experiment that can study each of these parameters independently of the others. Also, since the erosion rate usually is in the 1-100  $\mu$ gram/shot range, a substantial number of shots must be made before an easily measurable mass change has occurred.

It is generally assumed that the electrode erosion is closely related to the electrode surface temperature and resulting melting and vapor jet formation. Early, work was carried out by Llewellyn-Jones [64] and by Finkelburg [65]. For instance, Finkelburg calculates that the weight of metal lost from an electrode is given by

$$w = \frac{W}{Q} \frac{\text{grams}}{\text{sec-cm}^2} \quad (\text{IV-5})$$

where

$$W = j_c V_c \text{ for the cathode}$$

and

$$W = j_a (V_a + \phi) \text{ for the anode}$$

( $j$  = current density,  $V$  = electrode drop,  $\phi$  = work function,  $Q$  = energy needed to evaporate  $1g$  of electrode material and heat it to the jet temperature (in  $\frac{\text{watt-sec}}{g}$ )). A difficulty in comparing this calculation with experimental results is the lack of knowledge of the specific heat of metal vapors over this wide a temperature range. Calculations and experimental results generally disagree [66] by factors of 3-50. In the work by Llewellyn-Jones [64] certain constants had to be empirically determined and disagreements with experimental results were still a factor of 3. Later work by Belkin and Kiselev [67] claims better agreement, at least for copper, but they also have a somewhat arbitrarily determined constant in their theoretical expression. They find that the mass of metal eroded from the surface is given by

$$M = \frac{2kV_e Q_o R_{cr}}{3\pi c T_{mp} R} \quad (\text{IV-6})$$

where

$k = 0.4$  (somewhat arbitrarily chosen (experimental fit) as fraction of molten metal which is actually eroded)

$V_e$  = electrode voltage drop

$Q_o$  = initial charge on capacitor bank

$R_{cr} = 2\left(\frac{L}{C}\right)^{1/2}$ , the critical resistance of the discharge circuit

$R$  = effective resistance of discharge circuit

$c$  = specific heat of the electrode metal

$T_{mp}$  = melting point temperature of the electrode material.

For short discharges ( $t \sim 10^{-7}$  s) K. Schöbach [68] has derived an equation for the anode temperature, as shown below.

$$T_a = \text{const} \times (V_a + \phi + V_{th}) (\lambda \rho c)^{-1/2} (i_o/t_o)^{1/3} \quad (\text{IV-7})$$

where

$V_a$  = anode drop (ionization potential of gas)

$\phi$  = anode work function

$V_{th} = \frac{1}{e} \frac{3}{2} k T_e$ , ( $T_e$  = electron temp. in discharge)

$\lambda$  = thermal conductivity of anode material

$\rho$  = material density of anode

$c$  = specific heat of anode material

$k$  = Boltzmann's const.

$i_o$  = max. current

$t_o$  = time of max. current

This equation should also be generally correct for the cathode when the energy input term is changed to  $(V_c + V_{th})$ . Note that one should look for anode materials with high  $(\lambda \rho c)$  products in order to keep  $T_a$  low. The gas type determines the anode drop,  $V_a$ , and to some extent the electron temperature,  $T_e$  (e.g. gases with high ionization potential tend to produce higher anode temperatures).

Some calculated results, using this equation are shown in Fig. IV-12. At high  $(i_o/t_o)$  anode jets will form, resulting in violent expulsion of electrode material as shown in Fig. IV-13 which is adapted from the same reference. These curves agree

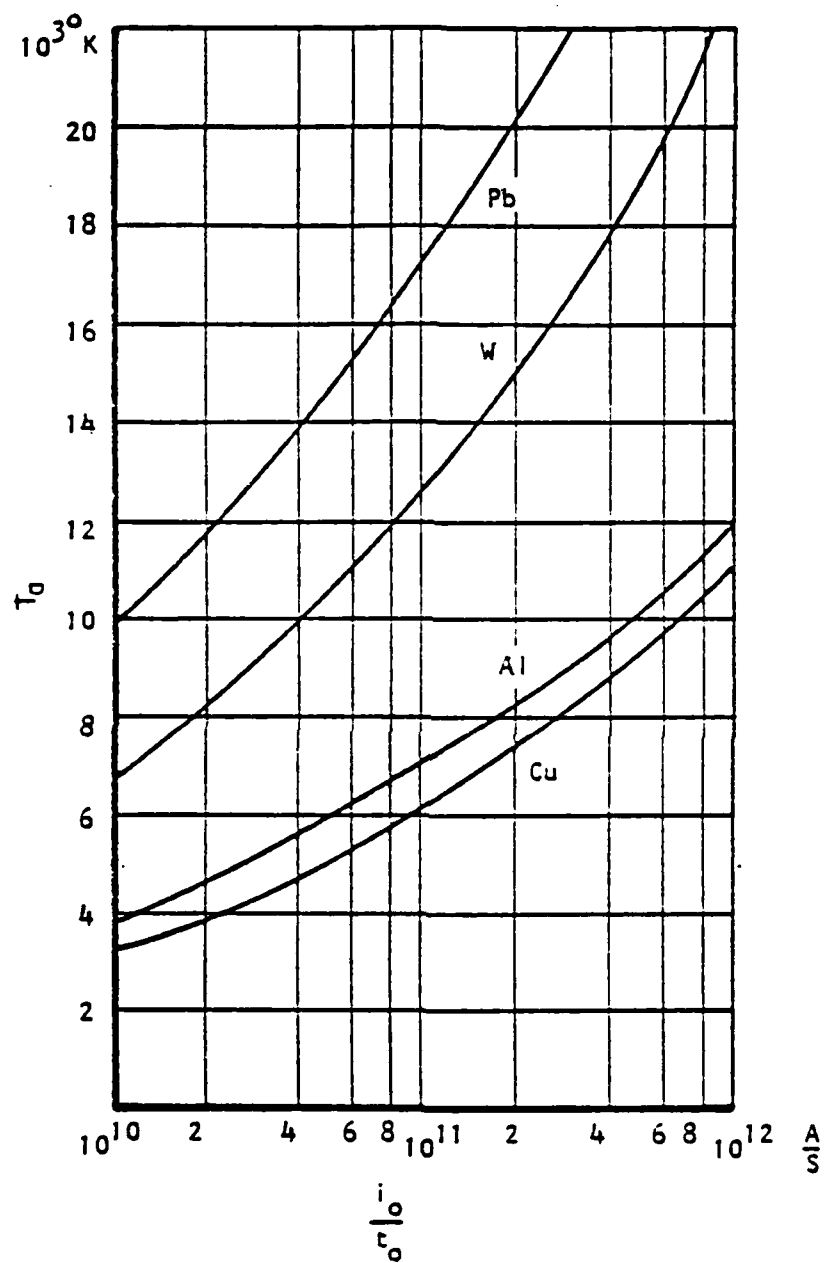


Fig. IV-12. ELECTRODE SURFACE TEMPERATURE vs RATE OF CURRENT RISE FOR COPPER, TUNGSTEN, LEAD AND ALUMINUM. [68]  
 ( $i_o/t_o \triangleq$  Peak Current/Quarter Period)

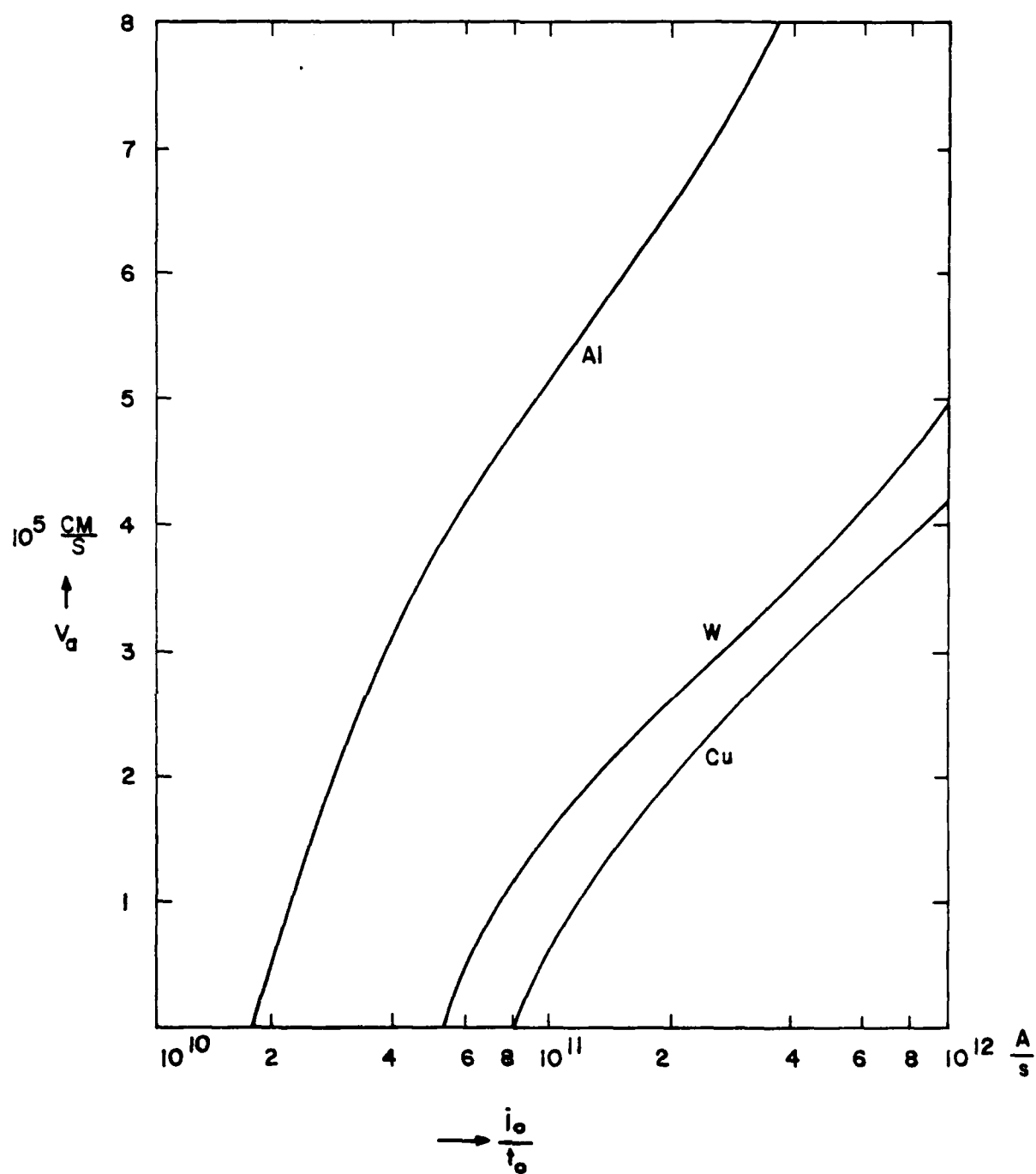


Fig. IV-13. Anode Jet Velocity vs Rate of Current Rise for Copper, Tungsten and Aluminum [68] ( $i_o/t_o$  = peak current/quarter period)

generally within 50% with experimental results [68]. For longer discharge times where radiation and convection become more important, the problem is less understood at the present time. An apparent cause for concern with regard to this [68] experimental work is that the electrode separation was so small (0.2 - 0.85 mm) that it is not clear how and if this scales to larger gap distances.

The electrode erosion problem has the additional aspect that besides surface melting and vapor jet expulsion there is also the chemical reactions between the ionized, high temperature gas and the electrode surface. None of the theoretical efforts have included chemical effects.

The published experimental results disagree in many cases but some general conclusions regarding electrode erosion in gas filled gaps are given below (largely the courtesy of Ian Smith).

- 1) Vacuum operation gives order of magnitude higher erosion rates than operation at roughly atmospheric pressure
- 2) Erosion increases with gas pressure in the 1-4 atm range
- 3) Erosion is material and gas dependent (In general, non-reactive gases and tungsten give lowest erosion rate)
- 4) Cathode and anode erosion rates normally differ (Gas dependent)
- 5) Erosion/Coulomb apparently increases with rep-rate
- 6) Erosion/Coulomb apparently increases with peak current.

In addition the following conclusions come from Belkin's work [67].

- 1) Erosion of metal from electrodes at high currents occurs primarily in the liquid phase.
- 2) The masses of molten and eroded metal depend linearly upon  $q = \int_0^t i dt$  at currents from 70-800 kA.
- 3) The portion of molten metal (the constant  $k$  in Eq. (IV-6)) does not depend upon magnitude or shape of current in the 70-800 kA range.
- 4) Below a certain threshold the linear dependence in 2) above is reduced.
- 5) The erosion is reduced when the external circuit inductance is reduced.

Some of the most extensive erosion tests reported are by J. J. Moriarty, et.al. [69] and by J. E. Gruber and R. Suess [70]. Moriarty, et.al. investigated the erosion of Elkonite 10W3 (75% W + 25% Cu by weight). The results are summarized in Table IV-6. Because so many parameters were varied it is difficult to draw any firm conclusions or plot any curves or trends from this work. The author's own conclusions generally agreed with those given above. These workers found no correlation between erosion and  $\int i^2 dt$  or the arc heating. One should also note that the gas was not circulated in these experiments. Some examples of gas decomposition products after switching are given in Table IV-7.



Table IV-6. Results of Electrode Erosion Tests  
(for Elkonite 10W3) [69]

Gas Mixture (by Volume)	Pressure (psia)	Voltage (kV)	Capacitance ( $\mu$ F)	Charge Flow (mCb)	PRF (pps)	Total Pulses	Total Erosion (mg)	Erosion Rate ( $\mu$ gm/Cb)
100% N <sub>2</sub>	65	-40	0.02	0.8	10	30,000	0.8	33
100% SF <sub>6</sub>	15	-34	1.84	62.6	0.2	5,059	3.3	10.4
	17	-16	1.84	29.4	1.1	31,151	16	17.5
	17	+20	1.84	36.8	1	25,000	12.1	13
	15	+17	1.84	31.3	1	29,084	14.9	16.3
	17	-28	0.02	0.56	10	324,000	4.7	25.9
	45	+40	0.02	0.8	10	100,600	29.2	362
75% C <sub>2</sub> F <sub>6</sub> +25% N <sub>2</sub> O	46	+40	0.02	0.8	10	275,400	38.8	176
50% Ar + 40% N <sub>2</sub> + 10% SF <sub>6</sub>	55	+34	0.02	0.68	10	250,800	26.8	158
50% Ar +	60	+40	0.02	0.8	10	278,000	28.2	130
38% C <sub>2</sub> F <sub>6</sub>	45	+20	0.02	0.4	10	228,600	8.8	96
12% N <sub>2</sub> O	45	-20	0.02	0.4	10	236,700	1.9	20

Table IV-7. Decomposition Products from Switch Discharges [69]

Initial Gas Mixture (By Volume)	Pressure (psia)	Erosion Rate ( $10^{-5}$ g/C)	Gas Analysis After Firing	Bulk Resistivity of Solid Residue (ohm-cm)
100% $\text{SF}_6$	45	36.2	$\text{SF}_6$ , $\text{SO}_2\text{F}_2$ , $\text{SiF}_4$ HF = 0.02%	No sample
75% $\text{C}_2\text{F}_6$ + 25% $\text{N}_2\text{O}$	46	17.6	$\text{C}_2\text{F}_6$ - 70% $\text{N}_2\text{O}$ - 2.8% $\text{CF}_4$ - 16% $\text{C}_2\text{F}_4$ - 3.26% + air & misc.	$7.9 \times 10^{12(c)}$
50% $\text{Ar}^{(a)}$ + 40% $\text{N}_2$ + 10% $\text{SF}_6$	55	15.8	$\text{SF}_6$ , $\text{SO}_2\text{F}_2$ (sizable) $\text{SiF}_4$ (small) HF = 0.13%	$< 0.2 \times 10^7$
50% $\text{Ar}^{(b)}$ + 38% $\text{C}_2\text{F}_6$ + 12% $\text{N}_2\text{O}$	60	13.0	$\text{C}_2\text{F}_6$ - 39% $\text{N}_2\text{O}$ - 1.6% $\text{Ar}$ - 40% $\text{CF}_4$ - 12.5% $\text{C}_2\text{F}_4$ - 2.5% + air & misc.	$> 3.3 \times 10^{11(c)}$ $3.9 \times 10^{12(d)}$

(a) Analysis of unfired sample showed  $\text{SF}_6$ ,  $\text{Ar}$ ,  $\text{N}_2$ ,  $\text{O}_2$  and  $\text{CO}_2$  present. There were no hydrolyzable fluorides (HF).

(b) Initial gas mixture is probably in error. Consistency with subsequent analysis would require initial mixture of 40%  $\text{Ar}$  + 45%  $\text{C}_2\text{F}_6$  + 15%  $\text{N}_2\text{O}$ .

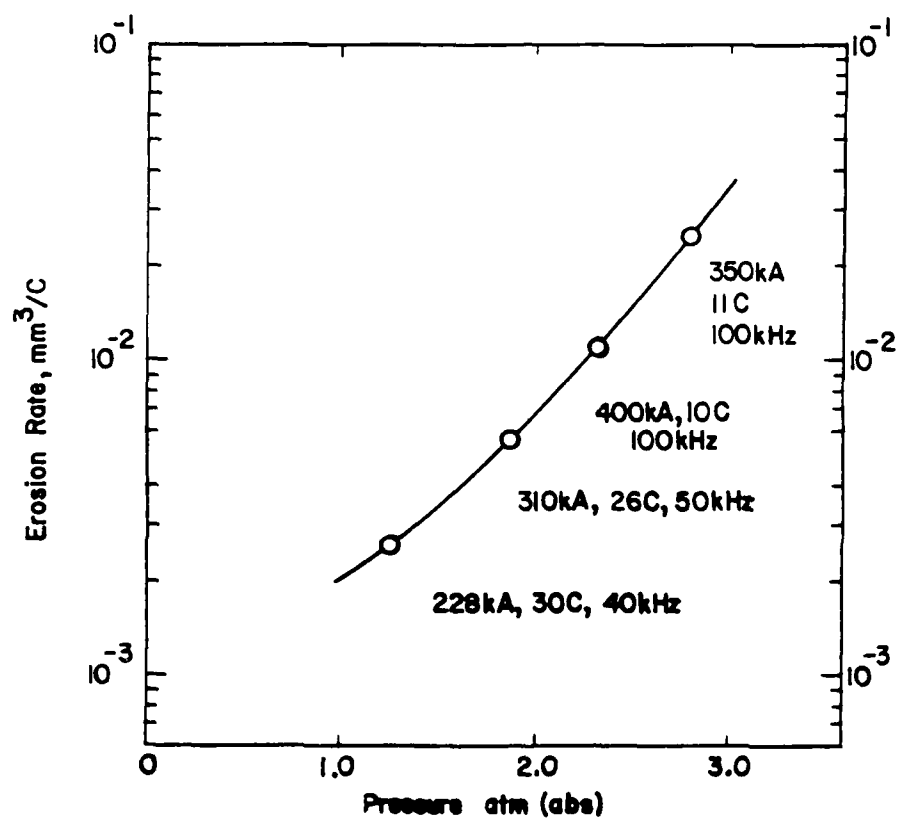
(c) A gray deposit collected in general area of the electrode.

(d) A "shellac-like" deposit found around center of electrode and obtained after wiping the gray (c) deposit away. This deposit (d) was soluble in acetone.

The strong increase in erosion with increased gas pressure has also been reported by R. A. Burden and T. E. James [25] as shown in Fig. IV-14. One should note, however, that the experimental conditions were not the same for all the data points. In the apparently very careful investigation by Gruber and Suess [70] this marked increase in electrode erosion with pressure was not observed. Their results are summarized in Fig. IV-15. Only copper shows a marked pressure dependence and this may be caused by chemical reactions with the air in the gap. The understanding of gas pressure effects on erosion is thus, at best, incomplete.

One should also note that J. C. Martin has observed [71] that vortex gas flow in a slowly rep-rated (3-10 pps) spark gap results in increased erosion rate (factor 10). This is presumably because the metal vapor is swept away before it gets a chance to re-deposit on the electrodes. The increase in erosion with flowing gas was not observed however, in an experiment [72] where the flow was more laminar. In many cases it is desirable to use a slightly reactive gas since this tends to remove whiskers on the electrode surface which otherwise would lead to unreliable switch operation. This will, however, also lead to higher erosion rates.

In the work by Gruber and Suess [70] all the tests were carried out with a damped sinusoidal discharge with a decay time constant of 50-200  $\mu$ s. Two different electrode separations



EROSION OF MK V GAP MAIN ELECTRODES [25]  
Electrode material - brass  
Air gap - 15mm

Fig. IV-14.

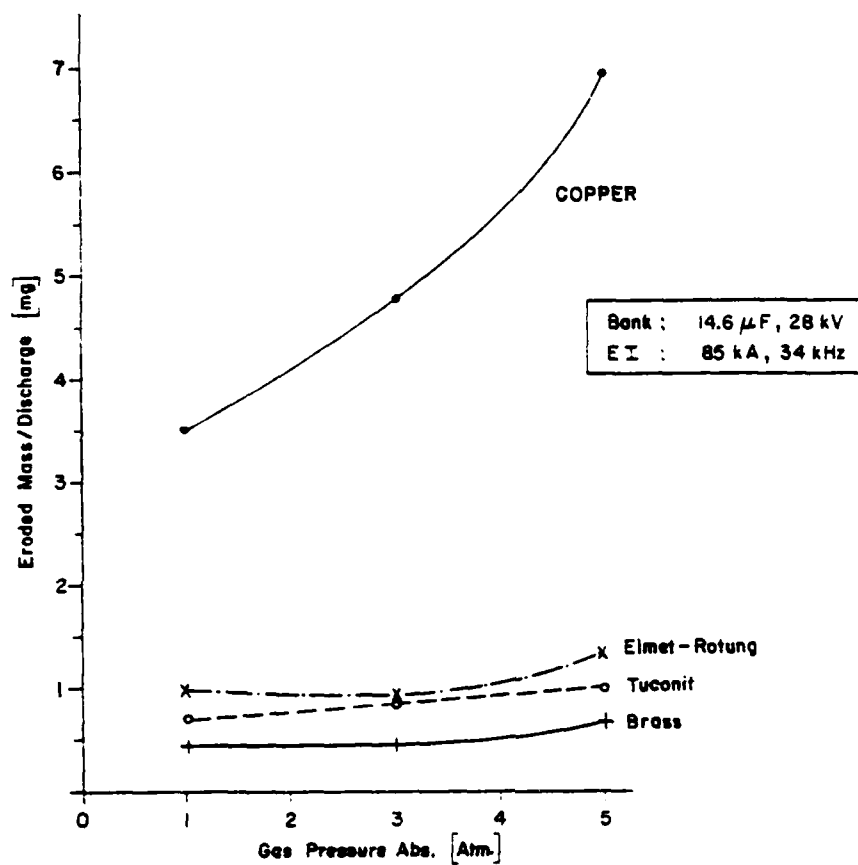


Fig. IV-15. Effect of gas pressure on erosion rate in a 2mm gap, electrodes 30mm diam.,  $Q = 7Cb$  const. [70]

were used (13 and 1.5 mm) and it was found that the erosion rate was much higher in the small gap (factor of 10). The predominant erosion effect was found to be  $\int idt$  but an  $i$ -dependence (at constant  $\int idt$ ) was also found. These results are summarized in Figs. IV-16 through IV-19. The erosion results for copper tend to support Belkin's results [67] but detailed agreement was not found. Tungsten-copper electrodes (80% W + 20% Cu, similar to Elkonite) were found to have the best erosion characteristics, in agreement with other reports [8, 69, 73]. The "discontinuities" in the erosion curves for copper and brass may be related to the "threshold" values discussed by Belkin [67, 79] and may be due to the onset of the molten phase over the entire electrode surface area.

Graphite electrodes of various kinds have also been tested for erosion [75] and compared with brass electrodes. The test conditions were: 10,000 shots, 100 kA, 0.5 C/shot. The erosion rates were about the same (slightly less) as for brass except that a whole chunk of material came loose from one of the graphite electrodes.

In an erosion study at the UKAEA Culham Laboratory [76] the effect of peak current ( $I_p$ ) on the erosion rate of brass (main electrodes) and heavy-metal (trigger electrode) in a field distortion spark gap was studied. It was found that the erosion is proportional to  $I_p^{1.7}$  and that the erosion/Coulomb was essentially constant below some current threshold ( $> 250$  kA).

For spark gap erosion studies it is important to decide the validity of using ringing discharges rather than sinusoidal or "square" unipolarity pulses. In many practical applications the pulses will be of one polarity rather than a ringing, damped discharge. With the ringing discharge the Coulomb transfer is much enhanced, however, since

$$q = CV \frac{1 + I_1/I_{\max}}{1 - I_1/I_{\max}} \quad (\text{IV-8})$$

where  $I_{\max}$  = max current at first half period  
 $I_1$  = max current at second half period  
 $V$  = Charging voltage of capacitor  
 $C$  = Capacitance of capacitor  
 $q$  = Charge transfer (Coulomb)

The ringing discharge is thus a relatively simple and inexpensive way to produce a large number of C/shot.

At first thought it appears that "a Coulomb is a Coulomb." It is, however, not so clear that one can interpret in a simple way erosion studies done in this manner since the erosion is undoubtedly also a function of peak current and electrode heating. It has been shown [23] that for a ringing discharge with 90.8% reversal the energy deposition per Coulomb (J/C) in the electrode was 3.4 times greater than in the case of no reversal. Careful comparisons of erosion studies with damped and ringing discharges has, to our knowledge, not been made but probably warrants a closer look since the ringing discharges can greatly simplify the test circuitry and power requirements.

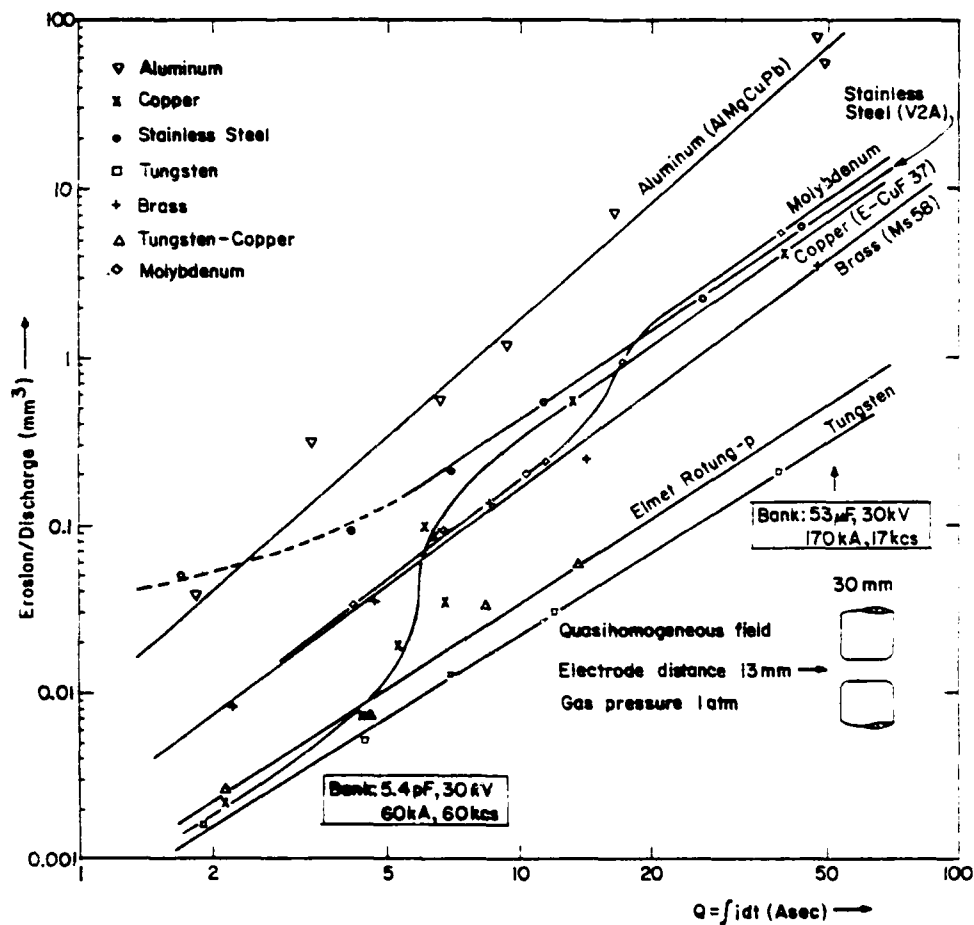


Fig. IX-16. Erosion Rate for Different Electrode Metals  
(13mm, 1 atm) [70]



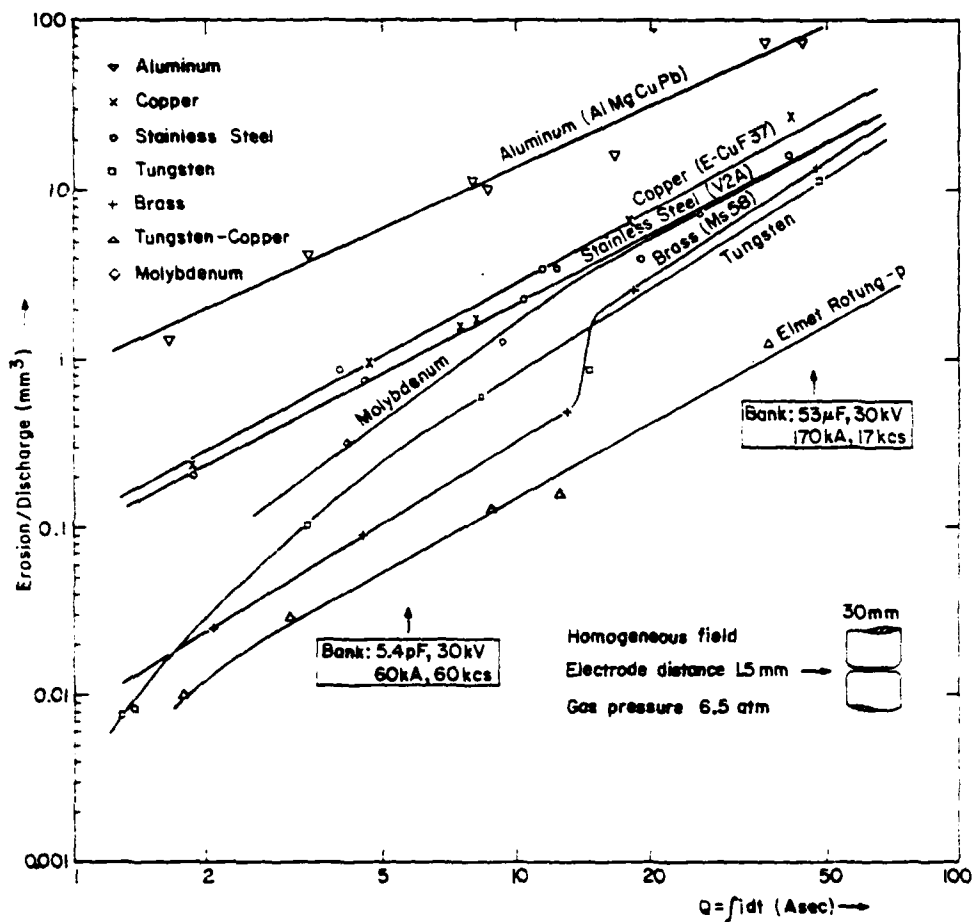


Fig. IX-17. Erosion Rate for Different Electrode Metals  
(1.5 mm, 6.5 atm) [70]

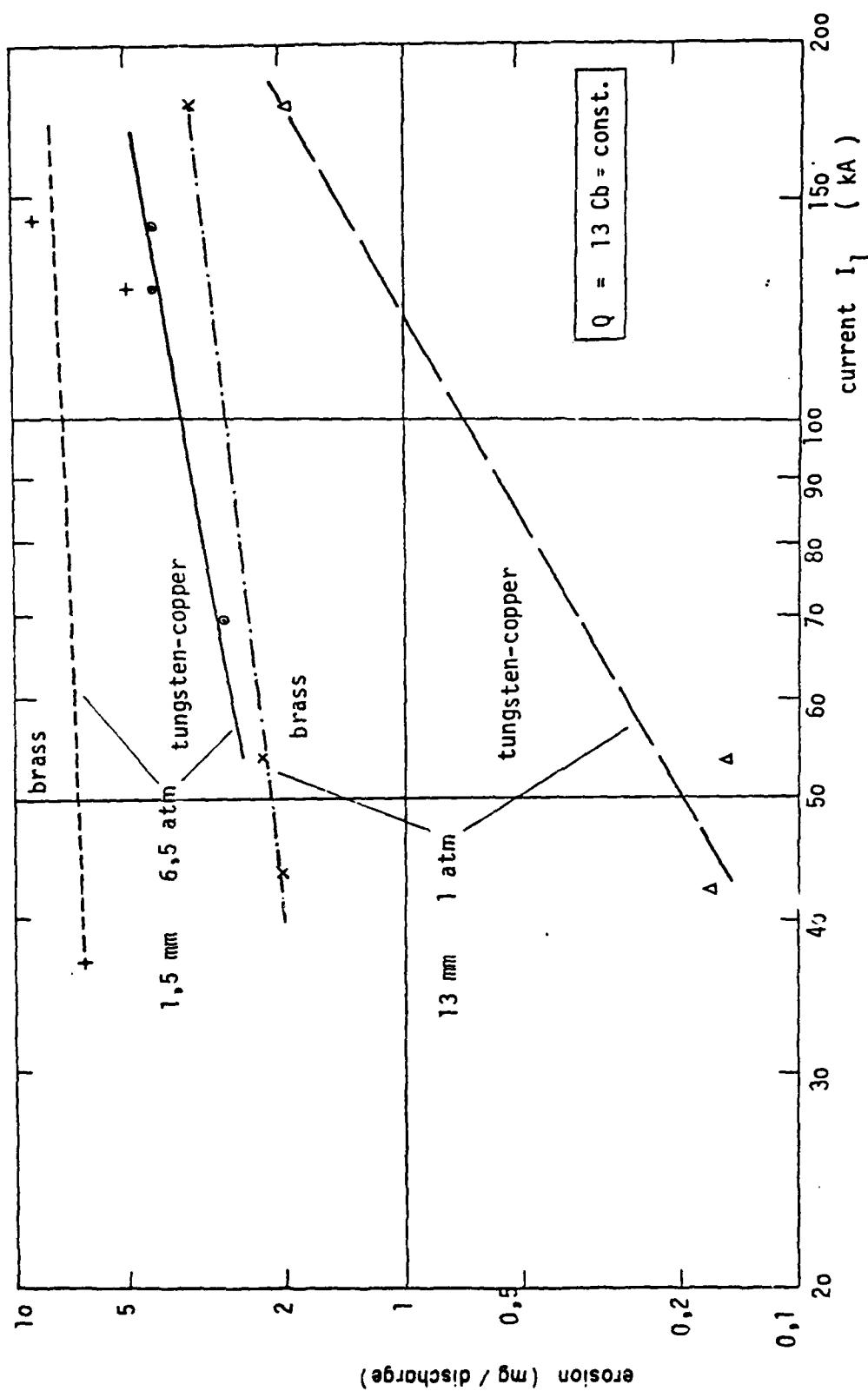


Fig. IV-18. THE EROSION AT A CONSTANT COULOMB RATING BUT VARYING CURRENT [70]

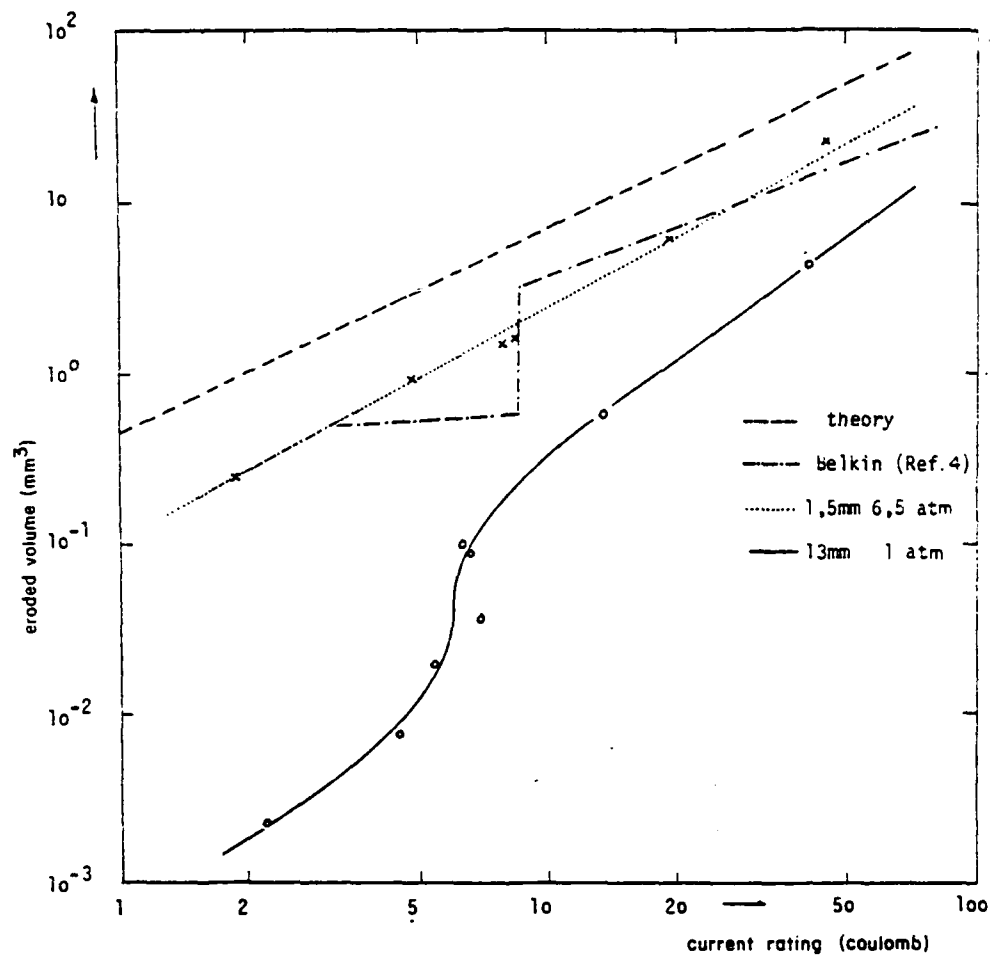


Fig. IV-19. THE EROSION OF COPPER [70]

## 6. Some Quantitative Spark Gap Parameters

Many important spark gap parameters have been extensively studied and many of them can be described empirically or theoretically. Some important parameters are described in the following.

### a. Discharge Impedance and Risetime

When calculating the risetime of a spark gap it is necessary to know the resistive and inductive time phases of the spark channel. The total e-folding risetime is usually taken as  $t_e = t_R + t_L$  but one may advance some arguments for using  $t_e = (t_R^2 + t_L^2)^{1/2}$ . To convert to 10% to 90% risetime use

$$t = 2.2t_e \quad (\text{IV-9})$$

The resistive time phase is given empirically by\*

$$t_R = \frac{88}{(Z_O)^{1/3} (E)^{4/3}} \left(\frac{\rho}{\rho_O}\right)^{1/2} \text{ ns} \quad (\text{IV-10})$$

This formula, whose symbols are defined below, has recently been found to differ from experimentally obtained values for risetime. It has been found that the risetime depends on the gas. Proposed empirical formulas [77] are:

for Nitrogen

$$t_R = 44 p^{1/2} / E Z_O^{1/3} \quad (\text{IV-11})$$

and for Helium

$$t_R = 6.4 p^{1/3} / E^{1/2} Z_O^{1/3} \quad (\text{IV-12})$$

\*J. C. Martin, UKAWRE, Aldermasten.

where  $Z_o$  = source (machine) impedance in ohms

$E$  = Electric field in gap in MV/m units

$\rho$  = gas density

$\rho_o$  = density of air at STP

$p$  = pressure in atmospheres

It should also be noted that O'Rourke [78] has proposed an equation similar to Martin's, namely

$$t_R = k \left( \frac{\ell \rho}{E^4 Z_o} \right)^{1/3} \quad (\text{IV-13})$$

where  $\ell$  = length of arc channel

$k$  = empirical constant

Time resolved measurements of the resistance during spark gap breakdown have recently been reported for the 0.1-1.5 ns range [79]. Their results are found to differ somewhat from those in Ref. [77] for nitrogen gas. The inductive time phase is given by

$$t_L = \frac{L}{Z_o} \quad (\text{IV-14})$$

where  $L$  = inductance of spark channel  $\sim \frac{\mu_o \ell}{2\pi} \ln \frac{b}{a}$  Henrys

where  $\ell$  = gap distance in meters

$$\mu_o = 4\pi \times 10^{-7} \text{ H/m}$$

$b$  ~ radius of electrode

$a$  ~ radius of channel

Although the channel radius is time dependent (see subsection on Arc Radius) the  $\ln$ -term makes the inductance relatively

insensitive to this fact and it seems that as a general rule  $L \sim 10-15$  nh/cm is a fairly good estimate. This is also supported by theoretical calculations [80].

#### b. Electrode Heating

Electrode heating is obviously very important in connection with spark gap erosion and it is desirable to keep the temperature as low as possible.

The heat flow through an electrode (anode) surface per unit time has been calculated by K. Schönbach [68] for rapid discharges.

$$\dot{Q}(t) = \frac{\lambda T_e}{a\sqrt{\pi t}} R^2(t) \quad (\text{IV-15})$$

where  $\lambda$  = thermal conductivity

$R$  = channel radius (see Eq. (IV-19))

$T_e$  = electron temperature

$a^2 = \kappa/c_v$

$\kappa$  = the thermal conductivity of the anode material

$c_v$  = the specific heat per unit volume of the anode material

The anode temperature is then given by Eq. IV-7. The same equation (Eq. (IV-7)) is also generally valid for the cathode as long as the energy input term is properly modified (i.e.

$$(V_a + \phi + V_{th}) \rightarrow (V_c + V_{th})).$$

## c. Arc Voltage

The arc voltage is important when calculating the gap dissipation and efficiency. Reliable data for the arc voltage have been difficult to obtain. The results of James and Browning [81] are difficult to apply in general since the necessary constants in the equation are generally not known. They find

$$V_a = (A + \ell_g E_\infty) \left(1 + \frac{E_0}{E_\infty} (1 - e^{-t/\tau})\right) \quad (\text{IV-16})$$

where  $A$  = constant for fixed  $p$ ,  $I$ , and electrode system  
(e.g.:  $A$  varies from 15-30 for  $p = 1$  atm and  $I$  varying from 1.5-40 kA)

$\ell_g$  = gap length

$E_\infty$  = Avg. electric field during pulse for long pulse times

$E_0$  = Avg. electric field during pulse for short times

$t$  = pulse length

$\tau$  = characteristic time const ( $\sim 1.5$  ms at  $p = 1$  atm)

These values can be deduced for argon and air at atmospheric pressure from the curves in Ref. [81].

Boicourt [82] has derived an empirical equation for the arc voltage in air filled spark gaps ( $p = 20$ -30 psi). He finds:

$$V_a = k_1 + k_2 |I| + k_3 |I|^2 \quad (\text{IV-17})$$

where  $k_1 = 99$   
 $k_2 = 8.9 \times 10^{-4}$   
 $k_3 = 2.25 \times 10^{-10}$

For the vacuum case [83] it is, for comparison, found that for  $I < 6.5$  kA

$$V_a = 20 + GI, \quad (\text{IV-18})$$

where  $G$  is a constant which depends upon electrode material, shape, and separation.

#### d. Arc Radius and Joule Losses

Information about the arc channel radius is important both to risetime and erosion (temperature) calculations. The questions of arc radius and growth are, however, still unresolved in the general case. For short discharge times ( $t < 100$  ns) the most commonly stated equation for the channel radius is [84]

$$R(t) \cong \left( \frac{4}{\pi^2 \rho_0 \xi \sigma} \right)^{1/6} \left( \int_0^t I^{2/3} dt \right)^{1/2} \quad (\text{IV-19})$$

where  $\rho_0$  = initial gas density

$\sigma$  = electrical conductivity of spark channel

$I$  = current

$$\xi = K_p \left( 1 + \frac{1}{(\gamma-1) 2 \dot{r}(t)^2} \ddot{r}(t) \right)$$

where  $K_p = 0.9$  (the coeff. of resistance in the pressure equation  $P = K_p \rho_0 \dot{r}(t)^2$ )

$\gamma$  = effective adiabatic constant

Reasonable agreements with this equation have been found [85-87] although it does not take into account the heat conduction losses from the channel. Recent investigations at



Technische Hochschule Darmstadt, FRG are re-examining both the theoretical development and the verification of this equation [88]. Under certain special assumptions about the conductivity of air ( $220 (\Omega \text{ cm})^{-1}$ ), its constancy and ionization number ( $Z = 1$ ), and about the current rise ( $I \propto t^{3/4}$ ), Equation (IV-19) can be written as

$$R(t) = A \rho_0^{-1/6} I^{1/3} t^{1/2} \quad (\text{IV-20})$$

where

$R$  is in mm

$\rho_0$  is in atm

$I$  is in kA

$t$  is in  $\mu\text{s}$

$A = 0.92$

For other theoretical calculations of  $R(t)$  under various gas shock conditions set up by the expanding channel see refs. [89, 90]. A review [91] of some Soviet work on arc channel evolution at  $p \leq 1$  atm claims good agreement with the theory development in ref. [89, 90].

For modest current levels of  $I_m < 250 p^{1/2}$  (where  $p$  is in atmospheres and  $I$  in kA), the joule losses in the discharge channel scale as [8]

$$P \propto (p^{1/3}, I_m^{4/3}) \quad (\text{IV-21})$$

For higher current values, it is found empirically that [8]

$$P \propto (p^{2/3}, I_m^{4/3}) \quad (\text{IV-22})$$

#### e. Breakdown Voltage

The self breakdown voltage of a gap is obviously a most important design parameter. For uniform DC fields in air, the breakdown field is given by [44]

$$E_{BD} = 24.6p + 6.7 \left(\frac{p}{d}\right)^{1/2} \text{ kV/cm} \quad (\text{IV-23})$$

where  $p$  = gas pressure in atm.

$d$  = electrode separation in cm.

For non-uniform fields, the  $E_{BD}$  can be considerably less than this and the "field enhancement" and "effective electrode distance" must be considered (see Ref. [44]). For pulse charged gaps with extremely divergent fields (e.g. points or edges), the breakdown field can be both time, polarity, and pressure dependent [44]. An approximate expression is

$$\bar{E}_{BD} (dt)^{1/6} = (k_{\pm}) p^{\beta} \quad (\text{IV-24})$$

where  $\bar{E}_{BD}$  = the mean field ( $V/d$ ) in kV/cm

$d$  = electrode separation in cm

$t$  = pulse time in  $\mu s$  (time when pulse is above 63% of max value)

$p$  = pressure in atm,

and where  $k_{\pm}$  depends upon the polarity of the sharp electrode

and is given below together with the exponent,  $\beta$ , for some gases.

	<u>Freon</u>	<u>SF<sub>6</sub></u>	<u>Air</u>
$\beta$	0.4	0.4	0.6
$k_+$	36	44	22
$k_-$	60	72	45

For long pulse times, the pressure dependence for air disappears [44].

## 7. References

- [1] E. L. E. Wheatcroft, Gaseous Electrical Conductors, Oxford Press 1938.
- [2] A. S. Denholm et.al., "Review of Dielectrics and Switching," AFWL-TR-72-88.
- [3] P. Felsenthal and J. M. Proud, "Nanosecond Pulse Breakdown in Gaps," Phys. Rev. 139, A 1976 (1965).
- [4] J. C. Martin, "Pressure Dependency of the Pulse Breakdown of Gases," Pulsed Electrical Power Dielectric Strength Notes PEP 5-1, Note 15, AFWL TR 73-167, April 1973.
- [5] P. D'A. Champney, "Some Recent Advances in Three Electrode Field Enhanced Triggered Gas Switches," Energy Storage, Compression and Switching, Plenum Press. N.Y. and London, 1976.
- [6] P. Felsenthal and J. M. Proud, "Nanosecond Switch Development," AFWL-TR-65-119, Nov. 1965.
- [7] Proceedings of the Workshop on Switching Requirements and R & D for Fusion Reactors, March 24-26, 1976, Rept. EPRI ER-376-SR (M. Kristiansen, Editor), Electric Power Research Institute, 3412 Hillview Avenue, Palo Alto, Calif. 94304.
- [8] V. S. Komelkov, Technology of Large Impulse Currents and Magnetic Fields, Translation FTD-MT-24-992-71.
- [9] S. Kassel and C. D. Hendricks, "Soviet Research and Development of High-Power Gap Switches," Rept R-1333-ARPA, Jan 1974, (ARPA Order No. 189-1).
- [10] C. Grey Morgan, "Irradiation and Time Lags" Chapter VI Contribution to new edition of Electrical Breakdown of Gases (Univ. Wales, Univ. College of Swansea).
- [11] E. L. Kemp, "Switching Requirements for Near-Term, Pulsed High-Beta Experiments," Proc. Workshop on Switching Requirements R & D for Fusion Reactors (M. Kristiansen, Editor) Rept. EPRI ER-376-SR, July 1977 Electric Power Research Inst., 3412 Hillview Avenue, Palo Alto, Calif. 94304.
- [12] S. Kassel, "Soviet Pulsed-Power R & D," Rand Rept R-2212-ARPA (preprint, 1978).

- [13] J. M. Proud and H. J. Huber, "Picosecond Risetime Switch Study," RADC-TR-67-400, Aug. 1967.
- [14] Maxwell Laboratories, Inc., "Investigating Means of Reducing the Weight of Large RES Generators," Rept. MLR-9C, AFWL EMP HAS 3-3, April 1970.
- [15] Gardner, et.al., "High Power Pulse Line Switching," Final Rept., Series 5, Issue No. 10 Contract W-28-099 ac-446, Univ. Calif., Microwave Lab., April 1952. (Also see J. B. Woodford, "Spark Gap Switches for Low-Jitter Radar Service, Report of a Literature Study," Rome ADC Contracts No. AF-30(602)-96 Phase 7 and No. AF-30(602)-915, Jan. 1954).
- [16] J. C. Martin, "High Speed Pulse Breakdown of Pressurized Uniform Gaps," UKAWRE Rept. SSWA/JCM/7081107 (Aug. 1970).
- [17] L. P. Bradley, "Highly Overvolted Gas Spark Gaps for Electron Beam Generators," Sandia Laboratories, Albuquerque, N.M. (undated).
- [18] J. E. Gruber and T. E. James, "Fast Pulse Breakdown of Non-uniform Field Pressurized Air Spark Gaps," CLM-Pl71, Culham Laboratories, 1968.
- [19] S. I. Andreev and M. P. Vanyukov, "Application of a Spark Discharge to Obtain Intense Light Flashes of Length  $10^{-7}$  -  $10^{-8}$  sec." Sov. Phys.-Tech. Phys 6, 700 (1962).
- [20] V. V. Baraboshkin, "Plasma Trigatron Spark Gap," Priory i Tekhnika Experimenta, No. 2, 131 (1977).
- [21] P. M. Barnes, et.al., "High Current Switching Using Low Inductance Field Distortion Spark Gaps Closely Connected in Parallel," CLM-R71, Culham Laboratories, 1967.
- [22] R. A. Burden and J. E. James, "Premature Breakdown and Electrode Erosion Studies in a High Current Spark Gap Switch," Int. Symp. High Voltage Technology, Munich, 9-14 March, 1972.
- [23] Ian Smith, ISI, Personal Communication.
- [24] A. E. Bishop and G. D. Edmonds, "A 250 Coulomb 40 kV Spark Gap," Proc. 5th Symp. Fusion Technology, Oxford, U.K., 1968.
- [25] R. A. Burden and T. E. James, "Statistical Performance Data for A High Current 60 kV Spark Gap Switch," Proc. 7th Symp. Fusion Technology, Grenoble, France, 24-27 Oct. 1972.

- [26] W. H. Borkenhagen, et.al., "Multichannel Spark Gap Technology for Staged Theta Pinch Machines," Proc. 6th Symp. Eng. Probs. Fusion Research, San Diego, 1975.
- [27] K. B. Riepe, LASL, Personal Communication.
- [28] G. Simcox, PI, Personal Communication.
- [29] J. C. Martin, "Short Pulse High Voltage Systems," Energy Storage, Compression, and Switching, Plenum Press, N.Y. and London, 1976.
- [30] F. B. A. Früngel, High Speed Pulse Technology, Vol. I, Sec. B, "Switching Means," Academic Press, N.Y. (1965).
- [31] F. Rose, NSWC, Personal Communication.
- [32] "High Power Spark Gap Optimization," Final Report on NSWC, Dahlgren Lab. Contract N 60921-76-C-0274, June 16, 1977., Maxwell Lab. Rept. MLR-670.
- [33] H. Milde, Ion Physics, Personal Communication.
- [34] J. D. Craggs, et.al., "The Development of Triggered Spark Gaps for High-Power Modulators," J. Inst. Elect. Eng. 93, Part III A, No. 5, March-May 1946.
- [35] L. B. Woolaver, "The Use of Triggered Spark Gaps as Crowbars," Proc. 7th Symp. on Hydrogen Thyratrons and Modulators, Fort Monmouth, N.J., May 22-24, 1962, p. 521.
- [36] P. I. Shkuropat, "Electrical Characteristics of Controlled High-Current Triggered Air Spark Gaps," Sov. Phys.-Tech. Phys. 11, 779 (1966).
- [37] D. Markins, "Command Triggering of Synchronized Megavolt Pulse Generators," Maxwell Laboratories, Inc. San Diego, Calif. (undated).
- [38] R. A. Fitch and N. R. McCormick, "Low Inductance Switching Using Parallel Spark Gaps," Proc. IEE (London) 106A Suppl. 2, 117 (1959) (Also see Proc. 4th Int. Conf. Phenomena in Gases, Vol. 2, Amsterdam, 1960).
- [39] T. E. Broadbent and A. H. A. Shlash, "The Hot-Wire Triggered Spark Gap at Very High Voltages," Brit. J. Appl. Phys. 13, 596 (1962).

- [40] R. A. Harraway, "An Exploding Wire Triggered Spark Gap," J. Sci. Inst. 41, 399 (1964).
- [41] W. A. Cilliers and S. Leeman, "Switching and Clamping by Means of Plasma Jet Switches," J. Sci. Inst. 39, 528 (1962).
- [42] T. Shimizu and M. Hirata, "On Starting an Electric Spark by Intense Ionization of the Sparking Space," Sci. Paper Inst. Phys. Chem. Res. Tokyo, 38, 317 (1941).
- [43] W. H. Borkenhagen, et.al., "Multichannel Spark-Gap Technology for Theta-Pinch Machines," 6th Symp. Eng. Problems of Fusion Research, 1975.
- [44] J. C. Martin, "Nanosecond Pulse Techniques," Circuit and Electromagnetic System Design Notes, Note 4, April 1970.
- [45] T. E. James, "High-Current 60 kV Multiple-Arc Spark-Gap Switch of 1.7 nH Inductance," Proc. IEE 117, 1448 (1970) (Also CLM-P212, Culham Laboratory, July, 1969).
- [46] P. M. Barnes, et.al., "The Parallel Operation of Low-Inductance High-Current Spark Gaps Without Transit Time Isolation," J. Sci. Inst. 44, 599 (1967).
- [47] A. H. Guenther and J. R. Bettis, "The Laser Triggering of High-Voltage Switches," to appear in J. Phys. D: Appl. Phys. 11, (1978).
- [48] H. I. Milde, "Dielectric Strength Recovery of a Spark Gap," Appendix D of Multimegavolt Modulator Feasibility Study, RADC-TR-68-241, pp. 143-158.
- [49] A. B. Parker, et.al., "The Measurement of Electrode Surface Temperature and its Role in the Recovery of High-Current Spark Gaps," Brit. J. Appl. Phys. 16, 851 (1965).
- [50] G. A. Farrall and J. D. Cobine, IEEE Trans. Power App. and Syst. PAS-86, 927 (1967).
- [51] E. P. Bel'kov, "Gas Cooling and Electric Strength Recovery After a Spark Discharge," Sov. Phys.-Tech. Phys. 16, 1321 (1972).
- [52] M. P. Vanyukov, et.al., "Dielectric Strength Recovery of a Spark Gap in a Repeating-Discharge Regime," Sov. Phys.-Tech. Phys. 7, 544 (1962).

- [53] Wayne Clark, "High Power Spark Gap Switch Development, Final Report," AFAPL-TR-75-41 (Maxwell Lab. Rept. MLR-489), May 1975.
- [54] J. F. Driscoll, et.al., "Fundamental Study of High Power Spark Switch Operation," DRDA Project 014436, Dept. Aerospace Eng., Univ. Michigan, May, 1977.
- [55] A. Ramrus, "Development of a 100 kV Multimegawatt Rep Rate Gas Switch," Proc. 13th Pulse Power Modulator Symposium, SUNY/Buffalo, N.Y., June 20-22, 1978.
- [56] M. T. Buttram and G. J. Rohwein, "Operation of a 300 kV, 100 Hz, 30 kW Average Power Pulser," Proc. 13th Pulsed Power Modulator Symp., SUNY/Buffalo, N.Y., June 20-22, 1978.
- [57] A. Faltens, et.al., "High Repetition Rate Burst-Mode Spark Gap," Preprint UCRL-80634, June 15, 1978 (Also Proc. 13th Pulsed Power Mod. Symp.).
- [58] K. Takeda and Y. Hatta, "High Frequency Discharges in High Speed Gas Flow," Proc. 2nd Int. Conf. Gas Discharges, London (1972).
- [59] J. C. Martin, AWRE, Personal Communication.
- [60] "Electron Beam Fusion Progress Report," April through September, 1977. Sandia Laboratories Rept. SAND 78-0080.
- [61] W. Hertz, et.al., "Investigations of the Properties of SF<sub>6</sub> as an Arc Quenching Medium," Proc. IEEE 59, 485 (1971).
- [62] Veradyne Corp. 330 No. Victory Blvd., Burbank, CA 91502, Coaxial Spark Gap Switch No. 50024, 50030, and 50035.
- [63] S. Kassel, et.al., "Soviet Research and Development of High-Power Gap Switches," DARPA Rept. AD/A-004599, Jan. 1974.
- [64] F. Llewellyn-Jones, "Electrode Erosion by Spark Discharges," Brit. Jour. Appl. Phys. 1, 60 (1950).
- [65] W. Finkelburg, "A Theory of the Production of Electrode Vapor Jets by Sparks and Arcs," Phys. Rev. 74, 1475 (1948).
- [66] C. M. Cundall and J. D. Craggs, "Electrode Vapour Jets in Spark Discharges," Spectrochimica Acta 7, 149 (1955).



- [67] G. S. Belkin and V. Ya. Kiselev, "Electrode Erosion in Pulsed High-Current Discharges," Soviet Phys.-Tech. Phys. 11, 280 (1966).
- [68] K. Schönbach, "Explosive Erosion in Stromstarken Funkenentladungen," Zeitsch. Angew. Phys. 32, 253 (1971).
- [69] J. J. Moriarty, et.al., "Megavolt Modulator Study," RADC-TR-70-107.
- [70] J. E. Gruber and R. Suess, "Investigation of the Erosion Phenomenon in High Current, High Pressure Gas Discharges," Institut für Plasmaphysik, Garching bei München, IPP 4/72, December 1969.
- [71] J. C. Martin, "Million Volt Repetitive Spark Gaps," Proc. Workshop on Switching Req and R & D for Fusion Reactors (M. Kristiansen, Ed) March 24-26, 1976, p. 1-C14, EPRI ER-376-SR.
- [72] W. Clark, ML, Personal Communication.
- [73] S. Levy, "Spark Gap Studies," U.S. Army Research and Development Lab., TR-2454, April 1964.
- [74] G. S. Belkin, "Vaporization of Metal Electrodes by Pulsed Currents," Sov. Phys.-Tech. Phys. 13, 1256 (1969).
- [75] J. E. Gruber, MPI, Personal Communication.
- [76] D. Bold and P. M. Barnes, "MK IV Spark Gap Switch," Pulse Technology Memo 22, 12 Nov., 1973 (Ref. PMB/DB/jlt/722) UKAEA Culham Lab. Abingdon, Oxfordshire, U.K.
- [77] T. P. Sorensen and V. M. Ristic, "Risetime and time-dependent spark-gap resistance in nitrogen and helium," Jour. Appl. Phys. 48, 114 (1977).
- [78] R. C. O'Rourke, "Note on cylindrical and plane-parallel spark channels," MLT 5-69, Maxwell Laboratories, Inc., February 1969.
- [79] W. C. Cary, Jr and J. A. Mazzie, "Time Resolved Resistance During Spark Gap Breakdown," Proc. 13th Pulse Power Modulator Symposium, SUNY/Buffalo, N.Y., June 20-22, 1978.
- [80] Nuclear Defense Research Corp., "Magpie Switching Study," Contract F 29601-69-C-0053, March 1970.
- [81] T. E. James and J. L. Browning, "Arc Voltage of Pulsed High Current Spark Gaps," IEE Gas Discharges Conf., Sept. 1970.
- [82] W. C. Nunnally, Personal Communication (Eq. credited to G. Boicourt, LASL).
- [83] G. R. Mitchell, Proc. IEE 177, 2315 (1970).

- [84] S. F. Braginskii, Sov. Phys. JETP 7, 1068 (1958).
- [85] J. Koppitz, "Die radiale and axiale Entwicklung des Leuchtens im Funkenkanal untersucht mit einer Wischkamera," Z. Naturforschg 22a, 1089 (1967).
- [86] S. I. Andreev, et.al., "Growth of the Spark Discharge Canal for a Discharge Circuit with a Rapidly Increasing Current," Sov. Phys.-Tech. Phys. 7, 37 (1962).
- [87] S. I. Andreev and B. I. Orlov, "Development of a Spark Discharge. I" Sov. Phys.-Tech. Phys. 10, 1097 (1966).
- [88] K. H. Schönbach, Univ. Darmstadt, Personal Communication.
- [89] S. I. Drabkina, J. Exp. Theo. Phys. (USSR) 21, 473 (1951).
- [90] A. Sakurai, Basic Developments in Fluid Dynamics, Academic Press, N.Y. 1, 309 (1965).
- [91] S. Mandelstam, "Excitation of the Spectrum in a Spark Discharge," Spectrochemica Acta, 255 (1959).

### C. Triggered Vacuum Gaps

#### 1. Basic Operation

Triggered vacuum gaps [1-4] are superficially similar to the pressurized spark gaps discussed in the previous section. The major difference is, of course, that the region between the anode and the cathode is evacuated rather than pressurized. Consequently the plasma necessary to form an arc across the evacuated gap must be generated from electrode material rather than, as in pressurized gaps, from filler gas. In both types of gaps the plasma is formed initially by a trigger pulse, but is maintained by power dissipation in the arc. Several features that distinguish triggered vacuum gaps from their pressurized counter-parts originate from differences between vacuum arcs (in metal vapor) and those in the gases typically used in pressured gaps. Consider an example [1]. For arcs in gases, the arc voltage,  $v$ , is relatively high at low gap current and decreases as the current,  $i$ , increases so that  $dv/di < 0$ . This result, taken together with the curvature of the typical gas arc  $v$ - $i$  characteristic, means that if two gas arcs are paralleled, one of them tends to take all the current. It is difficult, therefore, to run pressurized spark gaps in parallel. For vacuum arcs, on the other hand, usually  $dv/di > 0$  so that parallel operation is not difficult. Thus, vacuum gaps can be operated in parallel much more easily than pressurized gaps.

A second beneficial feature of vacuum arcs is their relatively low arc drop compared with that of a pressurized arc [1]. As a consequence, the dissipation and hence the electrode erosion rate in a triggered vacuum gap can be comparatively smaller (depending upon the magnitude of the pressure). Furthermore, rapid recondensation of the metal vapor in the gap onto the electrodes after the arc is extinguished permits the vacuum gap to recover its hold-off voltage in a few microseconds [2]. This is shorter than the recovery time for pressurized gaps in which the recovery depends primarily on electron-ion recombination in the arc medium and subsequent gas cooling rather than on recondensation, and hence the effective disappearance, of the arc medium as in vacuum gaps. Electron-ion recombination and gas cooling proceeds much more slowly in a pressurized gap because the relatively higher thermal capacity of the pressurized gaps keeps the high temperature in the gap longer. The rapid recovery time in vacuum gaps also helps to slow erosion of the gap by reducing dissipation.

The low pressure in triggered vacuum gaps forces them to operate below the minimum in the Paschen curve and hence allows small electrode spacings, typically 1 cm or less [1, 2, 5, 6]. The narrow gap spacing helps to reduce the recovery (recondensation) time, the switch inductance, and the size of the device.

Another important feature of triggered vacuum gaps is the capability of any particular gap to trigger reliably,

without adjustment, for a wide range of applied voltages. Somewhat surprisingly, the delay between application of the trigger pulse and the occurrence of the arc can be nearly independent of the applied voltage except for very low voltages. For example, one type of switch has been triggered from 1 kV to 100 kV with approximately constant delay [5]. Another switch was used between 300 V and 3000 V. At less than 1 kV, the delay was about 1  $\mu$ s whereas for higher voltages, it decreases to less than 0.1  $\mu$ s. Thus, the delay can increase at low voltages. Vacuum gaps have been triggered with main gap voltages of less than 50 V [6].

Other potential advantages of triggered vacuum gaps in comparison with pressurized gaps include relative immunity to strong radiation and the lack of audio (shock wave) noise. Although vacuum gaps offer many advantages relative to pressurized gaps, there are areas in which vacuum gaps are comparatively lack-luster performers. In particular, the turn-on time for a vacuum gap is about 0.1  $\mu$ s compared to perhaps 1 ns (or less) for a pressurized gap [2]. Jitter for a typical vacuum gap is about 20 ns in comparison to a few ns or less for pressurized gaps. Both the turn-on time and the jitter for a particular vacuum gap depend, of course, upon how the gap is triggered. The turn-on time seems to be limited by how quickly the plasma formed at an electrode can flow to fill the interelectrode volume. In a pressurized gap, the plasma is formed in the gas between the electrodes,

so no flow time is required. The jitter in a vacuum gap, as in a pressurized gap, generally decreases as the trigger voltage is increased.

## 2. Triggering

Of the several ways to trigger a vacuum gap, [2] perhaps the most convenient one that gives rapid breakdown and a minimum of jitter is the injection of a plasma into the main gap by striking an arc between two gas-loaded auxiliary electrodes that occupy a recessed region in one of the major electrodes. Hydrogen is the preferred gas since, as the lightest element, it fills the region between the main electrodes in a relatively short time. With titanium hydride auxiliary trigger electrodes in an appropriate geometry, a trigger pulse of a few kilovolts produces a trigger current of about 10 A and breaks down the main gap with 30 kV across it in less than 0.1  $\mu$ s with a jitter of about 30 ns [2]. Less than 0.01 J energy and  $10^{-8}$  g of titanium hydride are required per shot. Although trigger life was not determined experimentally, little deterioration in performance occurred after 6000 single shots. Although this vacuum gap, like many, was sealed, hydrogen buildup during normal single shot operation was not a problem because of gettering action of the various gap electrodes. At high repetition rates, however, hydrogen buildup in the gap could become a problem when this trigger scheme is used.

Other triggering methods used in vacuum gaps include direct plasma injection and laser triggering [4]. Another approach, used to reduce jitter and delay, is to introduce a low pressure gas into the interelectrode region [4], as discussed below. In this case, an arrangement analogous to the trigatron gas gap can be used.

### 3. Typical Parameters

A number of triggered vacuum gaps have been described in the literature [5-30]. We briefly consider some of their parameters.

Voltage Standoff-The maximum voltage standoff reported in a single triggered vacuum gap seems to be about 100 kV [5, 23]. A typical value is 50 kV. The individual units can presumably be stacked [3] or assembled in a graded sectioned configuration [22] to achieve higher standoff voltages. Such configurations exploit the fact that spontaneous breakdown of the gap is much less sensitive to pressure variations for small electrode spacings [3,4]. The maximum standoff voltage for a particular gap is determined by the electrode surface microstructure. Changes in the microstructure from shot to shot can cause sizable variations in the maximum standoff voltage [2]. Up to 350 kV has been maintained across an untriggered gap [2]. A commercially available triggered vacuum gap has a rated voltage standoff of 45 kV [28].

Peak Current-The maximum peak current reported in the literature for a single unit is [9] 3.5 MA. Currents of several

hundred kA have been reported several times [10, 11, 25, 26]. Of course, single vacuum gaps can be paralleled, as mentioned earlier, to achieve even higher currents. One commercially available gap has a rated peak current of 50 kA [28].

Pulse Width-The maximum pulse width reported for particular devices in the literature ranges up to 600  $\mu\text{s}$  [6] and even up to [2] about 10 ms (1/2 of a 60 Hz cycle) and apparently pulse lengths of up to a few 10's of ms are possible [29].

di/dt-For a vacuum gap operating at a typical pressure of  $10^{-6}$  torr, the turn-on time can be of the order of 0.1  $\mu\text{s}$  [1,2]. For a typical peak current of  $10^5$  A, this gives  $di/dt \sim 10^{12}$  A/s. The fundamental limit on di/dt is the dynamics by which the interelectrode region is filled with plasma. A value of  $5 \times 10^{12}$  A/s has been achieved in practice [10] by increasing the gap pressure to about  $5 \times 10^{-6}$  torr. This pressure increase decreases the turn-on time [22].

Delay Time-For pressures of  $\sim 10^{-6}$  torr, the delay time is about 0.1  $\mu\text{s}$ . The delay can be decreased to about 0.02  $\mu\text{s}$  by increasing the pressure up to about  $5 \times 10^{-6}$  torr [10, 22]. No further decrease in delay is seen for higher pressures in this range. One gap that is commercially available has a rated maximum delay of 0.1  $\mu\text{s}$  [28].

Jitter-Typical figures for jitter are in the range of 20 ns [2, 5] although in the relatively high pressure region ( $5 \times 10^{-6}$  torr), a figure of 8 ns has been reported [10]. One



commercially available gap has a rated maximum jitter of 0.1  $\mu\text{s}$  [28].

Pulse Repetition Rate-Most operating experience has been for single shot applications. Repetition rates of up to 35 kpps have been reported, however [5]. The maximum rate will be limited by the recovery time, discussed below. The repetition rate of one commercially available gap is 2 per minute [28].

Average Current-No information is presently available to indicate the average current limitation of the gap itself under repetitive operation.

Duty Cycle-No information is presently available to indicate the duty cycle limitation of the gap itself under repetitive operation.

Recovery Time-The reported minimum recovery time ranges from about 3  $\mu\text{s}$  [2] to 10  $\mu\text{s}$  [5].

dv/dt-From data in Ref. [2] it appears that the initial rate of recovery (for about 2  $\mu\text{s}$ ) is about  $10^{10}$  V/s.

A switch [5] comprised of four units in series held off 80 kV less than 10  $\mu\text{s}$  after passing a current of 20 kA. This result implies a dv/dt of about  $8 \times 10^9$  V/s. The ultimate limit here is set by the deionization rate.

Rise Time-The minimum reported rise time is 20 ns [10]. This low value was achieved by operating at relatively high pressure ( $\sim 5 \times 10^{-6}$  torr). For lower pressures the rise time increases [10]. For sealed gaps ( $\sim 10^{-6}$  torr) rise times

are typically 0.1 to 0.3  $\mu$ s [1,2]. The limit here is the time required to fill the inter-electrode region with plasma.

Coulombs per Shot-For a typical peak current of 100 kA and a pulse width of about 10 ms (roughly a half cycle width at 60 Hz) the Coulomb per shot would be [30] on the order of  $10^3$  C. The charge transfer per pulse for one commercially available gap [28] is 0.7 C.

Lifetime-Lifetime for the 3.5 MA peak current vacuum gap mentioned earlier is given as  $2 \times 10^4$  shots [9]. The lifetime of the 35 kpps repetitive gap mentioned before [5] was evidently greater than  $10^7$  shots.

#### 4. Summary and Conclusions

Triggered vacuum gaps, in comparison with pressurized gaps, offer the advantages of simplified parallel operation to achieve high currents, rapid recovery, low dissipation wide range of operating voltage, quiet operation, relative immunity to strong radiation, and small size. The primary disadvantage is the relatively higher delay and jitter. The delay is related to the time required for the trigger plasma to fill the evacuated region between the electrodes and therefore may be difficult to reduce. A study of alternate means of triggering vacuum gaps might lead to a reduction in jitter and improved schemes for repetitive triggering. The fact [2] that shot-to-shot changes in the electrode surface microstructure cause in vacuum gaps, in contrast to pressurized gaps,

a corresponding significant shot-to-shot variation in hold-off voltage makes it tempting to recommend additional studies of electrode surface preparation and materials. In view of the extensive number of studies of vacuum arc-electrode interactions, however, progress in these areas though significant, is expected to be unspectacular. Studies of electrode erosion at high currents are needed to complement the mainly low current measurements available at present. These data would provide better lifetime estimates and an indication of the Coulombs/shot limit at high currents. Direct measurements of lifetimes under repetitive operation and a study of the failure modes of particular designs would be especially useful.

## 5. References

- [1] George A. Farrall, "Vacuum Arcs and Switching," Proc. IEEE, Vol. 61, p. 1113-1136, August, 1973.
- [2] J. M. Lafferty, "Triggered Vacuum Gap," Proc. IEEE, Vol. 54, pp. 23-32, January, 1966.
- [3] V. S. Komel'kov, Technology of Large Impulse Currents and Magnetic Fields, Translation FTD-MT-24-992-71, pp. 95-163, Moscow (1970).
- [4] A. S. Denholm, J. J. Moriarty, W. R. Bell, J. R. Uglum, G. K. Simcox, J. Hipple, and S. V. Nablo, Review of Dielectrics and Switching, Technical Report No. AFWL-TR-72-88, Air Force Weapons Laboratory, Kirtland AFB, New Mexico 87117, February, 1973. pp. 480-493.
- [5] Helmut I. Milde, Curtis J. Schubert and Robert Harrison, "Repetitive High Power Switching Technology," in Proceedings of the Workshop on Switching Requirements and R&D for Fusion Reactors, M. Kristiansen, Editor, Special Report EPRI ER-376-SR, Electric Power Research Institute, 3412 Hillview Avenue, Palo Alto, CA 94304, July 1977, p. 1-C 41-47.
- [6] S. Kamakshaiah and R. S. N. Rau, "Low Voltage Firing Characteristics of a Simple Triggered Vacuum Gap," IEEE Transactions on Plasma Science, Vol. PS-5, pp. 164-170, September, 1977.
- [7] G. R. Govinda Raju, R. Hackam and F. A. Benson, "Breakdown Mechanisms and Electrical Properties of Triggered Vacuum Gaps," J. Appl. Phys., Vol. 47, pp. 1310-1317, April, 1976.
- [8] S. Kamakshaiah and R. S. N. Rau, "Delay Characteristics of A Simple Triggered Vacuum Gap," J. Phys. D: Appl. Phys., Vol. 8, pp. 1426-1429, 1975.
- [9] A. M. Andrianov, V. F. Demichev, G. A. Eliseev, P. A. Levit, A. Yu. Sokolov, and A. K. Terent'ev, "Pulse Generator Producing a High-Power Current," Instrum. Exper. Tech., Vol. 14, pp. 124-126, July, 1971.
- [10] Kenneth D. Ware, Joseph W. Mather, Arthur K. Paul J. Bottoms and James P. Carpenter, "Operation of a Fast High-Voltage Vacuum Switch," Rev. Sci. Instr., Vol. 42, pp. 111-115, 1971.

- [11] Ryvichi Akiyama, Sunao Kawasaki and Taijiro Uchida, "A Simple Vacuum Crowbar Switch up to 1 MA," Japan. J. Appl. Phys., Vol. 9, p. 150, 1970.
- [12] E. A. Azizov and V. S. Komel'kov, "Switching of Discharge Gaps by Plasma Jets," Sov. Phys.-Tech. Phys. Vol. 13, 468-475 Oct., 1968.
- [13] G. N. Aretov, V. I. Vasil'ev, M. I. Pergament and S. S. Tserevitinov, "Delay Characteristics of Vacuum Disc Switches," Sov. Phys.-Tech. Phys. Vol. 12, 90-96, July 1967.
- [14] G. N. Aretov, V. I. Vasil'ev, M. I. Pergament and S. S. Tserevitinov, "Electrical Strength of Vacuum Disc Switches," Sov. Phys.-Tech. Phys. Vol. 11, 1548-1555, May, 1967.
- [15] George A. Farrall, "Low Voltage Firing Characteristics of a Triggered Vacuum Gap," IEEE Trans. Elec. Div., Vol. ED-13, pp. 432-438, April, 1966.
- [16] R. Hancox, "Low Pressure Gas Discharge Switches for Use in Fusion Experiments," Proc. IEE, Vol. 111, pp. 203-213. January, 1964.
- [17] M. P. Reece, "The Vacuum Switch," Proc. IEE, Vol. 110, pp. 791-811, April, 1963.
- [18] G. D. Cormack and A. J. Barnard, "Low Inductance Low Pressure Spark Gap Switch," Rev. Sci. Instr. Vol. 33, 606-610, June, 1962.
- [19] J. G. Bannenberg and F. G. Insinger, "Improved Vacuum Switch for Capacitor-Discharge Service," Rev. Sci. Instr., Vol. 33, pp. 1106-1107, October, 1962.
- [20] R. Hancox, "Triggering Mechanism of Low-Pressure Spark Gaps," Rev. Sci. Instr., Vol. 33, 1239-1244, Nov., 1962.
- [21] V. V. Sokol'skii, A. I. Nastyukha and E. A. Lobikov, "Vacuum Gap with Electron Triggering," Instrum. Exper. Tech., Vol. 2, pp. 340-342, March, April, 1961.
- [22] J. W. Mather and A. H. Williams, "Some Properties of a Graded Vacuum Spark Gap," Rev. Sci. Instr. Vol. 31, pp. 297-303, March, 1960.
- [23] A. M. Rodin and V. V. Surenyants, "A High-Voltage Heavy-Current Vacuum Discharger VIR-100," Instrum. Exper. Tech., Vol. 6, pp. 919-922, June, 1960.

- [24] Goerge J. Brucker, "A Kilovolt, Kiloampere Low Pressure Switch," Nucl. Inst. and Meth. Vol. 8, pp. 236-238, No. 2, 1960.
- [25] William R. Baker, "High-Voltage, Low-Inductance Switch for Megampere Pulse Currents," Rev. Sci. Instr., Vol. 30, pp. 700-702, August, 1959.
- [26] D. C. Hagerman and A. H. Williams, "High-Power Vacuum Spark Gap," Rev. Sci. Instr., Vol. 30, pp. 182-183, March, 1959.
- [27] A. A. Brish, A. B. Dmitriev, L. N. Kosmarskii, Iu. N. Sachkov, G. A. Svitnev, A. B. Kheifets, S. S. Tsitsiashvili and L. S. Eig, "Vacuum Spark Relays," Instru. Exper. Tech., Vol. 5, pp. 644-649, September-October, 1958.
- [28] Technical Information Sheet on type ZR-7512 Triggered Vacuum Gap, Microwave Tube Operations, General Electric, Schenectady, NY 12305.
- [29] C. H. Titus, "Switching for Fusion Reactors," in Proceedings of the Workshop on Switching Requirements and R&D for Fusion Reactors, M. Kristiansen, Editor, Special Report EPRI ER-376-SR, Electric Power Research Institute, 3412 Hillview Avenue, Palo Alto, CA 94304, July, 1977, pp. 1-C 37 to 1-C 40.
- [30] Proceedings of the Workshop on Switching Requirements and R&D for Fusion Reactors, M. Kristiansen, Editor, Special Report EPRI ER-376-SR, Electric Power Research Institute, 3412 Hillview Avenue, Palo Alto, CA 94304, July, 1977, p. 2-5.

#### D. Liquid Spark Gaps

##### 1. Introduction

Various liquids, such as water, oil, glycerine, etc. have been used as the dielectric medium in high voltage spark gaps. The interest in liquid gaps is that they are self-healing, like gases, and have high hold-off voltages, which means less gap spacing and hence low inductance. In certain energy storage systems, such as water-filled Blumlein generators, it is also very convenient to include the switch in the storage medium. The major problem with liquid gaps is in designing them to withstand the strong shocks generated by the arc in the liquid. Much of the early work on breakdown and streamer propagation in liquids was carried out at the AWRE group at Aldermasten, UK. This work is summarized in references [1] and [2]. There are, however, still several unresolved issues with regard to, for instance, the effect of pressurization of the liquids. Recent work at the AWRE [3] suggests that pressurization of water [4] may indeed improve the breakdown strength but less so for large electrode surface areas.

Impurities in the liquids, especially if they are polar in nature or have a high dielectric constant, may have a serious effect on the breakdown strength [5]. For short times ( $< 100 \mu\text{s}$ ) these impurities do not have time to move

much in the electric field and the breakdown voltage degradation is not as severe. The highest breakdown voltage in a non-planar, non-uniform gap is when the electrode with the smallest radius of curvature has negative polarity.

Field enhancement points (rods) can cause reliable multichannel breakdown in a self-triggered gap [6] provided the time isolation between the points are more than one standard deviation ( $\sigma$ ) in breakdown time apart. For very short charging times ( $\sim 100$  ns) it is also found that the field enhancement (FE) factor has little effect on the breakdown [6]. This is probably because the charging time and the formative time lag are comparable.

Much theory which is applicable to gas filled spark gaps also pertains to liquid gaps. The exceptions are certain phenomena that are related to the liquid's higher density (e.g. heat capacity). In these cases the liquid's behaviour is more analogous to that of solid dielectrics.

The risetime of the pulse due to the resistive phase of a gap is [7]

$$t_R(\text{ns}) \approx \frac{5\rho^{1/2}}{Z_O^{1/3} E_B^{4/3}} \quad (\text{IV-25})$$

where

$\rho$  is the liquid density in  $\text{gm/cm}^3$

$Z_O$  is the driving impedance in ohms

$E_B$  is the breakdown voltage in  $\text{MV/cm}$ .



Megavolt gaps have held off 100's kV/cm. The exact value depends on the type of liquid and the hold-off time. The jitter depends upon the field enhancement factor [6] but is typically less than 10 ns (as low as 3 ns) for charging times in the 100 ns range. Channel-channel jitter [6] was similarly less than 10 ns. The spark resistance is  $\sim 10 \text{ m}\Omega/\text{cm}$  and each channel can handle [6] 10's kJ. Triggered liquid gaps have operated in the multimegavolt range [7]. These switches are generally of the field distortion type but waterfilled trigatron switches have been investigated [8] but the switch exhibited rather long formative delay times of  $\sim 10 \text{ }\mu\text{s}$ . Oil and water are the two most commonly used liquids and it is therefore useful to list some of these properties in pulsed power service [9] as shown in Table IV-8. The breakdown in these liquids is electrode dependent and initiated. The  $t^{-1/3}$  dependence on breakdown found by Martin (Eq. IV-26) maybe too strong for very large areas charged in the 1  $\mu\text{s}$  time scale (at least for oil) and may be more like  $t^{-1/4}$  or  $t^{-1/5}$  [9]. On small scales the breakdown voltage can be improved by a factor of about 2 by electrode coating, liquid degassing, pressurization, etc but this has not worked well on large systems.

Jitter of less than 2 ns in a multichannel ( $\sim 10$  channels) 2 MV, oil rail gap switch has been obtained [10]. The trigger

Table IV-8. Some Properties of Oil and Water [9]

	Oil	Water
Dielectric Constant	2.3	80
Useful Field Strength (pos. electrode)	200-300 kV/cm	100-150 kV/cm
Polarity Effect	(~1.5:1) Variable	2:1

voltage in this case rose to 1.5 MV in 20 ns ( $dv/dt \sim 8 \times 10^{13}$  V/s). The closure time was about 35 ns with a standard deviation of less than 2 ns and a risetime of 8 ns. The shortest risetime was 5 ns (with 14 channels/120 cm).

In a self-breakdown oil switch [11] the 10-90% risetime was 5.7 ns with 12 channels/137 cm and a jitter of 1-1.5 ns. The operating voltage was in the 2.5 MV range.

The breakdown field (for uniform fields) in a liquid is given approximately by [7]

$$E_{BD} t^{1/3} A_{\pm}^{1/10} = k_{\pm} \quad (\text{IV-26})$$

where  $E_{BD}$  = breakdown field in MV/cm

$t$  = pulse time in  $\mu\text{sec}$

$A$  = electrode area in  $\text{cm}^2$

and  $(\pm)$  refers to positive or negative electrode. For transformer oil  $k_{\pm} = 0.5$  but for water  $k_{+} = 0.3$  and  $k_{-} = 0.6$ .

For point or edge plane breakdown at 0.1-1.0 MV, the streamer velocity in various liquids follows the equation [7]

$$U = k_{\pm} V^{n_{\pm}} \text{ cm}/\mu\text{s}, \quad (\text{IV-27})$$

where  $V$  is in MV and  $k$  typically is in the range 30-200 and  $n$  in the range 0.5-1.75 (see Ref. [7]). For water the relationship is quite different and is best given by [7]

$$U_t^{1/2} = 88 V^{0.6} \text{ (pos)} \quad (\text{IV-28})$$

and

$$U_t^{1/3} = 16 V^{1.1} \text{ (neg)} \quad (\text{IV-29})$$

In the range of 1-5 MV in oil there is the relationship [7]

$$U_d^{1/4} = 80 V^{1.6} \quad (\text{IV-30})$$

where  $d$  is in cm and  $V$  in MV.

Repetitive liquid gaps are generally not successful because the breakdown strength of the liquid is reduced when the impurities do not have time to settle out. A modest repetition rate of  $\sim 10$  pps have been found to reduce the breakdown strength of an oil by 33%.

The narrow discharge channels in a liquid tend to result in relatively heavy electrode damage. Experimental investigations of various electrode materials have been reported [12, 13]. Large energy discharges in liquids result in massive shock waves with resulting large mechanical stresses. This can become a particularly severe problem with rep-rated gaps. Some efforts have been made to design shock dampers, such as gas filled expansion chambers or flexible walls, but it is always difficult to maintain the structural integrity of heavy duty, liquid gaps for very long.

Liquid gaps have also been laser triggered [14] using both oil and water dielectrics. As with laser triggering of

gas gaps, the best performance is obtained with a coaxial trigger arrangement. It was also found that positive polarity for the target gave the least delay. The laser triggering can reduce both the formative lag and the jitter of these switches.

## 2. References

- [1] "Pulsed Electrical Power Dielectric Strength Notes," C. E. Baum, Ed., AFWL TR 73-167.
- [2] A. S. Denholm, et.al., "Review of Dielectrics and Switching," AFWL-TR-72-88.
- [3] T. H. Storr and J. C. Martin, "Interim Notes on Water Breakdown (SSWA/JCM/785/147), AWRE, Aldermasten, U.K. (Unpublished).
- [4] A. P. Alkhimov, et.al., "The Development of Electrical Discharge in Water," Soviet Phys.-Doklady 15, 959 (1971).
- [5] G. N. Aleksandrov, et.al., High Voltage Technology (Ch VI), FTD-ID(RS)T-0030-78.
- [6] J. K. Burton, et.al., "Multiple Channel Switching in Water Dielectric Pulse Generators," Proc. Fifth Symp. Eng. Problems of Fusion Research, p. 679, Princeton Univ., Nov. 5-9, 1973.
- [7] J. C. Martin, "Nanosecond Pulse Techniques," Circuit and Electromagnetic System Design Note No. 4, AFWL (April 1970).
- [8] I. I. Aksenov, et.al., "Controlled Discharge in a Liquid," Sov. Phys.-Tech. Phys. 13, 1389 (1969).
- [9] I. Smith, "Liquid Dielectric Pulse Line Technology," Energy Storage, Compression, and Switching, Plenum Press, N.Y. and London, 1976.
- [10] K. R. Prestwich, "A 2 MV, Multichannel, Oil-Dielectric, Triggered Spark Gap," Energy Storage, Compression, and Switching, Plenum Press, N.Y. and London, 1976.
- [11] D. L. Johnson, "Untriggered Multichannel Oil Switching," Energy Storage, Compression, and Switching, Plenum Press, N.Y. and London, 1976.
- [12] V. E. Il'in and S. V. Lebedev, "Destruction of Electrodes by Electric Discharges of High Current Density," Sov. Phys.-Tech. Phys. 7, 717 (1963).
- [13] M. Motoki, et.al., "Electrode Erosion Due to Transient Arc Discharges in Dielectric Liquids," Elec. Engr. Japan 87, 75 (1967).
- [14] A. H. Guenther and J. R. Bettis, "A Review of Laser- Triggered Switching," Proc. IEEE 59, 695 (1971).

CHAPTER V  
MECHANICAL SWITCHES  
J. P. Craig

### A. Introduction

A mechanical switch consists of metallic contacts and depends on relative motion of the contacts to perform the opening and closing function. The mechanical motion itself does not open the circuit in most breakers. It requires the assistance of an externally produced current zero and some arc extinguishing techniques. Mechanical switches are classified in many other ways. Perhaps the most common classification is by the type of insulating medium the switch employs, i.e., liquid, gas or vacuum, or more specifically as oil, air,  $\text{SF}_6$ , etc. Alternatively, they may be classified according to their application. The major subdivision according to application is whether they are to be used in a-c or d-c circuits. Adjectives used to describe mechanical switches by application include isolating, disconnect, load break, contactors, motor starters, interruptors, sectionalizers, circuit breakers, reclosers, shorting or crowbarring, controllers, etc. An additional way to classify mechanical switches is by some distinguishing features or characteristic ratings such as air blast, voltage, speed, power or KVA.

From the above discussion, it is apparent that there is a broad variety of mechanical switches. To describe the state-of-the-art and assess the limiting factors, requires consideration of many parameters. These parameters are identified and discussed in Chapter II.



Although much of the current interest in high power switching is for special purpose, pulsed power applications, much of the development and research information and hardware have evolved for the electric power industry. Fortunately, (for the present application) short circuits on power systems are of a "pulsed power" nature. Therefore, section C of this chapter is devoted to power system circuit breakers and their ratings, designs and characteristics.

#### B. Mechanical Switch Characterization

One appropriate characterization is switch resistance in the closed position. The immediately obvious consequences of increasing the current flow are to produce an increased voltage drop between the terminals and an increased power loss in the device. The increased power loss produces a rise in temperature. The amount of temperature rise depends upon the conduction time, how much resistance there is and how it is distributed, the heat capacity of the current carrying parts and the cooling system. If the current conduction time is very short, the cooling system will not have time to carry away a significant amount of heat, and the heat capacity of the conducting parts and the integral of the power loss will determine the temperature rise. However, for long conduction times, or for high duty factors, the cooling provisions may be the limiting factor, rather than the heat capacity. The temperature distribution over the

conducting parts will not be uniform. In fact, most of the resistance is likely to be at the contact between the two electrodes, where the cooling is not efficient and welding of the electrodes may occur if the temperature of one or more spots is sufficiently high. The resistance of the conducting parts can be reduced by increasing their cross sectional area and decreasing the current path length. However, increasing the cross sectional area increases the inertia, weight and cost. Also, any increase in inertia of the moving electrode requires an increase in force to open or close the contacts in a given time. Of course, this means more power and energy from the mechanical mechanism. Another consequence of increasing the cross sectional area of the conducting parts is the effect on skin and proximity effects. The skin effect is quite pronounced for high rates of change of current ( $di/dt$ ). Hence,  $di/dt$  as well as the current itself can influence the temperature rise and distribution. Perhaps, even more important for reducing contact resistance is the pressure or force of the contacts on each other. The temperature of the contact spots at which welding may occur and the contact resistance both depend upon the electrode (or electrode surface) material. Also, the weld properties, and damage done by any such welding, depend upon the materials.

Perhaps a less obvious, but no less important, consequence of high currents is the magneto-mechanical forces acting

on the electrodes, their supporting structure and the switching mechanisms. The familiar lateral forces that are exerted upon a pair of current carrying conductors are present. Also, the current through the electrodes may produce rather large forces tending to open the contacts. (This force is just the  $\vec{j} \times \vec{B}$  force due to the non-parallel components of the current distribution within the contacts.) Even if the contacts do not separate, the pressure is reduced and the contact resistance is increased.

It is assumed that the insulation between the contactors and other conducting parts are adequate not to be a limiting factor on the voltage. However, it should be noted that the geometry, dielectric constant of the insulation and its dielectric strength will influence the various impedances associated with the switch, and will, therefore, affect its performance parameters. Also, any influence that the external circuit has on the potentials of the other conducting parts will affect the switch performance.

There are inherent capacitances between the electrode system and the other conducting parts of the switch. These capacitances, together with the external circuit will influence the rate of rise of potential differences within the switch. Therefore, the properties of the insulating medium must be selected to cope with these potential differences. Obviously, the application of the switch will have a strong influence on the voltage wave forms which must be withstood.

The above discussion concerning the elementary mechanical switch in the closed position has indicated a surprisingly large number of factors that will influence the switch performance and limitations. It may be well to summarize these factors before proceeding to the other three modes of operation of the switch. The factors are:

Continuous current	(temperature rise and cooling system)
maximum current	(magnetic forces)
$\int i^2 dt$	(heat capacity)
$di/dt$	(hot spots, resistance and current distribution)
combination of above	(welding)
voltage withstand	(live/dead tank, types of insulation, its properties and thermodynamic condition, conductor geometry)
$dv/dt$	(short time insulation strength)
cooling system	(may involve insulation properties and/or separate cooling medium, possibly at high potential)
electrode material	(resistivity, welding properties)

With the switch in the open position and with no conduction current through the gap between the electrodes, the two electrodes will be at different potentials, depending upon the external circuitry and the internal capacitances of the switch. The simplest capacitive equivalent circuit is shown in Fig. V-1. In the closed position, the partial capacitance,  $C_1$ , is of no consequence since it is effectively shorted by

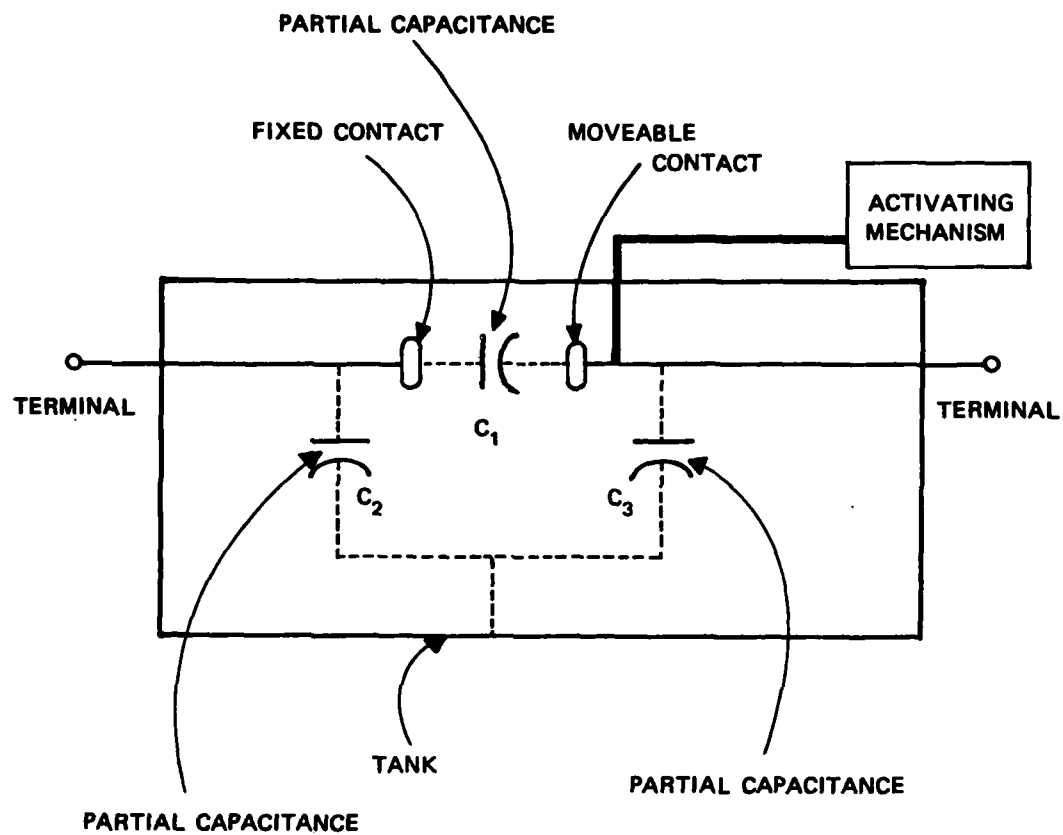


Figure V-1. Elementary Mechanical Switch Components.

the conducting contact between the electrodes. In the open position, however, the two electrodes need not be at the same potential and  $C_1$  is charged to whatever potential difference does exist. Of course, Kirchoffs voltage equation is satisfied around the capacitive loop, so that  $C_2$  and  $C_3$  form a voltage divider, fixing the potential of the enclosure if it is floating (live tank). If the enclosure is grounded (dead tank), then  $C_2$  and  $C_3$  are charged to their respective electrode voltages. It is apparent that the time variations of the capacitive voltages are functions of the external circuitry, live or dead tank, as well as the capacitances. Obviously, auxiliary capacitances could be paralleled with one or more of these capacitances to modify the various voltage wave forms and distributions. The voltage across  $C_1$  is the recovery voltage. The rate of rise of this voltage after conduction current has ceased on opening the switch is called the rate of rise of recovery voltage (r.r.r.v.). The two parameters, the recovery voltage and its rate of rise, are important parameters determining whether or not the conduction path is extinguished after the conduction current is momentarily zero. In order for the switch to successfully insert the desired high impedance between the two electrodes the insulation must be such that the voltages across  $C_1$ ,  $C_2$  and  $C_3$  do not break down. The things that affect breakdown voltages are the type, pressure and thermodynamic condition of the insulation, the electrode material,

electrode shape and surface condition and the voltage waveforms. More details on this are provided in references [1] and [2].

To the factors previously listed can be added:

the separation between the electrodes,  
the recovery voltage,  
and the rate of rise of recovery voltage.

The two additional modes of the switch are when it is intermediate between the open and closed positions, but is opening or closing, respectively.

In the opening mode of operation of the mechanical switch, two additional topics are introduced 1) an arc is formed and 2) the electrode positions and velocity with respect to each other are functions of time. How the arc properties are controlled are discussed in sections C.2, 3, 4, and in more detail in references [1] and [2]. Here it is simply noted that the presence and extinction of the arc introduce the following parameters for consideration:

arc cooling, motion, length, parallel and series  
splitting.

insulation type, pressure and flow patterns

magnetic fields and forces on arc

solid insulating and conducting plates

electrode geometry, materials, and surface treatment  
and conditions

mechanisms and energy storage system for controlling  
mechanical motion of electrodes.

timing devices for synchronizing contact separation  
with respect to point-on-wave for a-c or commutating  
current for d-c current interruption

jitter time in arc interruption

lifetime of mechanical mechanism and electrodes due  
to severe forces, acceleration and deceleration,  
and arcing

In the closing mode of operation, there is relative motion between the electrodes and an arc forms before the electrodes make physical contact. Therefore, the parameters are pretty much the same as those for the opening mode, except, now the interest is in how fast the arc can be formed rather than extinguished (jitter and  $di/dt$ ), and in being assured that the mechanical system is sufficiently strong to close and hold the electrodes together without the impact being violent enough to damage or weld the electrodes. Most of the commercial mechanical switches have not been designed for low inductance and high  $di/dt$ . Therefore, the energy in the prestrike arc is not as great as may be obtained in special pulse power switches designed for high closing  $di/dt$ . The increased arc energy will increase the probability of welding the contacts. This was a problem in vacuum interruption but alloys were developed which were antiwelding. One such alloy is bismuth copper [1]. The particular alloys used by manufacturers are sometimes proprietary.

### C. Power Circuit Breakers

#### 1. Introduction

Although the electric power industry utilizes many types



of mechanical switches as mentioned in section A, those within the scope of this report are the power circuit breakers. Since a large fraction of the art, science and technology in the high power mechanical switching area evolved from this application, it is appropriate to summarize the requirements of such devices and to briefly describe the types of breakers which have been developed. Typical ratings for oil, air break, air blast,  $\text{SF}_6$  blast and vacuum breakers are given in tables in their respective subsection in this chapter. These tables do not contain all the information needed to determine the switches' capabilities for pulsed power applications, but they do provide an appreciable amount of pertinent information that helps to define the state-of-the-art of mechanical switches. Unfortunately, these data require some interpretation, which requires some knowledge of circuit breaker ratings and standards. Appendix III gives a summary of the ratings and standards. These interpretations have been considered in the parameter evaluations in Section E.

## 2. Oil Circuit Breakers

The use of oil as an insulating and arc quenching medium was one of the first improvements made to extend the capabilities of power circuit breakers. Basically, the oil circuit breaker consists of an interrupter (or several interrupters in series), a mechanism for opening and closing the

interrupter(s), some stored energy for operating the mechanism and a means of charging the energy storage (usually a small electric motor). They are available in dead tank design up to 345 kV and live tank design up to 765 kV.

The interrupters consist of a pair of electrodes immersed in oil and surrounded by an arc control device. The arc control device is a metallic or insulating structure which channels the gas and oil flow in an optimum manner for arc cooling. The contacts can be opened to a few centimeters at average speeds of 2 to 10 m/s. Closing speeds are in the same range. Voltage ratings per interrupter are typically 10 to 170 kV. Only those below 60 kV are restrike free. In power systems the arc may restrike and then be interrupted on a later current zero. For pulse power applications, restrike free performance would be desired. Typical rms symmetrical current ratings are in the range of 20-70 kA, with the higher currents being associated with the lower voltages.

It is not appropriate to go into the details of the mechanical mechanisms in this report. Some drawings, photos and design details are provided in the manufacturers brochures listed in the references and in references [1] and [2]. It is sufficient to know that such mechanisms are available to provide the opening and closing speeds listed above. The closing energy required ranges from about 100 joules to several kilo-joules (See Table V-1).

Table V-1. Commercial Oil Circuit Breakers [2-7]

Nominal MVA Class	Rating							Related Capabilities		
	Voltage		Insulation Level		Current-kA		Interr. Time (cycles)	Current Values-kA		
	Rated Max. kV	Rated Voltage Range Factor K	Rated Withstand Test Voltage		Rated Cont. at 60	Rated S.C. at Rated Max. kV		Max. Symmetrical Interr.	3-Sec. Short Time	Closing and Latch- ing
			Low Freq. (kV, RMS)	Impulse (kV, Crest)						
500	15.5	1.29	50	110	1.2	18	5	23	23	37
500	25.8	2.15	60	150	1.2	11	5	24	24	38
1500	38	1.65	80	200	1.2	22	5	36	36	58
3500	72.5	1.10	160	350	1.2	26	5	29	29	46
5000	72.5	--	160	350	2.0	--	5	--	44	70
10000	121	1.0	260	550	3.0	63	3	63	63	101
20000	242	1.0	425	900	3.0	63	3	63	63	101
40000	525	--	--	--	2.5	--	-	--	--	--
55000	765	--	--	--	2.5	--	-	--	--	--

### 3. Gas Circuit Breakers

Several variations of circuit breakers using gas as the insulating and arc extinguishing medium have been developed. The commercial versions of available gas breakers differ in many details of design, but are categorized as air-break, air-blast or  $\text{SF}_6$ . The air-break circuit breakers are used on the lower voltage portions of the power system (utilization and distribution, i.e. up to  $\sim 35$  kV) with a single interruptor per phase. The air-blast and  $\text{SF}_6$  circuit breakers are used on the higher voltage portions of the power system (69 kV to 765 kV) and utilize up to 14 interrupters in series.

#### a. Air Break

In the air-break circuit breaker a set of contacts are mechanically parted in air at atmospheric pressure, forming an arc. The arc is horizontal and natural convection of the heated air provides some of the arc control. Basically, the arc is extinguished by a combination of two or more of

- arc elongation
- arc cooling
- arc splitting into several series arcs
- utilizing current zeros (due to external circuit).

There are several pairs of contacts. The main contacts are designed to have low resistance and carry most of the continuous current, and are often constructed as a number of

parallel contacts to improve current distribution. The materials that are best for the low resistance main contacts are not the ones that are best from the arc erosion standpoint. Therefore, the breaker is designed so that the main contacts open first and close last to minimize their arcing. By opening the main contacts first, the current is commutated to the intermediate or arcing contacts. The arc movement and elongation caused by the convection mentioned above is assisted by magnetic fields and their resulting  $\vec{j} \times \vec{B}$  forces. The magnetic fields may be produced by the current in the arc itself, by series or shunt coils, or by permanent magnets. The series coils are in the circuit permanently and must be of low resistance. The shunt coils are switched in by the arc itself. Also, air puffers are sometimes used to assist in low current interruptions. The arc movement is from the intermediate to the arcing contacts to arc runners. Various geometries of arc runners and splitter plates are used to aid in the arc elongation and cooling.

The splitter plates are contained in an arc chute and may be insulated or conducting. As the arc is forced into the arc chute, the conducting plates separate the arc into a number of series arcs. Since the anode and cathode drops for a heavy current between conducting plates is  $\sim 30$  V, the arc voltage increases to a value equal to about 30 times the number of plates. In addition heat

is conducted from the arc into the plates, thereby increasing the arc resistance and voltage. The insulating plates provide cooling and arc elongation.

The increased arc voltage is sufficient to decrease the current appreciably in the lower voltage power circuits. In fact, large arc chutes can be used to interrupt d-c current in 3 kV circuits, with continuous current ratings on the order of 10 kA. They interrupt short circuit currents of 40-60 kA in a few 10's of msec. Typical ratings for commercial a-c air break breakers are given in Table V-2.

b. Air Blast Breakers

Air blast circuit breakers expand compressed air through nozzles to produce a high velocity air flow axially along the arc for arc extinction. Pressures of a few to a hundred or more atmospheres are used to produce flow velocities on the order of Mach 1.

For system voltages up to about 35 kV, air blast breakers are used for their heavy current interrupting ability. They are commercially available, at lower current interrupting ratings, for use on transmission systems up to 800 kV. Their rate of rise of recovery voltage capability is approximately inversely proportional to the interrupting current for a given design. The interrupting current capability is approximately proportional to the nozzle areas.

Some of the advantages of the air blast breaker are:

Table V-2. Commercial Air Break Breaker Ratings [8, 9]

Nominal MVA Class	Rating						Related Capabilities			
	Voltage		Insulation Level		Current-kA		Current Values-kA			
	Rated Max. kV	Rated Voltage Range Factor K	Rated Withstand Test Voltage		Rated Cont. at 60	Rated S.C. at Rated Max. kV	Interr. Time (Cycles)	Max. Symmetrical Interr.	3-Sec. Short Time	Closing and Latch- ing
			Low Freq. (kV, RMS)	Impulse (kV, Crest)						
75	4.76	1.36	19	60	1.2	8.8	5	12	12	19
350	4.76	1.19	19	60	3.0	41	5	49	49	78
500	8.25	1.25	36	95	3.0	33	5	41	41	66
500	15	1.3	36	95	3.0	18	5	23	23	58
1000	15	1.3	36	95	3.0	37	5	48	48	77

- 1) the medium is cheap and presents no health hazard
- 2) its elasticity prevents pressure transients from being as severe as for oil
- 3) its nonflammability
- 4) the relative chemical inertness allows use of many different materials throughout the breaker
- 5) its dielectric strength increases with pressure
- 6) the compressed air is useful for pneumatic controls
- 7) can be designed for high voltage rating per interruptor.

The disadvantages of the air blast breaker are:

- 1) they are noisy
- 2) they are limited in the rate of rise of recovery voltage compared to other breakers
- 3) they tend to chop low currents
- 4) the cost of pressure vessels, compressors and filters are appreciable

Some typical ratings are given in Table V-3.

#### c. $\text{SF}_6$ Gas Blast Breakers

The  $\text{SF}_6$  gas blast breakers are similar in construction and performance to the air blast breakers; however, the  $\text{SF}_6$  is expensive enough to warrant closed systems. Two methods are used to obtain the high pressure to feed to the nozzles: 1) the two pressure system and 2) the puffer. The two pressure system is very similar to the air blast system and is the most widely used. The puffer system uses a piston motion



Table V-3. Commercial Air Blast Breakers [10, 11, 12]

Nominal MVA Class	Rating						Related Capabilities			
	Voltage		Insulation Level		Current-kA		Current Values-kA			
	Rated Max. kV	Rated Voltage Range Factor K	Rated Withstand Test Voltage		Rated Cont. at 60	Rated S.C. at Rated Max. kV	Interr. Time (Cycles)	Max. Symmetrical Interr.	3-Sec. Short Time	Closing and Latch- ing
			Low Freq. (kV, RMS)	Impulse (kV, Crest)						
2500	168		55	95			1	100	100	270
25000	242	1	425	900	3	63	2	63	63	101
55000	550	1	860	1800	2	63	2	63	63	101
75000	800	1	960	2050	2	63	2	63	63	101

at the time of interruption to produce the high pressure. Ratings of 140 kV per interrupter at 50 kA have been obtained with the puffer type.

The  $\text{SF}_6$  gas blast breakers are commercially available for the complete range of transmission line voltages. Typical ratings are given in Table V-4.

#### 4. Vacuum Breakers

Vacuum interrupters are simple, compact and quiet. The "simple" refers to the mechanical complexity, not the manufacturing processes. Indeed, problems with vacuum technology, glass and ceramic to metal seals, material purity, and contact welding prevented their commercial application until the last few years. The problems have been solved to the extent that several manufacturers are offering vacuum circuit breakers for a wide range of voltage and current ratings for a growing list of applications. The contact motion is transmitted through a bellows from a mechanism external to the vacuum interrupter.

Contact materials, sizes and shapes have been developed to the point where heavy currents can be interrupted. Also, axial magnetic fields have been found to be useful in extending the current interrupting ability of vacuum interrupters. (See Section D).

The fast recovery time of the vacuum arc is worthy of note. In fact Lee reports that after a  $di/dt$  of 185 A/ $\mu\text{s}$ ,

Table V-4. Commercial SF<sub>6</sub> Gas Blast Breakers [13, 14]

Nominal MVA Class	Rating						Related Capabilities			
	Voltage		Insulation Level		Current-kA		Current Values-kA			
	Rated Max. kV	Rated Voltage Range Factor K	Rated Withstand Test Voltage		Rated Cont. at 60	Rated S.C. at Rated Max. kV	Interr. Time (Cycles)	Max. Symmetrical Interr.	3-Sec. Short Time	Closing and Latch- ing
			Low Freq. (kV, RMS)	Impulse (kV, Crest)						
25000	242	1	425	900	3	63	2	63	63	101
35000	362	1	555	1300	3	63	2	63	63	101
55000	550	1	860	1800	3	63	2	63	63	101
75000	800	1	960	2050	3	63	2	63	63	101

a rate of rise of 24 kV/ $\mu$ s was withstood. "This is faster than any switching device that is known to man at the present time." [1] (1975) (Evidently, he intended to exclude fuses, see Chapter VI Section F.)

Some commercially available ratings are listed in Table V-5.

#### D. Other Mechanical Switch Examples

##### 1. Air Blast Breakers for Pulse Application

The 16.8 kV breaker listed in Table V-3 has been applied to pulsed power applications [18, 19]. Therefore, it is appropriate to provide some additional performance figures for it. See Table V-6 [11]. In this design both contacts are accelerated to about 12 m/s before one contact hits a stop and separation starts. It can interrupt 100 kA one hundred times without changing the contacts. Mechanically it is good for  $10^4$  operations without costly maintenance.

In the pulse application, a fusion experiment, the current through the breaker rises to 100 kA in 3 to 5 s. A charged capacitor is used to commutate the current into a resistor with a timing accuracy of  $\pm 40 \mu$ s, with an arcing time of 50  $\mu$ s.

##### 2. HVDC or Pulsed Power Vacuum Interruption

Vacuum interrupters have been tested together with commutation circuits, both for single interrupters and for two

Table V-5. Commercial Vacuum Breakers [15, 16, 17]

		Rating					Related Capabilities			
Nominal MVA Class	Voltage		Insulation Level		Current-kA		Current Values-kA			
	Rated Max. kV	Rated Voltage Range Factor K	Rated Withstand Test Voltage		Rated Cont. at 60	Rated S.C. at Rated Max. kV	Interr. Time (Cycles)	Max. Symmetrical Interr.	3-Sec. Short Time	Closing and Latch- ing
			Low Freq. (kV, RMS)	Impulse (kV, Crest)						
250	15.5		50	110	0.6	15.6	2	15.6	12*	19.2
	12.1	1	260	550	2.0	40	2	40	40	64
	145	1	310	650	2.0	40	2	40	40	64
	242	1	425	900	3.0	40	2	40	40	64
35000	362	1	555	1300	3.0	40	2	40	40	64
	550	1	860	1800	3.0	40	2	40	40	64
50000	800	1	860	1800	3.0	40	2	40	40	64

\* 4 sec. rating,

Table V-6. Air Blast Breaker Ratings

		50 Hz	60 Hz
Rated voltage	kV	15.4	16.8
Rated withstand voltage AC 50 Hz, 1 min., dry	kV	55	55
Rated peak withstand voltage 1.2/50 full wave	kV	95	95
Rated making current	kA	270	270
Rated short time current 3 s	kA	100	100
Rated peak short circuit current	kA	450	450
Rated Breaking current	kA	160	145
Making time	ms	65	65
Breaking time	ms	7	7
Precision	ms	$\pm 0.05$	$\pm 0.05$
Min. arcing time	ms	0.2	0.2
Rated pressure	bar	80	80
Air consumption			
Breaking	m <sup>3</sup>	1.8	1.8
Making	m <sup>3</sup>	0.5	0.5
Weight	kg	1 200	1 200
Dimensions			
Length	mm	3030	3030
Width	mm	760	760
Height	mm	1410	1410

in series [20, 21], to interrupt d-c power. Similar tests have been made for four interrupters in series and for three interrupters in parallel [22]. Experiments have also shown that axial magnetic fields on the order of 0.1 to 0.2 T, modify the tendency of the vacuum arcs to constrict at high current levels [20, 23]. This causes a reduction in the arc voltage of about a factor of 2. The axial magnetic field also was found to change the interrupting ability of a 7 inch (0.18 m) interrupter from 15 kA to 27 kA with the same  $di/dt$  and  $dv/dt$ . The interrupting ability of commercial interrupters of the same size have different current interrupting ability due to differences in contact materials and geometry. The highest interrupting ability for the commercial 7 inch interrupter tested in this test series was 35 kA with an axial field of 0.11 T, with 90% reliability. A special interrupter was constructed with different electrodes and an internal coil to generate the axial magnetic field of 0.27 T and interrupted 42 kA with 90% reliability.

Measurements have also been made [21] to determine the  $\int i^2 dt$  affects on the interrupting ability of 7" vacuum interrupters. It was found that an  $\int i^2 dt$  of  $4 \times 10^9 \text{ A}^2\text{s}$  had no effect on the probability of interrupting 10 kA, but reduced the probability of interruption to 80% at 15 kA, and to only 30% at 20 kA.

### 3. A Fast Closing, High Current Switch

A good example of how closing time can be decreased substantially when some other switch parameter requirements

are not too stringent is the switch described in reference [24]. Specifically, the hold off voltage requirements were less than 1 kV and the switch requires electrode replacement between pulses.

The switch consists of two fixed cylindrical electrodes separated axially by a small gap. The moving contact is a light-weight conducting, concentric ring which is only slightly smaller in diameter than the fixed electrodes. A still smaller diameter coil is concentric with the ring electrode. The switch is closed in about 33  $\mu$ s by magnetic forces expanding the ring electrode. The magnetic forces are produced by passing a large current through the inner coil yielding a pressure of 45 MPa on the ring. The ring attains a radial velocity of 200 m/s within about 30  $\mu$ s. Tests have indicated that a current rate of rise of  $1.27 \times 10^{13}$  A/s was obtained in the switch. The ring must be replaced after each closing operation. The switch has no opening function. Four of these are to be used in parallel to carry a peak of 1.88 MA, for approximately one half sine wave cycle of 2 ms.

#### 4. A Fast Mechanical Switch

A fast acting mechanical switch was developed to obtain a contact opening of 1.7 cm in a gas blast breaker in less than 0.8 ms [25]. In this design a rotary motion is used to minimize inertia. A specially designed, pulse driven electrodynamic drive motor has enabled an opening speed of 25 m/s



to be obtained. The switch contains two contacts in series and has a voltage recovery capability of 1 kV/ $\mu$ s using SF<sub>6</sub> at 4 atmospheres pressure.

## E. Parameters

### 1. Voltage

The voltage that a mechanical switch will hold off is dependent upon the spacing between the contacts, the dielectric strength of the insulation, the electric field distribution and the contact materials and surface condition. Considerations other than the voltage usually restrict the contact separation to a few centimeters. The dielectric strength depends upon the type of insulation, its condition (pressure, temperature, impurities) and the voltage waveforms. The characteristics of the commonly used insulations (oil, air, SF<sub>6</sub>, and vacuum) are well documented [1, 2, 26]. The field distribution is a function of the geometry which is usually arranged so that the field enhancement factor (ratio of average to maximum field intensity) is greater than 0.5. This, of course, does not count the microfield maxima that can occur at electrode surfaces.

It is not possible to give an upper practical limit on the voltage rating for mechanical switches. However, it is likely that for voltages greater than 100-200 kV, series switches will be more practical because of other parameter constraints. Series interrupters are commonly used on high voltage power systems. It has been found that the probability of interruption has improved with several breakers in series, with the same voltage per break.

## 2. Current

It has been pointed out that mechanical switches have several different current ratings. They typically have continuous current ratings of a few hundred to several thousand amperes. These values have been established by the applications, rather than by fundamental limitations. These ratings are limited by thermal effects and can obviously be extended by better cooling and by lowered resistance. The lower resistance can be obtained by using higher conductivity materials or by using larger area contacts with the necessary precautions to ensure suitable current distribution.

At the high end of the current scale is the closing and latching capability of the mechanical switch. This is determined by the mechanical strength of the electrode structure and operating mechanism. Peak values in the range of 100-500 kA are not unusual in practice.

For currents in excess of 100 kA, the  $\int i^2 dt$  becomes significant in a short time. Therefore, excess heating may limit the time such currents can be carried. The 3 second ratings for power circuit breakers give the order of magnitudes that a typical. That is, an rms symmetrical three second rating of  $10^5$  A, would indicate an  $\int i^2 dt$  of  $3 \times 10^{10} \text{ A}^2\text{-s}$ . For times much shorter than 3 seconds, the closing and latching rating may be the limiting factor, rather than the  $\int i^2 dt$  value.

The "interrupting current rating" of mechanical switches must be carefully interpreted for pulse power applications.

With the exception of low voltage (up to a few kV) d-c circuit breakers, the interrupting ability of mechanical switches rely on a current "zero" produced by external means. In a-c circuits there are two natural zeros per period. In high voltage d-c circuits the current zero must be produced by a commutation circuit. An example of d-c commutation is discussed in Section D. For a-c, consider a 345 kV, 2 cycle  $SF_6$  breaker with an interrupting capability of 63 kA, a 3 s rating of 63 kA and a closing and latching capability of 100 kA with a  $k$  factor of 1. This breaker could interrupt, in about 30 ms, a current that has been 180 kA about 8 ms prior to the end of the 30 ms period. It could handle a pulse with  $\int i^2 dt$  of  $1.2 \times 10^{10}$  A<sup>2</sup>-s with a current peak no higher than 270 kA. Whether or not it would interrupt this current would depend upon the characteristics of the commutating circuit. See discussions under  $di/dt$  and  $dv/dt$  below and in Section D.

### 3. Conduction Time (Pulse Width)

This is a category in which mechanical switches excel for long conduction times. Indefinitely long pulses may be used with mechanical switches for currents up to their continuous current ratings.

For high currents, the pulse width is limited by  $\int i^2 dt$  values for currents up to the peak currents limited by mechanical forces. (Typically from one second upward.)

The minimum conduction time that can be used with mechanical switches is limited by the contact opening and closing times

and the arc extinction time. The opening and closing times depend upon the acceleration of the contacts with respect to each other and the contact separation. The acceleration is limited by inertia and the force which can be practically applied. The arc extinction time depends upon the current, the  $di/dt$ , the arc extinction method and when the current zero occurs in the opening cycle. The arc extinction time could be eliminated by an appropriate commutating circuit to bring the current to zero prior to contact separation. The power and energy required for the mechanical mechanism and the commutating circuitry may put a practical limit on the minimum pulse width.

#### 4. Rep-rate

This is a category in which mechanical switches struggle, at best. The rate is limited by the time necessary to open and close the contacts, the deionization time and the time needed to recharge the energy storage necessary to operate the mechanism. Even if the rep-rate were high, their useful applications would be limited because it would not take long to use up its life (or maintenance requirements would be great). It is conceivable that rep-rates of a few per second are possible, but it is not considered likely without sacrificing some of the other desirable performance characteristics, and/or the closing and opening power and energy may become prohibitive.

### 5. Current Rate of Change ( $di/dt$ )

In the closing operation, the mechanical switch becomes an over-volted spark gap. The over voltage is triggered by reducing the gap. The limiting factor on the rate of rise of current are the same as those for spark gaps until the contacts close. Thereafter it is limited by circuit inductance. (See Chapter IV).

In opening low voltage circuits the arc voltage can influence the  $di/dt$ , but large values of  $di/dt$  are not produced this way. In higher voltage circuits the current zero is produced by natural zeros in a-c circuits and by commutating circuits in d-c circuits. Hence, the  $di/dt$  is determined by circuitry external to the switch. However, the successful interruption depends upon how high the  $di/dt$  is, as well as the cooling mechanism, the separation between electrodes at the time of the current zero, and any delay in voltage recovery and/or the  $dv/dt$ .

A 60 Hz breaker with a 100 kA interrupting rating has a  $di/dt$  of  $-5 \times 10^7$  A/sec. In the application for such a breaker the  $dv/dt$  could be in the range of  $10^8 - 10^9$  V/sec.

For pulsed power, with an appropriately designed commutation circuit to keep the r.r.r.v. near zero for a few tens to a few hundreds of microseconds, the  $di/dt$  would not be a limiting factor on the interrupting current.

#### 6. Voltage Rate of Change (dv/dt, r.r.r.v.)

The rate of rise of recovery voltage across the contacts of a mechanical switch is very important to the successful opening of the switch. There are two distinct modes of failure to extinguish the arc. First, a sufficiently high dv/dt may allow the current to build back up fast enough to re-ignite the arc thermally. Second, the dv/dt may be sufficiently high for a sufficient time to cause a new breakdown of the gap at its instantaneous separation. Typical values are  $10^8 - 10^9$  V/sec. A vacuum interrupter was reported that reached  $2.4 \times 10^{10}$  V/ $\mu$ s (Section 4)

#### 7. Delay

Delay on closing is on the order of ms after the mechanism is triggered to allow for significant travel of the contacts. Delay on opening is due to time required to separate the contacts to several mm plus some additional arcing time in some cases. The actual time may depend upon the point-on-wave at which the contacts separate in ac circuits or the relative timing of the contact separation and the commutation pulse in dc or pulsed systems. Typical delays are on the order of a fraction of to a few ms.

#### 8. Jitter

Jitter in mechanical switches is measured in 10's of microseconds, both closing and opening. However, this has

not prevented the successful operation of several series interrupters on EHV power systems.

#### 9. Life

For rep-rated pulsed power systems the lifetime of mechanical switches is rated "poor." The life of mechanical switches is limited by contact erosion and by mechanical wear and fatigue of the mechanism. Contact erosion is caused by arcing and is more severe in the gas blast breakers due to the high velocity gases. Some power system breakers require some maintenance after a very few operations under short circuit conditions. Under less severe conditions  $\sim 10^3$  operations may be obtained. The subject of erosion is discussed in more detail in Chapter IV. With contact replacement and other maintenance, the lifetime may be  $\sim 10^4$  operations.

#### 10. Contact Travel and Speed

In the open position, the typical contact separation is a few mm to a few cm. For gas blast breakers the optimum separation for arc quenching may be less than the maximum separation because of the flow patterns in the presence of the arc. Therefore, a pause may be built in at this optimum separation. Also, deceleration may be necessary at the extremes of the contact stroke before the stationary contacts hit the stops or stationary contacts.



High acceleration requires high forces (torque), power and energy. For conventional breaker construction, velocities up to about 10 m/s are used. Where high speeds are very important, the figure can be raised to  $\sim 25$  m/s. For non-conventional construction, the speeds can be raised at least an order of magnitude. (See Section D-3 and notes that the speed would be even higher if the separation were greater.)

### F. Summary

The basic advantage that mechanical motion has to offer high power, pulsed switching technology is that it enables the current pulse to be carried for a portion of the pulse time with essentially no damage to the device with relatively low cost and power loss. This enables them to handle a large value of Coulomb transfer per pulse efficiently and economically. For short pulses, the product of the peak current as limited by mechanical forces times the pulse time is the limiting factor. For long pulses and high duty factors, the rms continuous current rating together with the pulse time would determine the limiting factor. For intermediate pulse times and low duty factors the  $\int i^2 dt$  would determine the limit.

For pulse times in the range of a few tens to a few hundreds of ms, other required characteristics must be considered in determining whether or not a mechanical switch is preferred. However, a number of parameter requirements that would tend to make mechanical switches less favorable can be listed. For example, if the total number of pulses required are large ( $> \sim 10^4$ ), maintenance and/or replacement may be expensive. Or, if the rep-rate were more than a few per minute, the energy and power required for the mechanical mechanism would likely be prohibitive. Or, if fast rise times on closing are required some other switch type would

probably be preferred. Or, if jitter better than  $\sim \pm 10$   $\mu$ s were required on closing, the use of a mechanical switch would probably require the added complexity of a trigger system similar to those used with spark gaps. Similarly, several requirements that tend to favor the use of mechanical switches for this range of pulse widths can be enumerated, for example, large peak currents ( $\sim$  MA), large Coulomb transfer ( $\sim 10^6$  C), and large  $\int i^2 dt$  ( $\sim 10^{10}$  A<sup>2</sup>-s).

The characteristic values given in this chapter are primarily those of switches that were not developed for repetitive pulse power applications. A number were developed for power system applications; hence, they tend to cluster about particular combinations of parameter values. For applications such that any one parameter value is desired to be well outside those indicated in this chapter, there is an excellent chance that a mechanical switch could be developed (at least for some combinations of the other parameters). For example, very high voltage ratings could be obtained by using large separations between electrodes or by using higher pressures for the insulating medium (except for vacuum interrupters); however, opening times may be increased and current interruption values may be decreased. Or, current interrupting ratings could be increased by designs to limit the post arc  $dv/dt$ , or, alternatively by increasing nozzle area and gas flows for the gas blast type breakers. Or, the peak currents, Coulomb transfer and  $\int i^2 dt$  can be increased by increasing the cross-sectional area of the conducting parts

and contacts, at the expense of slower opening and closing times and/or more power and energy loss for the mechanical mechanism. Or, arcing times could be reduced either by faster contact motions or by commutation systems to force the current to zero before and/or during contact separation. Contact speeds much higher than 25 m/s for contructions similar to conventional breakers are not likely. However, for special cases, such as that discussed in section D-3, an order of magnitude higher is possible. Also, a continuously rotating contact holder may also be practical for rep-rated designs of the future where speeds in excess of 200 m/s could be used. It is also conceivable that a rotating design could increase possible rep-rate and lifetimes by an order of magnitude or more, particularly for the lower ranges of voltages and currents.

G. References

- [1] T. H. Lee, Physics and Engineering of High Power Switching Devices, MIT Press, Cambridge, Mass.
- [2] C. E. Flurschein, editor, Power Circuit Breaker Theory and Design, Peter Peregrinus Ltd., Soughth House, Stevenage, Herts. SG1 1HQ, England.
- [3] Allis-Chalmers brochure 71C1580-3 "Oil Circuit Breakers, Small Outdoor," Apr. 1975.
- [4] Allis-Chalmer brochure 71C1929-02 "Oil Circuit Breakers, Intermediate Form," Sept. 73.
- [5] Allis-Chalmer brochure, 71C5719, "Oil Circuit Breakers, Outdoor, Large," Oct. 75.
- [6] Westinghouse Descriptive Bulletin, 33-253, "Types GM, GMA and GMB Outdoor Oil Circuit Breakers," Sept. 77.
- [7] General Electric, GEA 5804 B, "FK Oil Circuit Breakers,"
- [8] Westinghouse Bulletin, 32-252, "Standarized Type DHP Medium Voltage Porcel-line Metal Clad Switchgear," April 1977.
- [9] D. Square, AIA File 1623, "Solenarc Metal-Clad Switchgear," 1974.
- [10] General Electric Switchgear Catalog, current.
- [11] AEG-Telefunken brochure E22.05.20/1076E, "Safety Circuit Breaker."
- [12] K. Kriechbaum, "High Voltage Circuit Breakers for Extra Duties," World Electrotechnical Congress," June 21-25, Moscow, 1977.
- [13] Allis-Chalmers brochure 71C10031, "SF<sub>6</sub> Gas-Insulated Circuit Breakers," Oct. 77.
- [14] Westinghouse Descriptive Bulletin, 33-555, "Type SFA Power Circuit Breakers," Nov. '77.
- [15] General Electric, GEA7813C, "Type VIB Vacuum Interrupter Breaker."
- [16] General Electric Switchgear Catalog, current.
- [17] R. B. Shover and V. E. Phillips, "High Voltage Vacuum Circuit Breakers," IFEE Trans. PAS 94, No. 5 Sept. 75, p. 1821.

- [18] K. Kriechbaum, "High Voltage Circuit Breakers For Extra Duties," World Electrotechnical Congress, June 21-25, 1977, Moscow.
- [19] P. Dokopouler and K. Krichbaum, "D.C. Circuit Breakers Arrangement, 73 kA, 24 kV for the Joint European Torus," (To be published in Elektrotechnische Zeitschrift-A).
- [20] R. W. Warren and E. M. Honig, "The Use of Vacuum Interrupters at Very High Currents," 1978 Thirteenth Pulse Power Modulator Symposium, June 20-22, 1978, Buffalo, N.Y.
- [21] R. W. Warren, "Vacuum Interrupters used for the Interruption of High DC Currents," Proc. Seventh Symposium on Engineering Problem of Fusion Research Vol. II, p. 1774, Knoxville, Tenn, Oct. 25-28, 1977.
- [22] A. N. Greenwood, P. Barkon and W. C. Kracht, "HVDC Vacuum Circuit Breakers," IEEE Trans. PAS-91, No. 4., July/Aug. 1972 p. 1575.
- [23] C. W. Kimblin and R. E. Voshall, "Interruption Ability of Vacuum Interrupters Subjected to Axial Magnetic Fields," Pro. IEE Vol. 119, No. 12, Dec. 72.
- [24] P. Wildi and J. Gully, "A Metallic Contact, Fast Closing, High Current Switch," Symposium on Engineering Problems of Fusion Research Vol. II, p. 1774, Knoxville, Tenn., Oct. 25-28, 1977.
- [25] G. A. Hofman, "Switching Devices for Fusion Reactors," Proc. of the Workshop on Switching Requirements and R&D for Fusion Reactors," EPRI ER-376-SR Special Report July, 1977.
- [26] Special issue on Atomic and Molecular Plasma, Proc. IEEE Vol. 59, No. 4, April 1971.

CHAPTER VI  
MISCELLANEOUS SWITCHES  
M. Kristiansen and M. O. Hagler

### A. Introduction

Several types of switches besides those considered so far in this report offer the possibility of improving certain switch performance measures or meeting special requirements in particular applications. Some of these switches are described briefly in the following pages. Others, such as solid state Hall switches [1], saturable inductors [2], plasma instability switches [3], and others [3] are not included because of limitations in time. Many of the factors and physical processes that limit the performance of the switches in this Chapter are not very well understood because the switches are at a relatively early stage of development compared with those we have discussed so far. As a consequence, the following material includes for each concept a brief account of the principles of operation, the salient potential advantages and disadvantages, and a short description of some state-of-the-art devices but not a comprehensive discussion of the factors that limit the various measures of switch performance.



References

- [1] E. K. Inall, A. E. Robson and P. J. Turchi, "The Use of the Hall Effect in a Corbino Disc as a Circuit Breaker," Proc. of the Sixth Symposium on Engineering Problems of Fusion Research, San Diego, CA., November 18-21, 1975, IEEE Pub. No. 75CH1097-5-NPS, p. 666.
- [2] Theory of Operation, High Power Magnetic Modulators, Aydin Energy Division, 3180 Hanover Street, Palo Alto, California 94303, August, 1972, reissued January, 1976.
- [3] O. Z. Zucker, "R & D Recommendations for Future ERDA Switch Requirements," Proc. of the Workshop on Switching Requirements and R & D for Fusions Reactors," March 24-26, Special Report EPRI ER-376-SR, (M. Kristiansen, Editor) Electric Power Research Institute, 3412 Hillview Avenue, Palo Alto, California 94304.

## B. Vacuum Arc Opening Switches

### 1. Introduction

Vacuum arc opening switches are the result of an effort to carry over many of the advantages of triggered vacuum gaps (discussed as closing switches elsewhere in Ch. IV) to opening switches [1, 2]. In these devices (See Fig. VI-1) electrons flow, primarily radially, from a rod-shaped cathode to a ring-shaped anode. A pulse to an ignitor electrode generates a metallic plasma in the interelectrode region, as in triggered vacuum gaps, and triggers the vacuum arc. The current through the device is controlled by applying an axial magnetic field. The ignitor electrode is separated from the cathode by an insulator on which the arc deposits a thin conducting metallic film. The arc is initiated by passing a current pulse through the conductive film to vaporize, ionize, and disperse it into the interelectrode region. The resulting plasma initiates the arc, which in turn, redeposits a film on the insulator. The arc current can be limited or extinguished by a coaxial magnetic field applied perpendicular to the plane of the anode ring. The magnetic field, perhaps 0.1 Tesla, impedes the flow of electrons from the cathode because they must move across it to reach the anode. More specifically, the magnetic field increases the arc voltage and hence tends to decrease the current flow.

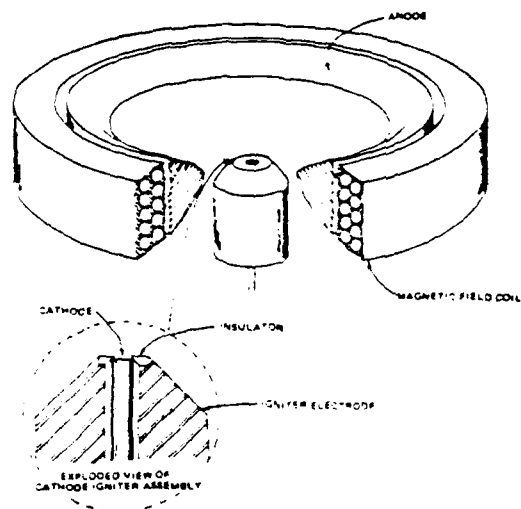


Fig. VI-1 VACUUM ARC INTERRUPTER [1]

Consider now some of the switch properties.

Voltage Standoff-The maximum reported so far is 25 kV although 50-100 kV is projected [1]. Ultimately, the hold-off voltage should be comparable to that of triggered vacuum gaps. Connecting the gaps in series should be possible.

Peak Current-At present, the maximum current interrupted is 4 kA. Eventually, it may be possible to interrupt 10-50 kA in a single unit [1]. The nice paralleling properties of vacuum arcs should mean that higher peak currents could be interrupted by using more than one unit in parallel.

Pulse Width-The conduction period for present units is 10  $\mu$ s-500  $\mu$ s [1] although times as great as 10 ms are expected in the future.

di/dt-Present turn-off times are about 2  $\mu$ s so that with a peak current of 4 kA, the implied value of di/dt is something like  $2 \times 10^9$  A/s [1]. This value may be difficult to maintain as the maximum interrupted current is increased to 10-50 kA since the turn-off time is projected to decrease only to less than 1  $\mu$ s [1]. Turn-on is somewhat faster [1].

Delay Time-No figures for the delay time are available.

Jitter-No figures for jitter are available.

Pulse Repetition Rate-The maximum repetition rate achieved so far is 1000 pps [1]. Rates greater than 10 kpps should be possible eventually.

Average Current-Figures available in the literature imply an average current of 40-2000 A [1]. Projected average currents are higher [1].

Duty Cycle-From the conduction time figures given above and the repetition rate of 1 kpps presently achievable, we find a maximum duty cycle of 0.5.

Recovery Time-Although no information is available on the recovery times for vacuum arc opening switches specifically, the recovery time should be similar to the vacuum arc in triggered vacuum gaps, perhaps a few microseconds.

dv/dt-No direct information available.

Risetime-The turn-on time for present devices is 1  $\mu$ s and may be decreased by a factor of 10 in the future [1]. The turn-off time is presently about 2  $\mu$ s and may drop to less than 1  $\mu$ s later on.

Coulombs/shot-The maximum Coulombs passed per shot is presently about 2 C/shot [1]. That figure might be stretched to 500 C [1].

Lifetime-Present lifetime is about 300 hours at an average current of 100 A [1]. Projected lifetimes extend to greater than 1000 hours at currents greater than 10 kA [1].

## 2. Summary and Conclusions

Vacuum arc opening switches are a possible means of introducing the advantages of arc switching into the realm of opening switches. These advantages include recovery speed, small size, and ease of operating them in parallel. A magnetic field is used to interrupt the arc. New approaches to triggering should be investigated to improve

the life of the switch (cathode and anode-cathode insulator). The mechanism of the interruption process by the magnetic field must be better understood so that better results can be stated for the ultimate limit to the turn-off time. One should also note that  $\text{LN}_2$  cooling of the cathode [3] has been found to increase the vacuum breakdown strength of a gap by a factor of 1.5-2.0. This effect may be worth further investigations for certain applications requiring extremely high hold-off voltage.

### 3. References

- [1] A. S. Gilmour, Jr., "The Present Status and Projected Capabilities of Vacuum Arc Opening Switches," Proc. IEEE International Pulsed Power Conference, Lubbock, Texas, 1976, p. IC1-1.
- [2] A. S. Gilmour, Jr. and D. L. Lockwood, "The Interruption of Vacuum Arcs at High DC Voltages," IEEE Trans. on Electron Devices, Vol. ED-22, pp. 173-180, April, 1975.
- [3] J. Salge, Tech. Univ. Braunschweig, personal communication.

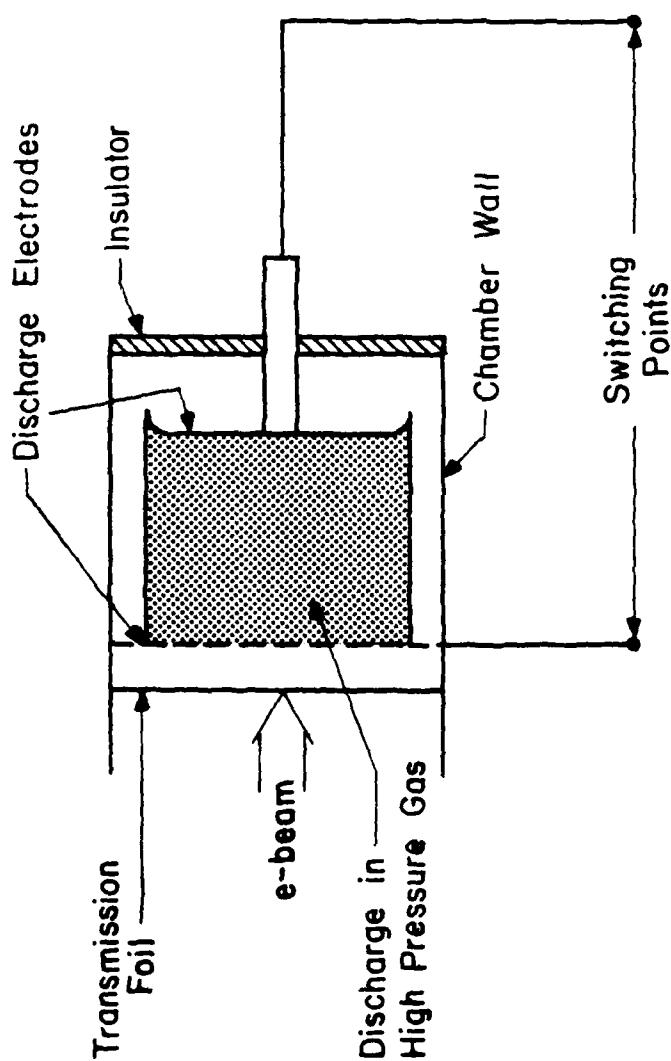
### C. Electron Beam Triggered and Sustained Switches

#### 1. Introduction

A special version of the thyatron and the triggered spark gaps are the electron beam sustained [1,2] and electron beam triggered [3-5] spark gaps. The basic physical arrangement is in both cases as shown in Fig. VI-2. The principal difference is that in the e-beam triggered mode the discharge is in the arc region and in the sustained mode in the glow discharge region. Although both concepts are in their preliminary phases of development and the available information is sparse, some very early work (1939) on electron beam triggering was carried out at the Leningrad Polytechnical Institute [6]. It was established [7] that the triggering was best with the beam along the electric field lines, from the negative to the positive electrode, but that the opposite polarity did not work very well. The original reference is unfortunately not available.

The operation of the e-beam sustained switch, also called an injection thyatron, is very much the same as that of the e-beam sustained CO<sub>2</sub> gas laser: The electrons injected by the e-beam are needed to maintain the discharge between the two electrodes. When the beam is turned off, the discharge ceases. This property permits the switch to be used as an opening switch. Theoretical calculations [1] by Kovaltchuk and Mesyats, ignoring electron attachment





A) e-beam trigger mode: Arc Discharge

B) e-beam sustained mode: Glow Discharge

This mode is also called an "injection thyatron"  
and can work as a fast opening switch.

Fig. VI-2 ELECTRON BEAM TRIGGERED AND SUSTAINED SWITCHES

in the gas, for an opening switch mode are summarized below.

Consider a voltage supply with voltage  $V_0$  and inductance  $L$  connected to the load through an e-beam sustained switch. The voltage across  $L$ , when the switch is activated, is given by

$$V_L = V_0 (1 + A\tau) e^{-(\tau + 0.5A\tau^2)}$$

where:  $\tau = \frac{t}{\theta}$ ,  $\theta = LSe\mu d^{-1} \left(\frac{\psi}{\beta}\right)^{1/2}$ ,

$$A = \psi LSe\mu d^{-1},$$

$S$  = discharge area

$d$  = anode - cathode separation

$\mu$  = electron mobility

$e$  = electron charge

$\psi$  = electron-ion pair generation by beam per sec per cm

$\beta$  = electron - ion recombination coefficient

$$\text{At the time } \tau_m = \frac{L(\sqrt{A}-1)}{AR_0}$$

$V_L$  has the maximum value  $V_{LM}$ , where

$$V_{LM} = V_0 \sqrt{A} e^{\frac{1-A}{2A}}$$

and

$$R_0 = \frac{d}{Se\mu} \left(\frac{\beta}{\psi}\right)^{1/2}$$

The breaking (opening) time, defined as the time when the electron concentration has decreased by a factor of 10, is given by  $\Delta t = 9(\psi\beta)^{-1/2}$ . In experiments carried out by

Kovaltchuk and Mesyats in a 1:1:3 mixture of  $\text{CO}_2:\text{H}_2:\text{He}$  at atmospheric pressure, a discharge current of 150 kA was maintained by a 15 kA ( $1.5 \text{ kA/cm}^2$ ) beam current and could be interrupted in 200 ns. Hunter [2] using a 250 kV beam with a current density of  $2\text{--}5 \text{ A/cm}^2$  in methane ( $\text{CH}_4$ ) over a  $1000 \text{ cm}^2$  area, switched 25 kA at 250 kV with a forward voltage drop of 1 kV. Experimental interruption values were  $\frac{di}{dt} \approx 2.5 \times 10^{11} \text{ A/s}$  and  $\frac{dv}{dt} \approx 5 \times 10^{11} \text{ V/s}$ . The design of a 0.1 MV, 1 MA switch with an interruption time of  $\Delta t \sim 100 \text{ ns}$  is believed [2] to be straightforward.

When the e-beam is used to trigger the switch the injected electrons constitute a large supply of initial electrons which practically reduce the statistical delay time (jitter) to zero and accelerate the process leading to the formation of an arc, the final state of operation of the switch. Once formed, the arc cannot be turned off by the beam. This concept is similar to the laser triggered spark (LTS) gap but not as well investigated and understood as the LTS. The purpose of this triggering method is to obtain a fast, low jitter discharge which may be diffuse or multi-channel. This last property will reduce the switch inductance and the electrode erosion.

Early experiments in the USSR [3] indicated that  $\pm 1 \text{ ns}$  jitter could easily be obtained for a 0.2 - 1 MV spark gap triggered by a 400 keV, 10 A, 5 ns electron beam. The least

breakdown delay, 20 ns, and jitter,  $\pm 1$  ns, was obtained using a 150 keV, 3 A e-beam in a gap with a gap voltage of 360 kV ( $.86 V_{BD}$ ), and a gap pressure of 8 atm.

With 16 atm pressure of nitrogen and an electric field  $E > 10^5$  V/cm arc-free discharges were produced [4] using a trigger beam with 350 keV maximum energy, 2000 A current, 10 ns width, 3 ns rise, and  $20 \text{ cm}^2$  aperture. Gap voltages as high as 1 MV were used. The maximum discharge current without arc channel formation was 40 kA at 700 kV in nitrogen at 7 atm pressure. The energy dissipation in the gap was  $10 \text{ J/cm}^3$ . In another experiment [5] channel free operation was demonstrated for a 1 cm x 40 cm cross-section discharge with a 400 keV, 1000 A injection beam.

## 2. Comparison and Conclusion

These switches are still too early in their development to enable one to make any firm conclusions. Potential problems with the e-beam sustained switch is related to a relatively high switch resistivity and hence the large cross-section which is needed to provide a low resistance switch. Research should be performed on determining conditions for minimum switch resistance and maximum possible current density.

The e-beam triggered switch has potential problems with arc damage of the beam transmission foil and it is still not clear that a diffuse conduction channel can always be established.

### 3. References

- [1] B. M. Kovaltchuk and G. A. Mesyats, First IEEE International Pulsed Power Conf., Nov. 9-11, 1976, Lubbock, Tx., paper IC7.
- [2] R. O. Hunter, Proc. First IEEE International Pulsed Power Conf., Nov. 9-11, 1976, Lubbock, Tx., paper IC8.
- [3] E. A. Abramyan, et. al., "Initiation of a Discharge in a Megavolt Gas Spark Gap by an Electron Beam," *Priory i Tekhnika Eksperimenta*, No. 1, pp. 117-118, Jan.-Feb. 1971.
- [4] B. M. Kovaltchuk, et. al., "Avalanche Discharge in Gas and Generation of Nanosecond and Subnanosecond High-Current Pulses," *DAN SSSR* 191, 76 (1970) (in Russian).
- [5] B. M. Kovaltchuk, et. al., "High-Pressure Gas Discharge Initiated by a Fast Electron Beam," *PMTF*, No. 6, p. 21 (1971) (in Russian).
- [6] V. S. Komel'kov, Technology of Large Impulse Currents and Magnetic Fields, Translation FTD-MT-24-992-71.
- [7] Unknown author, *Zh. Tekhn. Fiz.* 17, 589 (1947).

## D. Solid Dielectric Switches

### 1. Introduction

Solid dielectric switches are generally single shot or very slowly rep-rated closing switches. However, various Gatling gun arrangements or a continuous dielectric feed systems can increase the rep-rate. A major feature of such switches is that the use of solid insulation gives high standoff voltages with close electrode spacing so that the switch inductance can be low. There are two distinctly different types of these switches. One is essentially a spark gap with trigger electrode and a solid dielectric medium between the discharge electrodes. The other is essentially a mechanical switch where the solid dielectric is punctured by a solid object or a gas (which may be electromagnetically driven) so as to form a very low resistance contact. In solids, the breakdown field, down to a few nanoseconds, is independent of pulse duration and given by [1]

$$E_{BD} (\text{vol})^{1/10} = k$$

where  $E_{BD}$  is in MV/cm and the volume in  $\text{cm}^3$ . The factor  $k$  is in the range 2-4 for most practical dielectrics ( $k = 3.6$  for Mylar). For thin sheets, the breakdown becomes almost independent of the volume.

The field distortion, dielectric switch [2,3,4] is similar to a three electrode spark gap. The center electrode

of the dielectric switch is an aluminum strip sandwiched between two layers of dielectric sheets, as shown in Fig. VI-3. The strip and dielectric layers form a switch package that must be replaced after each switching action. The operational sequence of the switching action is summarized with the help of Fig. VI-3. Initially, the top switch electrode is held at the source voltage,  $V = V_0$ , while the bottom electrode is grounded,  $V = 0$ . The initial third electrode or trigger strip potential is determined by the capacitive voltage division of dielectric layers A and B, shown in Fig. VI-3. Switching action is initiated when the trigger system produces a large negative voltage pulse with a finite rise time at point x. When the electric field between point x and the trigger strip exceeds the dielectric breakdown of layer B, an arc occurs in the following sequence. The trigger strip voltage rapidly drops to the potential at x with a rise time much less than that of the trigger system. This action causes a large, fast distortion in the electric field between the trigger strip edges and the top electrode. The dielectric breakdown of A is exceeded and arcs are formed between the trigger strip edges and the top electrode. The rise time of the trigger strip voltage must be less than the arc formation time to produce multiple punctures in the dielectric. Once multiple arcs have formed between the trigger strip and the top electrode, the trigger strip voltage rises rapidly to  $V_0$ , the top electrode potential. Now the source

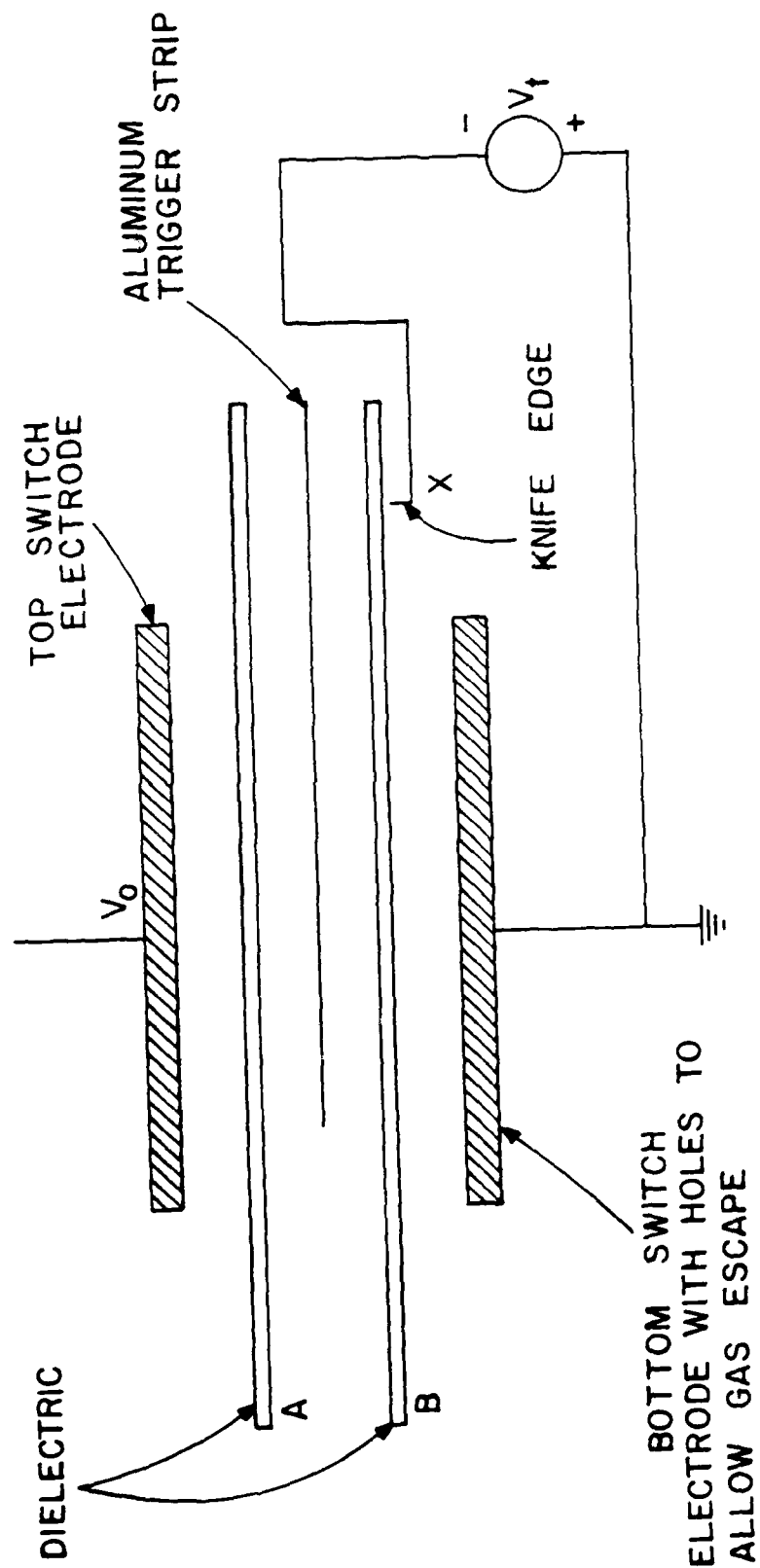


Fig. VI-3. DIELECTRIC SWITCH SCHEMATIC



voltage appears across dielectric layer B, whose dielectric strength is exceeded and multiple arcs again occur between the trigger strip and the bottom electrode. The top electrode voltage drops toward that of the bottom electrode, completing the switching action which occurs in nanoseconds.

The switch package is a very important part of the switch performance. The layers of dielectric, A and B in Fig. VI-3, are of different thicknesses and composed of several sheets. The thickness of layers A and B are determined by the source voltage and the trigger voltage magnitudes. For this switch, the initial trigger strip voltage is

$$V_{t0} = V_0 \ell_B / (\ell_A + \ell_B),$$

where  $\ell_A$  is the thickness of layer A, and  $\ell_B$  is the thickness of layer B. The total switch package thickness must hold off the maximum voltage appearing across the switch electrodes. The relative thicknesses of A and B are determined in order to produce multiple initial breakdown in layer A. Dokopoulos [2] determined an optimum ration  $\ell_A / \ell_B = 6$ , whereas Nunnally [3] found a value of  $\ell_A / \ell_B = 5/4$ . Ideally, the total thickness  $\ell_T = \ell_A + \ell_B$ , should be the minimum allowable to hold off the maximum switching voltage in order to produce fast, repeatable switching. The switch package construction is diagrammed in Fig. VI-4, illustrating the placement of the trigger strip. An important factor in the switch package placement is the physical symmetry of the trigger strip

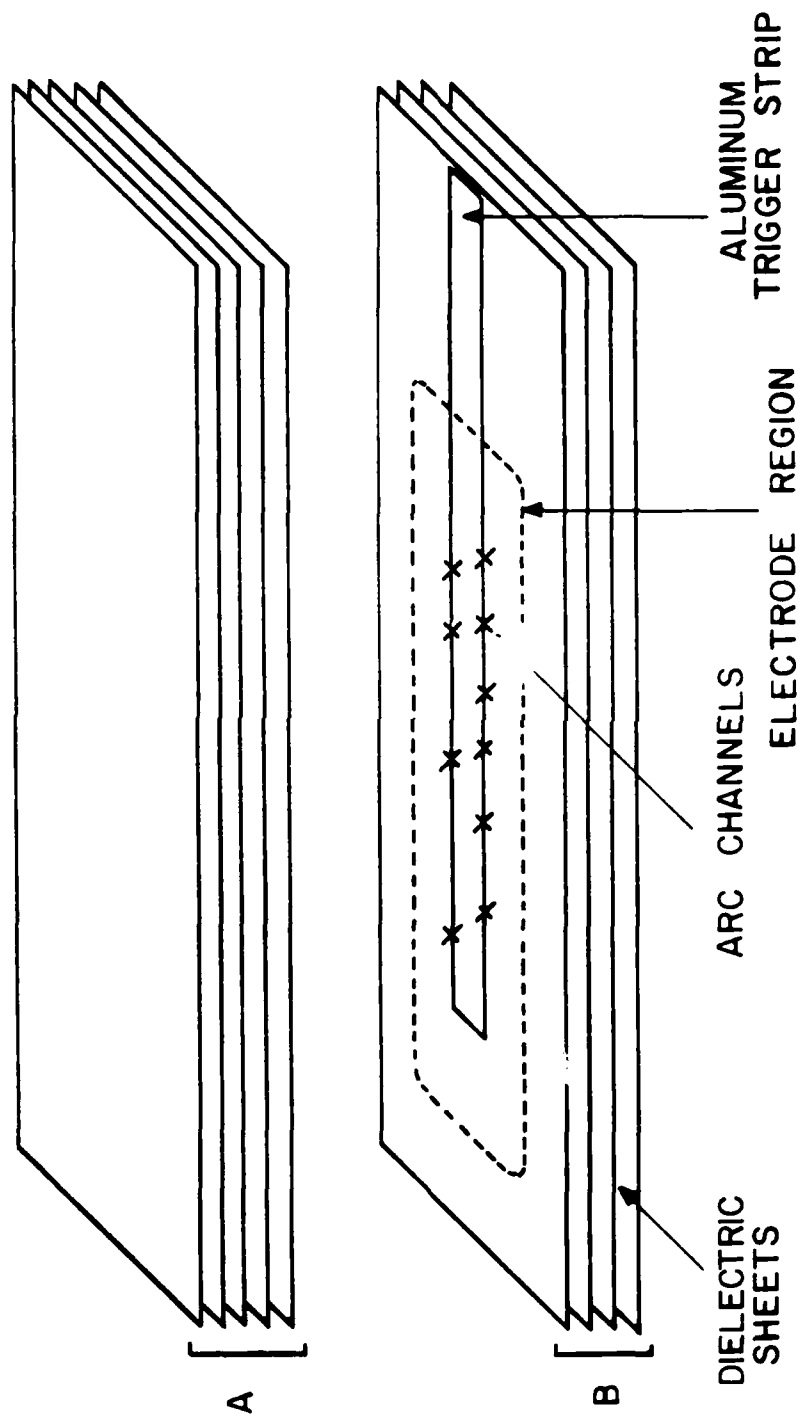


Fig. VI-4. TYPICAL SWITCH PACKAGE CONSTRUCTION

entrance into the electrode region. An unsymmetrical arrangement causes initial trigger breakdown at the entrance of the trigger strip into the electrode region. In addition, the trigger strip should not exit the electrode region opposite the trigger input, because of the inhomogeneous field situations created and the transmission line voltage doubling of the trigger pulse at the end of the switch trigger strip, which also causes switching outside the central electrode region. By using a partially prepunctured (stabbed) dielectric the dielectric can also be made to self-breakdown (similar to an untriggered spark gap) in several places. In this case stabs on the positive side seem to result in lower variation in the breakdown voltage than stabs on the negative electrode side.

A somewhat different arrangement has been described by Barnes et.al. [5]. In this case the triggering is caused by arcing through punctured dielectric layers between two trigger foils, as shown in Fig. VI-5. The resulting shock ruptures the main dielectric. Several trigger points can be used in parallel. A third modification [6] on this switch type utilizes an exploding foil trigger where the force of the explosion punctures the main insulation and drives pieces of it through holes drilled in the main electrode (see Fig. VI-6).

The characteristics of all these switches are that large forces are developed between the electrodes so they must be heavily clamped. The use of thin oil coatings between the

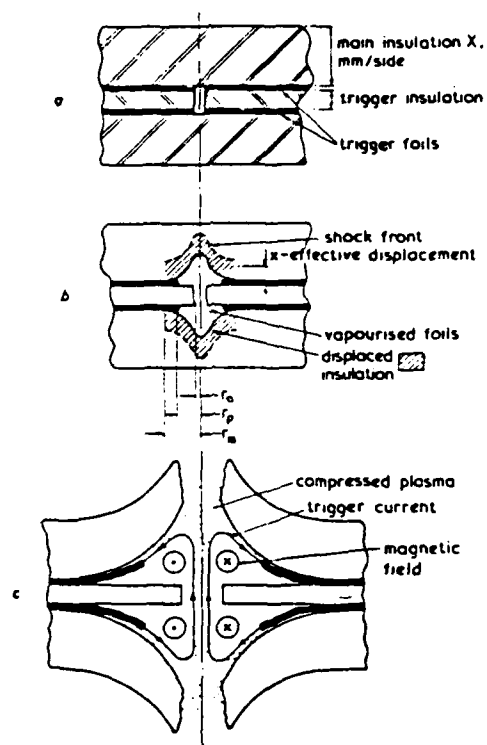
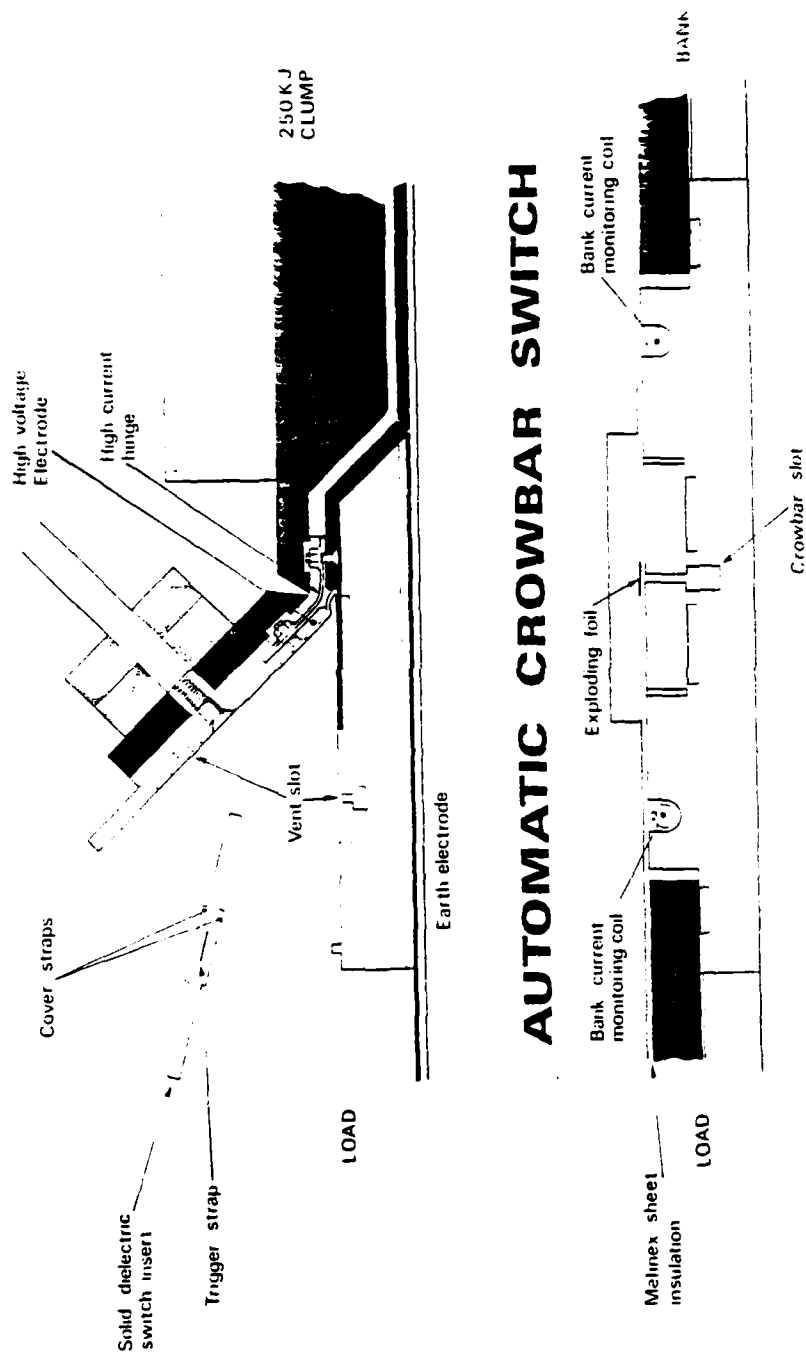


Fig. VI-5. SOLID DIELECTRIC SWITCH BREAKDOWN PROCESS [4]



### AUTOMATIC CROWBAR SWITCH

Fig.VI-6 MULTICHANNEL SOLID DIELECTRIC SWITCH (UKAWRE)

dielectric layers often helps the switch action by removing gas voids and by reducing surface tracking problems. Suitable vent holes or slots must be provided in the electrodes to allow gas escape and reduce electrode surface damage. The electrodes must typically be resurfaced after some 1000 shots. Because of the inherent stripline configuration of these switches it is easy to design them with  $L_s < 10 \text{ nh}$ . The closed switch resistance is typically less than  $1 \text{ m}\Omega$  (depending upon switch length and number of punctures). The switches can carry heavy currents (MA's) and pass a large number of Coulombs/shot ( $\gtrsim 1000 \text{ C}$ ). The switch closure time is  $\lesssim 1 \text{ }\mu\text{s}$  and the jitter is typically  $\sim 0.1 \text{ }\mu\text{s}$ , except for the field distortion switch which has closure times and jitter in the nanosecond range. The main problem with these switches is that the switch packages must be replaced after each switch operation and the switch can be acoustically noisy unless proper care is taken. The switch debris also tend to make the switch area somewhat messy after a while and care should be taken not to inhale the exhaust gases.

A related but different switch arrangement is to accelerate a metallic switch electrode so as to make a solid metal-metal contact. The physical arrangement is similar to those explained above. In this case, however, an exploding foil (A chemical explosive can obviously be used instead but there does not seem to be any obvious advantage to this) is used to deform a metal switch plate which punctures the solid dielectric and forms a metal-metal switch contact as

shown in Fig. VI-7. These switches have a very low resistance ( $< 10 \mu\Omega$ ). They can close [7] in less than  $5 \mu\text{s}$  with a jitter of  $0.1 \mu\text{s}$ . The switch electrodes must typically be refurbished after a few hundred shots. The switch has found its main application in crowbar service where a low resistance is particularly important.

The time from trigger current start to foil explosion is determined by the value of the action integral ( $g_t$ ) at blow-up [8]

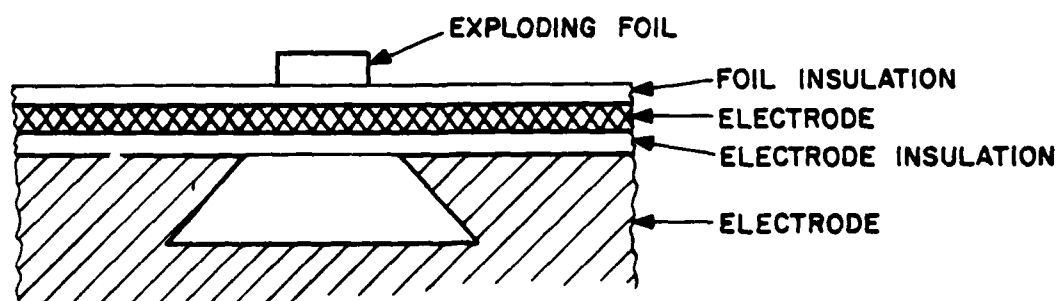
$$g_t = \int \frac{i^2}{A^2} dt$$

where  $i$  = foil current at time  $t$

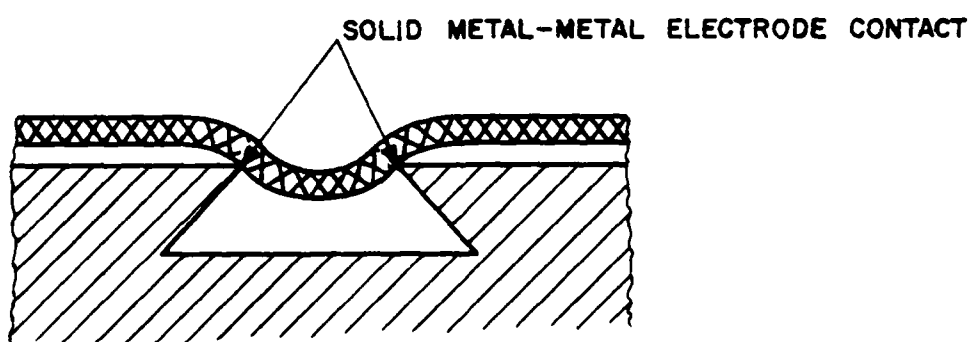
$A$  = cross-sectional area of foil in  $\text{cm}^2$

Measurements and calculations of the action integral to blow-up for various metal foils have been reported [9]. From this the foil cross-section to cause blow-up at a given time can be determined.

A second modification of the metal-metal switch accelerates a solid metal pellet through the dielectric and literally rivets [10] the two main electrodes. The pellet was electromagnetically driven. The switch was used in a 40 kV circuit with peak currents of up to 600 kA and a total charge passage of 2500 C. The switch closing time was  $50 \mu\text{s}$  and the jitter was  $\pm 1 \mu\text{s}$ . The metal-metal contact DC resistance was  $\sim 1 \mu\Omega$ . Solid dielectric switches have also been laser triggered [11] and delays as short as 3 ns with a jitter less than 1 ns were



Before Switching



After Switching

Fig. VI-7. METAL-METAL SWITCH



recorded while switching voltages from 30 to 80 kV. Komel'kov [12] has given survey of dielectric switch work before 1970.

## 2. Comparisons and Conclusions

The solid dielectric field distortion switch has the fastest switching time (few ns) and lowest jitter (few ns) while the metal-metal switch has the lowest resistance ( $R_{DC} \sim 1 \mu\Omega$ ) of these switches. All of these switches can hold-off high voltages ( $V > 100$  kV), pass high currents ( $I > 1$  MA), and transfer high Coulombs ( $C > 1000$ ). The main disadvantage is the single-shot nature of these switches and the resulting slow rep-rate of  $\sim 1/\text{min}$ .

Research into possible rep-rating methods for these switches using continuous feed dielectric systems, Gatling gun arrangements, etc. may be of interest for applications requiring extremely low switch resistance and high current and Coulomb handling. The basic operation of the switches seems to be fairly well understood.

### 3. References

- [1] J. C. Martin, "Nanosecond Pulse Techniques," Circuit and Electromagnetic System Design Notes, Note 4, April 1970.
- [2] J. C. Martin and A. MacAulay, Proc. 5th Symp. Fusion Technology, Oxford, U.K., 1968.
- [3] P. Dokopaulos and F. Lorbach, Proc. 6th Symp. on Fusion Technology.
- [4] W. C. Nunnally, et.al., "Simple, multiple arc, dielectric switch applied to a theta pinch," Rev. Sci. Inst. 45, 1361 (1974).
- [5] P. M. Barnes, et.al., "A Multiple Arc 100 kV 2.0 MA Solid Dielectric Switch," CLM-P209, 1969, UKAEA Culham Lab., U.K. Also Proc. IEE, 117, 225 (1970).
- [6] R. Bealing and P. G. Carpenter, J. Phys. E.: Sci. Inst. 5, 889 (1972).
- [7] D. E. Skelton, et.al., "Development Aspects of Fast Metal-Contact Solid-Dielectric Switches," UKAEA Culham Lab., U.K. (undated).
- [8] P. G. Carpenter, J. Phys. E.: Sci. Inst. 10, 1006 (1977).
- [9] R. Bealing and P. G. Carpenter, UKAWRE Report No. 02/76 (London: HMSO).
- [10] P. J. Rogers and H. R. Whittle, "An Electromagnetically Actuated Fast Closing Switch Using Polythene as the Main Dielectric," CLM-P180, UKAEA Culham Lab., 1968.
- [11] A. H. Guenther and J. R. Bettis, "The Laser Triggering of High Voltage Switches," Preprint, 1978. To be published in Journal of Phys. D. Appl. Phys. 11 (1978).
- [12] V. S. Komel'kov, Technology of Large Impulse Currents and Magnetic Fields, FTD-MT-24-992-71.

## E. Dielectric Surface Discharge Switches

### 1. Introduction

Creeping surface discharges have been used [2] in an interesting switch design as shown in Fig. VI-8. The same basic arrangement was also used as a preionization scheme for a gas laser [3]. This switch system which can also be wrapped in a coaxial arrangement simplifies the initiation of multichannel discharges, which result in low switch inductance. The surface discharge is initiated by a fast ( $10^{12}$  V/s), high voltage (50-70 kV) trigger pulse between the ground plane and the center electrode. Multichannel discharges result with spacings of 1.5 - 2 cm in air at atmospheric pressure and  $\sim 0.5$  cm at 300 Torr. The plasma discharge self-cleans the dielectric surface which can be of materials such as polyethylene or fiberglass laminate with thicknesses of 4 - 6 mm. The surface will, however, erode and result in a finite lifetime of  $10^3 - 10^4$  shots for the switch. Some experimental results for a 0.5 m wide switch are [1]:

Voltage range:	1-50 kV
Max. Current :	1 MA
Coulomb/shot :	20 C
Inductance :	< 5 nh
Delay :	40 ns
RMS jitter :	5 ns (estimated)
Life :	$10^4$ shots (before increased jitter and/or delay)

In another investigation [4] of self breakdown surface switches it was found that 29 channels/m in a 66 cm long

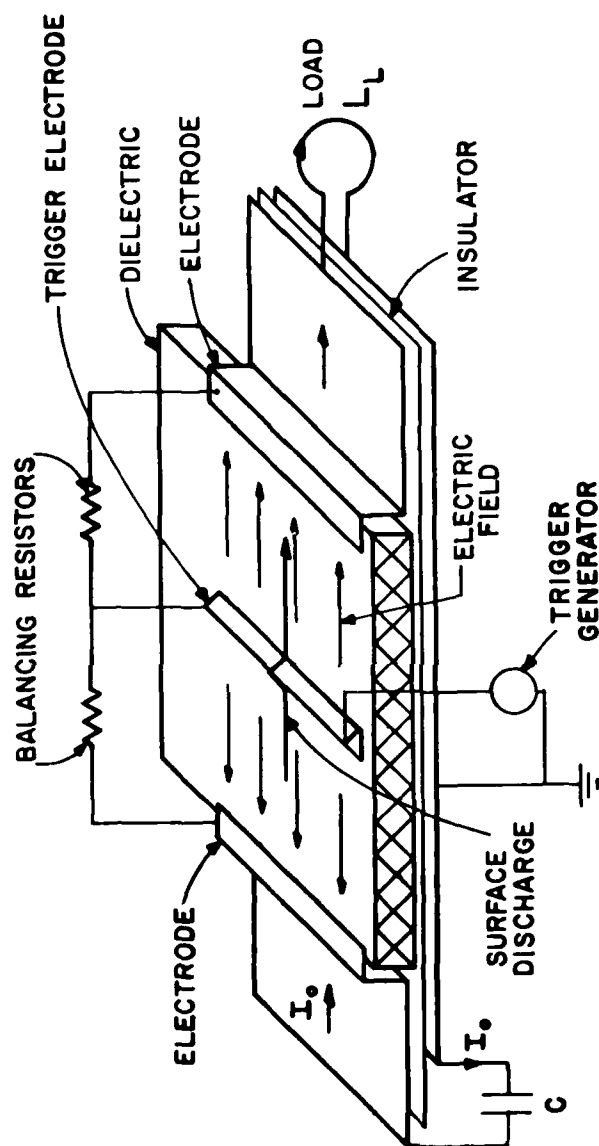


Fig. VI-8. DIELECTRIC SURFACE DISCHARGE SWITCH [1]

switch would close with a simultaneity of  $\sim 2$  ns for the first 500 shots, increasing to  $\sim 5$  ns and remain constant up to at least  $10^4$  shots. The hold off voltage was 120 kV but preliminary test were done up to 210 kV. Plans are to investigate voltages up to 1 MV. In rep-rated operation at 1 pps the substrate material ("G-30 modified polyamide rigid copper clad laminate" with the copper etched away) was found unsuitable. Initial tests with boron nitrate substrate look promising and a modest rep-rate capability of 10-20 pps is indicated.

These switches seem to have some interesting potential for high current, high Coulomb, low inductance, discharges. An investigation of the discharge resistance for various ambient gases and pressures and for various dielectric surface materials could lead to greatly improved performance.

## 2. References

- [1] P. N. Dashuk, et. al., "Commutation of Mega-Ampere Currents in Capacitive Accumulators of Power Supplies of Thermonuclear Reactors," Proc. All-Union Conf. Eng. Problems of Fusion Reactors, Leningrad, USSR, July 28-30, 1977.
- [2] J. S. T. Looms, "Switching by Surface Discharges," J. Sci. Inst. 38, 380 (1961).
- [3] D. Yu. Zaroslov, et.al., "The Use of the Gliding Discharge for the Preionization of the Pulsed Gas Discharge Laser," Proc. IX Nat. Conf. Coherent and Nonlinear Optics, Leningrad, USSR, 13-16 June, 1978.
- [4] W. J. Sarjeant, et.al., "Multichannel Surface Spark Gaps," Proc. 13th Pulsed Power Modulator Symposium, SUNY/Buffalo, N.Y., June 20-27, 1978.

## F. Fuse Opening Switches

### 1. Introduction

A fuse interrupts the current flowing through it after the joule dissipation from the current vaporizes the conductor. The interruption process can be very fast (typically 10  $\mu$ s) since heating increases the self-resistance which, in turn, increases the dissipation. Another feature, important for some applications, is the delay, after the current flow starts, before the fuse opens. For example, a fuse across a mechanical breaker can carry the current during the delay before vaporization and hence provide time for the mechanical contacts to separate enough to prevent arcing when the current is suddenly interrupted after the fuse vaporizes. An important feature, in practice, is that fuses are relatively cheap and easily fabricated. Perhaps the major disadvantage is that fuses are single-shot devices.

Fuses of a number of different materials and in several different geometrical configurations have been employed [1-20]. Materials used include Ag, Au, Al, Zn, W and Cu. Of these, Cu is often preferred for fuses in air because of its voltage hold-off and delay characteristics [13]. For fuses made of copper [10, 12], the time to explosion depends primarily on the current density, as shown in Fig. VI-9. Not surprisingly, operation at lower current densities delays the explosion. For a time to explosion of 1 ms, a typical opening time for a mechanical breaker, a current density of about 10 kA/mm<sup>2</sup> is required.

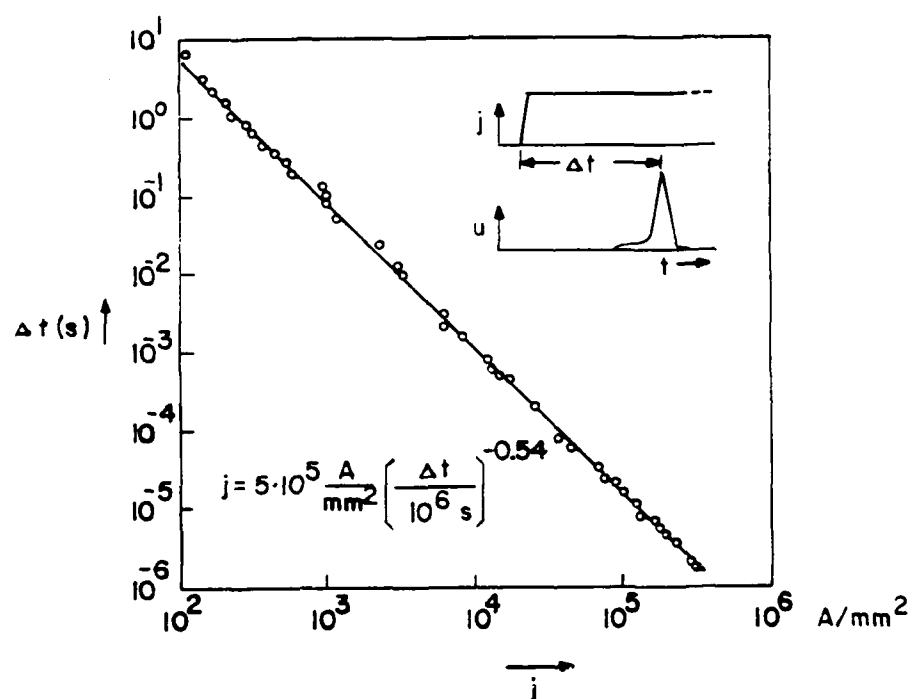


Fig. VI-9. TIME TO EXPLOSION  $\Delta t$  OF COPPER WIRES  
VERSUS CURRENT DENSITY  $j$   
(ADAPTED FROM REF. [10])



Figure VI-10 shows the peak voltage per unit length,  $V^*$ , across a copper wire in air, during a constant current discharge, vs the time to explosion. Because the data are for a constant current discharge, the peak in the voltage implies a peak in the fuse resistance. The increase in resistance before the peak is, as we mentioned, a result of the heating and vaporization of the fuse. The subsequent decrease in resistance is caused by "restrike," an arc through the vapor and debris left behind after the fuse disintegrates. For some applications, the restrike is a problem, of course. For now, however, notice the tradeoff between peak voltage (peak resistance) and the delay or time to explosion: the more delay we require, the lower the peak voltage (and resistance) for a given fuse.

Some interesting studies have been reported concerning geometrical effects for fuses. For example, a comparison of the peak voltages before restrike for a single wire, a group of parallel wires, and a foil, all of the same cross sectional area (to keep the current density constant), shows that parallel thin wires give higher peak voltages than either of the other alternatives [13].

The medium surrounding the fuse wire can be expected to affect the fuse performance significantly. A study [10, 12, 16] of fuses surrounded by air, by water, or by a small ( $\sim 1$  cm) tube filled with water shows, somewhat surprisingly, that the delay-peak voltage characteristic

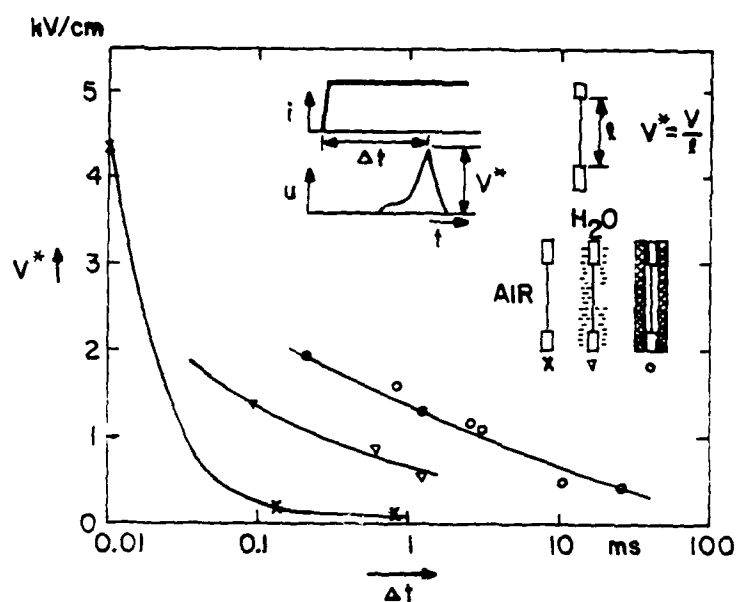


Fig. VI-10. PEAK VOLTAGE PER LENGTH  $V^*$  OF COPPER WIRES VERSUS TIME TO EXPLOSION. PARAMETER: SURROUNDING MEDIUM (ADAPTED FROM REF. [10])

is largely unaffected by changing the medium around the fuse. Thus, Fig. VI-9 is valid for all 3 cases. The peak voltage characteristic, on the other hand, is significantly different for each case, as shown in Fig. VI-10. The trade-off between delay time and peak voltage at restrike is still evident, however.

The high peak voltages of wires surrounded by water evidently result from thermal conduction cooling of the plasma from the fuse by the high pressure fluid around it. Without such cooling, the plasma density evidently remains relatively large so that an arc can be struck to re-establish a low resistance current channel. The higher peak voltages at shorter times to explosion seemingly result because the correspondingly high current densities produce a large  $dR/dt$  that permits a large voltage to develop across the switch during the time before restrike.

Figure VI-11 shows the voltage per unit length across the fuse during an essentially constant current discharge vs time for fuses in air, water and a water-filled tube [12]. Again, the switch resistance vs time is proportional to the voltage per unit length shown as the lower curve in Fig. VI-10. Notice that fuses surrounded by air and water break down or restrike after reaching the peak resistance. Fuses in a water-filled tube, on the other hand, recover and can hold off nearly 2 kV/cm of length. This feature is particularly important if a still faster switch is shunted

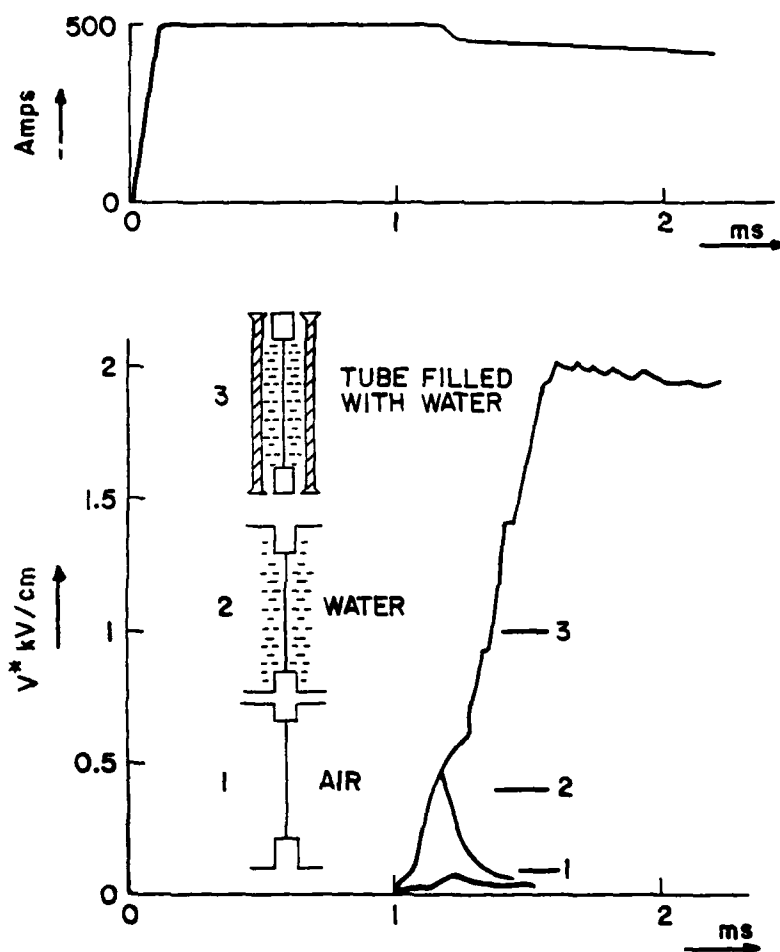


Fig. VI-11. PEAK VOLTAGE PER LENGTH  $V^*$  AND CURRENT SHAPES OF SLOWLY EXPLODING WIRES IN DIFFERENT SURROUNDING MEDIA. (ADAPTED FROM REF. [1])

across the fuse (in the same way that fuses are shunted across mechanical breakers) to achieve smaller switching times. Such successive staging of opening switches by connecting them in parallel and opening them one at a time in the order of increasing speed permits fast opening (large  $dR/dt$ ) with relatively low loss (fast switches typically have large resistances because their mass is kept small to make them fast). The price to be paid is that each switch must hold off the peak voltage across the load. Notice from Fig. VI-11 that  $dR/dt$  during switching is about  $\ell(6000)\Omega/\text{sec}$  where  $\ell$  is the length of the fuse in cm.

Using the tube-of-water fuses, 140 kV or 1.3 kV/cm was held off without restrike for 50 ms [16]. In other work [18], a foil fuse surrounded by quartz powder instead of water transferred currents up to 500 kA into a 200 nH load in 0.2  $\mu\text{s}$ . The voltage at the time the fuse exploded was 200 kV or 5.4 kV/cm. Restrike occurred after about 6  $\mu\text{s}$ . Peak opening voltages of up to about 450 kV and electric fields in the range 18-22 kV/cm have been reported [11] for copper fuses in water. Again, restrike occurred. Typical current densities are a few times  $10^7 \text{ A/cm}^2$ .

Various practical considerations typically limit the length of the fuse to 1 meter or less and hence limit the maximum voltage across the fuse. For example, as the fuse is lengthened, its finite resistivity in combination with the increased length produces a large voltage across the fuse, and hence across any associated breaker during

the time we are trying to open the breaker. This voltage might be reduced by increasing the cross sectional area of the fuse to decrease the wire resistance and increase the time to explosion (since increasing the cross section lowers the current density), but this change also tends to reduce  $dR/dt$ , as discussed earlier. Moreover, increasing both the length and area of the fuse simultaneously can decrease its efficiency by increasing the amount of energy required to explode the fuse. Increasing the cross sectional area to compensate for the fuse increases its inductance, which also can limit the switching speed. Some flexibility in design can be achieved by connecting individual fuses in series and/or parallel, however [9, 18].

If higher voltages cannot be realized in practice by increasing the fuse length beyond 1 meter, say, then how can they be achieved? One possibility is to use materials other than copper and water. Conte et.al., have reported [15, 18] using aluminum fuses in water and hydrogen peroxide to obtain maximum voltage stresses of approximately 6 kV/cm in water and  $H_2O_2$  with voltage risetimes in the range of 6-8  $\mu$ sec. No restrike or breakdown was observed. The improved performance is attributed to an exothermic chemical reaction (between the aluminum and the water or  $H_2O_2$ ) that provides energy in addition to joule heat to drive the fuse toward high resistance and explosion more quickly [15]. The net result is to reduce the lengths of the fuses necessary to achieve a

given voltage and hence to decrease both the energy required to explode the fuse and the fuse inductance. Fuses of Mg, Cu, and Ag were found to perform less satisfactorily, presumably because of their relatively lower chemical activity.

We now consider typical values for several parameters of fuse opening switches.

Voltage Standoff-The maximum standoff electric field reported, with restriking, is about 22 kV/cm for a copper fuse in water. For a fuse length of 1 m, this value would correspond to a standoff voltage of 2.2 MV. Without restriking, 6 kV/cm has been reported [15]. The maximum length is usually limited to less than one meter to reduce both the fuse inductance and the amount of energy necessary to drive the fuse open. The maximum reported [18] standoff voltage is 900 kV.

Peak Current-Larger fuse conductors or fuses in parallel can handle arbitrarily large currents. Two parallel copper fuses, for example, switched 2 MA into a 60 nH load in 6.5  $\mu$ s [17].

Pulse Width-If the pulse width is defined as the time delay before peak resistance, we know from Fig. VI-9 that the pulse width may be very wide, but at the price of a correspondingly decreased peak resistance (Fig. VI-10). A pulse width of about 1-2 ms is typical [11] but delays as short as 4  $\mu$ s have been reported [18]. Shorter delays are possible with increased current density.

di/dt-Values of up to  $1.5 \times 10^{12}$  A/s have been reported [2].

The value of di/dt can be increased at the expense of decreasing the delay before opening.

Delay Time-Fuses are not triggered, so delay time in the usual sense is not defined. See, however Pulse Width.

Jitter-Fuses are not triggered, so jitter in the usual sense is not defined. There will be variations, of course, in the delay time to peak resistance after current is applied.

Variations as low as 50 ns have been reported [18].

Pulse Repetition Rate-Although fuses are not ordinarily used repetitively, a maximum repetition rate of one shot every five minutes have been reported [12].

Average Current-Because fuses are not typically operated repetitively, average current in the usual sense is not meaningful.

Duty Cycle-Duty cycle in the usual sense has no real meaning for fuses, since they usually are used on an essentially one-shot basis.

Recovery Time-Fuses are, of course, opening switches so that recovery time in the usual sense has no meaning. If restrike does not occur, however, the peak voltage is held-off indefinitely.

dv/dt-The peak voltage is reached very fast [18] (e.g. 900 kV in 50 ns). The time required depends upon the foil or wire thickness. Measurements about how fast the voltage can be increased above the peak voltage when restrike does not occur are not available.



Risetime-Risetimes are determined by the current density in the fuse. Reported values range from 0.2  $\mu\text{s}$  [10] to 6-8  $\mu\text{s}$  [18] to about 500  $\mu\text{s}$  [12].

Coulombs/shot-This quantity clearly depends on the delay to opening, which depends in turn on the current density in the fuse. A value of more than 9 C has been achieved [12].

Lifetime-Fuses are single shot devices, although the holder can be reused [11].

## 2. Summary and Conclusions

Fuses are economic, fast opening switches that also provide a built-in delay before opening that is convenient in some applications. A major shortcoming is that they are basically single shot devices. Further work should be directed toward understanding the best materials for "tamping" the fuse (surrounding it with a solid (e.g.  $\text{H}_2\text{O}$  ice) or liquid medium) to improve its properties and to determine if repetitive operation (with a liquid conductor as the fuse for instance) might be possible. A better understanding of the conditions for preventing restrike at high electric fields would also be useful.

A recent, fairly detailed, investigation [19, 20] examines some of these problems for foil breakers and finds problems with foil edge effects which cause premature discharge channels. Methods to prevent this phenomenon are needed. It is also found that among air, polyethylene, paraffin, water and

quartz dust the latter is the best quenching material but a more comprehensive search is needed.

### 3. References

- [1] H. C. Early and F. J. Martin, "Methods of Producing a Fast Current Rise from Energy Storage Capacitors," Rev. Sci. Instr. 36, 1000 (1965).
- [2] Ch. Maisonnier, J. G. Linhardt and C. Gourian, "Rapid Transfer of Magnetic Energy by Means of Exploding Foils," Rev. Sci. Instr. 37, 1380 (1966).
- [3] J. N. DiMarco and L. C. Burkhardt, "Characteristics of a Magnetic Energy Storage System Using Exploding Foils," J. Appl. Phys. 41, 3894 (1970).
- [4] V. G. Artyukh, L. G. Lisenko and S. A. Smirnov, "Network for Fast Commutation of Large Currents in an Inductive Storage Device," translated from Priory i Tekhnika E'ksperimenta, No. 1, pp. 119-120, January - February, 1972.
- [5] V. G. Kuchinskii, V. T. Mikhkel'soo and G. A. Shneerson, "A Megaampere Switch with an Exploding Foil for the Investigation of Magnetic Cumulation," translated from Priory i Tekhnika E'ksperimenta, No. 3, pp. 108-112, May - June, 1973.
- [6] A. B. Andrezen, V. A. Burtsev, L. V. Dubovoy, M. P. Nadgornaya and A. B. Produvnov, "Fast-Response Foil Circuit Breaker," The USSR State Committee for the Utilization of Atomic Energy, The D. Y. Efremov Scientific Research Institute of Electrophysical Apparatus, Leningrad, USSR, 1973.
- [7] L. V. Dubovoi, I. M. Roife, E. V. Seredenko and B. A. Stokol'nikov, "A Powerful Foil Breaker for a Current of 0.5 MA which Actuates in 5  $\mu$ sec," translated from Priory i Tekhnika E'ksperimenta, No. 2, pp. 107-108, March - April, 1974.
- [8] V. A. Kotov, N. G. Kolganov and B. M. Koval'chuk, "A Fast Contact Breaker Based on Electrically Exploded Wires," translated from Priory i Tekhnika E'ksperimenta, No. 6, pp. 107-109, November - December, 1974.
- [9] L. V. Dubovoy, I. M. Royfe, Ye. V. Seredenko and B. A. Stokol'nikov, "Foil Breaker for Megaampere Current in the Microsecond Range," translated from preprint of NII EFA, No. T - 0177, 1974.

- [10] U. Braunsberger, J. Salge and U. Schwarz, "Circuit Breaker for Power Amplification in Poloidal Field Circuits," Proc. 8th Symposium on Fusion Technology, Noordwijkerhout, Netherlands, 1974, p. 399.
- [11] J. Benford, A. Calvin, I. Smith and H. Aslin, "High-Power Pulse Generation Using Exploding Fuses," in Energy Storage, Compression and Switching, W. H. Bostick, V. Nardi and O.S.F. Zucker, Eds., (Penum Press, New York, 1976), 39.
- [12] J. Salge, U. Braunsberger and U. Schwarz, "Circuit Breaker for Ohmic-Heating Systems," Proc. 6th Symposium on Engineering Problems of Fusion Research, San Diego, Calif., 1975, p. 643.
- [13] Yu. A. Kotov, N. G. Kolganov, V. S. Sedoi, B. M. Kovaltchuk and G. A. Mesyats, "Nanosecond Pulse Generators with Inductive Storage," Proc. First IEEE International Pulsed Power Conference, Lubbock, Texas, 1976, p. IA-1.
- [14] Ihor M. Vitkovitsky, "Development of Inductive Storage for Generation of High Voltage Pulses," Proc. First IEEE International Pulsed Power Conference, Lubbock, Texas, 1976, p. II D-2.
- [15] D. Conte, M. Friedman and M. Ury, "A Method for Enhancing Exploding Aluminum Foil Fuses for Inductive Storage Switching," Proc. First IEEE International Pulsed Power Conference, Lubbock, Texas, 1976, p. II D-7.
- [16] J. Salge, U. Braunsberger and U. Schwarz, "Circuit Breaking by Exploding Wires in Magnetic Energy Storage Systems," in Energy Storage, Compression and Switching, W. H. Bostick, V. Nardi and O. S. F. Zucker, Eds. (Plenum, New York, 1976), 477.
- [17] B. Antoni, Y. Landure' and C. Nazet, "The Commutation of the Energy Produced by a Helical Explosive Generator Using Exploding Foils," in Energy Storage, Compression and Switching, W. H. Bostick, V. Nardi and O. S. F. Zucker Eds. (Plenum Press, New York, 1976), 481.
- [18] V. A. Burtsev, et.al., "High Speed, High-Current Breakers on the Basis of Electrical Blast of Foil," Proc. All-Union Conf. Eng. Problems of Fusion Reactors, Leningrad, USSR, July 28-30, 1977.
- [19] V. A. Burtsev, et.al., "Electrical Explosion of Foils, I," Sov. Phys. Tech. Phys. 22 (8), 950 (1977).
- [20] V. A. Burtsev, et.al., "Electrical Explosion of Foils, II," Sov. Phys. Tech. Phys. 22 (8), 957 (1977).

## G. Explosive Opening Switches

### 1. Introduction

Explosive opening switches have been developed as a more rapidly opening alternative to mechanical breakers [1-7]. Opening times of less than 20  $\mu$ s have been achieved in comparison to about 1000  $\mu$ s for typical mechanical breakers. The short opening time, of course, reduces the effects of switch dissipation. In typical explosive opening switches, the current is interrupted by using an explosive to sever a conductor by blowing it apart or by forcing it against cutting rings.

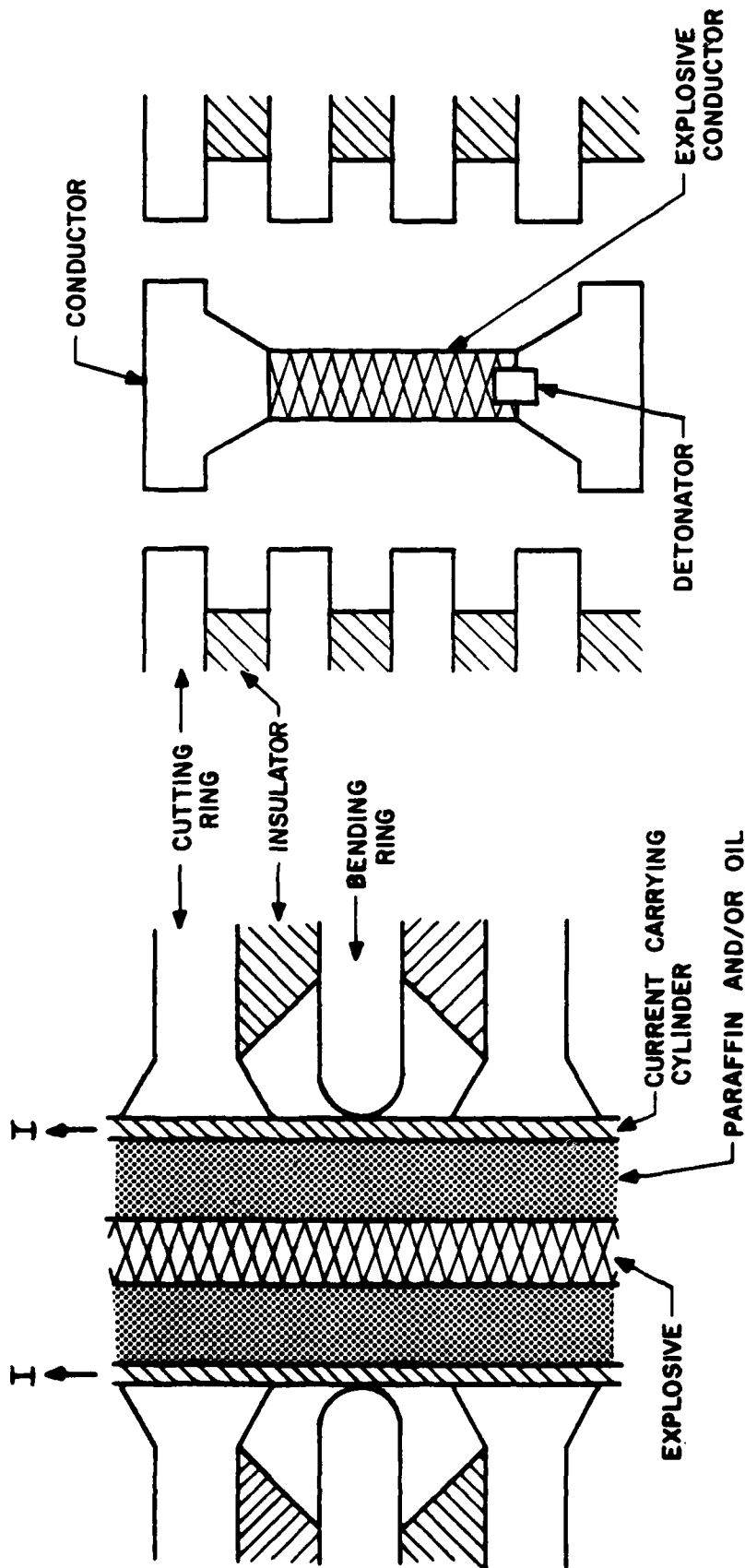
The explosion can be initiated with standard exploding bridgewire detonators [1] to realize jitter times of about 10  $\mu$ s. Such precise triggering permits series and parallel operation of single switch modules to achieve operation at higher voltages and currents. The major disadvantage of explosive opening switches is that repetitive operation, in the usual sense, is not possible. They offer [2] the possibility of precise timing and permit the delay before explosion to be controlled independently of the current flowing through the switch (with a minimum delay of  $\sim 40$   $\mu$ s).

In the USSR explosive charges in an oil bath surrounded by paraffin pushing a conducting cylinder against a set of cutting rings have been used [3] to interrupt 200 kA in 50-60  $\mu$ s and holding off 50 kV. A 2-stage series switch was tested to 70 kV (limited by the power supply but should test out at  $> 100$  kV) and opened in 7-10  $\mu$ s. The switch losses were

$\sim 100$  kJ in the first case and 25-30 kJ in the second case. It is felt [4] that a converging explosive shock type breaker may improve these results. There will then be problems with increased explosive mass but the possibility is being studied.

A new exploding switch concept where the explosive and the conductor is the same element has been reported [4]. This is achieved by mixing 10% explosive (Brandname TEN) and 90% copper powder (50-50% by volume) in a powder metallurgical process. The copper is in the form of  $100\ \mu$  "pellets." The mixture is pressed (cintured) at  $5000\ \text{kg/cm}^2$  and annealed in hydrogen. The product can be heated up to  $300^\circ\text{C}$  for short times and is "safe against impacts." Preliminary results exceeded their best results with the "conventional" explosive switch arrangement. The two arrangements are compared schematically in Fig. VI-12. The resistivity of the explosive conductor was initially about  $100\ \mu\Omega\text{-cm}$ . The explosive must, of course, be set off by a detonator.

Further developments [3] of this material using a "wetting agent" to "reduce pellet friction" (Molybdenum dichloride?) resulted in a higher packing factor and reduced the resistivity to  $\sim 20\ \mu\Omega\text{-cm}$ . With a 2 cm diameter, 2 cm long conductor-explosive element they have been able to interrupt 25 kA in 8-10  $\mu\text{s}$ , holding off 25 kV. Some of the main operational problems are with the end contacts where they use "waffled" copper disc surfaces and compression to achieve good electric contacts. The dielectric strength



"New" Explosive Switch

"Conventional" Explosive Switch

EXPLOSIVE CONDUCTOR MADE OF 90% CU AND 10%  
EXPLOSIVE (50-50 VOLUME %) IN A METALLURGICAL  
PROCESS  
 $\rho = 20 \mu\Omega\text{-cm}$   
PRELIMINARY RESULTS: 25 kA, 25 kV in  $\Delta t = 8-10 \mu\text{s}$

Fig. VI-12. EXPLOSIVE SWITCHES

of the switch recovers at a rate of  $3 \times 10^9$  V/s and the detonation velocity is  $\sim 5$  km/s with a mass flow rate of 2-3 km/s.

These investigations are in their infancy and it is difficult to predict what the ultimate results may be, but the concept is of sufficient novelty and merit to warrant further studies. It seems that this unique material may also have further, yet unexplored applications.

A somewhat different type of chemically exploding switch has been described by Kassel [5] in a recent review of Soviet Pulsed-Power R & D. In these cases the explosive cartridge is placed at right angle to the arc discharge. The explosively generated shock-wave and the explosion debris then extinguishes the arc (somewhat similar operation to an airblast breaker). The interrupted currents were fairly low (0.5 - 2.5 kA) but the interruption times,  $\Delta t$ , were quite low (2.1 - 39  $\mu$ s). We now describe the parameters of exploding opening switches that have resulted from one recent, fairly detailed study [1].

Voltage Standoff-After about a 10  $\mu$ s opening time, a multi-section series switch configuration has held off 100 kV without restrike, a figure corresponding to 3.3 kV/cm [1]. Up to 10 kV/cm is possible if a restrike after 20  $\mu$ s can be tolerated [1]. Switch lengths from 4 to 30 cm have been investigated. Tests show that 10-20 kV/cm may ultimately be possible.

Peak Current-A single switch module has carried peak currents of 100 kA [1]. This value could, of course, be increased by operating switch modules in parallel.



Pulse Width-The switch can carry rated current indefinitely before interruption occurs. Thus, the pulse width can be arbitrarily large.

di/dt-Interruption [1] of 100 kA in about 10  $\mu$ s indicates a di/dt of approximately  $10^{12}$  A/s.

Delay Time-The time delay after the trigger signal is applied to the detonator and before the switch ruptures ranges from 40 to 70  $\mu$ s [1], depending on the amount of explosive used and the types of materials used in the switch.

Jitter-A typical jitter time is about 10  $\mu$ s.

Pulse Repetition Rate-Since the conductor and the explosive must be replaced after every shot, repetition rates are once every few minutes.

Recovery Time-Recovery times of 40-50  $\mu$ s have been reported.

dv/dt-Voltage recovery rates in the range of  $10^9 - 10^{10}$  V/s. have been reported [1].

Risetime-The voltage risetime across the switch is in the range 10-20  $\mu$ s.

Lifetime-The conductor and explosive must be replaced after each shot. No lifetime information is available for the switch housing, which can be used repeatedly.

## 2. Summary and Conclusions

Explosive opening switches are a more rapidly opening alternative to mechanical breakers. Low jitter permits series-parallel connection of single switch modules for operation over a wide range of currents and voltages. The

major disadvantage is that repetitive operation, in the usual sense, is not possible. Voltage standoff and peak current for a single module will probably increase after further work. Triggering parameters (delay, jitter, and so on), already good in comparison to mechanical switches, are not likely to be improved without considerable efforts to develop a new means of detonation, although Larianov [3] found improved performance by using a coaxial arrangement of oil and paraffin rather than paraffin alone. The use of a limited number of different dielectric media has been investigated but this needs further research. The novel explosive conductor material [4] may also possibly be improved so as to make the resistivity approach that of copper. A USSR patent [7] suggests making the current carrying liner very thin (e.g. a thin film) so that it will vaporize and form a current carrying plasma with very low mass. This may result in reduced switch size, reduced explosives mass, higher working voltage, and faster opening speed.

The explosive switches have the advantage of indefinite current carrying ability and trigger command but are generally more complicated and expensive than the exploding wire fuse switches.

### 3. References

- [1] R. D. Ford and Ihor Vitkovitsky, "Explosively Actuated 100 kA Opening Switch for High Voltage Applications," NRL Memorandum Report 3561, July 1977.
- [2] D. Conte, R. D. Ford, W. H. Lupton and I. M. Vitkovitsky, "Two Stage Opening Switch Techniques for Generation of High Inductive Voltages," Proc. of the 7th Symposium on Engineering Aspects of Fusion Research, Knoxville, Tenn., 1977.
- [3] B. A. Larianov, ESRIEA, Personal communication.
- [4] B. A. Larianov, et.al., "Some Methods of Increasing the Response of Fast Breakers," Proc. All-Union Conf. Eng. Problems of Fusion Reactors, Leningrad, USSR, July 28-30, 1977.
- [5] S. Kassel, "Soviet Pulsed-Power R & D," Rept. R-2212-ARPA, Chapter X, Rand Co., Santa Monica, Ca (Preliminary Rept. (1978)).
- [6] E. A. Azizov, et.al., "Influence of a dielectric medium on the characteristics of a high-speed explosive circuit breaker," Sov. Tech. Phys. Lett. 2. 121 (1976).
- [7] A. M. Pavlovsky, et.al., "Explosive Pulsed Current Breaker," USSR Patent No. 490381, 25 Oct., 1976.

## H. Thermally Driven Opening Switches

### 1. Introduction

Thermally driven opening switches are the result of attempts to achieve the speed and economy of fuse opening switches but with the added advantage of repetitive operation [1-5]. The strategy is simple: let the wire heat almost to, but not beyond, its melting point so that its resistance increases several-fold and hence decreases the current. The wire can thus partially interrupt (decrease considerably) the current without melting or exploding and hence can be re-used. For some applications, partial interruption is sufficient. Basic design information for thermally driven opening switches is given in Ref. [1]. Reports on applications is given in Refs. [1-4]. At this point, both low carbon steel [3,4,5] and tungsten [1,4,5] have been investigated. For low carbon steel, cooled initially to  $-193^{\circ}\text{C}$  and allowed to heat to  $+800^{\circ}\text{C}$ , the resistance changes by a factor of 70 [3,4]. Reference [6] argues that it should be possible to design a bistable thermal switch - one with both a high and a low equilibrium temperature (resistance). Such a switch could be used without fear of it being destroyed by thermal runaway.

We now briefly consider some of the characteristics for thermally driven opening switches reported in the literature. Because the development of such switches is not

very far advanced, there is considerable uncertainty in the extent of development possible.

Voltage Standoff-The maximum reported voltage standoff is 20 kV [3,4]. Electric fields of about 1.7 kV/cm were held off in the work of Ref. [1]. Neither of these figures is likely to represent a real limit. However, the voltage standoff should be lower for thermally driven opening switches than for fuses because thermally driven opening switches do not vaporize.

Peak Current-The maximum peak current reported so far is 200 kA [3,4]. Higher currents can be realized successfully by paralleling elements since the V-I characteristics for thermally driven opening switches have the proper characteristics for stability ( $dv/di > 0$ ).

Pulse Width-In the applications reported so far, pulse widths of about 5  $\mu$ s [1] and 100  $\mu$ s [3,4] have been used. As with fuses, larger pulse widths ordinarily mean slower switching.

$di/dt$ -No direct  $di/dt$  information is available, although a turnoff time of about 6  $\mu$ s has been observed [1]. The current density basically determines the  $di/dt$ . Typical [4] current densities are about 15 kA/mm<sup>2</sup>.

Delay Time-The difference in time between when the current is initiated and when the peak in the current is reached is determined by the current density in the wire. No careful studies have yet been made. In one experiment, the delay time is about 1  $\mu$ s - very short.

Jitter-No relevant information is available.

Pulse Repetition Rate-This quantity is determined by how fast the wire can be cooled. After an initial cooling period of 15 min before the first shot, repeated cooldowns are possible at the rate of about 1 shot per minute [3,4] when the initial temperature is  $-193^{\circ}\text{C}$ .

Average Current-No relevant information is available.

Duty Cycle-No relevant information is available.

Recovery Time-Because the wire does not vaporize and ionize, the "recovery" is essentially instantaneous.

dv/dt-Appropriate information is not available.

Risetime-The best reported is 6-8  $\mu\text{s}$ , although this figure depends on the current density in the wire.

Coulomb/shot-For a pulse width of 100  $\mu\text{s}$  and a current of 200 kA, the charge transfer is about 20 C.

Lifetime-No quantitative data are available.

## 2. Summary and Conclusion

The main attractive feature of thermally driven opening switches is the promise of repetitive operation. At present, a major unknown is how well the wires will hold up under re-cycling. This factor should be investigated together with efforts to obtain a better characterization and understanding of the device performance.

### 3. References

- [1] Dah Yu Cheng, "Application of a Variable Resistance to Arrest Oscillations in a Pulsed Capacitor Discharge Circuit," Rev. Sci. Instr., Vol. 40, pp. 1153-1157, September 1969.
- [2] M. I. Bystrov, B. A. Larinov, V. P. Sinin, F. M. Spevakova and A. M. Stolov, "Pulsed Power Sources Based on Transformer Inductive Energy Storage Devices with Non-linear Elements," No. 2 in the series: Inductive Energy Storage Devices and Switching Apparatus for Thermonuclear Installation, Report of a Joint USSR-USA Seminar, USSR Atomic Energy State Committee, Leningrad, NII-EFA, 1974, (Translated by W. J. Grimes, P.O. Box 55, Hingham, Ma 02043, May 1975).
- [3] M. N. Bystrov, L. V. Dubovoy, Ye. A. Larianov, I. Monoszon, I. M. Royfe, A. M. Stolov, Ye. V. Seredko, V. P. Silin, B. A. Stekol'nikov and L. A. Sairochi, "Thermal Non-Linear Resistances in Energy Output Systems for Inductive Storage Devices," No. 5 in the series: Inductive Energy Storage Devices and Switching Apparatus for Thermonuclear Installation, Report of a Joint USSR-USA Seminar, USSR Atomic Energy State Committee, Leningrad, NII-EFA, 1974 (Translated by W. J. Grimes, P.O. Box 55, Hingham, Ma 02043, May 1975).
- [4] M. N. Bystrov, V. A. Krylov, B. A. Larionov, V. P. Silin and A. M. Stolov, "Impulse Power Source for Feeding the 'Pinch with Liner' Installation," Report II, Joint Soviet-American Seminar on Pulsed Fusion Reactors, September 23-27, 1975, ESRII, Leningrad, 1975.
- [5] A. S. Gilmour and J. D. Marshall, "Liquid Nitrogen Cooled Wires as Switchable High-Power Direct Current Limiting Elements," Proc. First IEEE Internat. Pulsed Power Conf., (76CH1147-8 Reg 5) IC-3, Lubbock, Texas, Nov. 9-11, 1976.
- [6] P. D. Coleman and M. O. Hagler, "Limitations of Thermally Driven Resistors as Opening Switches," in Pulse Power Systems Employing Magnetic Energy Storage, Final Report Under Naval Surface Weapons Center Contract N60921-76-C-0092, T. F. Trost, Principal Investigator, Department of Electrical Engineering, Texas Tech University, Lubbock, Texas 79409, May, 1977.

## I. Superconducting Switches

### 1. Introduction

Superconducting opening switches are generally used in connection with superconductive inductive energy storage. They represent an attempt to exploit the low temperature environment already present in the superconductive energy storage system in providing a conceptually simple means of repetitive switching. The switch is caused to change from the superconducting to the normal stage in some characteristic switching time  $\Delta t$ . The main problem with superconducting switches is the additional refrigeration required to remove the heat dissipated into the low temperature fluid when the switch goes normal.

This transition can be induced by three distinctly different trigger (quench) methods: Current, B-field, and thermal quench. The current from the source through the switch can be increased to cause self-quench or the current can be induced by one of several means from a separate external trigger source. An external magnetic field can be applied to cause B-field quenching. The magnetic field can be applied, with different results, parallel, or transverse to the current. With foil conductors, there is also a difference with  $\vec{B} \perp$  or  $\parallel$  to the foil surface while  $\vec{B}$  is  $\perp$  to  $\vec{I}$ . These differences are related to the shielding effect of the conductor. For foil conductors it has been found [1] that the best (fastest) quench occurs with  $\vec{B} \perp \vec{I}$



and tangentially to the foil surface as shown by  $\vec{B}_3$  in Fig. VI-13. The thermal quench can be induced by heating all or part of the switch with an external heating filament. The best way of ensuring uniform heating may be to use some form of radio frequency heating [2].

The thermal quench is the slowest [3] one with a  $\Delta t_{\min}$  of approximately 1 ms. The B-field quench has about 200 times faster  $dR/dt$  but involves generally bulkier and more complicated equipment. The simplest quench method for  $\Delta t < 10 \mu s$  appears to be the current induced one. One should note, however, that empirical results [2,4] show that in order to obtain a "firm quench" ( $\sim 90\%$  of max. switch resistance) a voltage of  $0.3 I_c R_{sw}$  must be applied to the switch or switch segment. Here,  $I_c$  = critical current in switch and  $R_{sw}$  = fully normal switch or switch segment resistance. For practical switch values, this can result in very high voltages which cause insulation problems, unless the switching voltage is applied across many switch segments. The quench proceeds from several points along the wire which goes normal. Opening times as short as 200 ns can be obtained with 200  $\mu m$  diameter wires [5]. One should also note that the switching condition must be maintained long enough to deliver enough energy (or extract it from the storage circuit) to raise the temperature of the switch and all associated material above the critical temperature [6].

When the switch is triggered, it is important that the entire switch goes normal so that a sufficient  $\Delta R$  will reduce

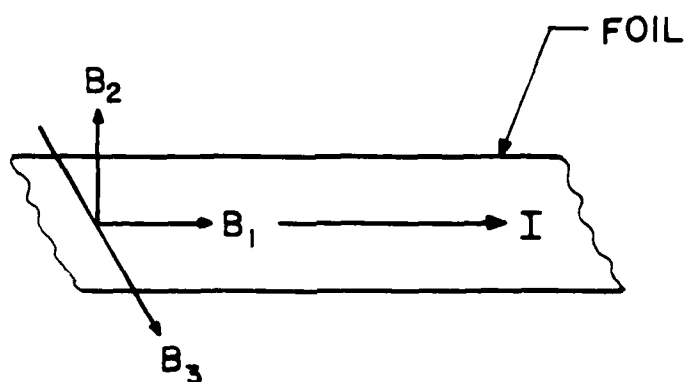


Fig. VI-13. Possible B-Field Orientations For S.C. Switch Quenching

the current enough to avoid switch burn-out. If the superconductor is stabilized sufficiently (Cu-matrix), then this is difficult. The switch is therefore either partly stabilized [7,8] (e.g. with 70% Cu, 30% Ni matrix) or not stabilized [9] at all. The power density in the switch ( $\text{MW}/\text{cm}^3$ ) is generally limited by the allowable temperature rise of the enclosing epoxy [10] ( $\sim 100^\circ\text{K}$ ). Typical values are 1-2  $\text{MW}/\text{cm}^3$ .

The repetition rate of the switch depends on how fast it recovers its superconducting stage which again depends upon the design details, total mass (matrix + s.c. + epoxy), cooling channels, etc. It is difficult to see how this kind of a switch can be rep-rated much above 100 pps and the losses (refrigeration power) would then probably be excessive. Recall that each Watt of dissipated power in the cryogenic volume must be paid for by

$$W_E = W_C \frac{T_O - T}{\eta T_O}$$

where  $W_C$  = power dissipated in cryogenic environment

$W_E$  = supplied refrigeration power

$\eta$  = % refrigerator efficiency compared to Carnot efficiency

$T_O$  = temperature of surrounding medium ( $\sim 300^\circ\text{K}$ )

$T$  = refrigeration temperature ( $\sim 4^\circ\text{K}$ )

Typically, this comes out as  $W_E \sim 250 W_C$ . A 95% switch efficiency does not sound as impressive when one realizes that the 5% loss power must be multiplied by a factor of 250 in terms of the overall system efficiency. This also demonstrates the desirability of using a different super-

conducting material, such as  $\text{Nb}_3\text{Sn}$ . With a superconducting temperature of say  $20^\circ\text{K}$ , the relationship for a practical refrigeration unit will be  $W_E \sim 50 W_C$ . It has been shown [6,11] that, for an unstabilized switch, the volume (which is approximately proportional to the price) is given by

$$V_{SC} = A\ell \frac{V_{\max} I_{\max}}{J_C^2 \rho_N},$$

where  $a$  and  $\ell$  are the cross sectional area and length,  $V_{\max}$  and  $I_{\max}$ , the peak voltage (during switching) and current,  $J_C$  the critical current density, and  $\rho_N$  the normal state resistivity of the superconductor. If a matrix is used with an area ratio of  $A_m/A_{SC} = a$ , then

$$V_{SC} = (a + 1) \frac{V_{\max} I_{\max}}{J_C^2 \rho_e},$$

where  $\rho_e$  is the effective resistivity of the superconductor and matrix in parallel in the normal state. This is given by

$$\rho_e = [(1 + a)\rho_m\rho_N]/(\rho_m + a\rho_N)$$

From these equations, it is clear that one wants to maximize  $J_C$ ,  $\rho_m$ , and  $\rho_N$  and to minimize  $a = A_m/A_{SC}$ .

The switch must be designed with a low inductance winding (bifilar) arrangement to allow fast switching (low  $\Delta t$ ) and with sufficient conductor length to give sufficiently large  $\Delta R$ . Too large a loop length in the switch coil can cause voltage breakdown problems between adjacent conductors. However, when the switch quenches high voltage spikes are

observed as a result of the high  $L \frac{di}{dt}$  (even though  $L$  is made as small as possible). Also, when accidental quenches occur, high voltage spikes occur along the switch where the quench occurs [8]. These spikes can be 10 times higher than the voltage which is seen with a normal (triggered) quench. The insulation must, therefore, be designed accordingly.

For a purely resistive transfer where the superconducting (s.c.) switch is shunted by a resistance, the energy dissipated in the cryogenic environment is given by [8,12].

$$E_{sw} = \frac{E_0}{1 + \frac{R_N}{R_{sh}}}$$

where  $E_0$  is the inductively stored energy,  $R_N$  is the normal resistance of the switch, and  $R_{sh}$  is the shunt resistance. Some considerations of switch losses and energy transfer times, which are also functions of the external circuit parameters, are discussed in Ref. [12]. The shunt resistor can also be used in parallel with the load (which may be inductive) in order to reduce the energy dissipation in the cryogenic volume. In order to achieve this, one must have [13,14]  $R_N > R_{sh}$ . However, high  $R_N$  also requires high switching voltage and power.

For fast switching, one must also keep the conductor dimensions small so as to limit magnetic and thermal diffusion times. The switching times of superconducting wires of various dimensions vs the switching  $di/dt$  have been measured [13]. For  $\dot{i} < 5 \times 10^7$  A/s, the switching times increase rapidly for decreasing  $\dot{i}$ .

The minimum energy per unit volume for warm-up of the composite switch and matrix is given by

$$Q_0 = \sigma_{\text{comp}} \int_{4.2^{\circ}\text{K}}^{10^{\circ}\text{K}} C_{\text{comp}} dt$$

where  $\sigma_{\text{comp}}$  is the average composite density and  $C_{\text{comp}}$  is the average specific heat. In actuality the supplied energy must be  $\sim 100$  times this in order to ensure a fast quench. For one specific case [4]  $Q_0$  was calculated to be  $22 \text{ mJ/cm}^3$ .

## 2. Experimental Results

At Kernforschungszentrum Karlsruhe several s.c. switches and inductive energy storage systems have been investigated. The largest storage system was 220 kJ but the switch in this case was designed to handle 1 MJ. The switches used approximately a ratio of 1.2:1 of 70% Cu, 30% Ni matrix to s.c. in a bifilar cylindrical winding arrangement. In most cases the s.c. was NbTi and it was measured and calculated that s.c. wires have higher  $dR/dt$  than s.c. foils for a thermal quench. Some of the experimentally obtained results are:

Power	: 40 MW
$V_{\text{max}}$	: 47 kV
$\Delta t$	: 20 $\mu\text{s}$
$dR/dt$	: 22 $\text{M}\Omega/\text{s}$
Switch Loss/shot	: 2.5% of stored energy
$\Delta R$	: 450 $\Omega$ (at $T = 10^{\circ}\text{K}$ )
Switch Recovery	: 162 sec
Rep-rate	: 4 shots/hr

The switch recovery rate was largely determined by the epoxy encapsulation and the rep-rate was set by the recovery of the storage inductor. (Smaller switches at the same facility have recovered in 10 sec.) The peak power density in the switch (s.c. + matrix) is  $2 \text{ MW/cm}^3$  and is limited by the maximum allowable temperature rise at the epoxy interface ( $\sim 100^\circ\text{K}$ ). Thermal triggering gave large jitter with a delay from trigger to switching of  $\sim 1 \text{ ms}$ . With current triggering the jitter was  $\sim 5.2 \mu\text{s}$ . A problem with the switch was that it would sometimes self-quench. This is attributed [10] to problems with the matrix and it is felt that there is a need for further research on suitable matrix materials for the switch. At the present time it appears that the work will not be continued. A detailed report of much of this work is being prepared [15].

At the D. V. Efremov Scientific Research Institute of Electrophysical Apparatus in Leningrad, USSR (ESRIEA) the research has been concentrated on building small, compact, modular s.c. switches [9]. They use NbTi foils with no matrix material and achieve a maximum power density of  $1 \text{ MW/cm}^2$  of superconducting material. The seemingly contradictory result that this is less than in the previously described switches where  $2 \text{ MW/cm}^2$  was obtained for a NbTi - matrix material combination is probably due to the temperature rise limitation of the encapsulating epoxy. It is also possible that they may have problems in feeding the relatively wide s.c. foils they used with uniform current density.

The S.C. switch is constructed as a bifilar pack of a 20  $\mu\text{m}$  thick strip of the s.c. foil as shown in Fig. VI-14. Insulating fiberglass gaskets impregnated with epoxy resin (at 40 atm pressure) are placed between the layers. Several switches have been constructed and tested as shown in Table VI-1. The switch dimensions are typically 1.5" x 2" x 6". The  $I_{\text{max}}$  and  $I_{\text{min}}$  in Table VI-1 gives the range over which the switch will self (current) quench. This range increases with increasing foil width and may be due to mechanical motions of the foil or "magneto-thermal effects" (flux jumping?). Thermal and B-field quenching were also investigated. The best magnetic field direction for externally controlled (triggered) quenching was  $\vec{B} \perp \vec{I}$  and tangentially to the s.c. foil surface.

Using the SCS6 switch listed in Table VI-1, they transferred a peak power of 25 MW (2.5 kA, 10 kV) from a 50 kJ inductive storage systems. The maximum current is 8 kA/unit and  $\Delta R \sim 20\text{--}50 \Omega$  @  $T = 20^\circ\text{K}$ . A particularly important feature of these switches is their potential modularity. This aspect is presently being studied at the ESRIEA [16]. The SCS22 and SCS23 switches were successfully operated in parallel as shown in Table VI-2. Successful parallel operation of superconducting switches was also demonstrated at LASL. Two switches which reached 6 kA and 7 kA individually were operated in parallel at 13 kA.



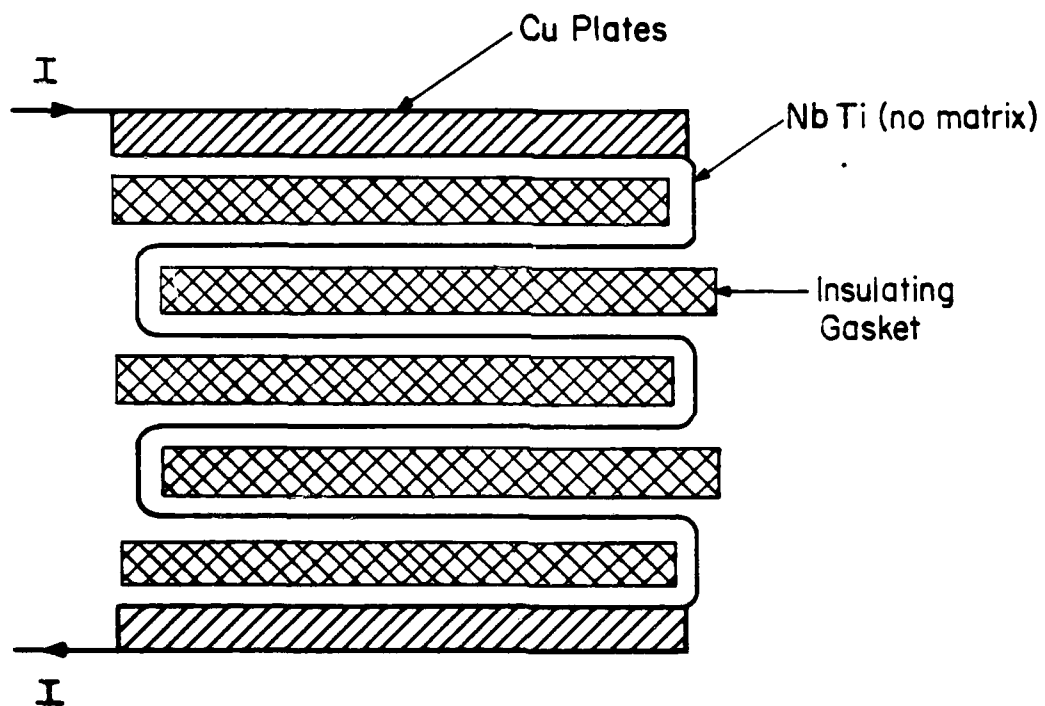


Fig. VI-14. SUPERCONDUCTING OPENING SWITCH (After References [1,9])

Table VI-1. The parameters and experimental results of SCS modules

	SCS6	SCS8	SCS14	SCS16	SCS18	SCS19*	SCS20*	SCS21	SCS22	SCS23
$I_{\max}, A$	2700	8240	4040	3900	3120	3120	5200	2800	3130	2820
$j_{\max}, 10^5 A/cm^2$	5.4	5.1	5.0	4.8	6.2	6.2	5.6	5.6	6.2	5.6
$I_{\min}, A$	2490	4320	3640	2990	2800	2530	3210	2520	2580	2560
$j_{\min}, 10^5 A/cm^2$	5.0	2.7	4.5	3.0	5.6	5.0	3.4	5.0	5.2	5.1
R SCS (20°K), Ohm	50	20	8.7	27	25	36	20	41	41	41
$\rho (20^\circ K)$										
$10^{-5} Ohm-cm$	6.4	6.4	7.0	7.0	7.2	7.2	7.2	7.0	7.0	7.0
$l, mm$ (foil width)	$25 \pm 1$	$80 \pm 1$	$40 \pm 1$	$40 \pm 1$	$25 \pm 1$	$25 \pm 1$	$46 \pm 1$	$25 \pm 1$	$25 \pm 1$	$25 \pm 1$

\*Mechanical foil connection, other switches were epoxied.

Table VI-2. Experimental results of SCS22 and SCS23 parallel operation

Name	$I_{\max}$ A	$I_{\min}$ A
SCS22	3130	2580
SCS23	2828	2560
SCS22+SCS23	6100	5680

The current stability ( $I_{\min} \rightarrow I_{\max}$  range) of these switches has been found to improve with increased operating temperature, although this reduces  $I_{\max}$ . Residual fields in the foils may also be a contributing factor to the current instability besides the previously mentioned mechanical motion and "magneto-thermal" effects. Although B-field quenching requires relatively bulky equipment, it provides trigger isolation from the main circuit and the work is therefore proceeding along these lines.

At los Alamos Scientific Laboratory superconducting switch work was pursued for several years in connection with the Magnetic Fusion Confinement Program. The work was discontinued for programmatic reasons. Some of their experimental results with a switch using a 70-30 Cu-Ni matrix with a 1.3:1 matrix to s.c. ratio were:

$$\begin{aligned} I_{\text{cmax}} &= 10 \text{ kA} \\ V_{\text{max}} &= 25 \text{ kV} \\ E_{\text{max}} &= 200 \text{ kJ} \\ \tau_{\text{transf}} &= \text{few ms} \\ \Delta R &= 34.2 \, \Omega \end{aligned}$$

Both a cylindrical braid and an accordion type configuration switch was used. The last one is similar in configuration to the Efremov switch shown in Fig. VI-13. Movements of the leads were found to cause stability problems as did stray fields from the storage coil.

### 3. Conclusions and Recommendations

Superconducting switches are the only truly reusable opening switches for inductive energy storage and may be important in relatively slow rep-rated systems. At high rep-rate it appears that the losses of refrigeration power may be excessive. Research on using higher temperature superconductors may be worth while. It appears that the unstabilized switch should have some advantages because of its low heat capacity. It is somewhat strange, however, that no mention is made of spontaneous self quenching for this switch, - especially in view of such problems with the partially stabilized switch. Also the epoxy encapsulation apparently poses a limitation on the maximum power density in the switch due to the maximum allowable temperature rise without mechanical damage. New encapsulation materials and new superconducting materials may, therefore, improve the switch performance and recovery rate. Different matrix materials can also be important.

#### 4. References

- [1] M. D. Machalek, "Foreign Travel Trip Report," April 14-August 4, 1977, USSR and Denmark, CTR Division, LASL.
- [2] D. M. Weldon, et.al., "Optimization of the Superconducting Switch Design in a Superconducting Magnetic Energy Storage System," LASL Rept. LA-5218-MS, March 1973.
- [3] K. Grawatsch, et.al., "Investigations for the Development of Superconducting Power Switches," Proc. Applied Superconductivity Conf., 1-2 Oct., 1974. Oakbrook, Ill.
- [4] H. L. Laquer, et.al., "Superconducting Magnetic Energy Storage and Transfer," LASL Rept. LA-DC-72-470.
- [5] H. L. Laquer, et.al., Proc. 6th Intersoc. Energy Conversion Eng. Conf., Boston, Mass., August 3-6, 1971, p. 1089.
- [6] H. L. Laquer, et.al., "Design Options and Trade-offs in Superconducting Magnetic Energy Storage with Irreversible Switching," LASL Rept. LA-5314-MS, June 1973.
- [7] J. D. G. Lindsay, et.al., "Development of a Superconducting Switch for Magnetic Energy Storage Systems," Proc. Appl. Supercond. Conf., 1-2 Oct., 1974, Oakbrook, Ill.
- [8] A. Ulbright, et.al., "The Study of High Voltage Problems in a Superconducting Power Pulse Generator, p. 50, 6th Int. Cryogenic Engineering Conf.
- [9] V. A. Glukhikh, et.al., "Results of Investigations of High Specific Breaking Power Superconducting Switches," Proc. 7th Symp. on the Eng. Prob. of Fusion Research, Knoxville, Tenn., Oct. 25-28, 1977, p. 912. Also Proc. All-Union Conf. Eng. Prob's. of Fusion Reactors, Leningrad, USSR, July 28-30 1977.
- [10] A. Ulbricht, Kernforschungszentrum Karlsruhe, Personal Communication.
- [11] R. R. Hake, "Single-Shot Pulsed Fields from Inductive Energy Stores," LASL Rept. LA-4617-MS (Aug. 1970).
- [12] P. Komarek and A. Ulbricht, "Investigations on Superconducting Energy Storage Systems Concerning Fusion Technology," Fifth Internat. Conf. on Magnet Technology (Interner Bericht 75-81-MAG, April 1975, Kernforschungszentrum Karlsruhe).

- [13] H. Laquer, et.al., "Superconductive Energy Storage and Switching Experiments," Proc. XIII Internat. Congress of Refrigeration, Vol. I, Wash., D.C., 1971.
- [14] O. K. Mawardi, U.S. Patent No. 3,384,762.
- [15] A. Ulbricht, Ph.D. Thesis, Kernforschungszentrum Karlsruhe (in print).
- [16] A. I. Kostenko, ESRIEA, Personal Communication.
- [17] P. J. Blevins and J. G. D. Lindsay, "Design and Performance of two 10 kA Superconducting Switches," LASL Rept. LA-UR-75-865.

APPENDIX I  
BASIC THEORY OF GAS BREAKDOWN  
E. E. Kunhardt



## 1. Introduction

The evolution of the ionization in an electric field, from a small number of initiatory electrons up to a final steady current is of fundamental importance in the development of high power switches. This evolution has been the subject of considerable investigation for the case of a uniform and constant electric field between parallel plate electrodes. The space between the plates is filled with different gases. This simple geometry is, under certain conditions, amenable to relatively easy theoretical analysis, and the results obtained, although not directly applicable to other geometries, are of fundamental importance since the basic concepts are the same. When a high voltage is applied to a parallel plate gap, the gas between the plates undergoes a transition from insulator to conductor. This transition may be divided into three phases. These phases correspond to the Townsend, the glow, and the arc discharge [1]. A schematic indication of the evolution of the gap voltage and current in the development of breakdown is shown in Fig. A-1.

The time elapsed from the application of the high voltage to the observed time of the appearance of the spark (i.e. to in Fig. A-1) is called the observation time lag. This time consists of two portions: the statistical time lag and the formative time lag. The statistical time lag is the time elapsed from the application of the voltage to the gap, to the appearance of an initiating electron. The formative time

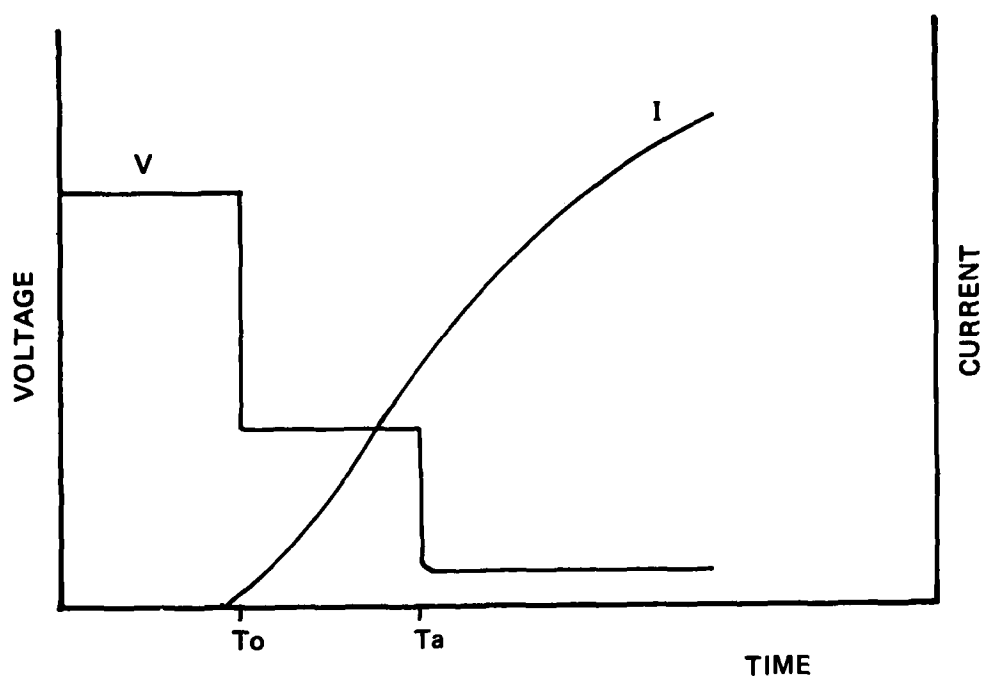


Figure AI-1. Evolution of Voltage and Current in Gap. Voltage is applied at  $t = 0$ .

lag is the time necessary for breakdown to develop from the initial electron. Presently, controversy still exists as to what are the fundamental physical processes at play in this process [1]. The process depends on a number of variables: electrode material, type of gas, pressure ( $p$ ), electric field strength ( $E$ ) and electrode separation ( $d$ ). However, it is generally thought that the development from an initial electron to breakdown may proceed via two different mechanisms depending on the conditions in the gap and the magnitude of the applied voltage. If the applied voltage does not exceed the self breakdown voltage by more than a few percent (this value is a function of gas pressure [2]), breakdown occurs via avalanche processes requiring secondary mechanisms for their maintenance. If  $N_0$  electrons/sec are generated at the cathode via some external means (i.e. UV radiation, electron beam, etc.), the number of electrons/sec reaching the anode, when secondary processes are absent, is given by [1]

$$N = N_0 e^{\alpha d}$$

where  $d \equiv$  gap width

$\alpha \equiv$  Townsend's first ionization coefficient

which is the number of ionizing collisions/unit distance.

An avalanche consists of a single initiating electron from the cathode and the  $e^{\alpha d}$  electrons it subsequently creates in traversing the gap. Thus  $N_0$  electron avalanches per second are maintained by the external field. If this external source

is shut off, the avalanches cease. The field-intensified (since  $\alpha$  is a function of  $E/p$ ) electron current at the anode is, under these conditions, stable.

When secondary processes are present, an instability in the current may develop which would lead to breakdown. The stable, field intensified current may become unstable if at least one electron/avalanche is produced via secondary processes. Under these conditions, a current would still exist in the gap even if the external source of electrons were cut off. This condition is defined as breakdown, i.e. the transition from a non-self sustaining state to one that is self sustaining. This state, or phase, is called a Townsend discharge. If the processes are not stabilized by some external means (i.e. restricting the current in the gap by adding a large resistance in series with the voltage source) further transitions to, first, a glow discharge and then an arc discharge would occur.

The secondary processes causing the instability can occur either at the cathode or in the volume of the gas. These are classified as follows [1]:

1. Gas ionization by positive ions or  $\beta$  processes, where  $\beta$  is Townsend's second coefficient of ionization.
2. Gas ionization by photo-ionization. At low pressures, this effect is negligible.
3. Secondary emission at the cathode due to incidence of positive ions, also referred to as  $\gamma$  processes.
4. Photo-electric effect at the cathode or  $\delta$  processes.

5. Secondary emission of the cathode due to incidence of excited atoms, or  $\epsilon$  processes.

When these processes are taken into consideration, the current in the gap is given by [1]:

$$I = \frac{I_0 (1 - \frac{\beta}{\alpha}) e^{\alpha d}}{e^{\beta d} [1 - \frac{\beta}{\alpha} + \frac{\beta(\delta + \epsilon)d}{\alpha} - (e^{(\alpha - \beta)d} - 1) \gamma + \frac{\delta + \epsilon}{\alpha - \beta} + \frac{\beta}{\alpha} (1 - (\delta + \epsilon)d)]}$$

When the conditions in the gap are such that the denominator in the above expression is zero, the instability leading to breakdown is said to develop.

Since  $\beta/\alpha$ ,  $\beta d$  and  $\delta d$  are generally  $\ll 1$ , the above expression reduces to:

$$n = \frac{n_0 e^{\alpha d}}{1 - \frac{\omega}{\alpha} (e^{\alpha d} - 1)} \quad (A-1)$$

where  $\omega = \beta + \alpha\gamma + \delta + \epsilon$ .

From this equation, although derived from steady state conditions, the breakdown criterion is obtained:

$$\frac{\omega}{\alpha} (e^{\alpha d} - 1) = 1 \quad (A-2)$$

This is known as Townsend's criterion for breakdown in uniform static fields. We observe that when Eq. (A-2) is satisfied, the current in Eq. (A-1) tends to infinity. This mathematical expression, obtained from the steady state Eq. (A-1), is physically interpreted as the condition which must exist in the gap so that a finite current flows without the need of an external ionization agent producing  $N_0$ , i.e. conditions for

a self sustaining discharge. Thus, for a given  $\omega$  and  $\alpha$  (which are functions of the electric field and pressure in the gap), Eq. (A-2) defines a distance  $d = d_s$  at which breakdown occurs, i.e. onset of a self-sustaining discharge. The time it takes for a gap to breakdown under these conditions is inversely proportional to the ion diffusion velocity, assuming that the secondary ionization processes are due to the ions.

Using Eq. (A-2), a functional relationship can be obtained between the electrode separation and the voltage at which breakdown occurs. This fact was observed experimentally by Dela Rue and Muller [3] and was extensively studied later by Paschen [4], to whom the law is ascribed.

Since  $\alpha/p$  is a unique function of  $E/p$ ; and if we assume that  $\omega$  is also a function of  $E/p$  (this has been experimentally confirmed), letting  $\alpha/p = f(E/p)$  and  $\omega/p = F(E/p)$ , Eq. (A-2) can be rewritten as [1]:

$$\frac{F(E/p)}{f(E/p)} (e^{f(E/p)pd_s} - 1) = 1$$

and since  $E = v_s/d_s$ ,

$$\frac{F(v_s/pd_s)}{f(v_s/pd_s)} (e^{f(v_s/pd_s)} - 1) = 1 \quad (A-3a)$$

or

$$v_s = \Phi(pd_s), \quad (A-3b)$$

which means that the breakdown voltage of the uniform field gap is a unique function,  $\phi$ , of the product of pressure and electrode separation for a given gas and electrode material. This is the Paschen Law. The functional relationships in Eq. (A-3) are generally very complicated and no single function, for example, can be used to represent the experimentally observed dependence of  $\alpha/p$  on  $E/p$ . In certain regimes, the functional relationship between  $\alpha/p$  and  $E/p$  can be approximated by [5]

$$\frac{\alpha}{p} = Ae^{-Bp/E} \quad (A-4)$$

where for a given gas, A and B are constants. Using Eq. (A-4) and the experimentally observed fact that  $\gamma$  (neglect all other process in  $\omega$ ) is a slowly varying function of  $E/p$ , over a wide range, Eq. (A-3) becomes (for  $\frac{\beta}{\alpha} \ll \gamma$ ),

$$\gamma \{ e^{[pd_s Ae^{-Bpd_s/V_s}] - 1} \} = 1$$

or

$$\frac{Bpd_s}{V_s} = \ln\left[\frac{A}{\ln\left(\frac{1}{\gamma} + 1\right)}\right] + \ln(pd_s).$$

Noting that the first term is practically constant with  $E/p$ , the above is rewritten as,

$$V_s = \frac{Bpd_s}{C + \ln(pd_s)} \quad (A-5)$$

where

$$C = \ln\left[\frac{A}{\ln\left(\frac{1}{\gamma} + 1\right)}\right]$$

Equation (A-5) is sketched in Fig. (A-2).

At large values of  $pd$  the breakdown voltage,  $V_s$ , increases with increasing  $pd$ . Note that the logarithmic function in the denominator has a lower increase with  $pd$  than the numerator, resulting in a net increase. This increase is physically due to the fact that as the pressure increases, the collision length decreases, thus higher applied fields are required for the electrons to gain, in these short paths, the necessary energy to ionize the gas. Similarly, at low values of  $pd$ ,  $V_s$  increases with decreasing  $pd$ . In this regime, for decreasing  $pd$ , the denominator decreases faster than the numerator resulting in a net increase. This behavior is physically due to the fact that at low pressures, the collision length is very large, larger than the gap separation, and very few electrons, in crossing the gap, ionize gas atoms. By increasing the applied voltage the number of ionizing electrons increases until the value is reached where breakdown occurs.

The breakdown voltage goes through a minimum in the transition from low to large values of  $pd$ . This minimum breakdown voltage is obtained from Eq. (A-5) by differentiating with respect to  $pd_s$  and equating the result to zero. This gives:

$$V_{smin} = 2.718 \frac{B}{A} \ln(1 + 1/\gamma) \quad (A-6)$$



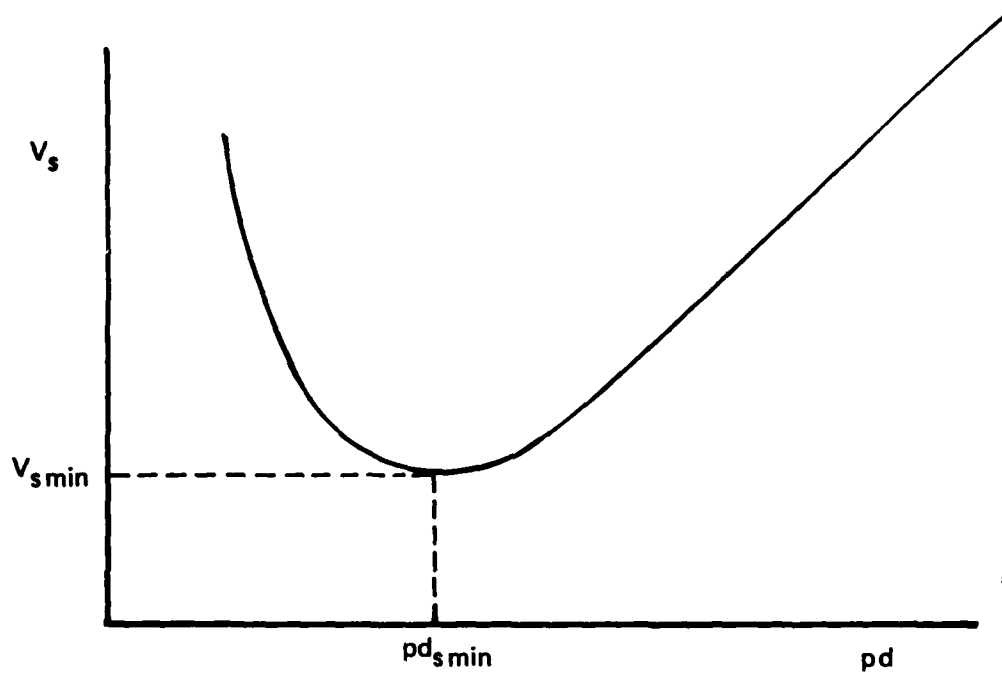


Figure AI-2. Typical Paschen Curve.

and

$$pd_{\text{smin}} = \frac{2.718}{A} \ln(1 + 1/\gamma).$$

With an applied voltage smaller than  $V_{\text{smin}}$ , it is impossible to cause breakdown of a uniform field gap no matter what the spacing or pressure is. The behavior of this curve has been experimentally confirmed for various gases and electrode material [1].

It is remarkable that the general results given above, obtained from a very simple theory, agree quite well, within the Townsend regime of parameter space, with experimental results. Because of this, the above results are very useful. Outside, this regime, variations from this law have been experimentally found and another theory has been proposed to explain the observed behavior [6].

It was at first thought that the deviations from the Paschen Law observed at high pressures (the boundary line is rather diffuse) were indicative of a different mechanism for breakdown [6]. However, it has now been established that it is the % overvoltage that really determines, at these high pressures, the process via which breakdown occurs [2]. For low overvoltages, breakdown develops as previously described. However, for overvoltages of a few percent or more (depending on pressure and type of gas [2]) breakdown is thought to develop via streamer formation [7].

A streamer is a filamentary ionization channel that develops from the head of a space charge due to photo ionization.

Streamers can propagate towards the cathode or both the cathode and anode, depending on the conditions in the gap [7]. Meek [6], who only considered the cathode directed streamer, developed the first mathematical criterion for streamer development. "A streamer will develop when the radial field above a positive space charge in an electron avalanche attains a value of the order of the external applied field"

If  $x_{cr}$  is the distance travelled by an avalanche before the transition to a streamer occurs, then the space charge field was experimentally found to become comparable to the applied field when [7].

$$\alpha x_{cr} \approx 20 \quad (A-7)$$

where  $\alpha$  is the Townsend ionization coefficient. This implies that  $n_{cr} = e^{\alpha x_{cr}} \sim 5 \times 10^8$  electrons assuming the streamer starts from a single electron. The critical number of electrons in the avalanche for a transition to a streamer to occur is  $n_{cr}$ . The time it takes to form the streamer is then

$$t_{cr} \sim \frac{x_{cr}}{V_e} \sim \frac{20}{\alpha V_e} \quad (A-8)$$

where  $V_e$  is the electron drift velocity in the applied field. The streamer velocity is

$$V_s = \mu E_0 \frac{a/R_0}{\ln \left[ \frac{2}{e} \sqrt{a/R_0} \right]} \quad (A-9)$$

where

$\mu$  = mobility of electrons

$E_0$  = applied electric field

$a$  = length of streamer

$R_0$  = Radius of charge distribution at time of  
streamer formation (only approximately known)

In overvolted gaps, where breakdown proceeds via streamer formation, the propagation time of the avalanche up to becoming critical,  $t_{cr}$ , determines the breakdown time since the streamer propagation velocity is very high. At fields above  $10^5$  V/cm, however, shorter delay times than those predicted from equation (A-2) have been observed. Those [9] have been explained by invoking multi-avalanche processes, i.e. many avalanches in series. The theory of streamer breakdown is highly qualitative and still a controversial subject [1, 2, 5, 6, 7].

## 2. References

- [1] F. L. Jones, "Ionization Growth and Breakdown," Encyclopedia of Physics, Springer, Berlin, Vol. XXII, 1956, pp. 1-52.
- [2] K. R. Allen and K. Phillips, Proc. Roy. Soc. A, 278, p. 188, (1963).
- [3] W. deLa Rue and H. W. Muller, Phi. Trans. Roy. Soc. Lond., 171, 109 (1880).
- [4] F. Paschen, Ann. Phys., 37, 69 (1889).
- [5] L. B. Loeb, Fundamental Processes of Electrical Discharge in Gases, John Wiley & Sons, London (1939).
- [6] J. M. Meek and J. D. Craggs, Electrical Breakdown of Gases, Clarendon, Oxford, 1953.
- [7] H. Raether, Electron Avalanches and Breakdown in Gases, Butterworths, London, 1964.
- [8] E. D. Lozanskii, Usp. Fiz. Nauk., 117, 493 (1975).
- [9] G. A. Mesyats, Y. I. Bychkov and V. V. Kremmer, Usp. Fiz. Nauk., 107, 201 (1972).

APPENDIX II  
HIGH POWER SWITCH DATA AND RATIONALE  
T. R. Burkes  
et. al.

## 1. Introduction

The switches described here are limited to vacuum tubes, thyratrons, spark gaps, ignitrons and silicon controlled rectifiers (SCR's). The emphasis is on "closing" rather than "opening" switches. The vacuum tube is the only concept discussed which clearly qualifies as an "opening" switch. Also, operation under "square pulse" conditions is utilized where data is available. Data on operation as phase control devices are not included in this evaluation.

Only the information found in the open literature and manufacturers' data sheets are utilized (except in some spark gap cases) in this Appendix even though the authors are aware of experiments in various laboratories that have not yet been published. Although it is unlikely that all available literature data have been found, sufficient information seems to have been gathered to define the state-of-the-art in high power switching in a reasonable way.

## 2. Data Base Rationale

The set of parameters chosen for evaluation are maximum rated voltage, peak repetitive current, current rate of rise ( $di/dt$ ), pulse repetition rate, Coulomb transfer per shot, total number of shots in expected life, and the total Coulomb transfer throughout the expected life. The data used in this evaluation is presented in Tables 1-5. Each entry represents a particular device performance under a specific set of operating conditions. Note that not all parameters were available for each entry.

Because switches can be operated to enhance one particular parameter at the expense of others, a reasonable set of parameters and operating conditions were chosen so that meaningful comparisons could be made. For instance, life expectancy in spark gaps and ignitrons is usually stated as a number of operations or shots under some set of conditions (hold-off voltage, peak current, and Coulomb transfer) whereas the life of vacuum tubes and thyratrons is usually expressed as a number of operating hours (usually  $10^4$  hours) and the life of solid state devices in years. In all these devices the life expectancy can be increased by reduction of the operating stress, i.e., lower voltage, current and Coulomb transfer or pulse width, as well as a reduced rate of current rise. This is generally true because of lower energy dissipation in the switch.

For thyratrons, the set of operational conditions used are simultaneous operation at rated voltage and pulsed current and operation at rated average current and pulse repetition rate as determined by the anode heating factor and a 10,000 hour life. From this set of data it is relatively easy to calculate the chosen set of parameters (Table I). In some cases, it was found that this procedure resulted in inconsistencies with other operating parameters such as the rms current, etc. However, a sufficiently consistent data set were found for the present purposes.



Vacuum tubes are somewhat more difficult to evaluate. Little information was, for instance, found on  $di/dt$ . This is because  $di/dt$  is a function of the driving power one is willing to invest for a particular tube. A pulse width limitation was stated in several cases. The data shown in Table II were derived by postulating operation at rated voltage and current, maximum pulse width and rated anode dissipation. A 10,000 hour life was assumed. Some of the tubes are developmental types and only incomplete data were available.

Ignitrons are mostly rated for crowbar and ringing capacitor discharge service. A very limited life results from such operation (1000's of shots) and manufacturer's data tend to be very conservative. It is well known that the ignitron life in rectifier service is many years. However, this type of operation is not within the present meaning of "high power switching." Some data are available on operation of ignitrons in high repetition rate, square pulse service and these data were included. Otherwise, the data supplied by manufacturers on the crowbar or capacitor discharge operation form the data base (Table I).

Spark gap data (Table IV) are particularly difficult to compare since most spark gaps are individually designed and built by the user for a particular application. As a result the gaps are also usually tested in a limited parameter range for the given application. Many lifetests, for instance, have been terminated before the device actually failed because there was no need at the time for longer life

or because there was no funding for continuing the test. As a result it is felt that the indicated lifetimes for spark gaps are quite conservative. The few manufacturer's specifications that exist for spark gaps are generally uninteresting in that they usually describe rather low performance devices. The information used in this paper was gleaned mostly from conference papers and technical reports supplemented by interviews where obvious holes in the data base existed.

The data (Table V) for solid state devices were obtained from manufacturers' data sheets for high power inverters. Phase control devices are not included. The voltage  $V_T$  represents the repetitive forward or reverse blocking voltage. For SCRs the peak current,  $I_p$ , is the maximum peak current obtained for a trapezoidal pulse with a leading edge ramp of 100 A/ $\mu$ sec. The maximum values of  $di/dt$  (shown in parenthesis in Table V) for these inverters are based on dissipation constraints, and, except for the lowest value, which was obtained repetitively (a European test condition), are non-repetitive values. The remaining data were obtained from the open literature. For the RSR  $V_T$  is the forward breakover voltage; the values for the LASS devices are conventional SCR blocking voltages. Pulse shapes for these data were more or less rectangular. For the RSR  $di/dt$  was measured repetitively, and is related to the turn-on efficiency of the device. The  $di/dt$  value for the LASS devices were obtained from pulse risetimes and peak

TABLE I. Thyatron Data

$V_T$	$I_p$	$di/dt$	$Q_T$	$N_T$	$Q_s$	$f_r$
kV	kA	A/ $\mu$ s	Coul	Shots	Coul/shot	pps
50	80	$2(10^5)$	$9(10^8)$	$1.35(10^{10})$	$6.67(10^{-2})$	375
50	5	$10^4$	$2.88(10^8)$	$5.76(10^{10})$	$5(10^{-3})$	$1.6(10^3)$
80	12	$10^4$	$4.32(10^8)$	$1.(10^{10})$	$4.32(10^{-2})$	291
120	6	$10^5$	$2.16(10^8)$	$.7(10^{10})$	$3.(10^{-2})$	194
160	6	$10^5$	$2.16(10^8)$	$5.2(10^{10})$	$4.1(10^{-2})$	146
40	10	$10^4$	$5.4(10^8)$	$1.8(10^{10})$	$3(10^{-2})$	500
25	1	$5(10^3)$	$4.5(10^7)$	$7.2(10^{11})$	$6.2(10^{-5})$	$20(10^3)$
44	44	$2(10^4)$	$2.2(10^6)$	$5(10^6)$	.44	125
44	11	$2(10^4)$	$1.1(10^6)$	$5(10^6)$	.22	250
260	4	$10^4$				

TABLE II. Vacuum Tube Data

$V_T$	$I_p$	$di/dt$	$Q_T$	$N_T$	$Q_s$	$f_r$
kV	Amp.	Amp/ $\mu$ Sec.	Coul	Shots	Coul/shot	pps
40	350	$1.1(10^5)$	$1.44(10^9)$	$4.1(10^{11})$	$3.5(10^{-3})$	$1.14(10^4)$
200	225					
65	800	$1.5(10^5)$	$2.88(10^9)$	$3.6(10^{11})$	$8(10^{-3})$	$10^4$
75	2 KA	$1.5(10^5)$	$7.2(10^8)$	$3.6(10^8)$	2	10
65	1.2KA		$2.6(10^7)$	$2.16(10^5)$	120	.006
320	30					
200	200					
100	90				90	D.C.

TABLE III. Ignitron Data

$V_T$	$I_p$	$di/dt$	$Q_T$	$N_T$	$Q_s$	$f_r$
kV	kA	A/ $\mu$ s	Coul.	Shots	Coul/shot	pps
25	300		$2(10^5)$	$10^3$	200	2/min
50	15		$.15(10^5)$	$10^3$	15	2/min
50	65			$10^3$		
25	100				400	
75	60				120	
75	150				45	
35	1.1		$1.26(10^6)$	$4.5(10^8)$	$2.78(10^{-3})$	360
30	75		$2.25(10^5)$	$2(10^5)$	11.25	
25	80	200			400	.2
	21	$1.7(10^4)$				
35	7.4		$2.86(10^6)$	$1.3(10^8)$	.0222	60

Table IV. Spark Gap Data

$V_T$	$I_p$	$di/dt$	$Q_T$	$N_T$	$Q_s$	$f_r$
kV	kA	A/ $\mu$ s	Coul.	Shots	Coul/shot	pps
120	25	$25(10^3)$	$>.14(10^6)$	$2.6(10^6)$	$53(10^{-3})$	2 - 5
54	1	$200(10^3)$	$>10^3$	$>10^5$	.1	$(10^3)$ *
90	4.5				$240(10^{-3})$	250 ++
$10^3$	500	$5(10^7)$			$50(10^{-3})$	single shot
240	43					
60	330	$(10^9)$				**
60	140		$4.5(10^4)$	$5(10^3)$	9	
60	60	$2.1(10^4)$	$.7(10^6)$	$2(10^6)$	.35	.1
125	500	$4(10^6)$	$5(10^3)$	$5(10^3)$	1	
60	6				$360(10^{-3})$	250 ++
80					1.2	100 ++
80					.56	200 ++
80	~4				.28	400 ++
80					.24	500 ++
20					.56	500 ++
60	400	$\sim 2(10^5)$	$1.3(10^6)$	$1.6(10^5)$	8	.13
60	$10^3$				50	
45	400		$\sim 4(10^5)$	$13(10^3)$	30	1/60
40	750			$10^3$	50	
$12(10^3)$	$10^3$	$>10^7$				*
100	$.6(10^3)$	$8(10^5)$				*
30	$4(10^3)$					*
$10(10^3)$	100	$>10^6$				*

\* (single shot  $di/dt$ )\*\* ( $di/dt$  and  $I_p$  under short ckt conditions)

++ synthetic testing

TABLE V. Solid State Switch Data

$V_T$	$I_p$	$di/dt$	$Q_t$	$N_T$	$Q_s$	$f_r$
kV	kA	A/ $\mu$ s	Coul	shots	Coul/shot	pps
1.3	1.8	100(200)			18	50
1.3	10.0	100(800)			0.5	218
2.1	10.0	100(800)			2.1	60
1.2	5.0	2500			0.1	250
2.0	10.00	$1.1 \times 10^6$			0.001	1000
2.0	24.0	$4.0 \times 10^4$			.96	1000

currents. No lifetime data were available for any of the tabulated devices, but it is to be expected that they will have the very long lifetimes (in the order of 20 years) generally associated with semiconductor power devices.



### 3. Bibliography

"Proc. Workshop on Switching Requirements and R&D for Fusion Reactors," EPRI ER-376-SR, July 1977, M. Kristiansen, Editor.

"High Power Spark Gap Switch Development," Maxwell Lab. Rept. MLR-484, May 1975 (Final Rept. to AFAPL).

"High Power Spark Gap Optimization," Maxwell Lab. Rept. MLR-670, June 16, 1977 (Final Rept. to NSWC).

"Investigation of the Erosion Phenomenon in High Current, High Pressure Gas Discharges," J. E. Gruber and R. Suess, Proc. 6th Symp. on Fusion Tech, Aachen, FRG, Sept. 1970.

"A 250 Coulomb 40 kV Spark Gap," A. E. Bishop and G. D. Edmonds, Proc. 5th Symp. on Fusion Tech., Oxford, UK, 1968.

"Arc Voltage of Pulsed High Circuit Spark Gaps," T. E. James and J. L. Browning, Proc. IEE Gas Discharge Conf., Sept. 1970.

"Statistical Performance Data for a High Current 60 KV Spark Gap Switch," R. A. Burden and T. E. James, Proc. 7th Symp. on Fusion Technology, Grenoble, Oct. 1970.

"Gas Cooling and Electric Strength Recovery After a Spark Discharge," E. P. Bel'kov, Soviet Phys-Tech Phys., 16 1321 (1972).

"Multimegavolt Modular Study," J. J. Moriarty, H. I. Milde and J. E. Hipple, RADC-TR-70-107.

"Multichannel Spark-Gap Technology for Staged Theta Pinch Machines," W. H. Borkhagen, et.al.

"Explosive Erosion in Stromstarken Funkenentladungen, K. Schonbach, Zeitsch Angew. Phys., 32, 253 (1971).

"Professional Electron Tubes," Abridged Data, G.E.C. Electronic Tube Company Limited, 1976/77.

Fred Vorwerk, "Evaluation of the Z-5233 Ignitron," Technical Report. ECOM-2512.

G. Bronner, J. Murray and S. Duritt, "Ignitron Long Pulse Testing," MATT-1104 Jan. 76, Plasma Physics Laboratory, Princeton University.

A. Booth and J. Holliday, "High-Voltage Mercury-Arc Switch for Heavy Current Pulse Duty," Proceedings of IEE, Vol. 110, Nov. 63.

D. Cummings, "Development of Switching Tubes for Controlled Fusion Research," Electrical Engineering, 79, 1960.

H. Knight, L. Herbert and R. Maddison, "The Ignitron as a Switch In High-Voltage Heavy-Current Pulsing Circuits," IEE, April 59.

"Ignitron Excitation Circuits and Their Requirements," G-E Power Tube Department Publication PT-50, Dec. 60.

"Ignitrons, Capacitor Discharge and Crowbar Service," G-E Tube Products Department Publication M-1256, Nov. 74.

E. B. Forsyth, "A General Purpose Hundred Kilojoule Pulser," Proceedings of the Ninth Modulator Symposium, May 66.

J. Romanelli, "Pulse Characteristics of a GL-5630 Ignitron," Proceedings of the Eighth Symposium on Hydrogen Thyratrons and Modulators, May 64.

Performance of Ignitrons in Pulse Service, T. F. Turner and H. S. Butler, Proceedings of Seventh Symposium on Hydrogen Thyratrons and Modulators.

P. Faugeras, H. Kuh and J. Zanasco, "Generation of High Current, Long Duration Rectangular Pulses," Conference Record of Eleventh Modulator Symposium, Sept. 73.

"Electronic Control Devices for Industry," National Electronics, Inc. Geneva, Illinois.

"A Sixty-Megawatt Hard-Tube Modulator," H. D. Doolittle, H. Langer, J. A. Randmer and B. Singer, Proceedings of Eighth Symposium on Hydrogen Thyratrons and Modulations, May 1964.

"Development of a 325-Kilovolt, High-Vacuum Switch Tube, L. J. Fox, Proceedings of Eighth Symposium on Hydrogen Thyratrons and Modulators, May 1964.

"A 200-MW Hard-Tube Modulator," Philip A. Ingwersen, Proceedings of the Ninth Modulator Symposium.

"Drive Requirements for High Voltage Low-Grid-Current Tubes," George W. Taylor, Proceedings of the Ninth Modulator Symposium.

"Design Consideration for 180 KV Floating Deck Modulator, Glenn Grotz, Proceedings of the Ninth Modulator Symposium.

"Development and Test of a 50-Megawatt High-Vacuum Pulse-Modulator Tube," J. J. Tritchler and W. L. Wills, Proceedings of the Tenth Modulator Symposium, May, 1968.

"High Voltage Switch Tubes for Neutral Beam Injectors-A New Design Approach," D. H. Preist, Conference Record of the 12th Modulator Symposium, Feb. 1976.

"600 kW Peak High Repetition Rate Hard Tube Modulator," Rulldolf A. Ecken and Leonard Genova, Conference Record of Eleventh Modular Symposium Sept., 1973.

"Long Pulse Switch and Power Amplifier Tubes for Phased Array Radar," R. E. Byram and J. T. Mark, Conference Record of Eleventh Modular Symposium Sept., 1973.

"4CW 100,000 Tetrode Pulse Tests at RADC," Paul Byran and Howard Beard, Conference Record of Eleventh Modular Symposium Sept., 1973.

"Long Pulse Switching of High Power Tetrodes, Bobby R. Gray, Conference Record of the 12th Modulator Symposium Feb., 1976.

"Advanced Reverse Switching Rectifier Modulator," E. H. Hooper and B. L. Jordan, Air Force Weapons Laboratory Report AFWL-TR-75-100, Kirtland Air Force Base, New Mexico, October, 1975.

"Light Activated Semiconductor Switches," L. R. Lowry and D. J. Page, 1977 NAECON Record.

"Megawatt Nanosecond Switching of High Power Laser Activated Silicon Switches," O. S. Zucker, J. R. Long, U. L. Smith, D. J. Page and J. S. Roberts, 12th Modulator Symposium, New York, February 1976.

"Professional Electron Tubes, Abridged Data," G.E.C. Electronic Tube Company Limited, 1976/77.

H. Menown, "Gaseous Switches: The Past and Present State-of-the-art," Proceedings IEEE International Pulsed Power Conference, Nov. 1976.

Evaluation of State-of-the-Art Hydrogen Thyratrons at Extended Ratings, Bobby R. Gray, Hqs. Rome Air Development Center, Conference Record of Eleventh Modular Symposium Sept. 1973.

J. Hamilton and D. Turnquist, "Forty Kilovolt Megawatt Average Power Thyatron (MAPS 40)," Technical Report ECOM-76-1352-F, US Army Electronics Command, Fort Monmouth, N.J. July 77.

"Silizium-Thyristoren," Siemens Datenbuch, 1976,77.

"Electronic Control Devices for Industry," National Electronics, Inc., Geneva, Illinois.

G.E. Semiconductor Data, Semiconductor Products Department, Syracuse, N.Y.

Ed. Hooper and B. Jordan, "Advanced Reverse Switching Rectifier Modulator," Final Report, AFWL-TR-75-100, Oct. 75.

APPENDIX III  
POWER CIRCUIT BREAKER DUTIES AND RATINGS

J. P. Craig

## 1. Introduction

The circuit breaker duties include both opening and closing of electric circuits with inductive, capacitive and resistive loads over a wide range of values from no-load short lines, to rated-loads, to short circuits. The majority of applications have been for 50 and 60 Hz systems, but there is some experience with DC, 25 and 400 Hz. Transients of several kHz are possible on such systems.

The typical duty of the power circuit breaker is to carry current (from a fraction up to its continuous rating) continuously for long periods of time, to interrupt these currents occasionally and, on rare occasions, interrupt short circuit currents. Automatic reclosing is frequently used for fault, or short circuit conditions. Thus, the breaker is called upon, not only to close circuits on no load (charging currents) and normal load currents (plus transients), but also on severe short circuits. In addition to its current carrying and opening and closing duties, it must stand off both transient voltages immediately after opening as well as normal, steady state values for extended periods of time. Also, in both the open and closed position, it is called upon to withstand lightning surges.

Reliability is of utmost importance, since failures can be catastrophic, not only to the breaker itself, but also to other expensive equipment with which they invariably interconnect. A standard practice to increase reliability in

power system applications is to use backup circuit breakers (or fuses). However, this backup capability is not normally obtained by duplication of facilities, but rather is obtained from other breakers installed to control and protect a larger portion of the power system. For many of the pulsed power applications, for which this report is of interest, such backup will not automatically be installed. Therefore, more emphasis should be placed on the primary switches' reliability.

For short circuit conditions on a-c power systems, the switch opening time is measured in cycles of the normal frequency ( $16 \frac{2}{3}$  ms for 60 Hz systems). Typical values of opening times are  $1 \frac{1}{2}$  to 8 cycles after the relays call for the breaker to interrupt. Some breakers can operate in slightly less than one cycle. The opening time for the general case will not be less than  $\frac{1}{2}$  cycle, since the normal current zeros are relied upon for arc extinction. (Current chopping is avoided and forced commutation is not practiced on a-c power systems.) However, both power system stability and arc erosion of the breaker electrodes favor short opening times.

This appendix is not intended to show the details of how transient switching voltages and short circuit currents are calculated or to present the complete circuit breaker ratings standards, either ANSI or IEC. The references at the end of the chapter provide the reader with an extensive

list of books and articles on these topics. A good review of the history and current state of ratings standards is included in the IEEE text Application of Power Circuit Breakers [1]. Greenwood's book [2] provides excellent insight into the voltage transients on power systems. Power Circuit Breaker Theory And Design, edited by Flurschein, [3] also has a chapter on network switching conditions. The AIEE [4] and the two IEEE PAS bibliographies [5, 6] cover pertinent literature up through 1973.

However, for the reader's convenience, a summary of the fundamentals is presented here. For a balanced, three phase circuit, the MVA through the breaker is

$$\text{MVA} = \sqrt{3} V I, \quad (\text{A3-1})$$

where  $V$  is the rms line to line voltage in kilovolts and  $I$  is the rms current in kiloamps. The largest currents that the breakers have to interrupt are due to short circuits on the system. The short circuits may be three phase, line-to-line, line-to-ground, etc. Depending upon the instant of time during the cycle that the short circuit occurs, the resulting transient current may have a damped d-c offset as shown in Fig. A3-1. The peak value of the sinusoidal component of the current wave is  $\sqrt{2}$  times the rms value of that component. A term called "total rms current" is defined as

$$\text{total rms current} = \sqrt{(\text{ac})^2 + (\text{dc})^2}, \quad (\text{A3-2})$$



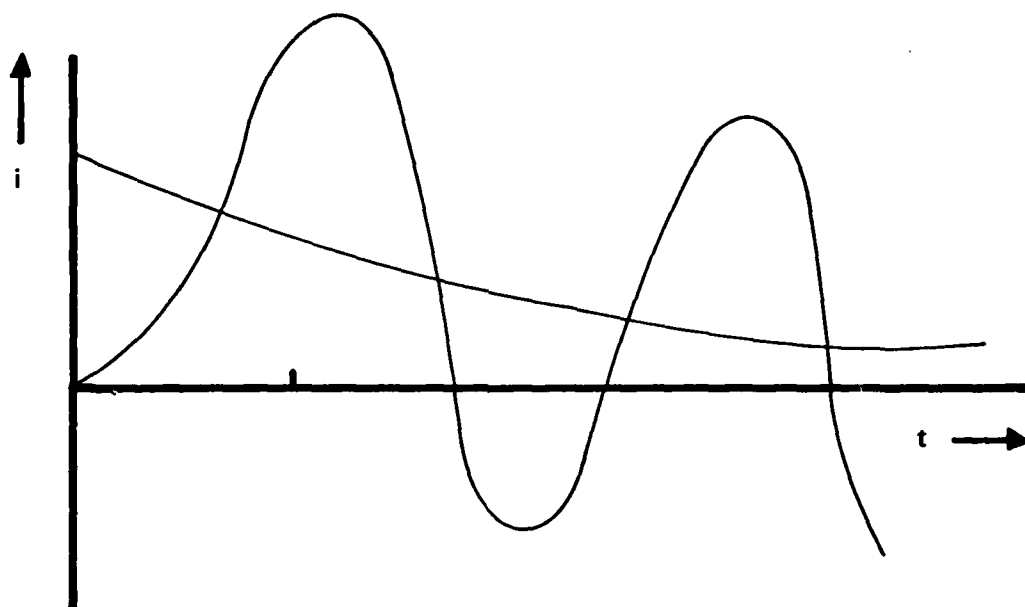


Figure A3-1. Short Circuit Current with Decaying D-C offset.

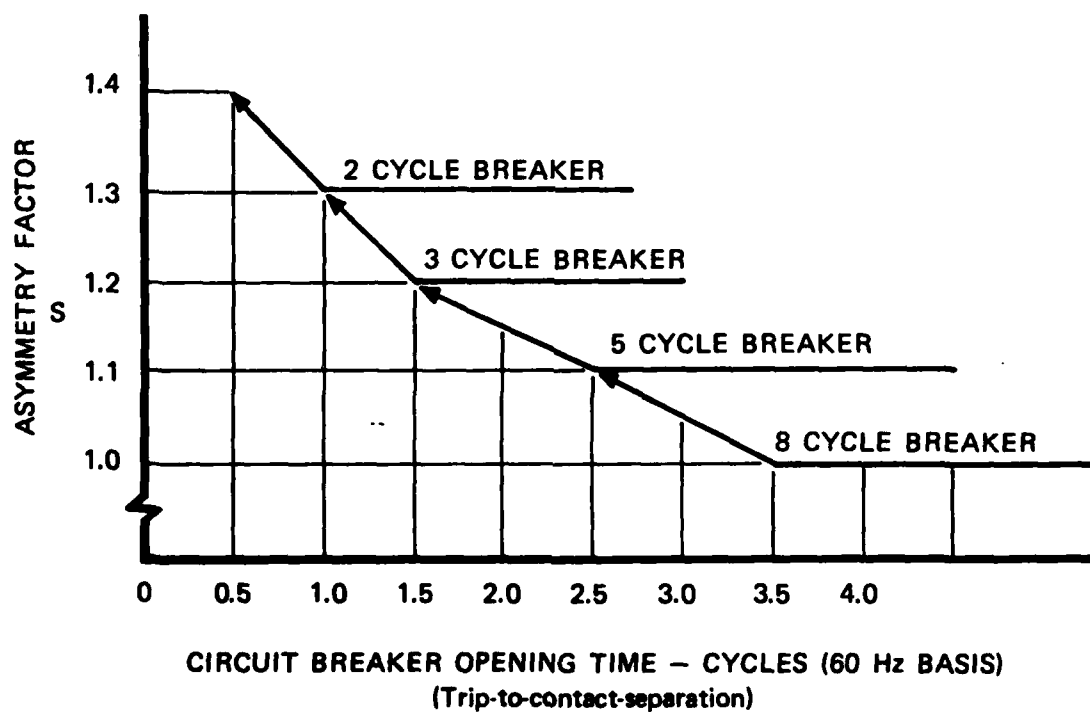


Figure A3-2. Asymmetry Factor for Symmetrical Rating Standard.

which is a function of time, where (ac) is the rms value of the sinusoidal component and (dc) is the value of the decaying dc current at the time that the breaker electrodes first separate. This quantity was used in the older "Total Current Basis of Rating." Obviously, the instantaneous value of the current at the time of contact separation may be considerably higher or lower than this value. The "Symmetrical rating standard" uses the rms value of the sinusoidal component only, together with an asymmetry factor, S. The asymmetry factor is shown in Fig. A3-2.

The abscissa is measured in cycles of a 60 Hz wave from the trip signal to contact separation. The various cycle breaker times listed include a relaying time and extend to current interrupt, rather than contact separation.

Another factor, K, the rated voltage range factor, is used in the symmetrical rating standard. The breaker has a maximum rated voltage, which is the highest rms line-to-line voltage for which the breaker is designed. Over the range of voltage from this maximum voltage down to  $1/K$  times this voltage, the rated current interrupting capabilities are  $V_{\max}/V$  times the rated current interrupting ability with  $V_{\max}$ .

It should be apparent that this maximum rated voltage is neither the withstand voltage nor the maximum voltage that can occur across the contacts of an interrupter. Other factors that can influence these voltages appreciably are the

$\sqrt{2}$  ratio between the peak to rms value of sine waves, the  $\sqrt{3}$  ratio between the line-to-line and line to neutral voltages of a balanced three phase system, the fact that there may be several interrupters in series, lightning and lightning arrester characteristics, and voltage transients which may follow interruption.

The closing and latching capability of the breaker shall be 1.6 K times the (rms symmetrical) rated short circuit current. Or the peak value is 2.7 K times the rated short circuit current. The breaker must be able to carry this current for 3 seconds. It must be able to carry this current for 2 seconds and then interrupt it, for rated voltages of 72.5 kV and below. The required carrying time before interrupt for breakers rated 121 kV and above is reduced to 1 second.

Breakers rated 121 kV and above must be capable of the following full-rated interruption duty cycle. Close-open, wait 15 seconds; close-open, wait 15 minutes; close-open, wait 15 seconds; close-open, wait 1 hour; close-open.

The high voltage breakers use several intersystems in series. Typical numbers of interrupters are given in Table A3-1.

Table A3-1. Interrupters in Series [7]

Breaker Voltage kV	Type Breaker			
	Oil	SF <sub>6</sub>	Air Blast	Vacuum
145	2-4	1	2	3
242	4-6	2	2	5
362	6-8	2	4	7
550	10-12	3	6	11
800	12-14	4	8	14

## 2. References

- [1] R. E. Friedrich, editor, Application of Power Circuit Breakers, IEEE Course Text 75CH0975-3-PWR, 1975.
  - [2] A. N. Greenwood, Electrical Transients in Power Systems, Wiley-Interscience, 1971, N.Y.
  - [3] C. H. Flurscheim, Power Circuit Breaker Theory and Design, Peter Peregrinus Ltd., Southgate House, Stevenage Herts, SG1 1HA, England, 1975.
  - [4] Committee Report, "Bibliography of Switchgear Literature," AIEE Trans. Vol. 61, pp. 1077, 1942.
  - [5] Committee Report, "Bibliography of Switchgear Literature," IEEE Trans, PAS 91 No. 5, Sept/Oct. 1972.
  - [6] Committee Report, "Bibliography of Switchgear Literature," IEEE Trans. PAS Vol. 94, No. 3, May/June 1975.
  - [7] R. B. Shover and V. E. Phillips, "High Voltage Vacuum Circuit Breakers," IEEE Trans. PAS-94, No. 5, Sept./Oct. 1975, p. 1821.
- 